DISPERSION OF VAPOR FROM LNG SPILLS AT ENERGY TERMINAL SERVICE CORPORATION: SIMULATION IN A WIND TUNNEL

by

K. M. Kothari

R. N. Meroney

Prepared for

Energy Terminal Services Corporation

80 Park Plaza

Newark, New Jersey 07101

Fluid Dynamics and Diffusion Laboratory
Department of Civil Engineering
Colorado State University
Fort Collins, Colorado 80523

November 1981

CER80-81KMK-RNM59

EXECUTIVE SUMMARY

A 1:250 scale model of Energy Terminal Service Corporation (ETSC) facility at Staten Island was placed in the Environmental Wind Tunnel to study the dense gas cloud behavior resulting from an accidental LNG release under neutral stability. A total of three wind speeds, five LNG release locations, three wind directions, two boiloff rates for unlimited spill duration, one boiloff rate for 10 minute spill duration, and three vapor barrier fence heights were investigated. The experimental measurements resulted in the following conclusions:

- The flammable methane-air cloud mixture (i.e., peak concentrations greater than LFL) remains within the property boundaries of the ETSC facility during 10 minute pipe failure situations for all cases investigated.
- An increase in the vapor barrier fence height reduced the ground level concentration.
- The LNG plume dispersion was enhanced by the wakes of two tanks for wind directions of 270° and 315°. This confirms that aerodynamic mixing in the wakes of obstacles plays a very important role in accelerating the dispersion of LNG plumes.
- Maximum concentrations at property boundaries were observed for a wind direction of 215° and during LNG spills in the process area.
- The LNG plume dispersion was enhanced by an increase in the wind speed.
- Vertical profiles of gas concentration indicated that the maximum concentration was at the ground.

ACKNOWLEDGMENT

The authors wish to acknowledge the fiscal support of Energy Terminal Services Corporation, Newark, New Jersey. The successful completion of this work depended on the encouragement of Mr. Benjamin H. Bakerjian, Energy Terminal Services Corporation.

TABLE OF CONTENTS

TABLE OF CONTENTS (Continued)

LIST OF TABLES

LIST OF FIGURES

LIST OF FIGURES (Continued)

LIST OF FIGURES (Continued)

LIST OF SYMBOLS

Dimensions are given in terms of mass (m), length (L), time (t), moles (n), and temperature (T)

Symbol	Definition	
A	Area	$[L^2]$
C_p	Specific heat capacity at constant pressure	$[L^2t^{-2}T^{-1}]$
D	Source diameter	[L]
g	Gravitational acceleration	$[Lt^{-2}]$
k	Thermal conductivity	$[mLT^{-1}t^{-3}]$
L	Length	[L]
m	Mass	[m]
$\dot{m}$	Mass flow rate	[m/t]
M	Molecular weight	$[mn^{-1}]$
n	Mole	[n]
c	Exponent of velocity distribution power law	
P	Pressure	$[mL^{-1}t^{-2}]$
Q	Volumetric rate of gas flow	$[L^3t^{-1}]$
T	Temperature	[T]
ΔT	Temperature difference across some reference layer	[T]
t	Time	[t]
U	Velocity	$[Lt^{-1}]$
u_*	Friction velocity	$[Lt^{-1}]$
₩	Volume	$[L^3]$
W	Plume vertical velocity	$[Lt^{-1}]$
x	General downwind coordinate	[L]
y	General lateral coordinate	[L]
z	General vertical coordinate	[L]
z_o	Surface roughness parameter	[L]

LIST OF SYMBOLS (Continued)

Symbol	Definition	
α	Power law exponent	[-]
δ	Boundary layer thickness	[L]
ν	Kinematic viscosity	$[L^2\ t^{-1}]$
$\Delta\rho$	Density difference between source gas and air	$[ML^{-3}]$
ρ	Density	$[ML^{-3}]$
χ	Mole fraction of gas component	
Ω	Angular velocity of earth = 0.726×10^{-4} (radians/sec)	$[t^{-1}]$
λ	Wave length	[L]
Λ	Integral length scale of turbulence	[L]

Subscripts

a	Air
Ar	Argon
g	Gas
i	Cartesian index
LNG	Liquified Natural Gas
LFL	Lower Flammability Limit
m	Model conditions
o	Reference conditions
p	Prototype conditions

1.0 INTRODUCTION

Natural gas is a highly desirable source of energy for residential, commercial and industrial uses, and its consumption is achieved with very little environmental impact. The nature of residential and commercial loads is such that very high demands are made in the winter months on the gas delivery system. These very high demands or "peak" periods are met by supplemental gas supplies such as liquified natural gas (LNG). LNG is cooled to a temperature of -162°C to store at approximately atmospheric pressure. At this temperature if LNG was released to the surrounding environment, rapid boiling of the LNG would occur and a flammable mixture would result. It has been demonstrated (Neff et al., 1976, 1978; Meroney et al., 1980; AGA, 1974) that the LNG vapor plume will remain negatively buoyant for a majority of its lifetime representing a ground level hazard. This hazard will extend downwind until the atmosphere has diluted the LNG vapor below the lower flammability limit (LFL, a local concentration for methane in air below 5% by volume).

It is important that accurate predictive models for LNG vapor cloud physics be developed, so that the associated hazards of transportation may be evaluated. Various industrial and governmental agencies have sponsored a combination of analytical, empirical, and physical modeling studies to analyze problems associated with the transportation and storage of LNG. Since these models require assumptions to permit tractable solution procedure one must perform prototype tests to verify their accuracy. In some cases these assumptions are so conservative that they grossly overpredict downwind hazard zones and eliminate the practicality of energy development completely. In such cases physical model studies can be performed to account for the effects of building

and terrain interaction otherwise unaccounted for in analytical or numerical models.

The current DOT-LNG facility regulations (DOT-LNG, 49CFR Part 193) require that the flammable vapor resulting from specified design accidental releases of LNG be confined within a vapor dispersion exclusion zone. For tanks with all piping connections through the roof, the design accident is a 10-minute spill at maximum flow rate from any piping. Capacity applied for after March 1, 1978 must meet the requirements of Part 193. In the case of ETSC the added capacity is 360 MMSCFD or 3015 gpm. It is the intention of this study to demonstrate that the vapor dispersion exclusion zone requirement is met by the planned use of a vapor fence at the ETSC facility. A wind-tunnel dispersion simulation is used to demonstrate this condition as provided for by the DOT regulations.

A 1:250 scale model of the Energy Terminal Services Corporation (ETSC) facility and surroundings was placed in the Environmental Wind Tunnel (EWT) at Colorado State University to determine the dispersion of hypothetical LNG vapor plumes. The tests were performed with a variety of spill rates, spill durations, and vapor barrier fence heights. The meteorological and source conditions for the various tests are summarized in Table 1. The tests were performed under a hazard analysis strategy designed to identify critical cases and assure conservative compliance with DOT regulations.

The methods employed and the appropriateness of physical modeling of atmospheric and plume motion are discussed in Chapter 2. The concept of a conservative hazard analysis strategy is explained in Section 2.4. The details of model construction and experimental measurements are described in Chapter 3. Chapter 4 discusses the test program and results obtained and Chapter 5 summarizes the conclusions of this study.

2.0 WIND-TUNNEL SIMULATION OF LNG VAPOR PLUMES

Evaluation of the potential hazards arising from accidental spills of LNG on land requires the simulation of the appropriate fluid physics. There are two fundamental approaches to simulation-physical modeling and mathematical modeling. Both procedures are based on the same laws of motion and energy. Mathematical modeling generally requires an explicit specification of all physical interactions and boundary conditions in symbolic mathematical notation. This is feasible, however, only for rather a limited set of all situations, and only after many simplifying assumptions. Physical modeling must also be constrained to a subset of all likely conditions; however, it is generally possible to examine satisfactorily a greater range of complex boundary conditions and interactions without a prior understanding of these behaviors in all their detail. In the following section a short review is provided of the historical context of physical simulation including recent experiments to verify, evaluate, and validate LNG spill models. Succeeding sections discuss full and partial simulation of plume matter and outline the conservative simulation strategy utilized for the ETSC model.

2.1 Applications of Wind Tunnels to Investigations of Wind Engineering Problems

Laboratory simulation is used routinely today to predict wind loads on tall buildings, surface cladding pressures, pedestrian environment in cities, dispersion from fossil fuel stacks, and hazards associated with releases from nuclear power stations. The consideration of the disciplines of meteorology, fluid dynamics, and aerodynamics has resulted in a new field - wind engineering. Current methods and capabilities in wind engineering are demonstrated by a review of problems related to

atmospheric advection and dispersion of air pollutants, wind forces on buildings and structures, and control of winds (Cermak, 1975).

Physical modeling of boundary layer-type winds and wind effects by measurements on small-scale models placed in meteorological wind tunnels currently provides the most reliable source of data for wind engineering. Coordinated measurements on full-scale systems and their small-scale models are available to confirm similarity for a large number of situations.

The turbulent atmospheric boundary layer can be simulated in long test-section wind tunnels with the exception of effects caused by Coriolis acceleration. Rotational effects can be simulated in special rotating flow systems; however, existing systems are too limited in scale to satisfy the boundary-value similarity requirements for near planar-homogeneity as is found in the atmosphere. Fortunately, experimental data from the laboratory and the atmosphere do not show evidence of measurable differences in surface-layer turbulence structure as a result of Coriolis acceleration in the atmosphere.

Counihan (1975) identified important characteristics of the adiabatic atmospheric surface layer to be friction velocity, surface roughness, velocity power law profile, vertical variation of turbulence integral scales, and vertical variation of longitudinal and vertical turbulence intensities. Boundary-layer wind tunnels can reproduce these values in a consistent manner for a wide range of scale ratios. This simulation is obviously not automatic and requires the appropriate selection of upstream roughness and wind tunnel turbulence generators (Cermak, 1971, 1975).

Time averages of micro-scale features within the lower 15% of thermally stratified turbulent boundary layers formed in wind tunnels are in excellent agreement with corresponding data measured within the atmospheric surface layer. This agreement is restricted to boundary layers formed over a sufficiently long boundary to produce near planar-homogeneity within the simulated surface layer. A length of 20-30 m yields data which agree with atmospheric data well within the errors of measurement when scaled with the Monin-Obukhov length and velocity scales. The same statement can be made for turbulence spectra down to a wave number determined by the boundary-layer thickness when scaled with the Kolmogorov length and velocity scales.

The mean velocity distribution of turbulent boundary layers over modeled areas of the earth several miles in extent (small-scale) when covered by high roughness elements such as the buildings of a city are in good agreement with the atmospheric counterparts. This is the case when geometric similarity is preserved, the Reynolds number is sufficiently large to guarantee invariance of flow patterns over sharp edged buildings and the approach flow is similar to the atmospheric boundary layer. Under these conditions, the turbulence structures are expected to be similar also; however, essentially no turbulence data have been obtained in the atmospheric boundary layer over a city to check this expectation.

The aerodynamics of buildings in the atmospheric boundary layer involves the nonlinear interaction of nonhomogeneous, nonuniform, turbulent approach flows with three-dimensional turbulent boundary layers and separated flow over the building, none of these complex flow types are well described even when unperturbed by the others. Consequently, wind-force information on buildings has been determined

previously from measurements on small-scale models on actual structures. Indeed it is now standard practice before final design to perform wind-tunnel simulation of all large high rise structures. Pressure measurements by Dagleish (1974) indicate that mean pressures on small-scale models of sharp-edged buildings in appropriate boundary layers closely represent full-scale values even though the model Reynolds number may be 100-500 times smaller than the prototype Reynold's number.

Meteorologists are frequently faced with problems requiring quantitative estimates of air flow patterns and turbulence characteristics over complex terrain. Use of the wind flow information includes air pollution zoning, siting of fossil fuel burning industrial facilities and wind turbine siting. Wind tunnels have been used to reproduce flow fields and dispersion over mountainous terrain and even valley draingage flow situations (Meroney, 1980) Meroney et al. (1980) and Chien et al. (1980) report field/model flow field comparisons over a complex mountain gorge region in New Zealand and over a mountainous penninsula in Oahu, Hawaii, respectively. A correlation by rank of relative wind speeds for the data pairs revealed simulations near 0.95. Quantitative correlations of wind speed magnitude was of the order of 0.80. Neal and Stevenson (1980) report rank and quantitative correlations for a field/model study of flow over a pass in a New Zealand mountain range as 0.97 and 0.90 respectively.

Physical modeling of mass transport in wind tunnels capable of simulating the atmospheric boundary layer has become an important source of data for treatment of many air-pollution and safety problems. Determination of concentrations of SO_2, radioactive gases, and H_2S from fossil fuel, nuclear, and geothermal power plants; CO, hydrocarbons, and

NO_x from parking garages and dense traffic; methane from liquid natural gas (LNG) spills; and toxic fumes from chemical spills are the most common cases involving the dispersion of gases. The transport of solids is encountered in dispersion of silver iodide over complex terrain for cloud seeding, snow drifting and soil and sand movement. When the boundary geometry is complex (composed of buildings, trees, uneven terrain) the uncertainty of concentrations calculated from the numerical or mathematical dispersion models for small distances from the source becomes very large. These are the conditions for which dispersion modeling in wind tunnels is the most accurate and achievable. Several examples of mass transport problems that have been studied by physical modeling in wind tunnels will be described to illustrate the methods used.

One of the most common problems associated with gaseous exhausts from power and other industrial plants is downwash. The problem may occur for an existing plant where stacks are too low or exit velocity too small. On the other hand downwash must be avoided by proper design for proposed plants. In both cases, data on plume behavior are needed to select a minimum stack height with reasonable gas exit velocities that will insure downwash-free operation. This is a short-range dispersion problem that is most pronounced for strong winds; therefore, it can be treated effectively by physical modeling in a wind tunnel boundary layer with neutral thermal stratification. Kothari et al. (1981) compare measurements over a 1:500 scale model and field measurements of concentration made near the Rancho Seco Nuclear Power Station, California. Centerline concentrations as well as the horizontal spread of the plume were reproduced. On the average the wind tunnel

predictions were some 40 times more accurate in predicting field data than the conventional Pasquill-Gifford analytic dispersion algorithms.

Release of a dense gas from short stacks or near the ground is accompanied by initial descent and horizontal spreading caused by gravitational forces. Buoyancy forces tend to suppress advection by wind shear and dispersion by atmospheric turbulence. Such clouds will drift downwind from the source location at ground level, providing an opportunity for ignition if the gas is flammable or perhaps for acute toxic effects to life in its path. These dense clouds interact with surface topography and obstacles to produce complex time dependent concentration patterns. In Appendix E of this report is provided a review by Meroney (1980) of wind-tunnel experiments performed with dense plumes and simulation evaluation by comparison with field measurements and analytic models. Controlled field experiments of dense plume behavior are sparse. Often important information concerning boil-off rates, spill size, and wind conditions are missing or questionable. Nonetheless, one notes good reproduction of time varying concentrations for the Capistrano 044 LNG Land Spill in Figure E-4, and the Parton Freon Releases in Figure E-5. A comparison of wind tunnel and field data for the 6-cubic meter LNG spill series at China Lake is displayed in Figure E-6.

A comparison of field/model measurements for the 40-cubic meter spill series at China Lake has just been completed (Meroney and Neff, 1980; Neff et al., 1981). Velocity profiles and turbulence measured at the China Lake Site were accurately reproduced over a 1:85 scale model of the spill site. It was found that the peak plume centerline concentration decay with downwind distance was accurately reproduced for all

tests. Annual time, rise time characteristics and peak concentrations were almost identical when approach wind profile conditions reproduced the field conditions.

2.2 Physical Modeling of the Atmospheric Boundary Layer

In order for the flow in any laboratory model to be of value in interpreting or predicting the observed flow in the atmosphere, it is essential that the two flow systems should be dynamically, thermally and kinematically similar. This means that the flow in the two systems must be described by the same equations after appropriate adjustments of the units of length, time and other variables.

A number of authors including Cermak (1975) and Snyder (1972) have derived the governing parameters for atmospheric heat, mass, or momentum transport by dimensional analysis, similarity theory, and inspectional analysis. Another group justify similitude by considerations of turbulence theory and recent reviews of full scale wind data which represent the characteristics of the prototype atmospheric wind on a parametric basis (Counihan, 1973). Although all investigators do not agree concerning details, most would concur that the dominant mechanisms can now be identified and are understandable. The following sections review similitude criteria as they relate to adiabatic atmospheric shear flow.

The atmospheric boundary layer is that portion of the atmosphere extending from ground level to approximately 100 meters within which the major exchanges of mass, momentum, and heat occur and is described mathematically by equation of conservation of mass, momentum, and energy (Cermak, 1971; Snyder, 1981). The general requirements for laboratory-atmospheric-flow similarity may be obtained by fractional analysis of these governing equations (Kline, 1965). This methodology is

accomplished by scaling the pertinent dependent and independent variables and then casting the equations into dimensionless form. Performing these operations on such dimensional equations yields dimensionless parameters commonly known as:

Reynolds number $\quad Re = U_o L_o / \nu_o \quad = \frac{\text{Inertial Force}}{\text{Viscous Force}}$

Bulk Richardson number $\quad Ri = \frac{g_o}{T_o} \frac{(\Delta T)_o L_o}{U_o^2} \quad = \frac{\text{Gravitational Force}}{\text{Inertial Force}}$

Rossby number $\quad R_o = U_o / L_o \Omega_o \quad = \frac{\text{Inertial Force}}{\text{Coriolis Force}}$

Prandtl number $\quad Pr = \nu_o / (k_o / \rho_o C_{p_o}) \quad = \frac{\text{Viscous Diffusivity}}{\text{Thermal Diffusivity}}$

Eckert number $\quad Ec = U_o^2 / C_{p_o} \, (\Delta \bar{T})_o$

For exact similarity between different flows which are governed by the same set of equations, each of these dimensionless parameters must be equal for both prototype and model systems. In addition to these requirements, there must be similarity between the boundary conditions.

Boundary condition similarity requires equivalence of the following features:

a) Surface-roughness distributions,

b) Topographic relief, and

c) Surface-temperature distribution.

If all the foregoing requirements are met simultaneously, all atmospheric scales of motion ranging from micro to mesoscale could be simulated within the same flow field for a given set of boundary conditions (Cermak, 1975). However, all of the requirements cannot be

satisfied simultaneously by existing laboratory facilities; thus, a partial or approximate simulation must be used. This limitation requires that atmospheric simulation for a particular wind-engineering application must be designed to simulate most accurately those scales of motion which are of significance for the given application.

2.2.1 Partial Simulation of the Atmospheric Boundary Layer

A partial simulation is practically realizable only because the kinematics and dynamics of flow systems are independent above a critical Reynolds number (Schlichting, 1968; Zoric, 1972). The magnitude of this critical Reynolds number will depend upon the geometry of the flow system being studied. Halitsky (1969) reported that for concentration measurements on a cube placed in a near uniform flow field the Reynolds number required for invariance of the concentration distribution over the cube surface and downwind need only exceed 11,000. A value as low as 3000 may be used if measurements are restricted to regions away from the immediate building surface. Because of this invariance, exact similarity of Reynolds parameter was unnecessary in the present research since characteristic values always exceeded 4000.

Too low a model Reynolds number implies greater dominance of viscous forces than is found in the prototype situations. Greater viscous effects result in higher dissipation rates for turbulence and a lower rate of scalar dispersion. For the circumstances of the ESTS test configuration any mismatch in Reynolds number physics should result in higher LNG vapor concentrations and a conservative prediction of concentraton levels at plant boundaries (see extended discussion on conservative nature of tests in Section 2.5).

When the flow scale being modeled is small enough such that the turning of the mean wind directions with heights is unimportant, similarity of the Rossby number may be relaxed. For the case of dispersion of LNG near the ground level the Coriolis effect on the plume motion would be extremely small and the exact Rossby number similarity was also considered unnecessary.

The Eckert number for air is equivalent to $0.4\ M_a^2\ (\frac{T_o}{\Delta T_o})$ where M_a is the Mach number (Hinze, 1975). For the wind and temperature differences which occur in either the atmosphere or the laboratory flow the Eckert number is very small; thus, the effects of dissipation of kinetic energy into thermal energy is negligible for both model and prototype. Eckert number equality is not required.

Prandtl number equality is obtained since it is dependent on the molecular properties of the working fluid which is air for both model and prototype.

Bulk Richardson number equality may be obtained in special laboratory facilities such as the Meteorological Wind Tunnel at Colorado State University (Plate, 1963). For neutral flow conditions, bulk Richardson number equality is obtained in the present research.

Quite often during the modeling of a specific flow phenomena it is sufficient to model only a portion of the boundary layer or a portion of the spectral energy distribution. This relaxation allows more flexibility in the choice of the length scale that is to be used in a model study. When this technique is employed it is common to scale the flow by any combination of the following length scales, δ, the portion of the boundary layer to be simulated; z_o, the aerodynamic roughness; Λ, the integral length scale of the velocity fluctuations, or λ_p, the wave

length at which the peak spectral energy is observed. Unfortunately, many of the scaling parameters and characteristic profiles are difficult to obtain in the atmosphere. Counihan (1975) has summarized measured values of some of these different descriptions for the atmospheric flow at many different sites and flow conditions.

2.3 Physical Modeling of Plume Motion

In addition to modeling the turbulent structure of the atmospheric boundary layer in the vicinity of a test site it is necessary to scale the plume source conditions. The similitude approach, (Kline, 1965), determines scaling parameters by reasoning that the mass ratios, force ratios, energy ratios, and property ratios should be equal for both model and prototype. The dynamics of gaseous plume behavior leads to the following nondimensional parameters of importance (Hoot, 1974; Skinner, 1978; Snyder, 1972,1981; Halitsky, 1969):[1,2]

$$\text{Mass Ratio} = \frac{\text{mass flow of plume}}{\text{effective mass flow of air}}$$

$$= \frac{\rho_s W_s A_s}{\rho_a U_a A_a} = \frac{\rho_s Q}{\rho_a U_a L^2} ,$$

$$\text{Momentum Ratio} = \frac{\text{inertia of plume}}{\text{effective inertia of air}}$$

$$= \frac{\rho_s W_s^2 A_s}{\rho_a U_a^2 A_a} = \frac{\rho_s Q^2}{\rho_a U_a^2 L^4} ,$$

---

[1] It has been assumed that the dominant transfer mechanism is that of turbulent entrainment. Thus the transfer processes of heat conduction, convection, and radiation are negligible.

[2] The scaling of plume Reynolds number is also a significant parameter. Its effects are invariant over a large range thus making it possible to scale the distribution of mean and turbulent velocities and relax exact parameter equality.

Densimetric Froude No. (Fr)

$$= \frac{\text{effective inertia of air}}{\text{buoyancy of plume}}$$

$$= \frac{\rho_a U_a^2 A_a}{g(\rho_s - \rho_a)\forall_s} = \frac{U_a^2}{g(\frac{\rho_s - \rho_a}{\rho_a})L}$$

Volume Flux Ratio

$$= \frac{\text{Volume flow of plume}}{\text{effective volume flow of air}}$$

$$= \frac{Q}{UL^2}$$

In order to obtain simultaneous simulation of these four parameters, it is necessary to maintain equality of the plume's specific gravity ρ_s/ρ_a. This constraint is often found over-restrictive as discussed in the following section.

2.3.1 Partial Simulation of Plume Motion

The restriction to an exact variation of the density ratio for the entire life of a plume is difficult to meet for plumes which simultaneously vary in molecular weight and temperature. To emphasize this point more clearly, consider the mixing of two volumes of gas, one being the source gas, $\forall_s$, the other being ambient air, $\forall_a$. Consideration of the conservation of mass and energy for this system yields (Skinner and Ludwig, 1978):[1]

$$\frac{\rho_g}{\rho_a} = \frac{\frac{\rho_s}{\rho_a}\forall_s + \forall_a}{\left(\frac{T_a}{T_s}\forall_s + \forall_a\right)\left(\frac{C_{p_s}M_s}{C_{p_a}M_a} + \forall_a\right)\Big/\left(\frac{C_{p_s}M_s}{C_{p_a}M_a}\frac{T_a}{T_s}\forall_s + \forall_a\right)}$$

[1]The pertinent assumption in this derivation is that the gases are ideal and properties are constant.

If the temperature of the air, T_a, equals the temperature of the source gases, T_s, or if the product, C_pM, is equal for both source gas and air then the equation reduces to:

$$\frac{\rho_g}{\rho_a} = \frac{\frac{\rho_s}{\rho_a} V_s + V_a}{V_s + V_a} .$$

Thus for two prototype cases: 1) an isothermal plume and 2) a thermal plume which is composed mostly of air, it does not matter how one produces the model density ratio as long as the initial density ratio value is equal for both model and prototype.

For a plume whose temperature, molecular weight, and specific heat are all different from that of the ambient air, i.e., a cold natural gas plume, equality in the variation of the density ratio upon mixing is not possible if one is to model utilizing a gas different from that of the prototype.[1] In most situations this deviation from exact similarity is very small. This point is discussed further in Section 2.5 where it is argued the influence on a modeled plume is conservative, i.e., the modeled plume should predict larger distances to LFL.

Scaling of the effects of heat transfer by conduction, convection, radiation, or latent heat release from entrained water vapor cannot be reproduced when the model source gas and environment are isothermal. Fortunately the effects of heat transfer by conduction, convection, and radiation from the environment are small enough that the plume buoyancy essentially remains unchanged. The absence of these effects are argued

[1] If one was to use a gas whose temperature is different from that of the ambient air then consideration of similarity in the scaling of the energy ratios must be considered.

to be conservative for the purposes of hazard predictions. The influence of latent heat release by moisture upon the plume's buoyancy is a function of the quantity of water vapor present in the plume and the humidity of the ambient atmosphere. Such phase change effects on plume buoyancy can be very pronounced in some prototype situations. Figure 1 displays the variation of specific gravity from a spill of liquified natural gas in atmospheres of different humidities. Humidity effects are expected to reduce the extent in space and time of plume buoyancy dominance on plume motion. Hence a dry adiabatic condition should be conservative in terms of distances to lower flammability limit (LFL).

Equality of densimetric Froude number results in the following relationship between model and prototype velocity fields:

$$\left(U_a\right)_m = \left(\frac{S.G._m - 1}{S.G._p - 1}\right)^{1/2} \left(\frac{1}{L.S.}\right)^{1/2} \left(U_a\right)_p$$

where S.G. is the specific gravity, (ρ_s/ρ_a), and L.S. is the length scale, (L_p/L_m). When the prototype velocity is low, the equivalent model velocity utilizing the above relationship is also extremely low. This factor tends to control the minimum prototype wind speed which may be simulated. A performance envelope suggesting the range of spill conditions possible in the EWT are noted in Figure D-4 and D-5 of Appendix D.

2.4 Modeling of Plume Dispersion at Energy Terminal Service Corporation (ETSC) Facility

In the sections above a review of the extent to which wind tunnels can model plume dispersion in the atmospheric boundary layer has been presented. In this section these arguments are applied to the specific

case of an LNG spill at the Energy Terminal Service Corporation facility.

2.4.1 Physical Modeling of the ETSC Atmospheric Surface Layer

The neutral boundary layer was generated in the Environmental Wind Tunnel (EWT) using spires in the entrance of the tunnel and 2.54 cm (1 in.) roughness on the floor. The wind speeds are referenced to a 6.1 m (prototype) height. The aerodynamic roughness, z_o, and power law exponent, α, were specified such that the boundary layer profile is similar to that expected at the ETSC facility.

2.4.2 Physical Modeling of the ETSC Spill Plume

The buoyancy of a plume resulting from a LNG spill is primarily a function of both the mole fraction of methane and temperature. If the plume entrains air adiabatically, then the plume would remain negatively buoyant for its entire lifetime. If the humidity of the atmosphere were high then the state of buoyancy of the plume will vary from negative to weakly positive. These density variations are shown in Figure 1, which illustrates the specific gravity of mixtures of methane initially at boiloff temperature with ambient air and water vapor.

Since the adiabatic plume assumption will yield the most conservative downwind dispersion estimates, this situation was simulated. Several investigators have confirmed that the densimetric Froude number is the parameter which governs plume spread rate, trajectory, plume size and entrainment during initial dense plume dilution (Hoot and Meroney, 1974; Bodurtha, 1961; Van Ulden, 1974; Boyle and Kneebone, 1973; and Neff and Meroney, 1979; Meroney, Neff, and Kothari, 1980). Argon was used as an isothermal model gas to simulate the behavior of a cold methane plume. Argon provides almost eight times the detection

sensitivity for instantaneous concentration measurements as the carbon dioxide used in some previous studies (Meroney, 1977). The variation of specific gravity with equivalent observed mole fraction of methane and Argon is plotted in Figure 2. The variation of Froude number with equivalent mole fraction of methane for the simulation gas used, Argon, is plotted in Figure 3. Over the concentration range where the buoyancy forces are dominant, the variation of the Froude number is conservatively simulated. Undistorted scaling of velocity components was maintained which implies the undistorted scaling of source strength for all three prototype wind speeds of 2.90 m/sec (6.5 mph), and 4.46 m/sec (10 mph) and 6.69 m/sec (15 mph). The boiloff areas and rate values used for modeling were provided by Arthur D. Little, Inc. for ETSC.

Preliminary calculations (Aravamudan and Drake, 1981) showed that the expected concentrations are small in magnitude near the property line of ETSC for a LNG spill rate of 7000 gpm over a 10 minute duration as a result of a pipe failure. Hence, the preliminary tests were performed for a 7000 gpm spill rate for unlimited time duration (continuous spill) to determine the worst case scenerio. This continuous high spill rate would result in the conservative estimate of the concentration at the property line of ETSC. Next additional tests were performed with half the initial spill area of the dike or process area but the same spill rate. The tests were then conducted for a LNG spill rate of 3500 gpm for unlimited time duration. The Materials Transportation Bureau (MTB) vapor exclusion zone requirement is based on a 2.5% mean gas concentration or one half the lower flammable limit of 5% for methane in air. The turbulently dispersing vapor contains regions of instantaneous concentrations higher and lower than the average. Thus MTB is allowing

a peak to average ratio of two to reduce the likelihood of localized flammable concentrations of vapor beyond the vapor dispersion exclusion zone. The tests were also performed with the approach flow velocity profile having the more conservative lower turbulence characteristics of a rural atmosphere. Three worst case sceneries from the preliminary tests were selected and resimulated with the LNG spill rate of 7000 gpm but for 10 minute spill duration. Concentration time histories at downwind locations were recorded to determine peak expected concentration levels.

Since the design spill duration (10 minutes) is finite, concentrations are time dependent or nonstationary. In this case it is inappropriate to interpret the instantaneous concentrations measured as mean concentrations. Indeed classical Pasquill-Gifford type analysis are calibrated with field concentration measurements averaged over 10 minutes. A running mean of the concentration time histories have been produced for equivalent averaging time of 1, 2, 3 and 10 minutes. Ten minute averages are generally at least two times smaller than peak concentrations recorded during the model tests.

Since the thermally variable prototype gas was simulated by an isothermal simulation gas, the concentration measurements observed in the model must be adjusted to equivalent concentrations that would be measured in the field. This relationship which is derived in Appendix A is:

$$\chi_p = \frac{\chi_m}{\chi_m + (1 - \chi_m)\frac{T_s}{T_a}}$$

where

χ_m = volume or mole fraction measured during the model tests,

T_s = source temperature of LNG during prototype conditions, and

T_a = ambient air temperature during prototype conditions.

2.5 A Conservative Simulation Strategy

It is desirable during mathematical or physical modeling of LNG vapor plume behavior to provide the maximum degree of conservatism possible to allow for the uncertainties of model development, instrument resolution, and statistical variability. A basic premise of the hazard analysis strategy followed herein is that:

> A meteorological and spill configuration which meets DOT regulations under conservative constraints will definitely meet regulations under specified design conditions.

A conservative constraint is one which can logically be expected to produce higher ground level concentrations at the plant boundaries. When concentrations below 2.5% mean are produced under conservative conditions, the situation may be considered to meet DOT requirements.

On the other hand if conservative criteria produce concentrations greater than 2.5% mean at plant boundaries, then it is necessary to successively decrease the degree of conservatism to determine if a less-conservative scenario will comply with regulations. In no case does this imply tests with less than the DOT regulation specified spill conditions. The specified design release would be a 10 minute spill at a rate of 3015 gpm.

Conservatisms were introduced into the physical model at two levels. There are specified initial conditions which can be varied such as source spill rate, spill area, source spill duration, and vapor barrier fence height. There are inherent conservatisms associated with

the nature of the model method selected such as the use of isothermal model gases, zero humidity, zero wall heat fluxes, and neutral atmospheric stratification. The nature of each of these assumptions are discussed separately below.

Overestimation of Source Spill Rate

The specified design spill is based on rupture of a single transfer pipe (or multiple pipes that lack provisions to prevent parallel flow) which has the greatest overall flow capacity, discharging at maximum potential capacity. In the case of ETSC for the proposed new facility, this would be 360 MM SCFD or 3015 gpm. All model tests were performed with either 7000 or 3500 gpm equivalent flow rates. Since concentrations are expected to vary more or less directly with source strength this implies a factor of safety of 2.32 and 1.16 respectively.

Underestimation of Vapor Detention Space

The vapor detention areas provided for the tank area by the existing earthen dike (D) and for the process area by a proposed vapor barrier fence (P) are 58,700 m^2 and 34,900 m^2 respectively. When a source is released over a smaller area but retains the same overall source strength larger concentrations are expected at plant boundaries. A concentrated area source maintains its identity for a larger time since the larger eddy sizes merely displace the resultant plume rather than dilute it. Six tests during the model test series were performed over release areas approximately one-half those of the areas permitted by DOT regulations (i.e., D/2 and P*/2).

Overestimation of Source Spill Duration

Forty eight of the fifty one model scenarios were simulated with a continuous rather than a finite duration spill. The design basis

accident specifies a minimum release time of 10 minutes. During a continuous plume release successive puffs travel downwind to overlap in time and space. This superposition of scalar transport results in higher local concentrations than would occur from any finite release alone. Experiments performed by Meroney et al. (1976) for LNG vapor dispersion downwind of tank/dike complexes found that mean concentration measurements made at constant boiloff rates always upper bound conditions of the maximum concentrations detected during any transient boiloff situation.

Underestimation of Vapor Barrier Fence Height

Model vapor barrier fence heights of 2.44, 4.88, and 7.32 m were examined. The minimum height considered exceeds that required to enclose the total methane volume generated during the specified design spill but is less than the proposed vapor barrier height to be installed. Vapor dispersing over the top of a vapor barrier fence has an increased rate of dilution over ground surface releases. In addition mechanical mixing behind wind breaks or fences increase directly proportional to fence height. Tests performed with low fence heights underestimate this additional vertical dispersion, increases dispersion distances and over estimates the dispersion hazards.

Physical Model Implies Zero Humidity

Latent heat release during condensation and freezing of water vapor mixed with cold methane plume decreases the density of the methane cloud (see Figure 1). The decrease in density results in less inhibition of mixing by buoyancy, smaller concentrations, deeper clouds, and the LFL will occur closer to the source. Since the model experiment is

performed in a room-temperature environment, humidity plays no role; thus the model overestimates dispersion hazards.

Physical Model Implies a Zero Surface Heat Flux Condition

Radiation and surface heat transport to cold methane plumes normally act to decrease the bulk density of the cloud. This results in increased mixing within the cloud, greater rates of air entrainment, smaller concentrations, and an LFL which occurs closer to the source. Indeed, in calm situations heat transport is expected to eventually result in a buoyant cloud which would rise vertically above the plant site. An isothermal model gas behaves as a cold plume undergoing adiabatic entrainment (i.e., no heat transport across plume boundaries). Such a plume over estimates dispersion hazards.

Isothermal Plume Mixing Results in Less Persistent Density Effects

The bulk plume negative buoyancy can be represented as $(g \frac{\Delta\rho}{\rho a} \forall)$, where $\Delta\rho/\rho a$ is fractional density excess over air density and $\forall$ is total vapor volume. During adiabatic entrainment of an isothermal dense gas this function is a constant. However, for cold methane gases mixed adiabatically with air this negative buoyancy increases by nearly one half. This results from the difference between specific heat capacities and gas constants of methane and air (Fay, 1980; Equation (4.1)). This effect will offset some of the conservatism claimed in other areas. Nonetheless the Froude number is nearly correct for significant dilutions (see Figure 3), and model calculations predict equal or higher concentration values at equivalent times and distances when the model results are corrected to prototype source strength.

Physical Model Implies a Neutral Atmospheric Stability

Climatological data for the International Airport, Newark, New Jersey suggests that Pasquill-Gifford stability conditions of A, B, C, and D occur about 75% of the time (Aravamudan and Drake, 1981). Greater atmospheric mixing normally occurs during A, B, and C situations; therefore a plume released during class D (neutral) conditions will maintain higher concentrations during advection under equivalent wind speed conditions. On the other hand experiments performed by Meroney et al. (1977) for model releases in category D and F simulated atmospheric boundary layers produced no significant difference in plume dispersion in the near field behind tanks and dikes (i.e., the $x/H \sim 20$). Kothari et al. (1979) have performed extensive measurements of mean velocity, mean temperature, and turbulence intensity in the wake of buildings placed in a stably stratified turbulent boundary layer. These tests showed that the effects of buildings persisted as long as 60 heights downstream of the buildings in the test. The measurement showed the higher turbulence intensity and excess temperature in the building wakes. Because of the observed excess temperature in the wake, the wake stability was approximately two categories more unstable than that suggested by the Pasquill-Gifford curves for the background flow stability. A similar conclusion was obtained by Allwine et al. (1980) in their stable flow diffusion experiments in the presence of building wakes. Thus, it can be concluded that even if the present experiments would have been performed in the stable approach flow, the stability would have been destroyed by the fences and tanks and the experimental results would be essentially the same as for the neutral stability case.

Therefore, the "F" stability condition called for in the DOT regulations (Part 193) is not relevant in this case because of the introduction of turbulence by the tanks, fence and other structures in the immediate area.

In summary the conservative simulation strategy followed was to:

1. Initially test with maximum specifiable conservative test conditions. If the 2.5% mean concentrational level is not exceeded for a given spill area, wind speed, or wind direction proceed to the next condition.
2. If the 2.5% mean concentration level is exceeded at plant sites during a conservative test successively reduce the level of conservatism by
   a) increase of vapor barrier fence height,
   b) decrease of LNG spill rate, or
   c) reduction in duration of spill.
3. Since at a minimum certain nonspecifiable conservative assumptions are retained the ETSC facility may be shown to meet DOT regulations.

3.0 DATA ACQUISITION AND ANALYSIS

The experimental model scale measurements and the necessary conversion of these quantities to meaningful field equivalent quantities are described in this section. Attention has been given to the limitations of the techniques. Some of the methods are conventional and require little elaboration.

3.1 Wind Tunnel Facilities

All concentration measurements were performed in the Environmental Wind Tunnel (EWT). A schematic of the tunnel is shown in Figure 4. This tunnel is designed to study atmospheric flow phenomena. It has special features such as an adjustable ceiling, rotatable turntables, transparent boundary walls, and a long test section to permit reproduction of micrometeorological behavior at lower scales. Reference (model) wind speeds of 0.10 to 12 m/s and a boundary layer thickness up to 1 m at a downstream distance of 6 m from the tunnel entrance can be obtained with the use of the vortex generators and trip at the entrance of the test section and surface roughness on the floor. Additional flow straightener tubes were installed at the front of the test section to produce a larger wind tunnel pressure drop which permits the blower to be run at higher and more stable rotational speeds. A flexible test section roof facilitates an adjustment in test section height to obtain a zero longitudinal pressure gradient. The vortex generators at the test section entrance were followed by 11 m of a false floor with roughness elements 2.54 cm (1 in.) in height.

3.2 Model

A 1:250 scale model of the Energy Service Terminal Corporation facility was constructed from masonite sheet. The LNG tanks (number 3

and 5), process area buildings and vaporizers were constructed from plexiglass. The vapor barrier fence and dike were also constructed to a scale of 1:250. The dike sides have a constant slope of 2:1. The proposed vapor barrier fence will enclose all sides of the process area except that adjacent to the earthen dike. Refer to figure 16 for the fence location for the "P" and "D" tests. The vapor barrier fence was modified at the North-East end to enclose all sides of the P^* process area except that adjacent to the dike during tests identified as P^*, $P^*/2$ orD/2 as shown in Figure 17. Although the vapor barrier fence proposed will be thin- and sharp-edged, the fence used in the model had a broad, flat top. A sharp-edged thin barrier produces maximum wake dimensions and turbulence levels. Hence the more streamlined, flat-topped barrier used in the model will produce a conservative prediction of concentration levels at plant boundaries (see extended discussion Section 2.5). The masonite plate was cut in the dike and process area and replaced with cardboard plate with numerous holes of approximately 2.54 cm (1 in.) diameter. A fine metallic mesh grid was glued above the cardboard in the dike and the process area. The dike area under the cardboard was divided into 33 smaller areas of approximately 17.8 cm x 17.8 cm (7 in. x 7 in.) size. The process area was divided into six areas. Each area was separated and sealed with weather strips (see Figure 6).

The source gas, Argon, was stored in a high pressure cylinder and passed through a flowmeter and then directed into a manifold having fifty outlet ports. Thirty-three equal length tygon tubes having an inside diameter of 0.16 cm (1/16 in.) were connected to the manifold outlets. The rest of the manifold ports were interconnected or blocked to avoid leakage. The tygon tubes from this manifold were fed

underneath the wind tunnel, one to each of the thirty-three smaller areas under the cardboard plate. The gas passed through the flowmeter and into the manifold. The gas was divided evenly into the thirty-three tygon tubes and then passed into each of the smaller areas under the cardboard. The gas exited through the cardboard holes and fine metallic grid with an even surface distribution.

During the process area releases, the source gas from the argon cylinder was measured through a flowmeter and directed into the wind tunnel through a tygon tube of inside diameter 2.5 cm (1 in.). This tygon tube was connected to a brass tube running parallel to the process area fence and at the center of the process area. Holes of 0.16 cm (1/16 in.) diameter were drilled approximately 3.0 cm apart along the length of the tubes. Each hole was facing downward towards the wind tunnel floor. The source gas was directed from the flowmeter and tygon tube to the brass tube. The gas was subsequently emitted out of each of the small holes on the brass tube. The gas exited through the cardboard holes and fine metallic grid with even distribution. The ETSC model installed in the wind tunnel and the 33 model LNG release areas under the cardboard plate are shown in Figures 5 and 6, respectively.

3.3 Wind Profiles and Turbulence Measurements

Measurements of mean velocity and turbulence intensity were accomplished with a single hot-film anemometer with film axis horizontal. The instrumentation used was a Thermo-Systems constant temperature anemometer model 1050 connected to a 2.54×10^{-3} cm diameter platinum film sensing element 0.0508 cm long. The output of the constant temperature anemometer was directed to an on-line data acquisition system consisting of a Hewlett-Packard 21 MX Computer, disc unit, card reader,

printer, Digi-Data digital tape drive and a Preston Scientific Analog-digital converter. The data was processed immediately into mean velocities and turbulence intensities at each corresponding height and stored on the computer disc for printout or further analysis.

Calibration of the hot-film anemometer was performed using a calibrator suitable for low velocity and developed by CSU staff. The calibration data were fit to a variable exponent King's law relationship

$$E^2 = A + BU^n$$

where E is the hot-wire output voltage, U is the velocity and A, B, and n are coefficents selected to fit the calibration data. All measurements were performed with a sample rate of 100 samples per second for 60 seconds, and by means of the above calibraton relationship converted to the mean velocity. The King's law relationship is not normally used for very low velocities where the heat transfer from the sensor is governed by mixed force/free convection; hence, the absolute accuracy of velocity measurements is ±10% at such low velocities, however, relative magnitudes are consistent. The fluctuating velocity may be characterized by the statistic U_{rms} (root-mean-square velocity). It was calculated from

$$U_{rms} = \frac{2E\ E_{rms}}{Bn\ U^{n-1}}$$

where E_{rms} is the root-mean-square of voltage output from the anemometer and A, B and n are calibration constants. The local turbulence intensity, U_{rms}/U was then calculated. The hot-film was mounted on a vertical traverse and positioned over the measurement location on the model to obtain the mean velocity and turbulence intensity profiles. The velocity data reduction flow chart is shown in Figure 7.

3.4 Concentration Measurements

The local concentrations of methane produced during an LNG spill are time dependent; hence it is necessary to have a transducer with a fast response time to concentration fluctuations. A set of eight aspirating hot wire probes was utilized for the present study.

3.4.1 Hot Wire Aspirating Probe

The basic principles governing the behavior of a hot wire aspirating probe have been discused by Blackshear and Fingerson (1962), Brown and Rebollo (1972); and Kuretsky (1967). A schematic of eight probes is presented in Figure 8. A vacuum source sufficient to choke the flow through the small orifice just downwind of the sensing elements was applied. The wires were operated in a constant temperature mode at a temperature above that of the ambient air temperature. Feedback amplifiers maintained a constant overheat resistance through adjustment of the heating current. The change in output voltage from each sensor corresponds to a change in heat transfer between each hot wire and the sampling environment.

The heat transfer rate from a hot cylindrical wire to a gas flowing over it depends primarily upon the wire diameter, the temperature difference between the wire and the gas, the thermal conductivity and viscosity of the gas, and the gas velocity. For a wire in an aspirated probe with a sonic throat, the gas velocity can be expressed as a function of the ratio of the probe cross-sectional area at the wire position to the area at the throat, the specific heat ratio, and the speed of sound in the gas. The latter two parameters, as well as the thermal conductivity and viscosity of the gas mentioned earlier, are determined by the gas composition and temperature. Hence, for a fixed probe

geometry and wire temperature, the heat transfer rate, or the related voltage drop across the wire is a function of only the gas composition and temperature. Since all tests performed in this study were in an isothermal flow situation, the wire's response was only a function of gas composition.

During probe calibration known compositions of Argon-air mixtures were circulated through a pre-heat exchanger to condition the gas to the tunnel temperature environment. These known compositions were drawn from a bottle of prepared gas composition provided by Matheson Laboratories. Figure 9 displays the measured variation of the voltage drop with percentage of Argon in an Argon-air mixture for the overheat ratio of 1.65. It should be noted that voltage $\bar{E}$ shown in Figure 9, is the amplified voltage of the constant temperature anemometer. Thus, the actual sensitivity voltage is ten times smaller. For this overheat ratio (temperature of wire/ambient temperature) the voltage drop varies linearly with Argon concentration. This particular overheat ratio of 1.65 was used during all wind tunnel measurements.

The eight instantaneous concentration sensors were operated by an eight channel Thermo-Systems, Inc., anemometer system. The output voltages from the anemometers were conditioned by a d.c. suppression circuit, a passive low-pass filter circuit tuned to 100 Hz, and an operational amplifier of times ten magnitude and then fed to the analog-digital converter. The time series data were stored in the computer and analyzed at a later time. The schematic of the system is shown in Figure 10.

3.4.2 Errors in Concentration Measurement

The travel time from the sensor to the sonic choke limits the upper frequency response of the probe. At high frequencies the correlation

between concentration fluctuation and velocity fluctuations (velocity fluctuations are a result of the changes of sonic velocity with concentration) at the sensor begin to decline. The CSU aspirated probe is expected to have a 1000 Hz upper frequency response, but, to improve signal to noise characteristics, the signal was filtered at 100 Hz. This is well above the frequencies of concentration fluctuations that were expected to occur.

The errors caused by a linearity assumption in the reduction of concentration data are approximately the component value (percent Argon) ±0.75 percent. The errors caused by calibration change due to temperature drift are approximately 0.1 percent of the component value per degree centigrade. Since the tunnel temperatures vary at most ±5°C during a given test period the maximum error due to temperature drift would be 0.5 percent of the component value. Finally, peak results were only accepted when they reproduced the same signal output within 10% of component value of the calibration gas (i.e., at 0, 1, 5, 15 and 100%) argon). Final concentration magnitudes are expected at worst to be accurate to within ±0.8% methane at equivalent concentrations of 2.5% methane in air.

Instantaneous concentration fluctuations have been time averaged over a 10 minute period during the continuous spill rate tests to produce the values tabulated as mean (or average) concentrations in Appendix A (See Table I). These values are equivalent to those obtained during 10 minute sampling time at full scale. This is consistent with accepted atmospheric dispersion analysis which incorporates dispersion coefficients that have been determined by time-averaging. Thus they are suitable for comparison with analytic or numerical models based on the

generally used 10 minute time-averaging statistic. Peak concentrations reported during the continuous spill and 10 minute spill tests are equivalent to values which may be exceeded less than 1% of the time.

4.0 TEST PROGRAM

The test program examined LNG spill behavior inside of either a vapor fence or an earthen dike. The program included two source configurations: a) continuous or unlimited spill duration, and b) transient or 10 minute spill duration. The continuous spill rate obviously results in an overly conservative estimate of the expected concentrations as discussed previously. A total of three wind speeds, five different release locations, three fence heights, three wind directions and two boiloff rates were examined in the wind tunnel.

A summary of all tests simulated in the laboratory is presented in Table 1. Table 2 presents a comparison of prototype and model conditions. All dimensions reported in the following discussions have been converted to equivalent full scale values appropriate to the Energy Terminal Service Corporation facility with the origin at the center of the line joining the axis of tank number 3 and tank number 5. The positive axis is in the direction of the prevailing wind. A right hand coordinate system is utilized throughout the report.

Wind approach angles studied were 215°, 270°, and 315°. These were selected to include minimum distances between potential spill areas and plant boundaries as well as those cases where the secondary flows and wakes introduced by the storage tanks were either most or least pronounced. Based on past experience, it was felt that a wind direction of 215° would produce the least turbulence from tank wakes on the vapors resulting from a process area spill thus resulting in the longest

downwind distances. Angles of 270° and 315° provided an opportunity to observe increased entrainment produced by the tank wake regions.

4.1 Results and Discussion

4.1.1 Approach Velocities

The approach flow velocity profiles were measured upstream of the model. The neutral flow situations were performed in the EWT and the approach flow mean velocity and turbulence profiles are shown in Figure 11. The average velocity profile power-law index was 0.27. The frictional velocities measured, u_*, were 5.7, 3.1, and 1.8 cm/sec; equivalent to prototype values of 108, 59, and 34 cm/sec. These in turn correspond to 2.9 (6.5 mph), 4.46 (10 mph) and 6.69 (15 mph) m/sec wind speed at a 6.1 m height. Figure 12 shows an approach velocity and turbulence profile for a smooth spread surface condition representing a rural atmosphere. The velocity profile power-law exponent was 0.22. The frictional velocity, u_* was 1.9 cm/sec; equivalent to a prototype value of 36 cm/sec which corresponds to a 4.46 m/sec (10 mph) wind speed at 6.1 m height.

4.1.2 Concentration Measurement Results for LNG Spill Rates of 7000 gpm and 3500 gpm and Unlimited Time Duration

The preliminary experimental measurements of concentration were performed for three wind directions, 215°, 270° and 315°, two wind speeds, 4.46 m/sec (10 mph) and 6.69 m/sec (15 mph), two boiloff areas, dike and process, two fence heights, 2.44 m (8 ft) and 4.88 m (16 ft), with LNG spills of 7000 gpm and unlimited time duration. Subsequently, additional tests were performed at 2.9 m/sec (6.5 mph), modified boiloff areas and a 3500 gpm spill rate. The concentration measurements were performed with Argon at room temperature and various downwind positions.

Figures 13, 14, and 15, show the concentration measurement locations. Figures 16, 17, and 18 show the various release areas and their identification. Run numbers 1 through 23 were performed with the vapor barrier fence enclosing process area P as noted on Figure 16. Run numbers 23 through 51 were performed with the vapor barrier fence modified to enclose the process area P* as noted in Figure 17.

For each position and run computer disc files were created and concentration data were stored for further analysis. In order to extract the data from each file name, the following file name convention is used throughout the report:

1. The first alphanumeric letter on each file indicates rake position,
2. Next digit indicates the replication,
3. Next two digits indicate run number and
4. Last two digits relate sampling position for the particular rake position.

The peak concentration, mean concentration and root-mean-square of concentration fluctuation for the various measurement locations and conditions are given in Appendix B, and location of the peak or mean concentration isopleths are displayed on Figures 19 to 54.

It was noticed that for the same conditions, increase in the fence height reduced the concentration at a fixed location. Dispersion of the LNG plume was enhanced by the wakes of the two tanks for two wind directions, 270° and 315°. The measured concentrations were smaller in magnitude then those found during a 215° wind direction test. As expected, the concentration measurements were larger for 4.46 m/sec (10 mph) than for 6.69 m/sec (15 mph). From these preliminary measurements it was

concluded that concentrated vapor was carried farther downwind for a 2.44 m (8 ft) fence (run #9), than for a 4.88 m (16 ft) fence (run #10). For both these runs a 2.5% mean concentration was observed outside the ETSC property line. It should be noted that because of the unlimited spill duration, this is a conservative estimate. To reduce mean concentration, even for an unlimited time duration of LNG spill it was decided to examine an alternative fence combination as shown in Figure 17. This situation where the fence is farther from plant boundaries will be referred to as P*. Two additional runs (#31 and 32) were performed. It was determined that with continuous release, 4.46 m/sec (10 mph) wind speed, 215° wind direction and 4.88 m (16 ft) fence (run #32), the mean concentration were below 2.5% outside the ETSC facility boundary.

Analysis of the preliminary data showed that the plume extended farther downwind for the lower wind speed. It was deemed advisable to also measure concentration with a 2.9 m/sec (6.5 mph) wind speed (the minimum wind speed at which the wind tunnel was steady and reliable). This set of runs is identified by numbers 33 and 34. It was found that the 2.5% mean concentration extended slightly outside the ETSC facility boundary. Additional measurements were performed with half the P* area (run #39) and half the dike area (run numbers 43 and 44) for a LNG spill rate of 7000 gpm for unlimited time duration with 2.9 m/sec (6.5 mph) wind speed. The mean concentrations exceeded 2.5% outside the ETSC facility. One concentration measurement, run (#41), was performed with approach flow smooth floor characteristics in the EWT which reproduces a characteristic rural atmosphere. Again, the 2.5% mean concentrations exceeded the critical values outside the ETSC facility. Six runs (numbers 45 through 51) were also performed for a LNG spill rate of

3500 gpm for unlimited time duration with 2.9 m/sec (6.5 mph) wind speed. It was determined that the mean concentrations at the ETSC facility boundary were below 2.5%. It was determined that for continuous spills, worst conditions exist with 215° wind direction, 2.9 m/sec (6.5 mph) wind speed, and boiloff in P* area and P*/2 area, corresponding to run numbers 33, 39, and 41. At zero wind speed the vapor would not be expected to disperse laterally from the vapor fence area.

4.1.3 Concentration Measurements Results with LNG Spill Rate of 7000 gpm for 10 minutes Duration

These tests were also performed with Argon at room temperature as a simulation gas. For each position and run, the disc files were created and concentration data were stored for further analysis. It should be noted that the convention to extract data from each file name is the same as that used for continuous LNG release data.

The times of arrival, peak concentrations, and times of passage of the plume for the various measurement locations are given in Appendix C. Location of the peak and concentration isopleths are displayed in Figures 55 to 58 for three transient runs (numbers 36, 40 and 42). For all three runs, the distances to Lower Flammability Limit (peak concentration of 5% by volume of methane) were inside ETSC property. Instantaneous peak concentrations of 2.5% by volume of methane were observed outside the ETSC facility; however, measured instantaneous concentration fluctuations never exceeded the LFL (5% level).

The conventional formulae referenced in 49 CFR 193, Appendix B of the report "Evaluation of Vapor Control Methods," 1974, uses dispersion parameters specified by Gifford developed from data time averaged over

intervals varying from 3 minutes to one hour. The final tables of dispersion coefficients, σ_x and σ_y, versus distances, x, are considered to approximate 10 minute sample time results. When running averages are made of the instantaneous concentrations signals in runs 36, 40 and 42 for averaging times of 1, 2, 3 and 10 minutes the adjusted curves look like Figure 58. In no case does a 10 minute mean concentration exceed 2.5% mean levels at plant boundaries.

Meroney et al. (1980) and Kothari et al. (1981) observed that the maximum ground level concentration occurs at an intermediate wind speed rather than at a maximum or minimum wind speed when there is little or no interaction with surface obstacles. This was shown during wind-tunnel simulation of the 40 cubic meter spill series at China Lake for wind speeds of 3, 5, and 7 meters/sec. Results suggest maximum distances to LFL occurred between 5 and 7 m/sec (11 and 16 mph). Subsequent field tests also suggest that for spill rates in this size range maximum distances to LFL occur for velocities near 7 m/sec. A 3500 gpm spill over a 10 minute period is somewhat larger than 40 cubic meters; however the effects of wind speed should be similar. The vapor barrier fence will act to further diminish any tendency for the maximum LFL to occur at low wind speeds. The vapor barrier fence will also diminish any effect of variation in approach surface velocty profile as the wind approaches over different upwind terrain. Since tests in the ETSC model series were performed at 3 m/sec and above, it is felt that the highest possible levels of concentration at plant boundaries were measured. For the present worst case and the wind direction of 215°, the interaction of LNG plume with surface obstacles is minimal. The 4.88 m (16 ft) fence around the process area acts as a containment

device for the negatively buoyant LNG plume. Reductions of the wind speed would result in less LNG vapor advection due to lower shear displacement over the fence. Thus, the expected value of concentration at the ETSC facility would be reduced by a reduction in the wind speed. It is concluded that the flammable LNG mixture remains within the ETSC facility, given a 4.88 m (16 ft) fence around the P* area or the P*/2 area, for the wind tunnel tests investigated.

4.2 Summary

The critical final consideration for approval of the ETSC facility is whether concentrations greater than 2.5% mean exist at plant boundaries during a specified design release. Table 1 summarizes this feature for each model test. It is noted in each case whether concentrations at a plant boundary equal or exceed 5% mean, 5% peak, 2.5% mean, 2.5% peak, or 1% mean. The table specifies a simple yes (Y) or no (N) in each case.

In no case does a 7000 gpm spill for 10 minutes exceed the 2.5% mean concentration at the ETSC property line.

5.0 CONCLUSIONS

A 1:250 scale model of the Energy Terminal Service Corporation (ETSC) facility LNG storage tanks (numbers 3 and 5) and surroundings was placed in the Environmental Wind Tunnel (EWT) at Colorado State University to determine the dispersion of LNG vapor plumes under neutral stability approach flow. Three wind speeds measured at 6.1 m above the ground were simulated: 2.90, 4.46, and 6.69 m/sec, approaching from the SW (215°), the W (270°) and the NW (315°) wind directions. Two areas; process and dike; and two different spill rates for unlimited spill duration (3500 and 7000 gpm) were investigated. Additional concentration measurements were also performed with spills onto half the process area and half the dike area with unlimited spill duration and with ten minute spill duration. Three fence heights (2.44, 4.88, and 7.32 m) acting as vapor barriers were examined.

The experimental measurement program revealed the following plume behavior:

1. The flammable methane-air cloud remains within the ETSC property boundaries during all 10-minute pipe failure situations investigated. Concentrations never exceeded 5.0% (LFL) beyond the plant boundaries. Mean concentrations did not exceed 2.5% at the plant boundaries.

2. A progressive increase in fence height reduced the downwind distance and the total surface area intercepted by concentrations greater than the LFL. In some cases taller fences moved both mean and peak 2.5% isoconcentration contours within plant boundaries.

3. For wind directions of 270° and 315° the large storage tanks produced a highly turbulent wake region which intercepted the surface plume. Plume dispersion was considerably enhanced by this additional

aerodynamic mixing present in the tank wakes to the extent that even for a maximum continuous spill in these directions, the average concentration did not exceed 2.5% at the property line.

4. Maximum concentrations at property boundaries were observed for a wind direction of 215° and during LNG spills in the process area. Higher concentrations exist when a given spill rate quantity is released in smaller spill areas.

5. LNG plume dispersion was enhanced by an increase in the wind speed during unlimited duration spills. This conforms to experience for passive gas dispersion. Peak plume concentrations during 10 minute spills measured were only slightly influenced by wind speed.

6. Vertical profiles of gas concentration and plume visualization indicated the dense plume inhibited vertical mixing and remained near the surface. Maximum concentrations were measured at ground level.

7. The conservative nature of the test results in larger downwind distances to 2.5% average or 5% peak concentrations than would be expected under real conditions.

REFERENCES

Allwine, K. J., Meroney, R. N., and Peterka, J. A., (1980), "Rancho Seco Building Wake Effects on Atmospheric Diffusion: Simulation in a Meteorological Wind Tunnel," U.S. Nuclear Regulatory Commission Report NUREG/CR1286.

A. D. Little, Inc. (1974) Evalution of LNG Vapor Control Methods, Report to American Gas Association, 139 pp.

American Gas Association (1974) "LNG Safety Program, Interim Report on Phase II Work," Report on American Gas Association Project IS-3-1, Battelle Columbus Laboratories.

Aravamudan, K. and Drake, E. (1981) "Analysis of Vapor Fence Effectiveness in Limiting Dispersion Hazard Zones," A. D. Little Report C-83881, Prepared for ETSC, New Jersey, 32 pp.

Arya, S. P. S. and Plate, E. J. (1969) "Modeling of the Stately Stratified Atmospheric Boundary Layer," Journal of Atmospheric Science, Vol. 26, #4, pp. 656-665.

Blackshear, P. L., Jr., and Fingerson, L. (1962) "Rapid Response Heat Flux Probe for High Temperature Gases," ARS Journal, Novmeber 1962, pp. 1709-1715.

Bodurtha, F. T., Jr. (1961) "The Behavior of Dense Stack Gases," J. of APCA, Vol. 11, No. 9, pp. 431-437.

Boyle, G. J. and Kneebone, A. (1973) "Laboratory Investigation Into the Characteristics of LNG Spills on Water, Evaporation, Spreading and Vapor Dispersion," Shell Research, Ltd., Report to API, March.

Brown, G. L. and Rebollo, M. R. (1972) "A Small, Fast Response Probe to Measure Composition of a Binery Gas Mixture," AIAA Journal, Vol. 10, No. 5, pp. 649-752.

Burgess, D. S., Biardi, J., and Murphy, J. N. (1972) "Hazards of Spillage of LNG Into Water," Bureau of Mines, MIPR No. Z-70099-9-12395.

Cermak, J. E. (1971) "Laboratory Simulation of the Atmospheric Boundary Layer," AIAA Jl., Vol. 9, No. 9, pp. 1746-1754, September.

Cermak, J. E. (1975) "Applications of Fluid Mechanics to Wind Engineering, A Freeman Scholar Lecture," J. of Fluid Engineering, Vol. 97, Ser. 1, No. 1, pp. 9-38.

Chien, H. C., Meroney, R. N. and Sandborn, V. A. (1980) "Sites for Wind-Power Installations: Physical Modeling of the Wind Field Over Kahuku Point, Oahu, Hawaii," 3rd Int. Symposium on Wind Energy Systems, Copenhagen, Denmark, Aug. 26-29, 1980, pp. 75-90.

Counihan, J. (1973) "Simulation of an Adiabatic Urban Boundary Layer in a Wind Tunnel," Atmospheric Environment, Vol. 7, pp. 673-689.

Counihan, J. (1975) "Adiabatic Atmospheric Boundary Layers: A Review and Analysis of Data from the Period 1880-1972," Atmospheric Environment, Vol. 9, pp. 871-905.

Dagleish, W. A. (1974) "Clodding Pressures on Commerce Count Tower, Toronto," Symposium on Full Scale Measurements of Wind Effects on Tall Buildings and Other Structures," University of Western Ontario, London, 13 pp.

Fay, J. A. (1973) "Unusual Fire Hazard of LNG Tanker Spills," Combustion Science and Technology, Vol. 7, pp. 47-49.

Fay, J. A. (1980) "Gravitational Spread and Dilution of Heavy Vapor Clouds," Second International Symposium on Stratified Flows, Trondheim, Norway, June 24-27, 1980, pp. 471-494.

Halitsky, J. (1969) "Validation of Scaling Procedures for Wind Tunnel Model Testing of Diffusion Near Buildings," Geophysical Sciences Laboratory, Report No. TR-69-8, New York University, New York.

Hinze, J. O. (1975) Turbulence, McGraw-Hill, 790 pp.

Hoot, T. G. and Meroney, R. N. (1974) "The Behavior of Negatively Buoyant Stack Gases," 67th Annual Meeting APCA, June 9-13, 1973, Denver, Colorado, Paper No. 74-210, 21 pp.

Isyumov, N. and Tanaka, H. (1979) "Wind Tunnel Modeling of Stack Gas Dispersion--Difficulties and Approximations," Fifth International Conference on Wind Engineering, Colorado State University, 8-14 July 1979, Vol. II, pp. VIII-3-1 to VIII-3-15.

Kline, S. J. (1965) Similitude and Approximation Theory, McGraw-Hill, 229 pp.

Kothari, K. M. and Meroney, R. N. (1979) "Building Effects on National Transonic Facility Exhaust Plume," Fluid Dynamics and Diffusion Laboratory Report CER79-80KMK-RNM35, Colorado State University, Fort Collins, Colorado, 43 pp.

Kothari, K. M., Meroney, R. N., and Neff, D. N. (1981) "LNG Plume Interaction with Surface Ostacles," Draft Report GRI Contract No. 5014-352-0203, September 1981.

Kothari, K. M., Peterka, J. A., and Meroney, R. N. (1979) "Stably Stratified Building Wakes," U.S. Nuclear Regulatory Commission Report NUREG/CR-1247.

Kuretsky, W. H. (1967) "On the Use of an Aspirating Hot-Film Anemometer for the Instantaneous Measurement of Temperature," Thesis, Master of Mechanical Engineering, University of Minnesota, Minneapolis.

Meroney, R. N. (1980) "Wind Tunnel Simulation of the Flow Over Hills and Complex Terrain," Jour. of Industrial Aerodynamics, 5, pp. 297-321.

Meroney, R. N. (1980) "Physical Simulation of Dispersion in Complex Terrain and Valley Drainage Flow Situations," 11th NATO/CCMS Int. Tech. Meeting on Air Pollution Modeling and Its Applications, Amsterdam, Netherlands, Nov. 25-28, 1980, 21 pp.

Meroney, R. N. and Neff, D. E. (1980) "Physical Modeling of Forty Cubic Meter LNG Spills at China Lake, California," 11th NATO/CCMS Inter. Tech. Meeting on Air Pollution Modeling and Its Applications, Amsterdam, Netherlands, Nov. 25-28, 1980, 21 pp.

Meroney, R. N., Neff, D. E., and Kothari, K. M. (1980) "Behavior of LNG Vapor Clouds: Tests to Define the Size, Shape and Structure of LNG Vapor Clouds," Gas Research Institute Report GRI79/0073.

Neal, D. and Stevenson, D. C. (1980) "Prospecting for Wind Energy: A Field Assessment of Physical Modeling," 7th Australian Hydraulics and Fluid Mechanics Conference, Brisbane, August 18-22, 1980, pp. 27-30.

Neff, D. E., Meroney, R. N., and Cermak, J. E. (1976), "Wind Tunnel Study of Negatively Buoyant Plume Due to an LNG Spill," Report Prepared for R & D Associates, California, Fluid Dynamics and Diffusion Laboratory Report CER76-77DEN-RNM-JEC22, Colorado State University, Fort Collins, Colorado, 241 pp.

Neff, D. E. and Meroney, R. N. (1979) "Dispersion of Vapor from LNG Spills--Simulation in a Meteorological Wind Tunnels of Spills at China Lake Naval Weapons Center, California," Fluid Dynamics and Diffusion Laboratory Report CER78-79DEN-RNM41, Colorado State University, Fort Collins, Colorado, 77 pp.

Neff, D. E. and Meroney, R. N. (1981) "The Behavior of LNG Vapor Clouds, Wind Tunnel Simulation of 40 m^3 LNG Spill Tests at China Lake Naval Weapons Center, California," Final Report to Gas Research Institute, Contract No. 5014-352-0203, Colorado State University, 155 pp.

Pasquill, F. (1974) Atmospheric Diffusion, D. von Nostrand Co., 429 pp.

Plate, E. J. and Cermak, J. E. (1963) Micro-Meteorological Wind Tunnel Facility: Description and Characteristics," Fluid Dynamics and Diffusion Laboratory Report CER63-ELP-JEC9, Colorado State University, Fort Collins, Colorado.

Schlichting, H. (1968) Boundary Layer Theory, McGraw-Hill, New York, New York.

Skinner, G. T. and Ludwig, G. R. (1978) "Physical Modeling of Dispersion in the Atmospheric Boundary Layer," Calspan Advanced Technology Center, Calspan Report No. 201, May.

Snyder, W. H. (1972) "Similarity Criteria for the Applicatio of Fluid Models to the Study of Air Pollution Meteorology," Boundary Layer Meteorology, Vol. 3, No. 1, September.

Snyder, W. H. (1981) Guideline for Fluid Modeling of Atmospheric Diffusion, U.S. Environmental Protection Agency Report EPA 600/8-81-009, 185 pp.

Van Ulden, A. P. (1974) "On the Spreading of a Heavy Gas Released Near the Ground," Loss Prevention and Safety Promotion Seminar, Delft, Netherlands, 6 pp.

Zoric, D. and Sandborn, V. A. (1972) "Similarity of Large Reynolds Number Boundary Layers," Boundary-Layer Meteorology, Vol. 2, No. 3, March, pp. 326-333.

Table 1. Summary of Tests and Results

Run Number[1]	Wind Direction (degree)	LNG Boiloff Area	Fence Height (m)	LNG Spill Rate (gpm)	LNG Spill Duration (minutes)	Wind Speed at 6.1 m (m/sec)	Concentration Value at Property Boundary Exceeded 5% Mean[2]	5% Peak	2.5% Mean	2.5% Peak	1% Mean[2]	Notes
1	315	P	2.44	7000	UL	4.46	N	N	N	Y	N	
2	315	P	4.88	7000	UL	4.46	N	N	N	N	N	
3	315	P	2.44	7000	UL	6.69	N	N	N	N	N	
4	315	P	4.88	7000	UL	6.69	N	N	N	N	N	
5	270	P	2.44	7000	UL	4.46	N	N	N	Y	N	
6	270	P	4.88	7000	UL	4.46	N	N	N	Y	Y	
7	270	P	2.44	7000	UL	6.69	N	N	N	Y	Y	
8	270	P	4.88	7000	UL	6.69	N	N	N	N	Y	
9	215	P	2.44	7000	UL	4.46	N	Y	Y	Y	Y	See Run 10
10	215	P	4.88	7000	UL	4.46	N	N	Y	Y	Y	See Run 42
11	215	P	2.44	7000	UL	6.69	N	Y	Y	Y	Y	See Run 12
12	215	P	4.88	7000	UL	6.69	N	N	N	Y	Y	
13	315	D	2.44	7000	UL	4.46	N	N	N	N	N	
14	315	D	4.88	7000	UL	4.46	N	N	N	N	N	
15	315	D	2.44	7000	UL	6.69	N	N	N	N	Y	
16	315	D	4.88	7000	UL	6.69	N	N	N	N	Y	
17	270	D	2.44	7000	UL	4.46	N	N	N	N	Y	
18	270	D	4.88	7000	UL	4.46	N	N	N	N	Y	
19	270	D	2.44	7000	UL	6.69	N	N	N	N	Y	
20	270	D	4.88	7000	UL	6.69	N	N	N	N	Y	
21	215	D	2.44	7000	UL	4.46	N	N	N	N	N	
23	215	D	2.44	7000	UL	6.69	N	N	N	N	Y	
31	215	P*	2.44	7000	UL	4.46	N	Y	Y	Y	Y	See Run 32
32	215	P*	4.88	7000	UL	4.46	N	N	N	Y	Y	
33	215	P*	4.88	7000	UL	2.90	N	Y	Y	Y	Y	See Run 34
34	215	P*	7.32	7000	UL	2.90	N	N	Y	Y	Y	See Run 36
36	215	P*	4.88	7000	10.0	2.90	N	N	N	Y	Y	
39	215	P*/2	4.88	7000	UL	2.90	N	Y	Y	Y	Y	See Run 40
40	215	P*/2	4.88	7000	10.0	2.90	N	N	N	Y	Y	
41□	215	P*/2	4.88	7000	UL	4.46	N	Y	Y	Y	Y	See Run 42
42□	215	P*/2	4.88	7000	10.0	4.46	N	N	N	Y	Y	
43	270	D/2	4.88	7000	UL	2.90	N	N	N	Y	Y	
44	215	D/2	4.88	7000	UL	2.90	N	N	N	Y	Y	
45	315	P*/2	4.88	7000	UL	2.90	N	N	N	Y	Y	
46	215	D/2	4.88	3500	UL	2.90	N	N	N	N	Y	
47	215	P*/2	4.88	3500	UL	2.90	N	N	N	Y	Y	
48	270	D/2	4.88	3500	UL	2.90	N	N	N	Y	Y	
49	270	P*/2	4.88	3500	UL	2.90	N	N	N	Y	Y	
50	315	D/2	4.88	3500	UL	2.90	N	N	N	N	Y	
51	315	P*/2	4.88	3500	UL	2.90	N	N	N	N	Y	

□ = Runs performed with approach velocity profile having smooth floor characteristics.
UL = Unlimited time duration i.e. continuous boiloff at spill rate of 7000 gpm or 3500 gpm.
P = LNG Boiloff onto 100% process area (see Figure 16).
D = LNG Boiloff onto 100% process area (see Figure 16).
P* = LNG Boiloff onto slightly reduced process area (see Figure 17).
P* = LNG Boiloff onto half of P* area (see Figure 18).
D/2 = LNG Boiloff onto half of D area (see Figure 18).
All runs performed with neutral stability.

Y = Yes
N = No

[1] Run numbers are not consecutive, numbers were determined by computer storage location available at the test time, all experiments performed are listed below.

[2] "Mean" signifies a time average of 10 minutes.

Table 2. Comparison of Prototype and Model Conditions

Characteristics		Prototype Conditions	Model Conditions
Tank Diameter, D	(m)	40.97	0.164
Release Volume Rate, $\forall_{LNG}$	(gallons/min)	7000,3500	-
, $\forall_{LNG}$	(m^3/sec)	0.442,0.221	-
, $\forall_{NG}$	(m^3/sec)	101.66,50.83	85.4×10^{-6}, 42.7×10^{-6}
Spill Duration		Continuous, 10 minutes	Continuous, 45.6 sec
Specific Gravity of Source Gas		1.55 at boiloff temperature	1.38 at room temperature (~27°C)
Wind Speed (U) at 6.1 m	(m/sec)	6.69,4.46,2.90	.35,.235,.153
Stability		D	D
Density ratio, $(\frac{\rho_{NG}-\rho_{air}}{\rho_{air}})$		0.55	0.38
Reynolds number $\frac{UD}{\nu}$ at 6.1 m		1.96×10^7, 1.37×10^7, 8.49×10^6	4.1×10^3, 2.8×10^3, 1.76×10^3
Froude number $\frac{U^2}{g\frac{\Delta\rho}{\rho}D}$ at 6.1 m		2.0×10^{-1}, 9.0×10^{-2}, 3.8×10^{-2}	2.0×10^{-1}, 9.0×10^{-2}, 3.8×10^{-2}
Length scale 1:250			
$\nu = 0.14 \times 10^{-4}$ m^2/sec			

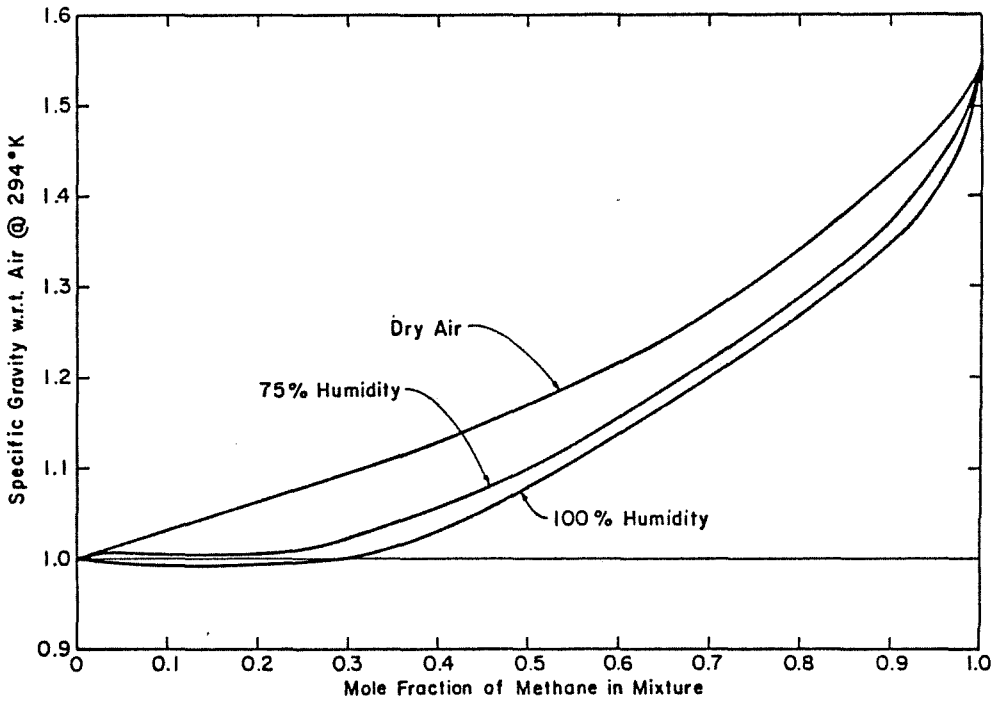

Figure 1. Specific Gravity of LNG Vapor-Humid Atmospheric Mixtures

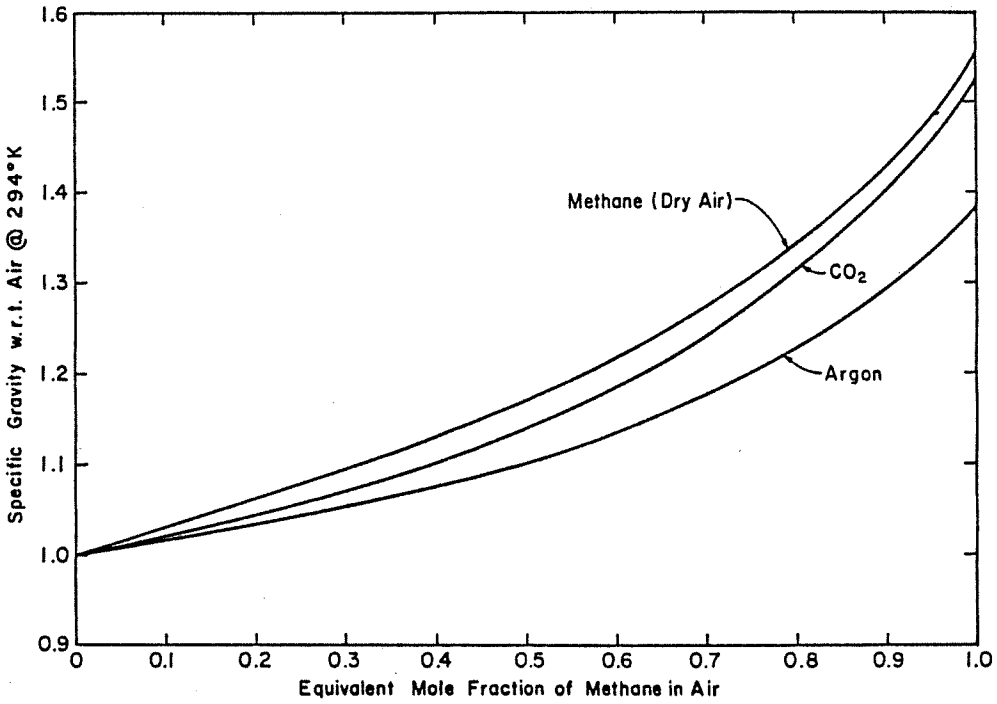

Figure 2. Specific Gravity of Gas-Air Mixtures

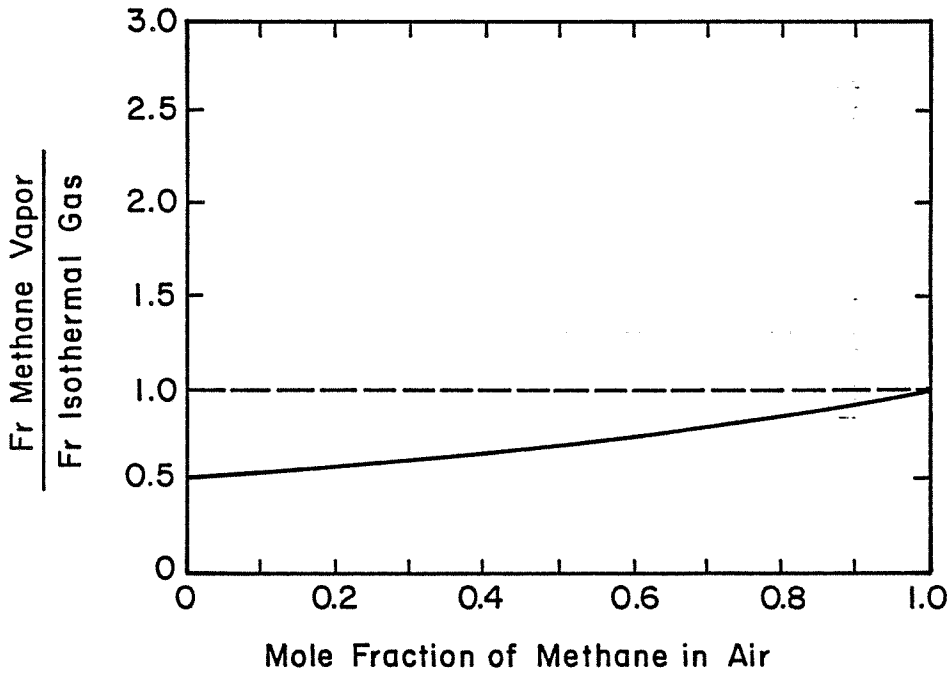

Figure 3. Variation of Froude Number for Gas-Air Mixtures

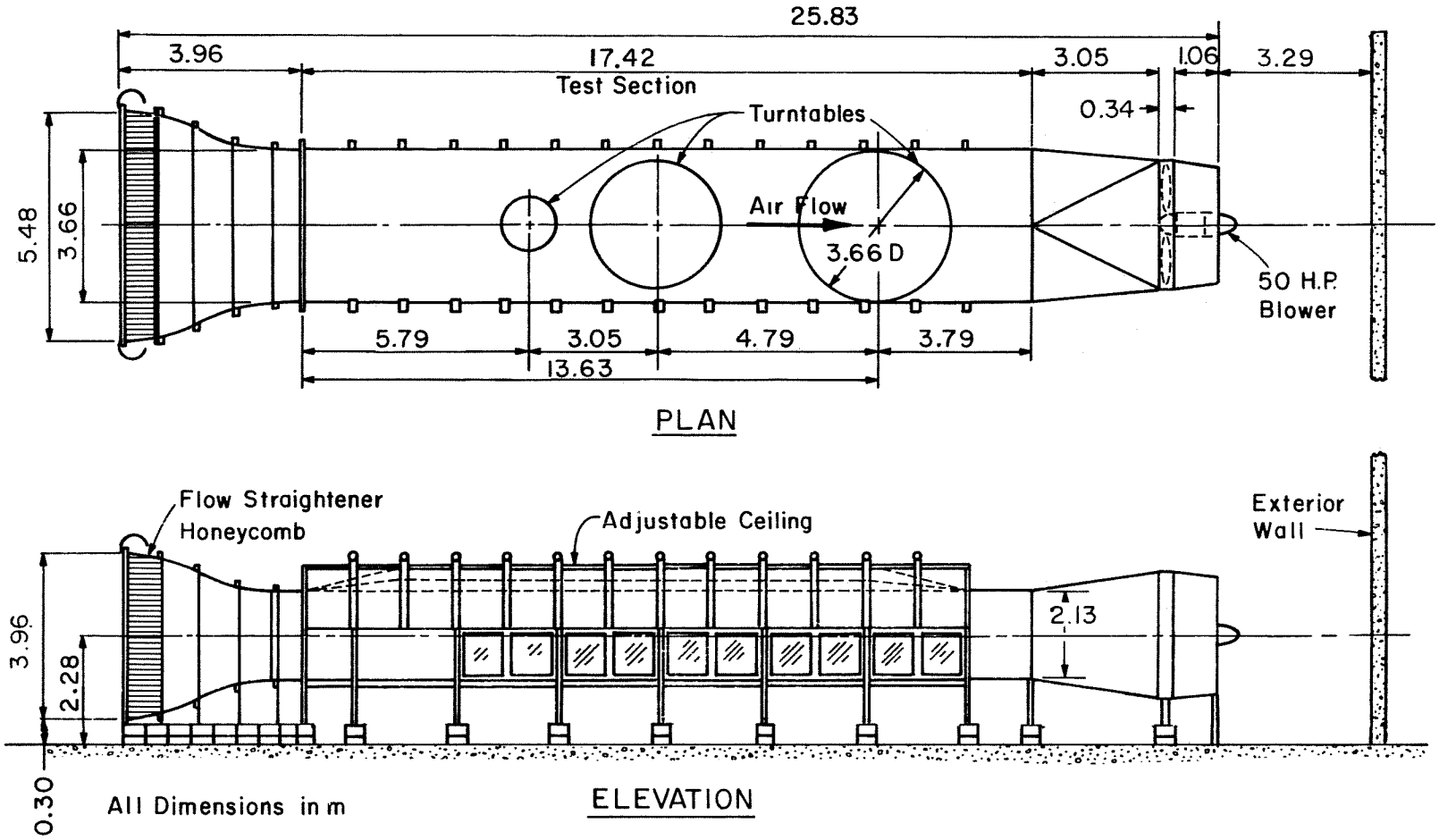

ENVIRONMENTAL WIND TUNNEL

Figure 4. FLUID DYNAMICS & DIFFUSION LABORATORY
COLORADO STATE UNIVERSITY

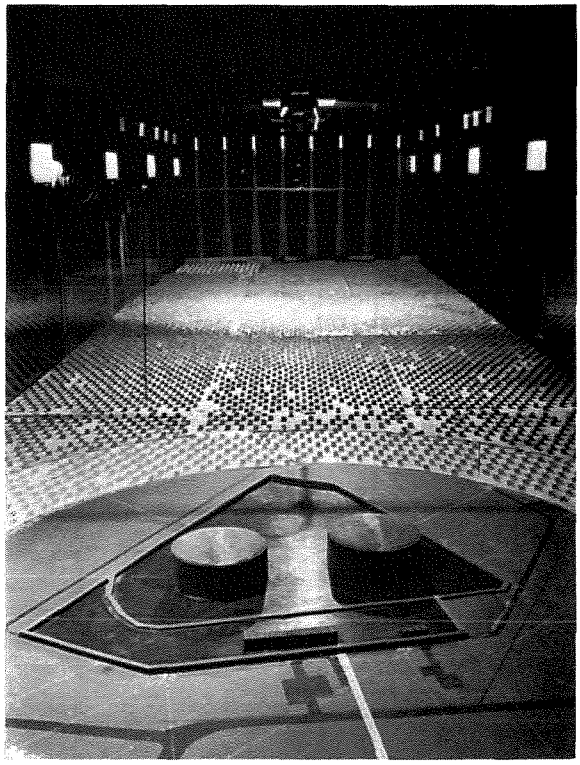

Figure 5. Energy Terminal Service Corporation Model in the Environmental Wind Tunnel

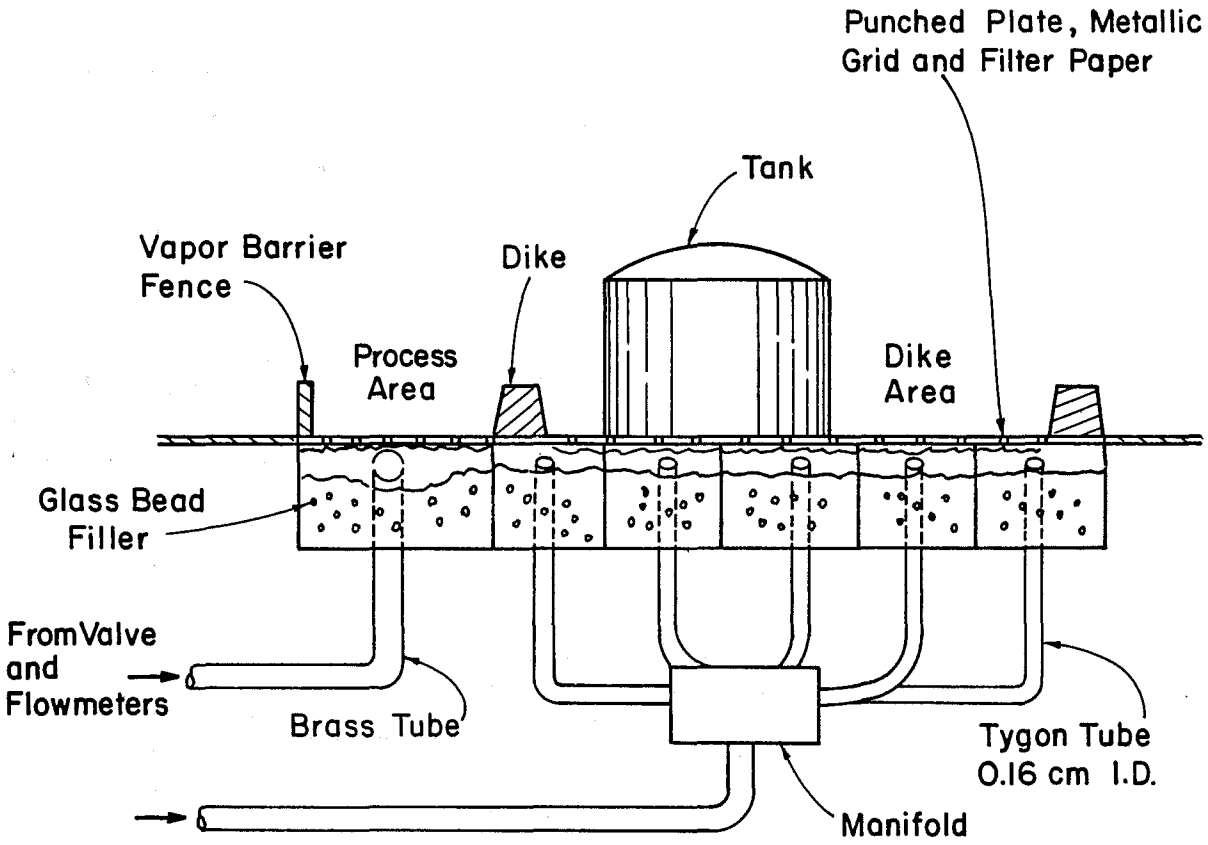

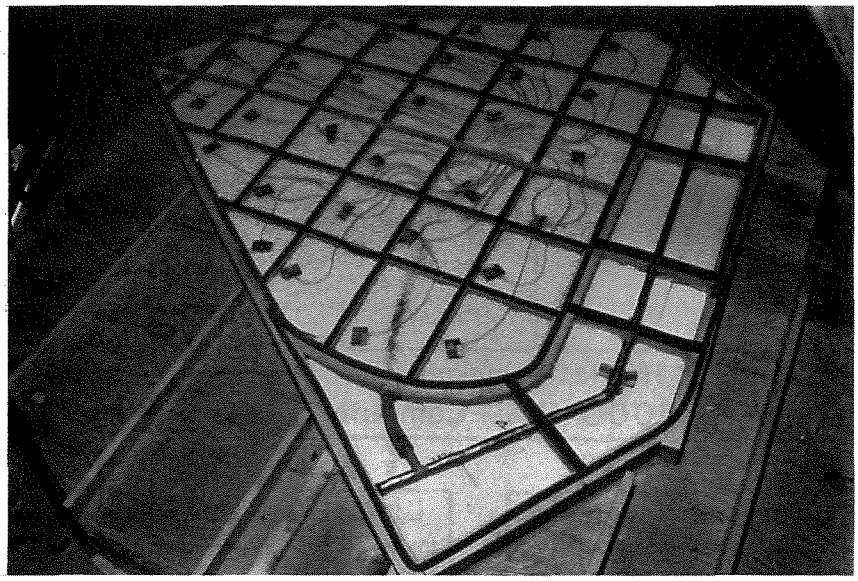

Figure 6. Argon Release Area under Energy Terminal Service Corporation Model

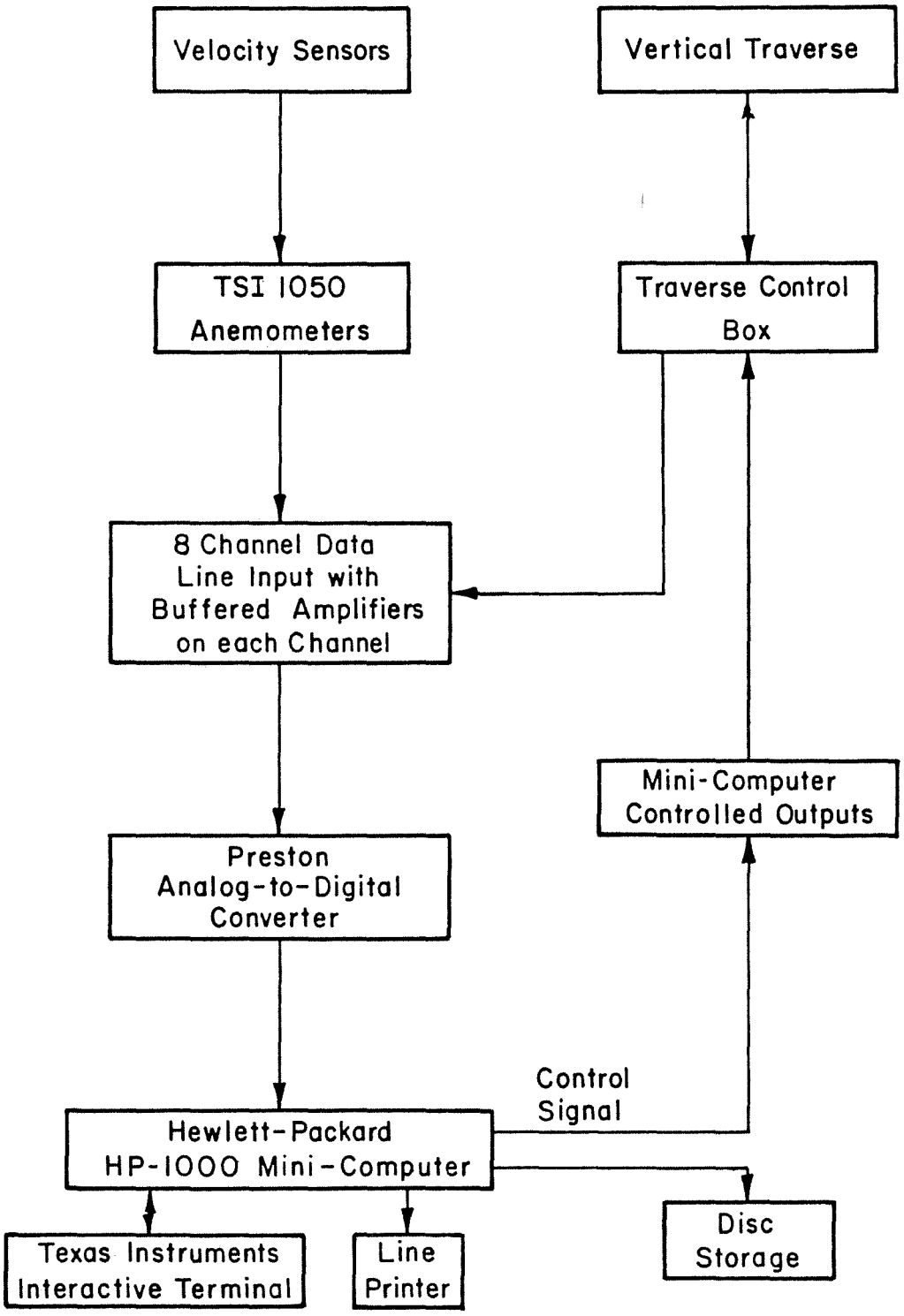

Figure 7. Velocity Data Reduction Flow Chart

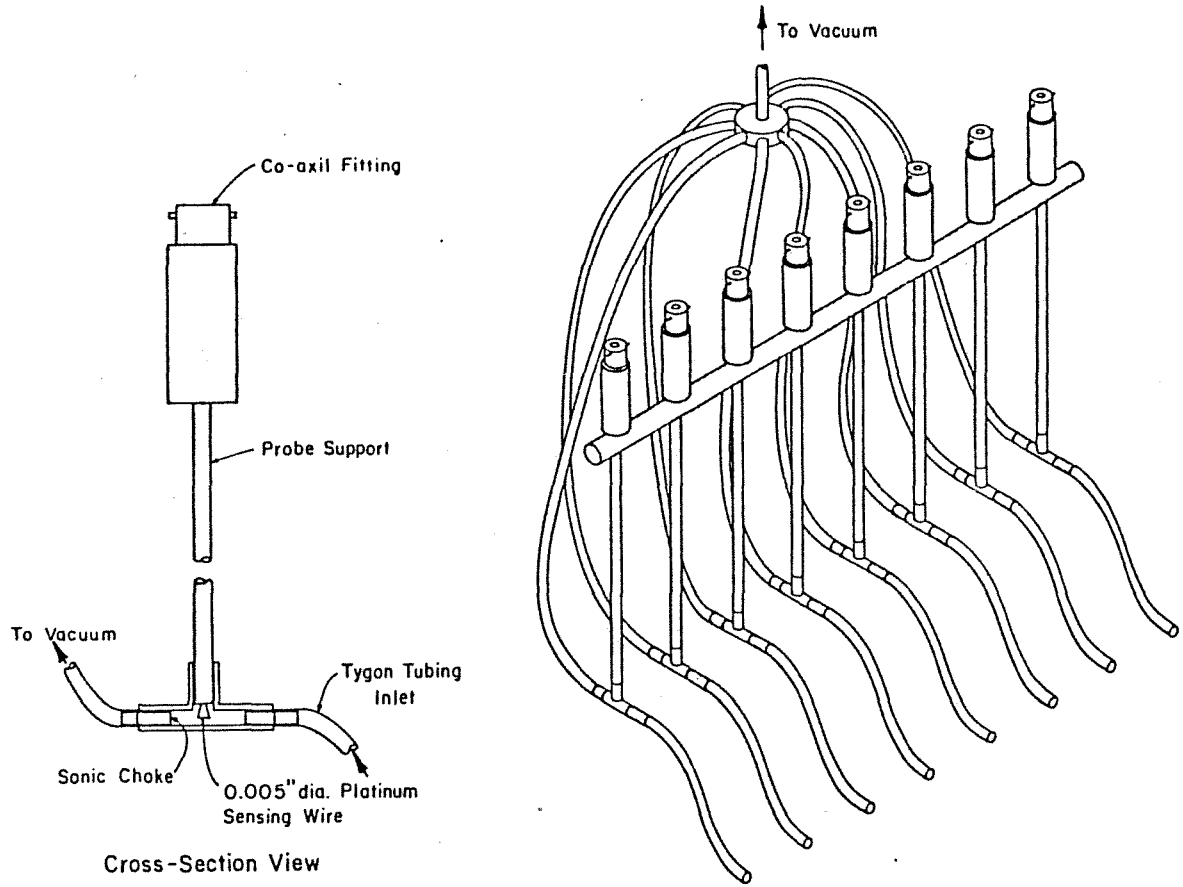

Figure 8. Schematic of the Aspirated Probe

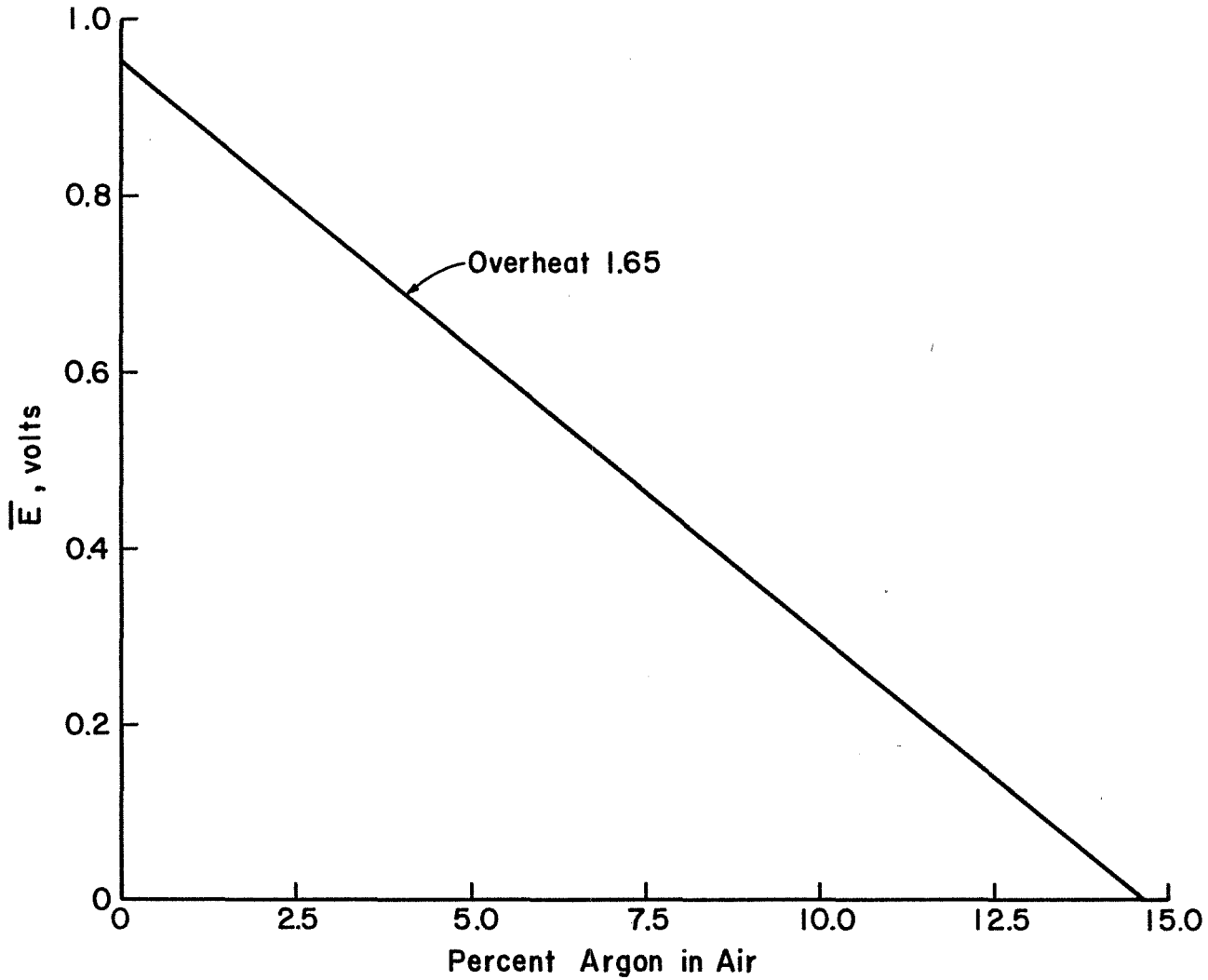

Figure 9. Typical Response of the Hot Wire Aspirated Probe

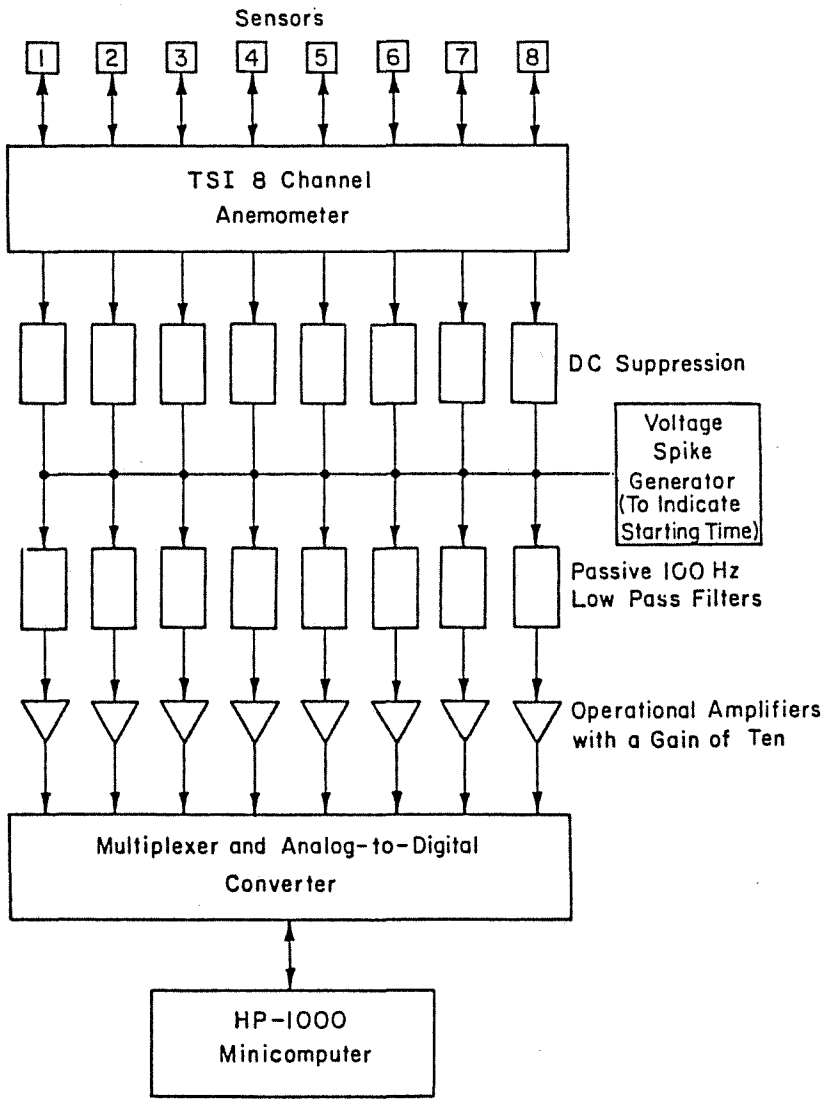

Figure 10. Schematic of the Concentration Measurement System

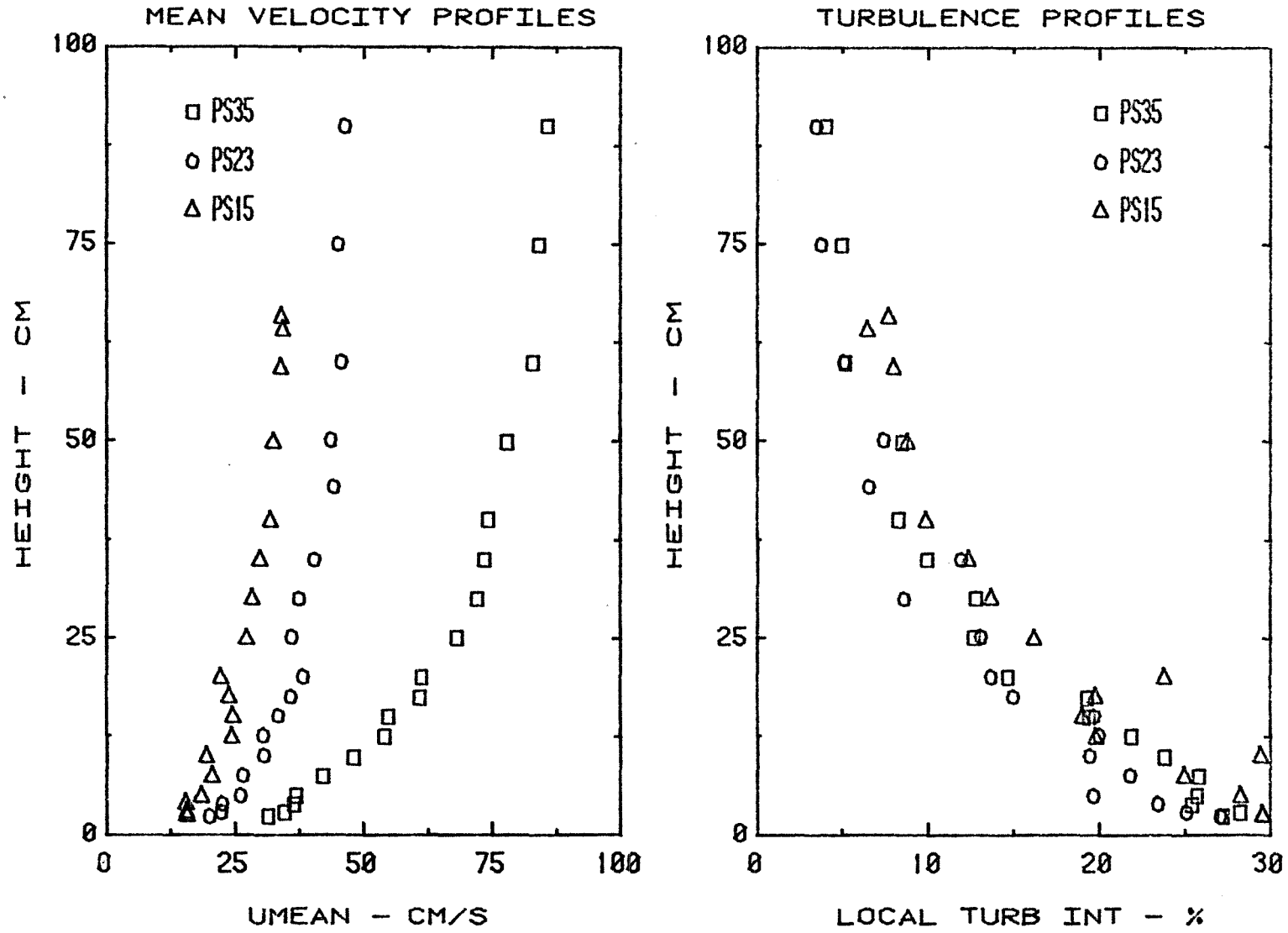

Figure 11. Velocity and Turbulence Profiles for Neutral Flow with Surface Roughness

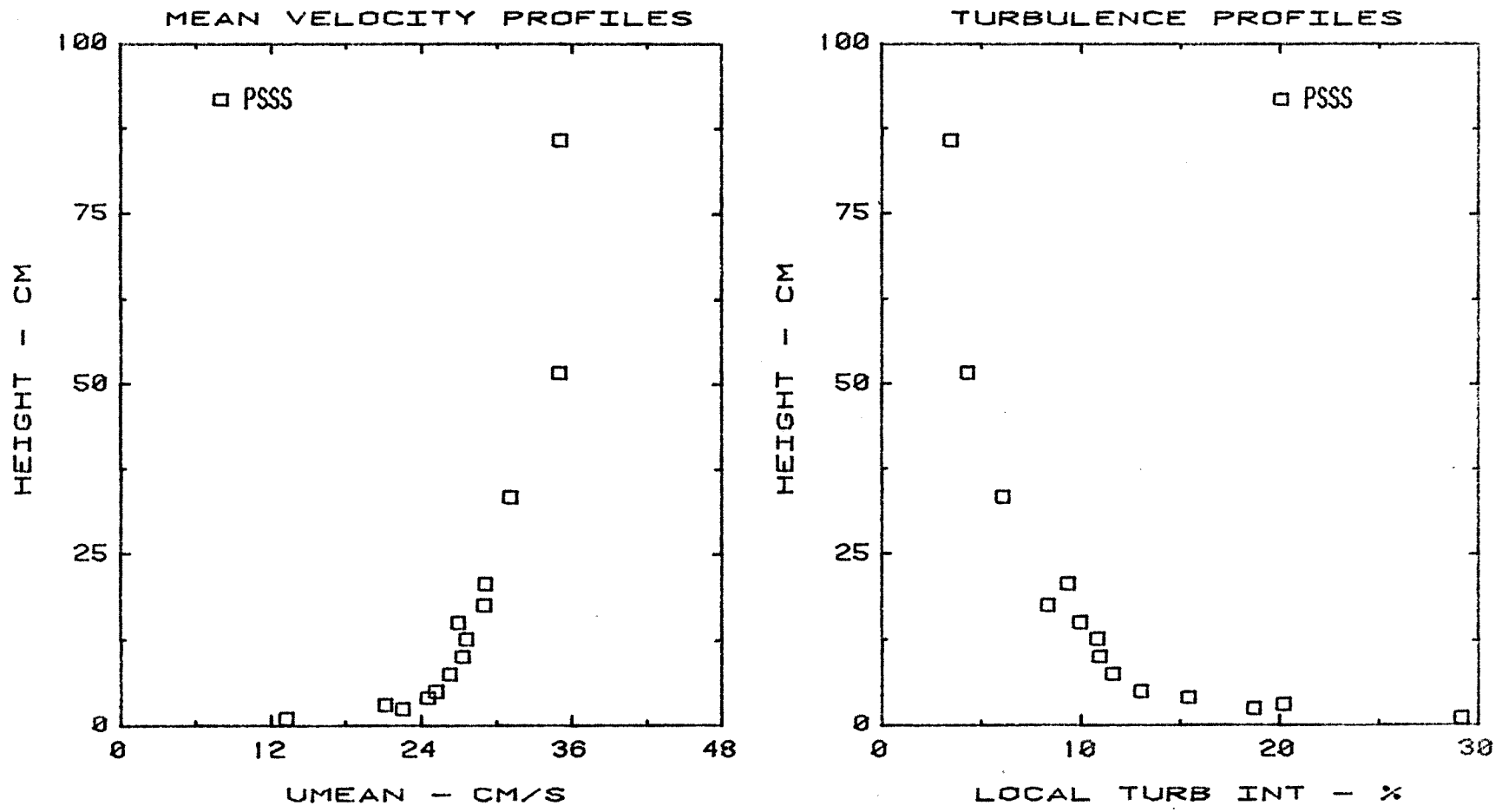

Figure 12. Velocity and Turbulence Profiles for Neutral Flow with Smooth Floor

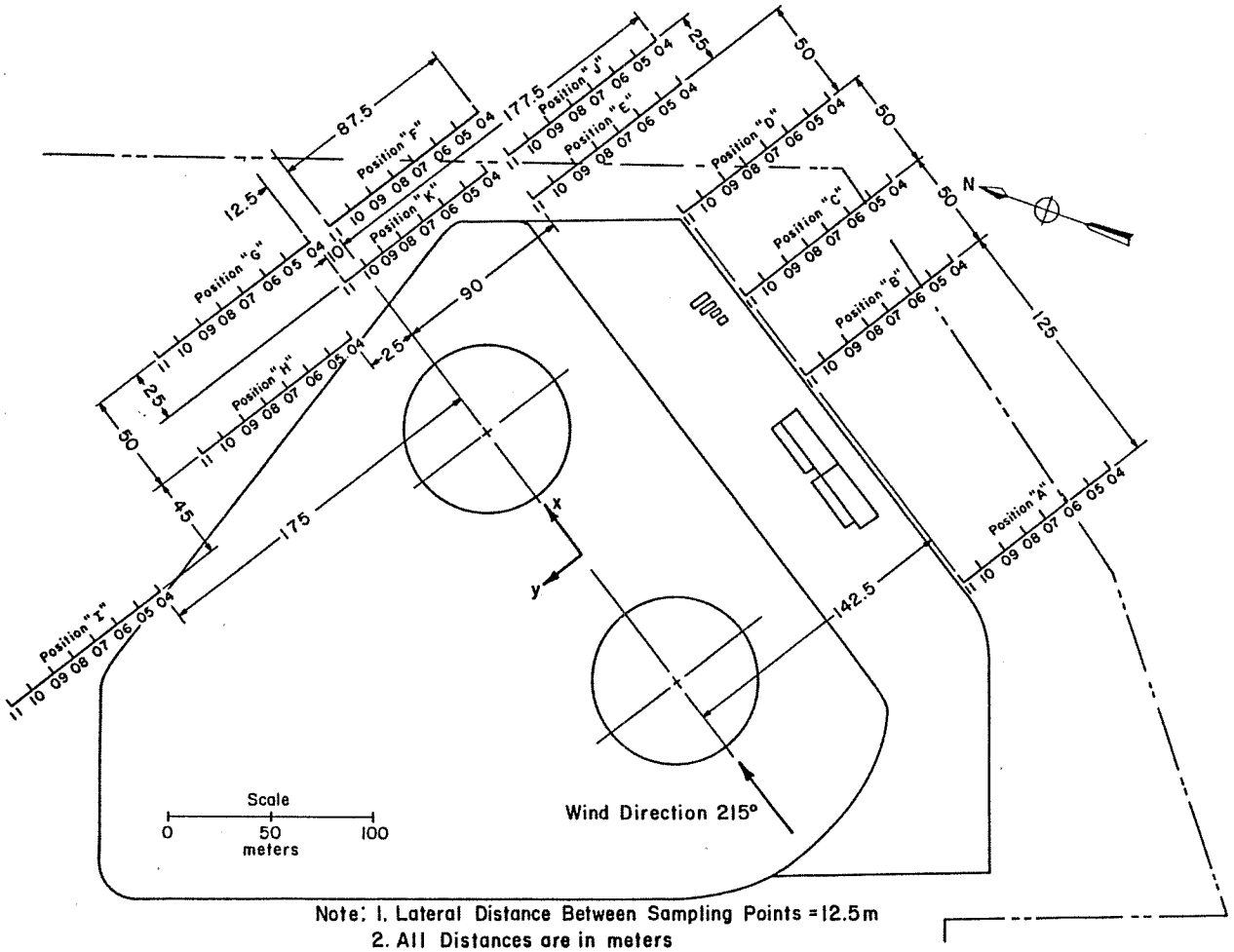

Figure 13. Concentration Measurement Locations for Wind Direction of 215°

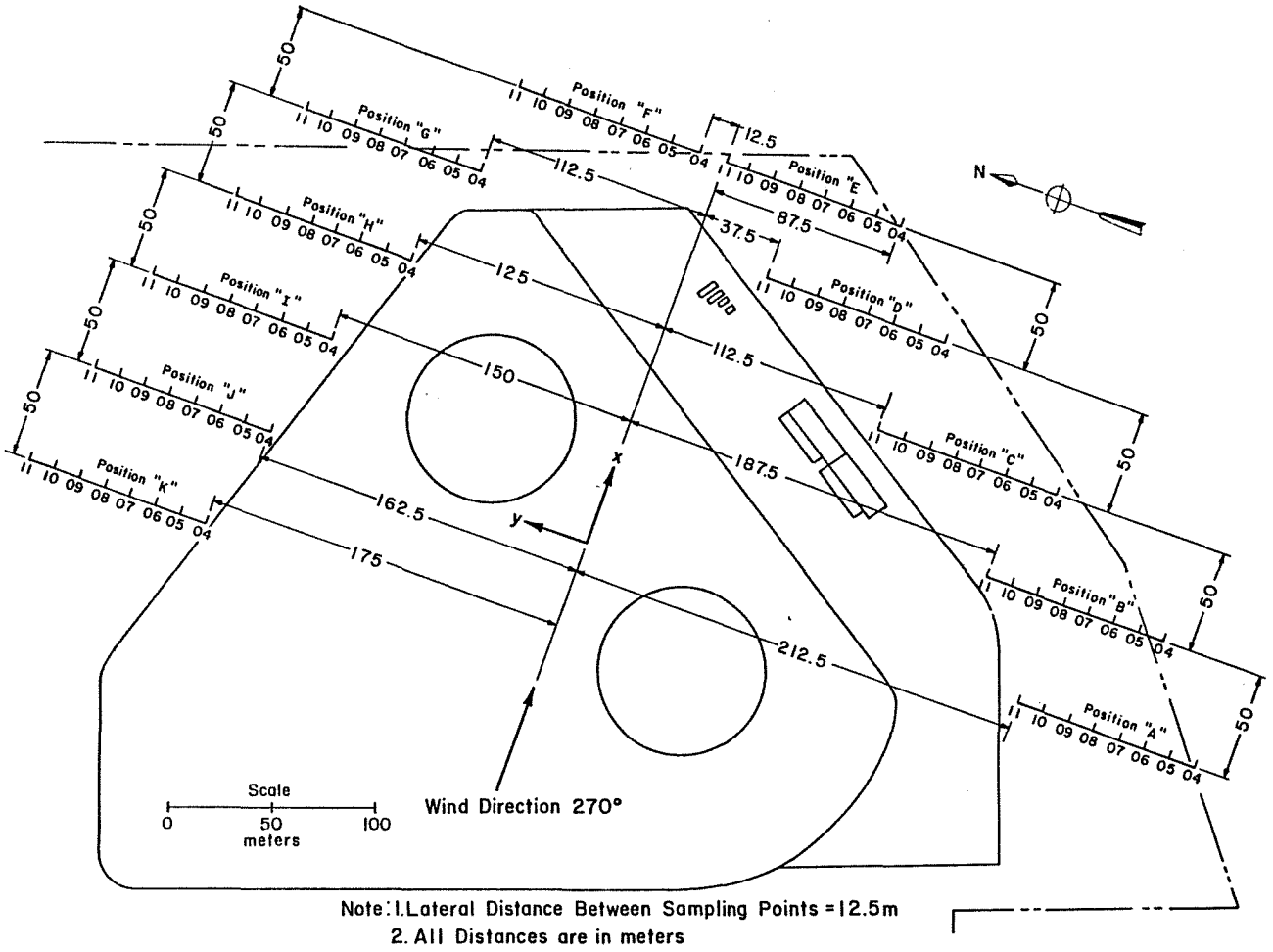

Figure 14. Concentration Measurement Locations for Wind Direction of 270°

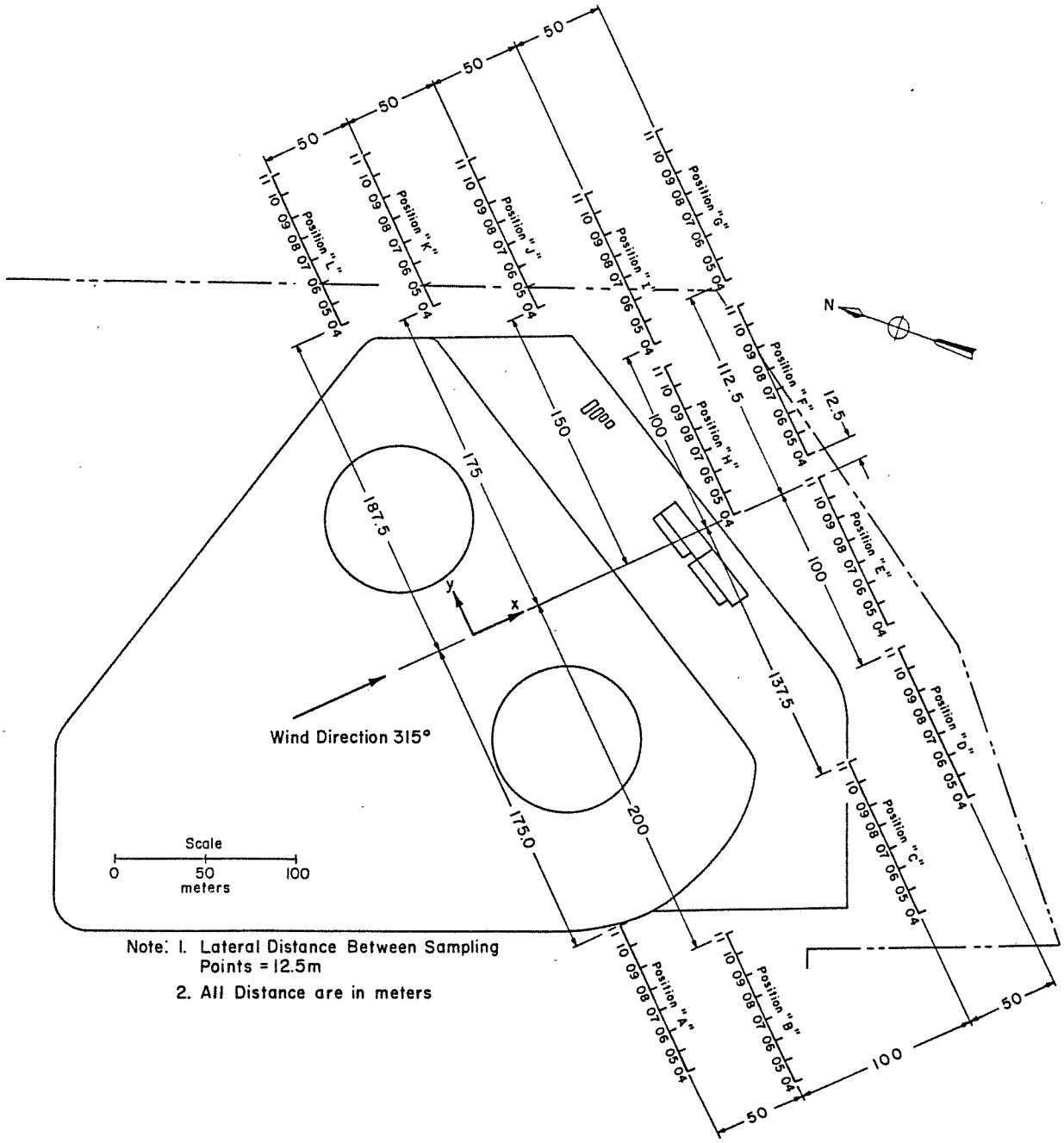

Figure 15. Concentration Measurement Locations for Wind Direction of 315°

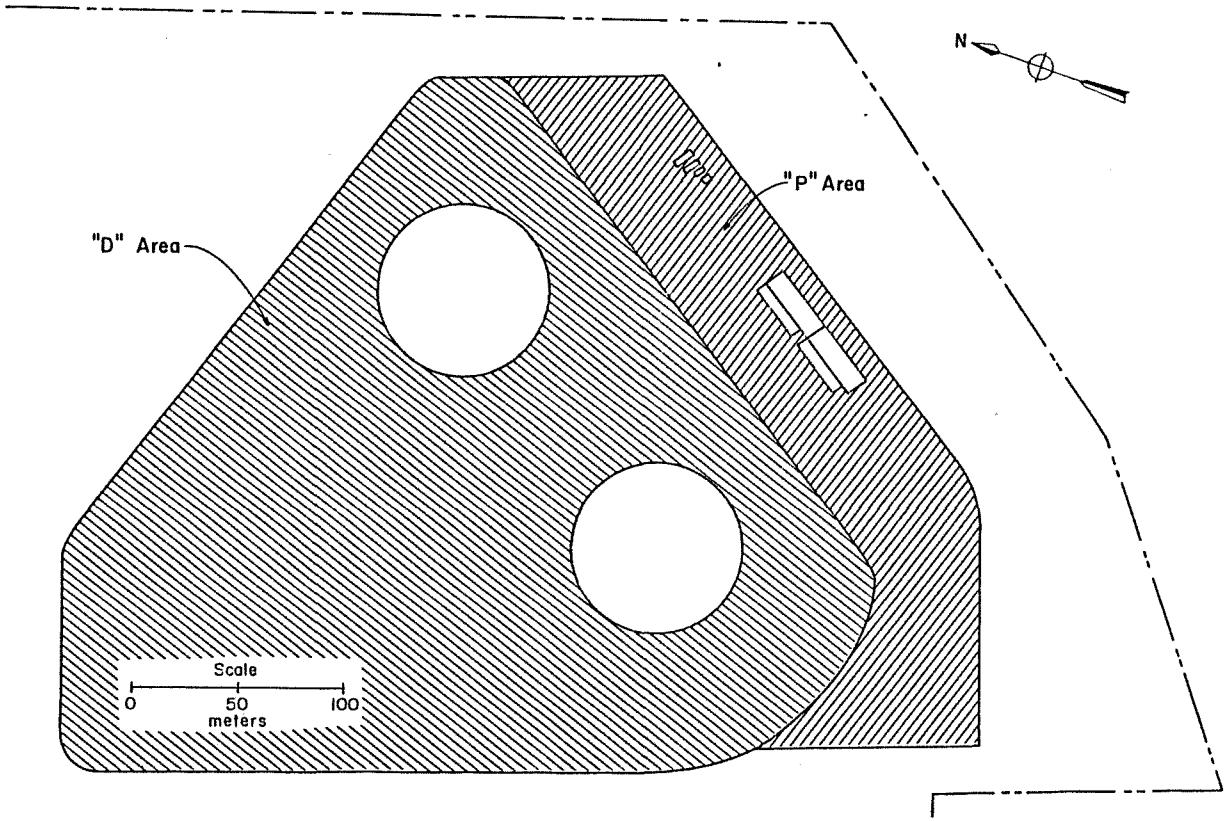

Figure 16. LNG Release Areas "P" and "D"

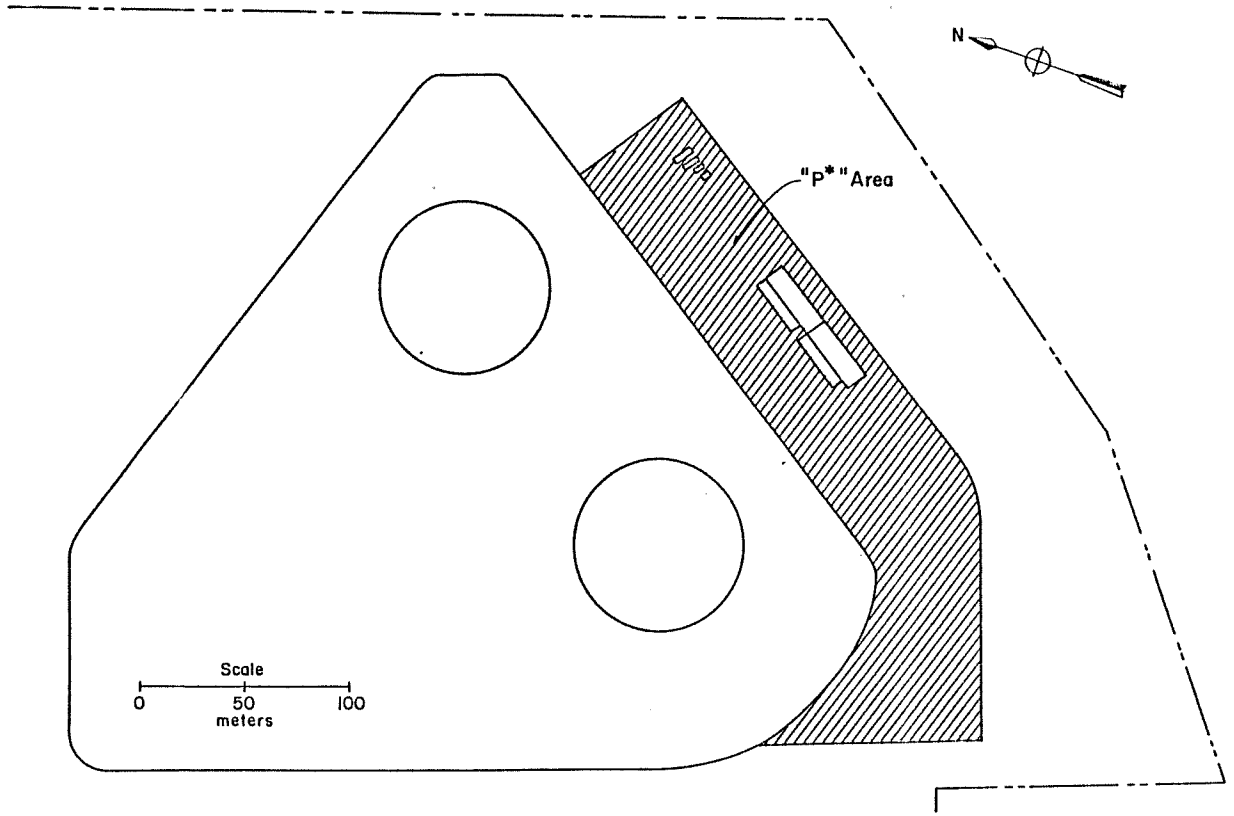

Figure 17. LNG Release Area "P*"

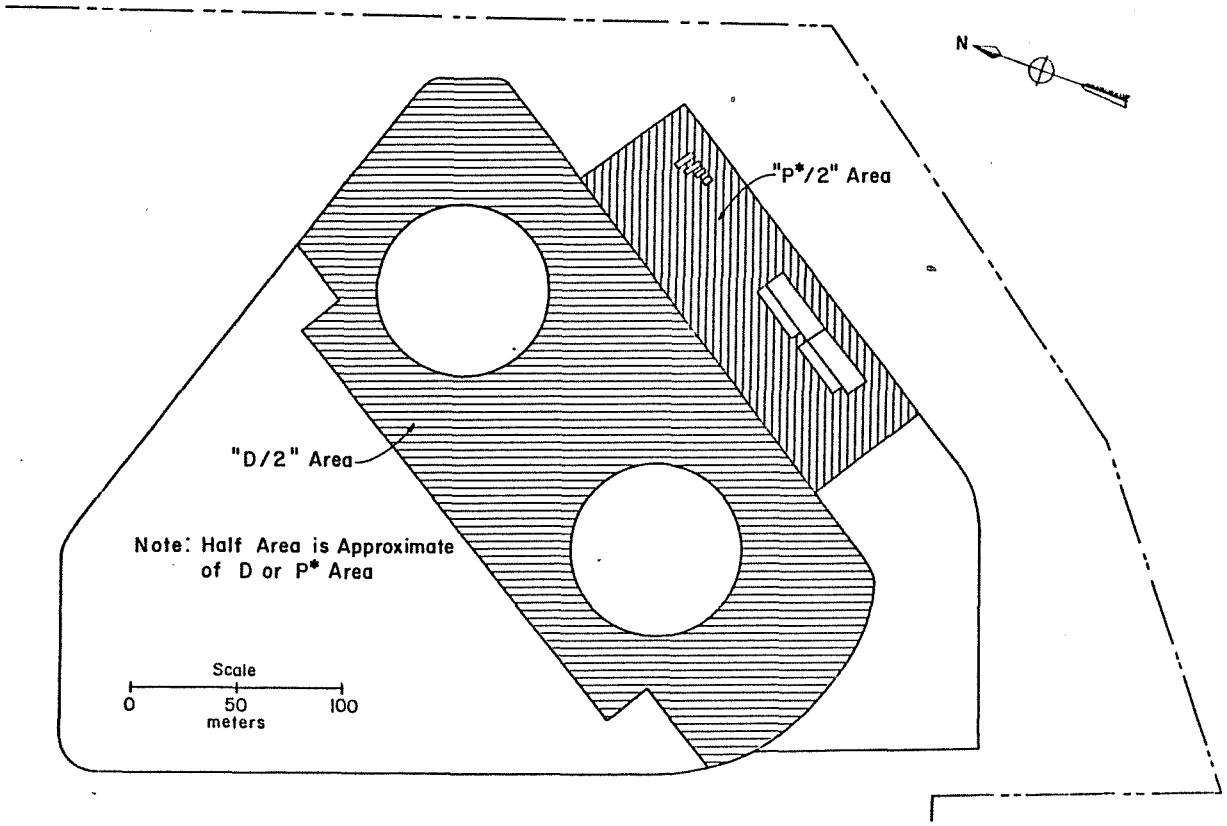

Figure 18. LNG Release Area "P*/2" and "D/2"

Run #1
Wind Direction 315°
LNG Boiloff Area P
Fence Height 2.44 m (8.0 ft)
LNG Spill Rate 7000 gpm for
Unlimited Time Duration
Wind Speed 4.46 m/sec (10 mph)
at 6.1 m Height

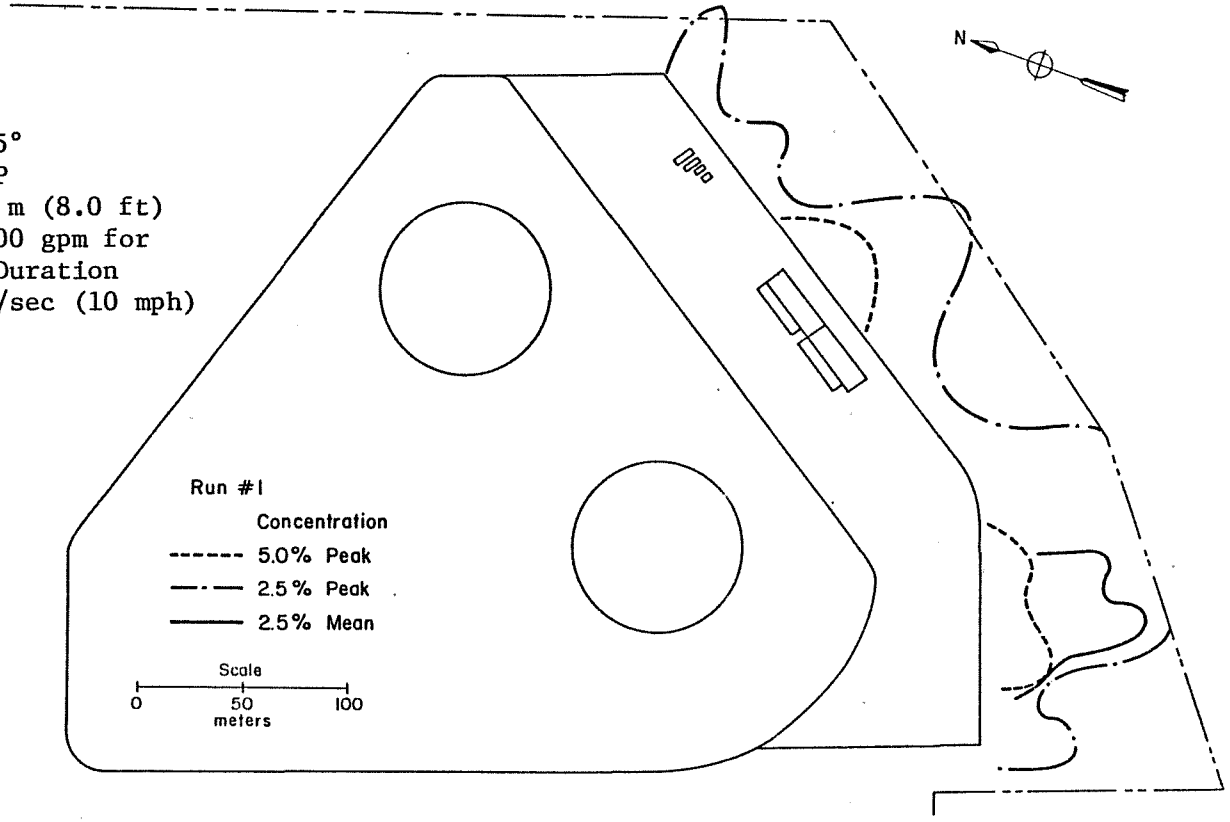

Figure 19. Concentration Isopleths

Run #2
Wind Direction 315°
LNG Boiloff Area P
Fence Height 4.88 m (16.0 ft)
LNG Spill Rate 7000 gpm for
Unlimited Time Duration
Wind Speed 4.46 m/sec (10 mph)
at 6.1 m Height

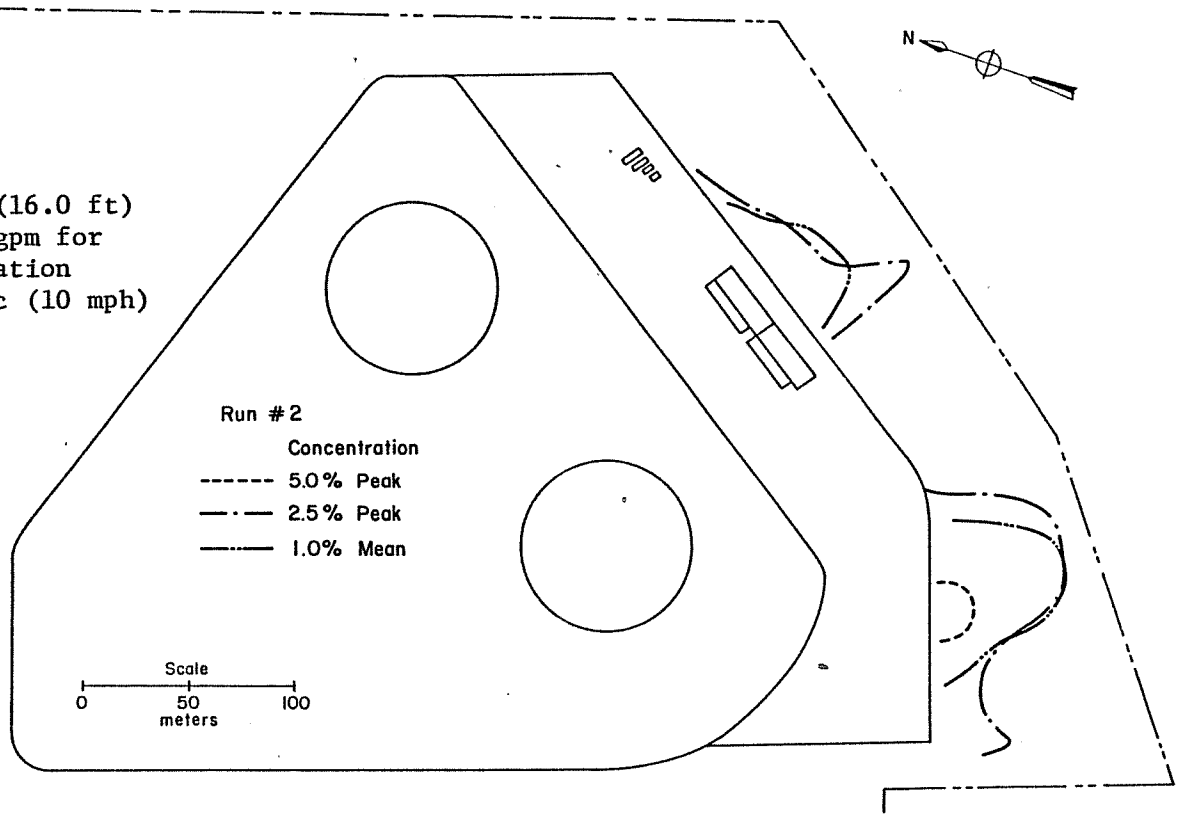

Figure 20. Concentration Isopleths

Run #3
Wind Direction 315°
LNG Boiloff Area P
Fence Height 2.44 m (8.0 ft)
LNG Spill Rate 7000 gpm for
Unlimited Time Duration
Wind Speed 6.69 m/sec (15 mph)
at 6.1 m Height

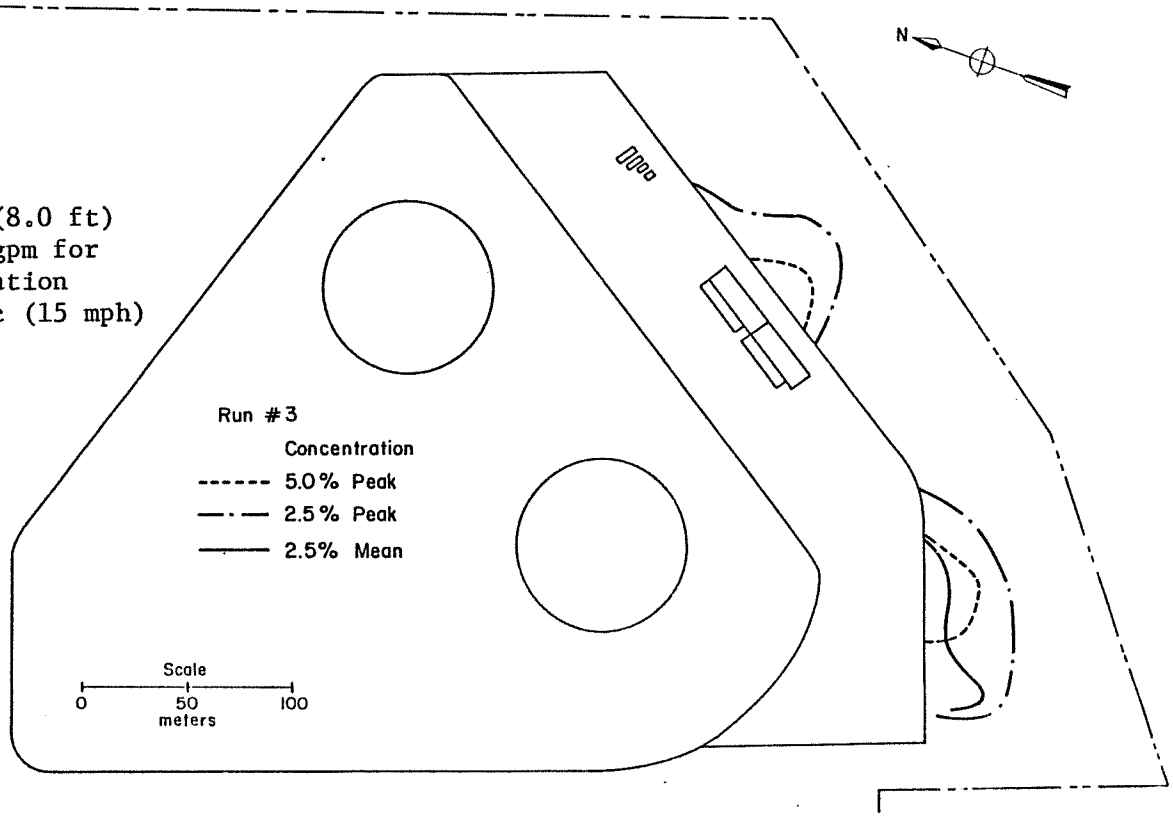

Figure 21. Concentration Isopleths

Run #4
Wind Direction 315°
LNG Boiloff Area P
Fence Height 4.88 m (16.0 ft)
LNG Spill Rate 7000 gpm for
Unlimited Time Duration
Wind Speed 6.69 m/sec (15 mph)
at 6.1 m Height

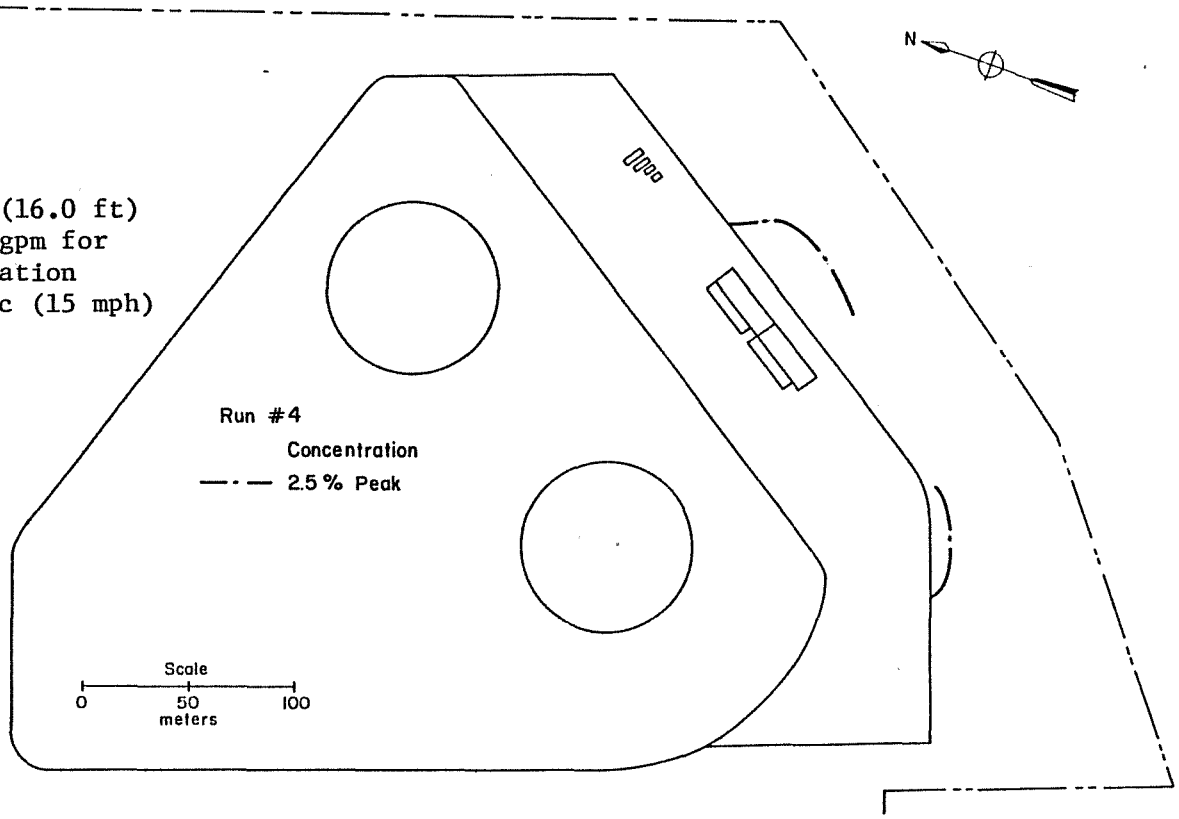

Figure 22. Concentration Isopleths

Run #5
Wind Direction 270°
LNG Boiloff Area P
Fence Height 2.44 m (8.0 ft)
LNG Spill Rate 7000 gpm for
Unlimited Time Duration
Wind Speed 4.46 m/sec (10 mph)
at 6.1 m Height

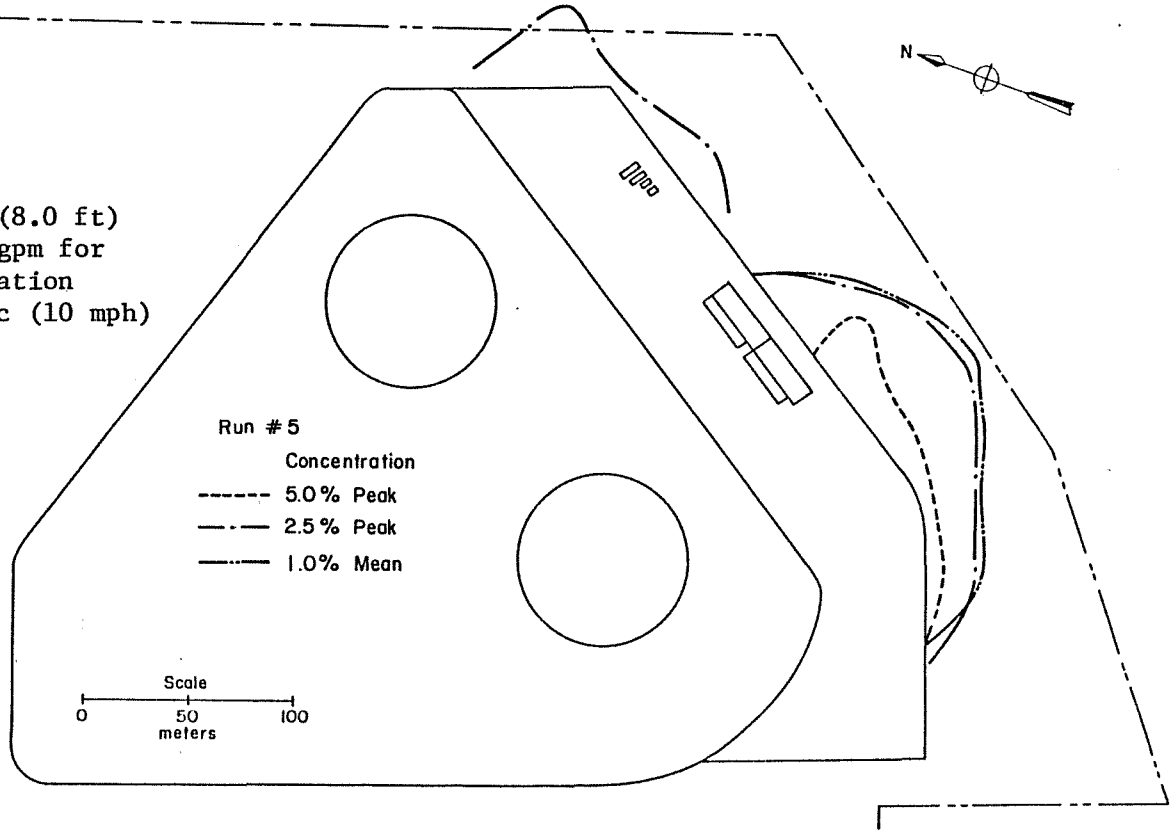

Figure 23. Concentration Isopleths

Run #6
Wind Direction 270°
LNG Boiloff Area P
Fence Height 4.88 m (16.0 ft)
LNG Spill Rate 7000 gpm for
Unlimited Time Duration
Wind Speed 4.46 m/sec (10 mph)
at 6.1 m Height

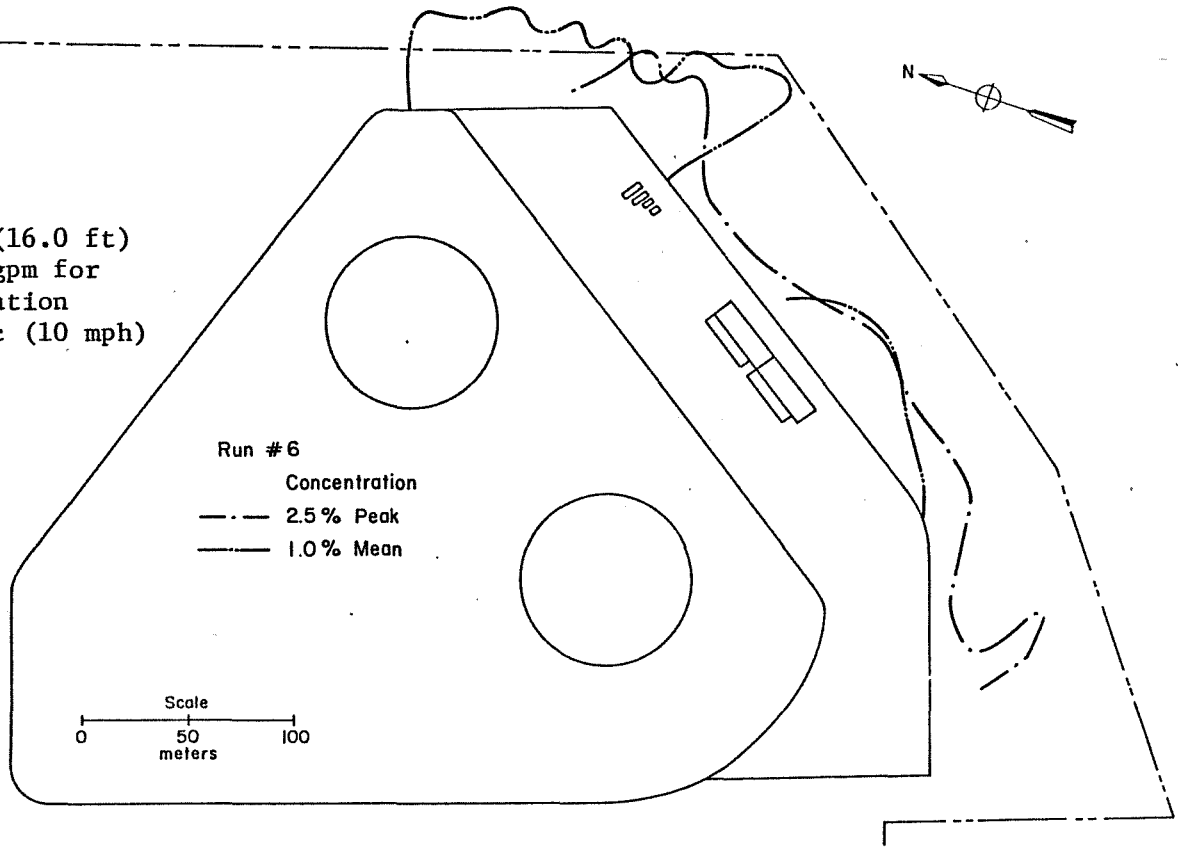

Figure 24. Concentration Isopleths

Run #7
Wind Direction 270°
LNG Boiloff Area P
Fence Height 2.44 m (8.0 ft)
LNG Spill Rate 7000 gpm for
Unlimited Time Duration
Wind Speed 6.69 m/sec (15 mph)
at 6.1 m Height

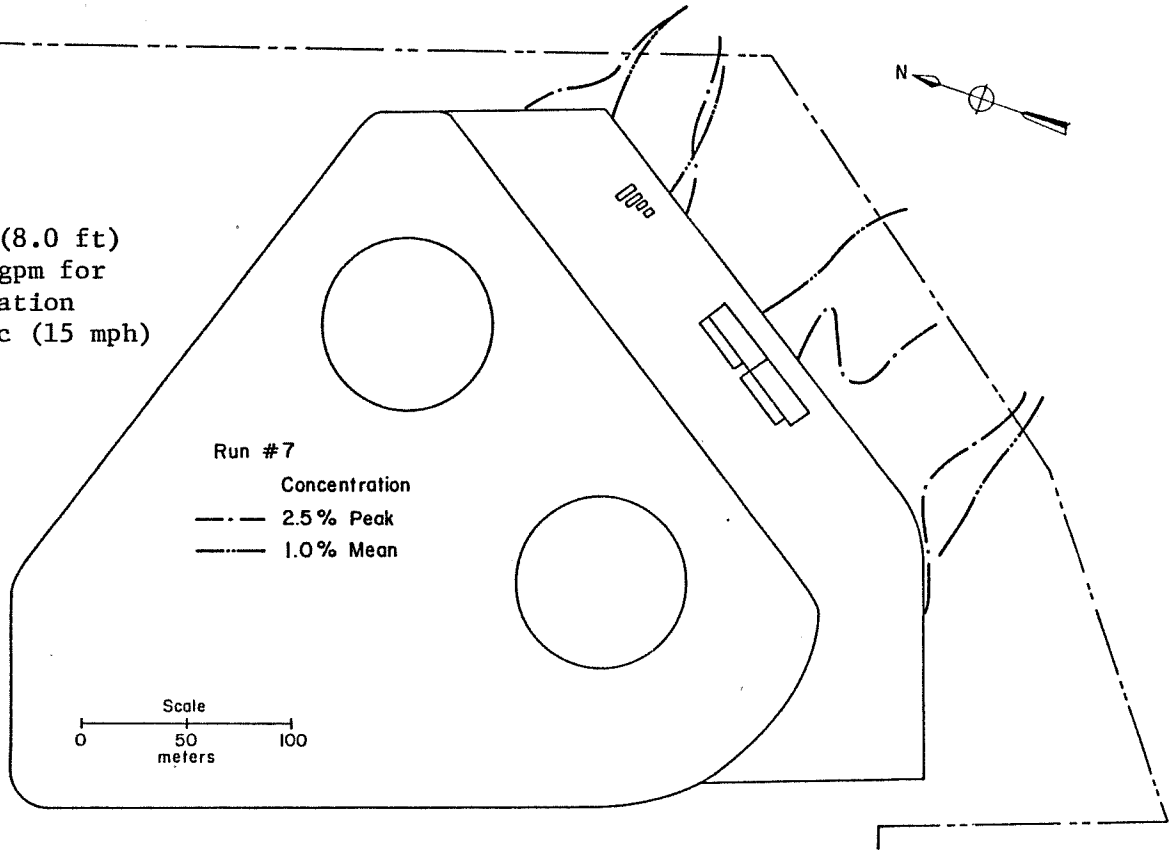

Figure 25. Concentration Isopleths

Run #8
Wind Direction 270°
LNG Boiloff Area P
Fence Height 4.88 m (16.0 ft)
LNG Spill Rate 7000 gpm for
Unlimited Time Duration
Wind Speed 6.69 m/sec (15 mph)
at 6.1 m Height

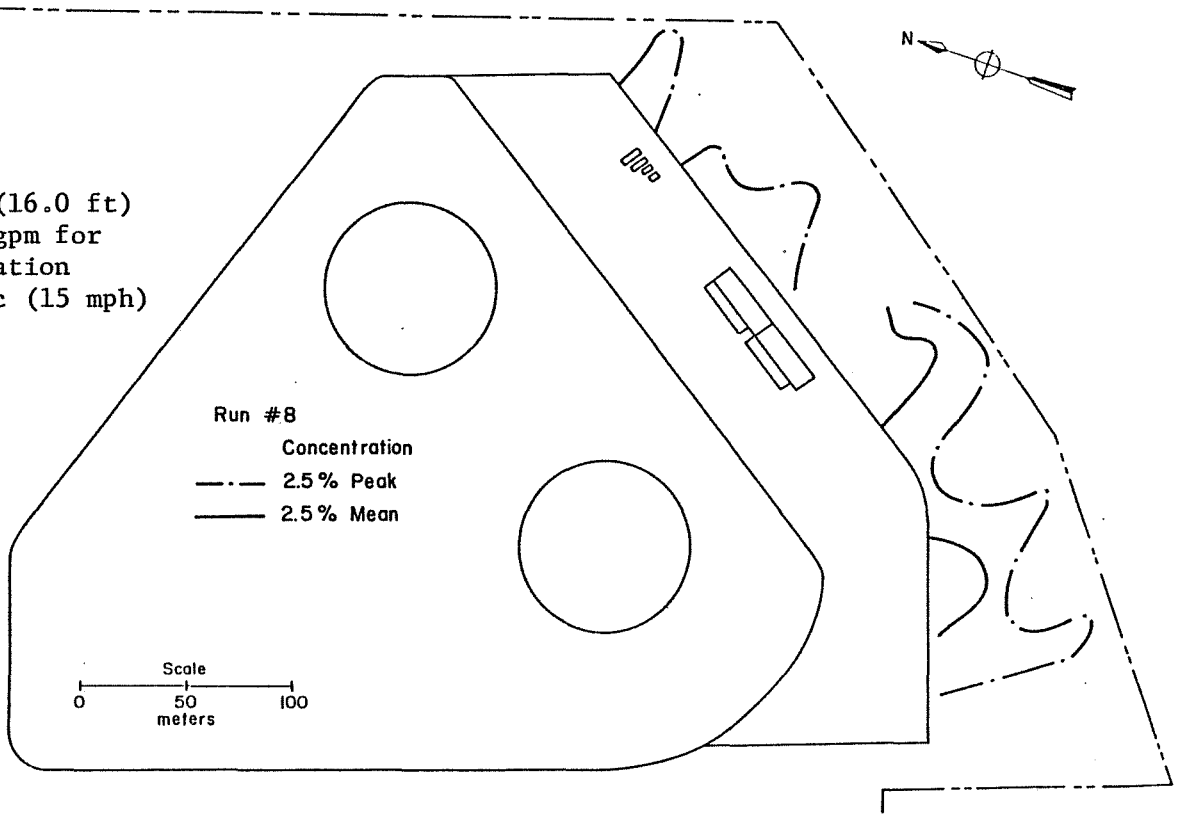

Figure 26. Concentration Isopleths

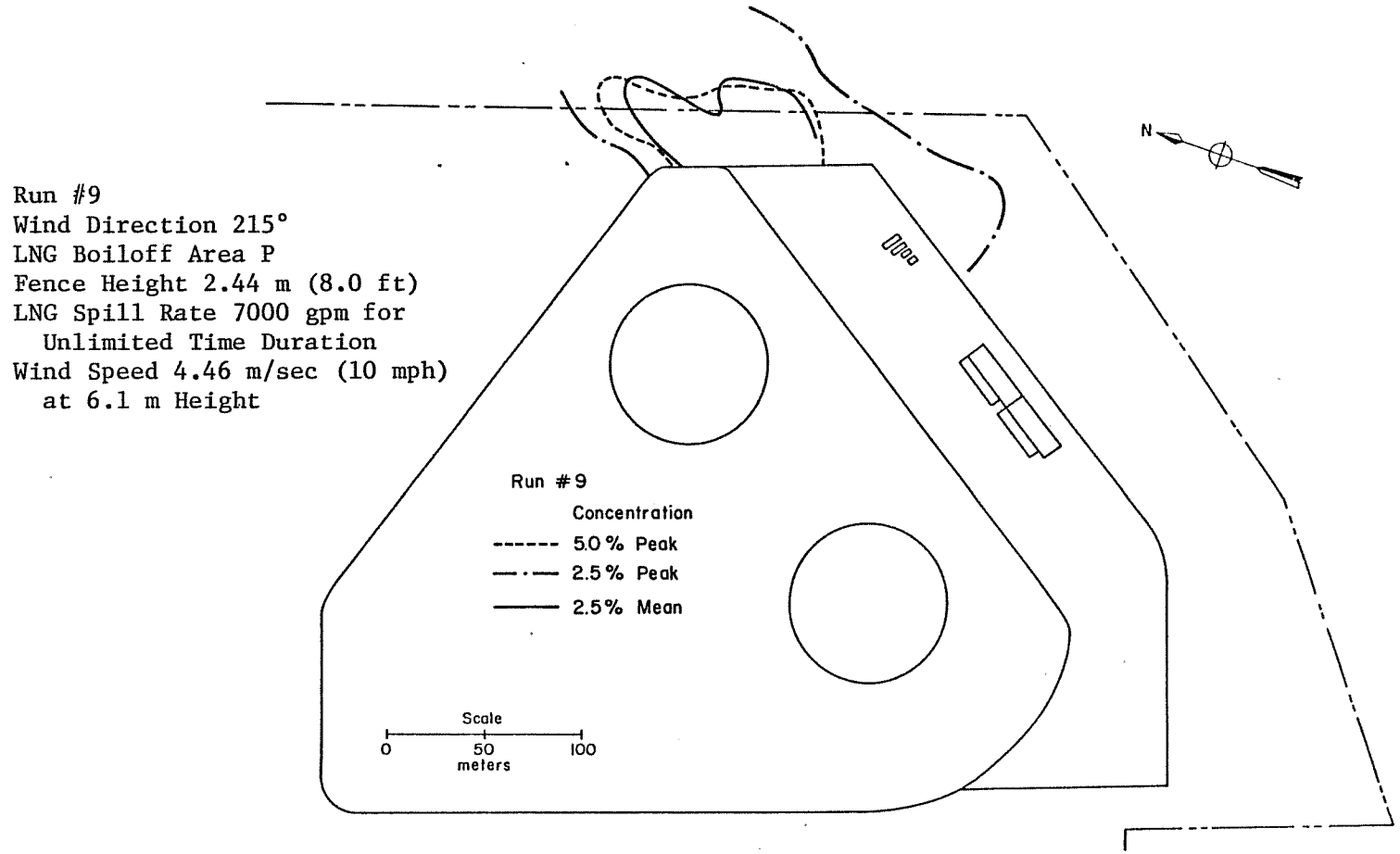

Figure 27. Concentration Isopleths

Run #10
Wind Direction 215°
LNG Boiloff Area P
Fence Height 4.88 m (16.0 ft)
LNG Spill Rate 7000 gpm for
Unlimited Time Duration
Wind Speed 4.46 m/sec (10 mph)
at 6.1 m Height

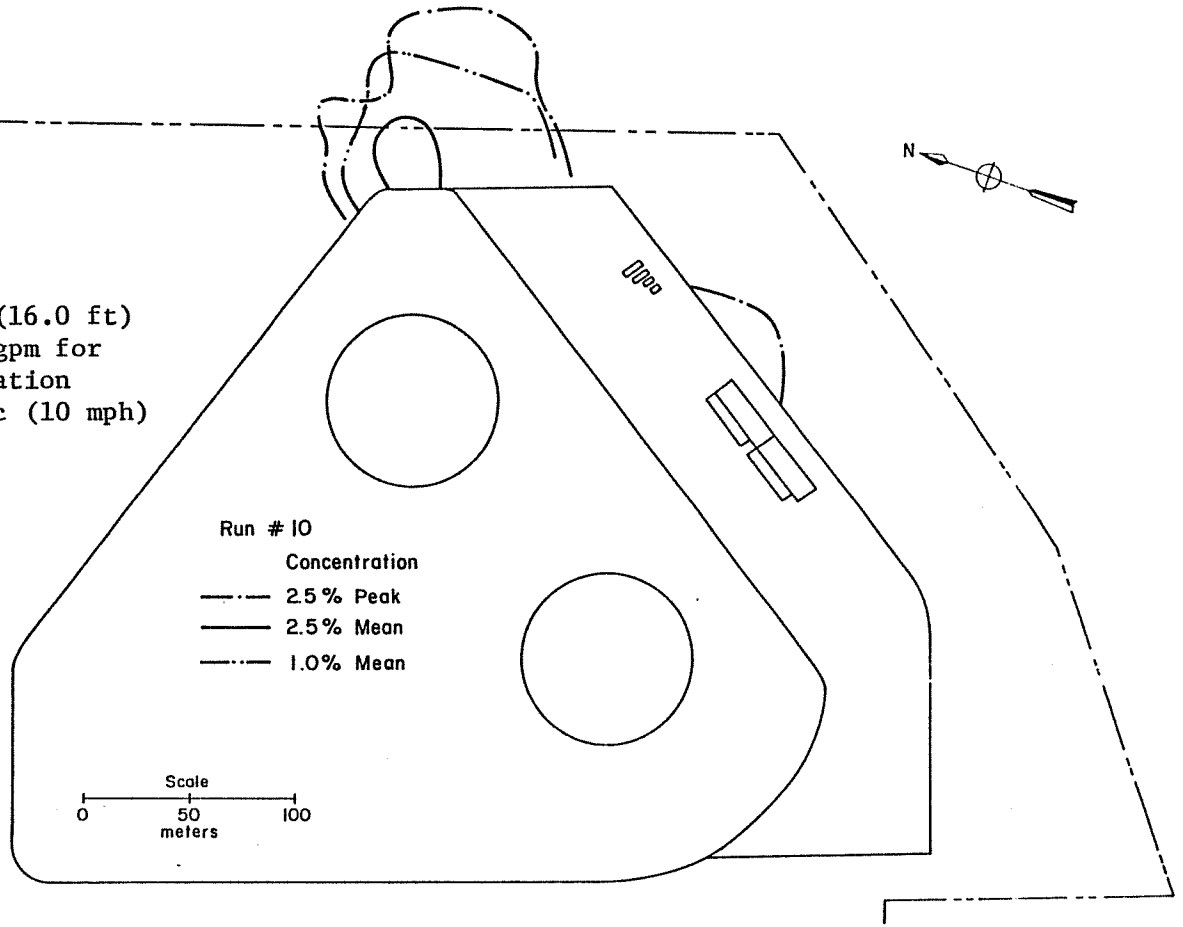

Figure 28. Concentration Isopleths

Run #11
Wind Direction 215°
LNG Boiloff Area P
Fence Height 2.44 m (8.0 ft)
LNG Spill Rate 7000 gpm for
Unlimited Time Duration
Wind Speed 6.69 m/sec (15 mph)
at 6.1 m Height

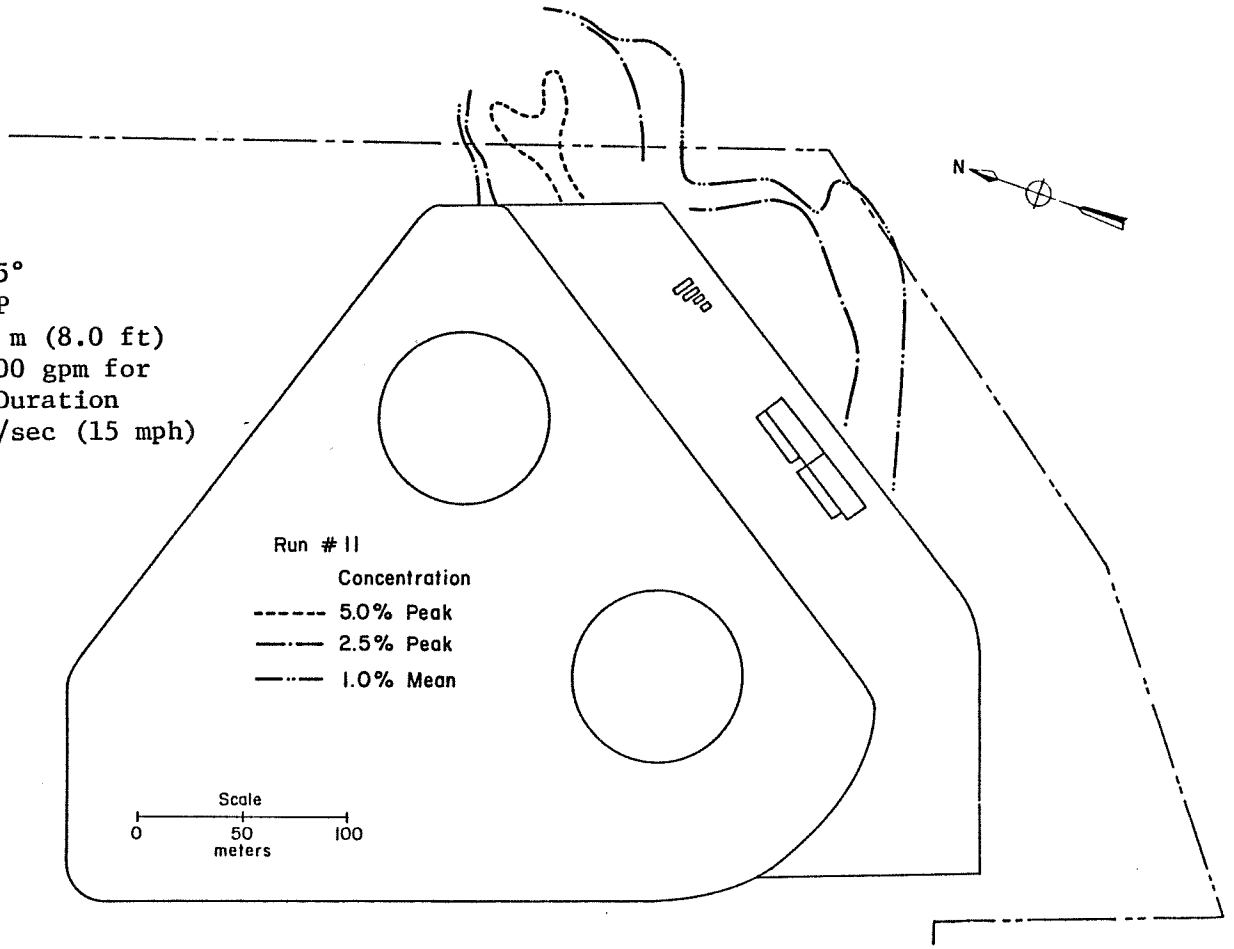

Figure 29. Concentration Isopleths

Run #12
Wind Direction 215°
LNG Boiloff Area P
Fence Height 4.88 m (16.0 ft)
LNG Spill Rate 7000 gpm for
Unlimited Time Duration
Wind Speed 6.69 m/sec (15 mph)
at 6.1 m Height

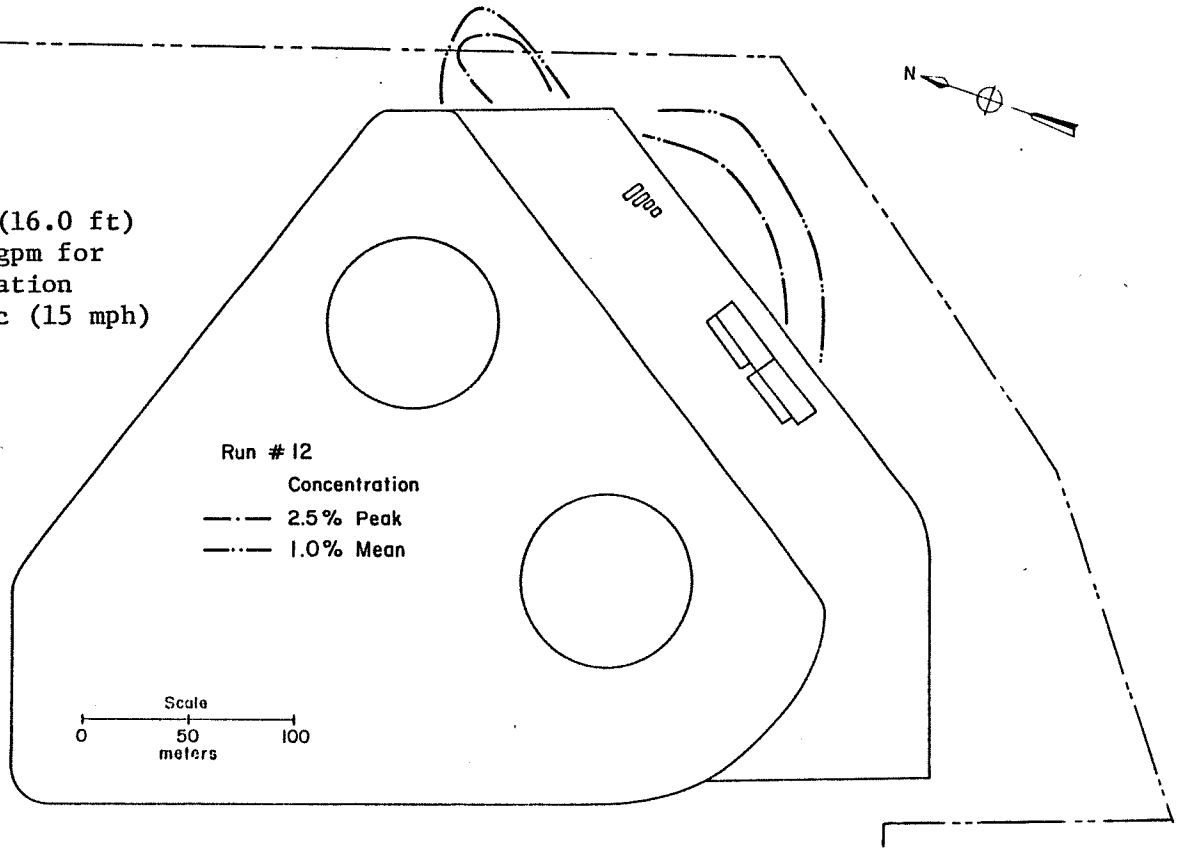

Figure 30. Concentration Isopleths

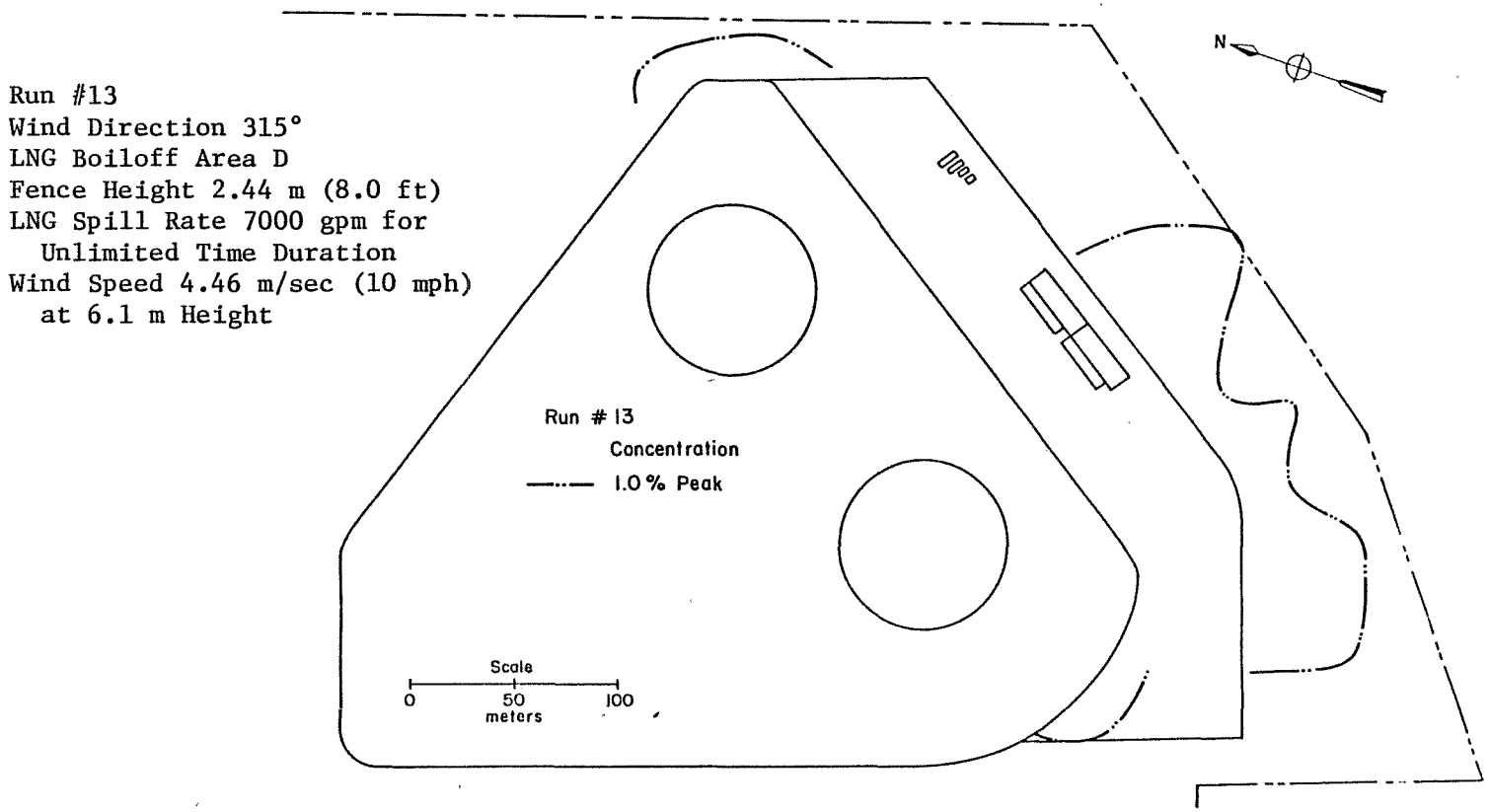

Figure 31. Concentration Isopleths

Run #14
Wind Direction 315°
LNG Boiloff Area D
Fence Height 4.88 m (16.0 ft)
LNG Spill Rate 7000 gpm for
Unlimited Time Duration
Wind Speed 4.46 m/sec (10 mph)
at 6.1 m Height

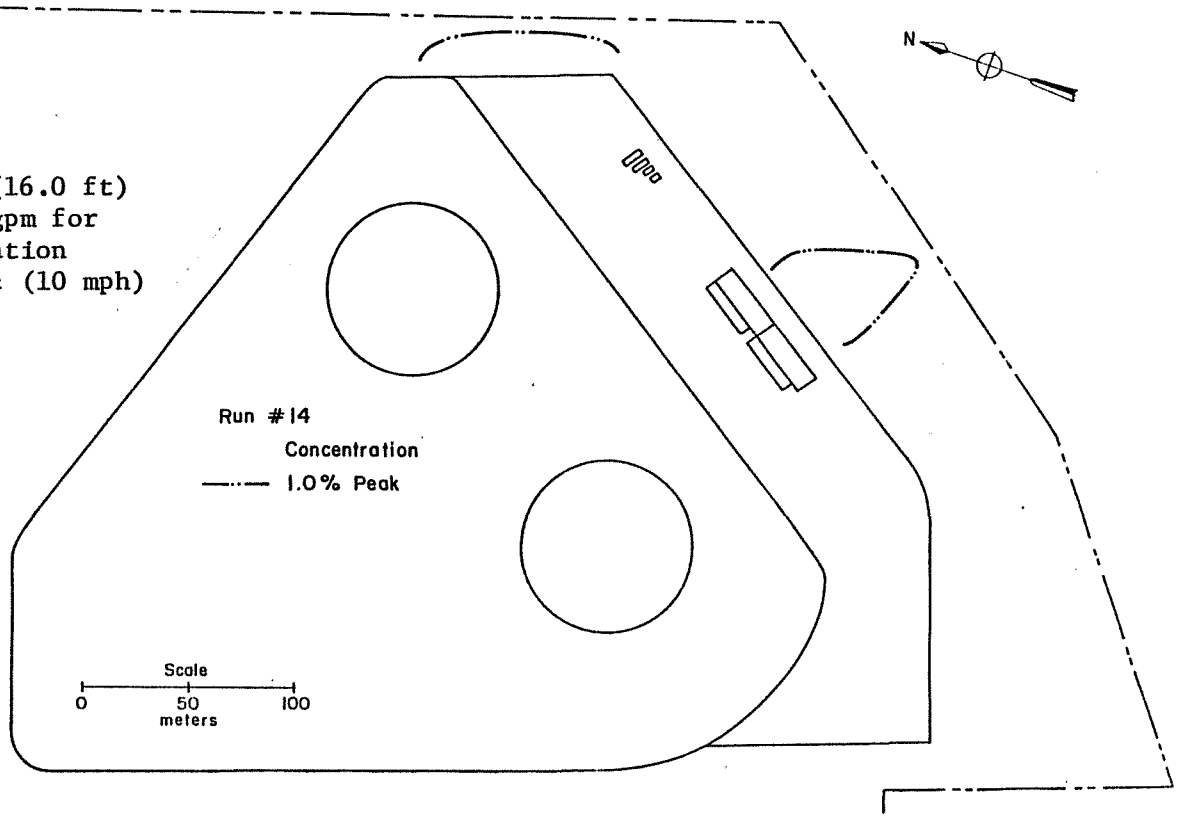

Figure 32. Concentration Isopleths

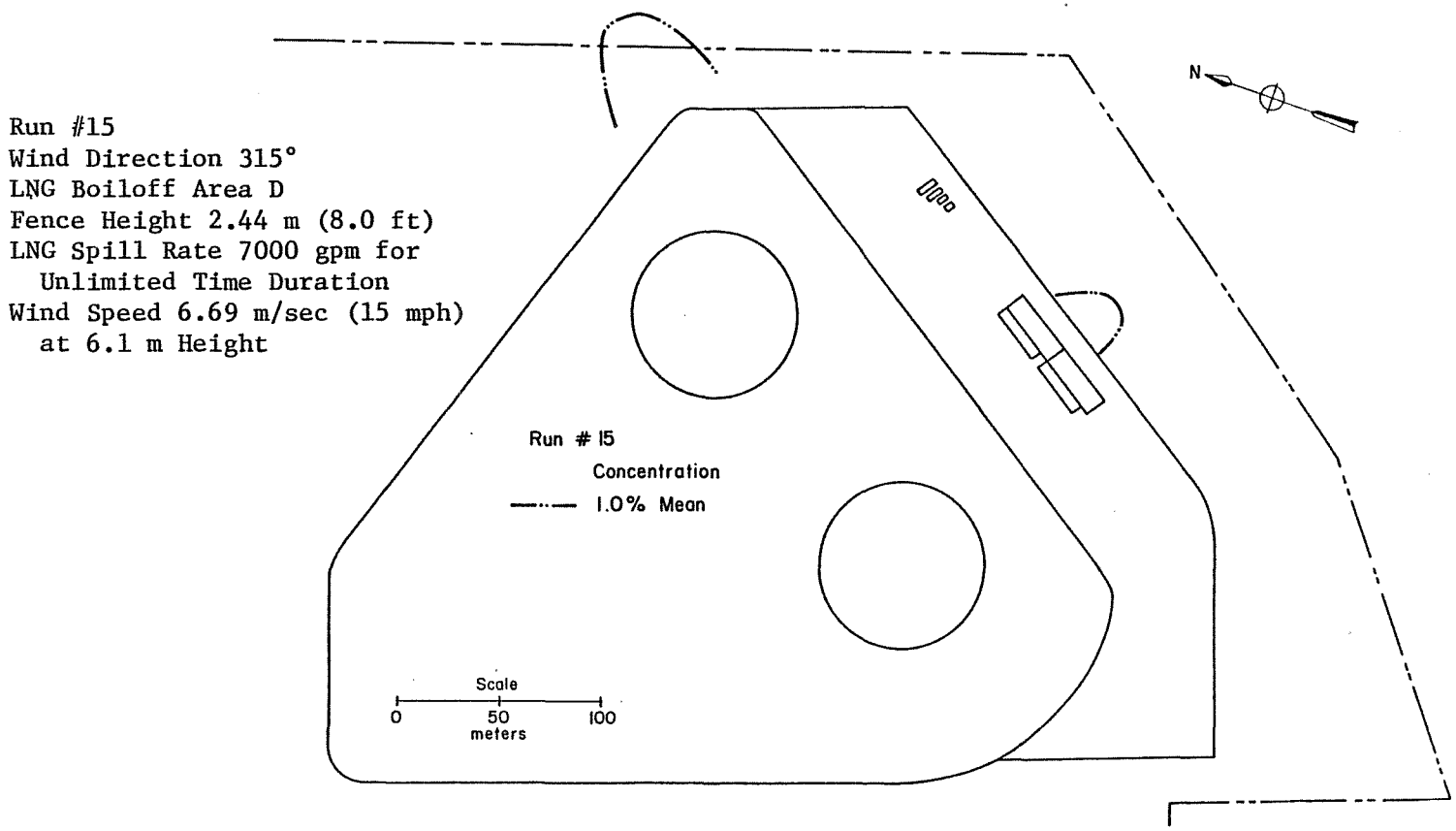

Figure 33. Concentration Isopleths

Run #16
Wind Direction 315°
LNG Boiloff Area D
Fence Height 4.88 m (16.0 ft)
LNG Spill Rate 7000 gpm for
Unlimited Time Duration
Wind Speed 6.69 m/sec (15 mph)
at 6.1 m Height

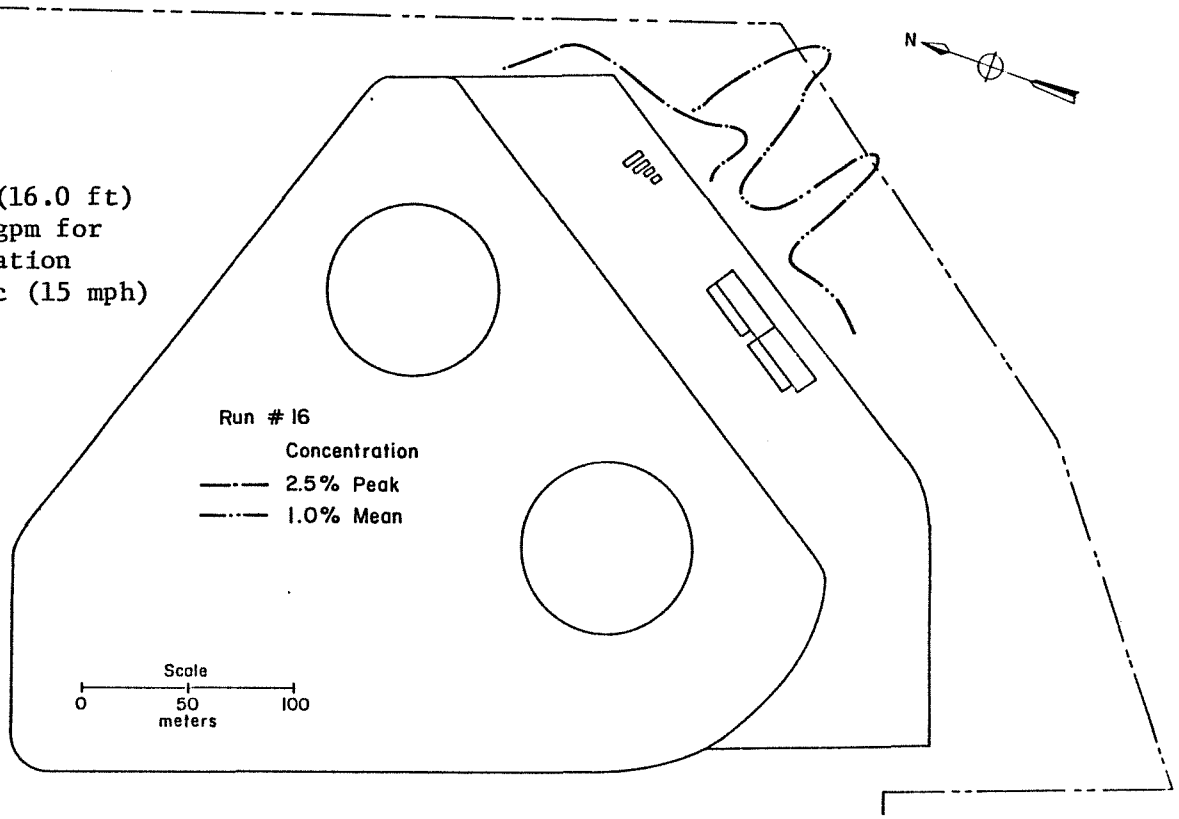

Figure 34. Concentration Isopleths

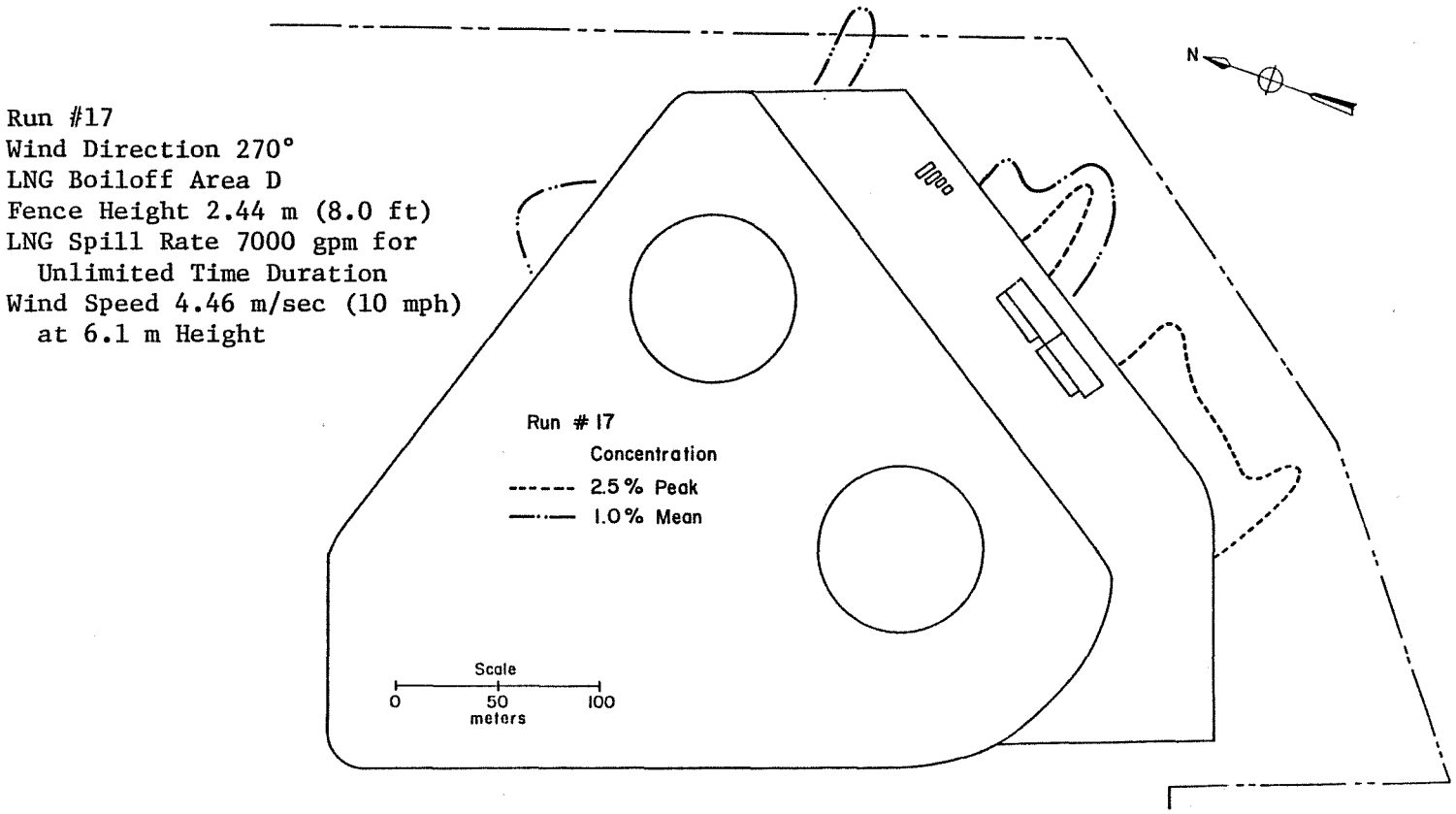

Figure 35. Concentration Isopleths

Run #18
Wind Direction 270°
LNG Boiloff Area D
Fence Height 4.88 m (16.0 ft)
LNG Spill Rate 7000 gpm for
Unlimited Time Duration
Wind Speed 4.46 m/sec (10 mph)
at 6.1 m Height

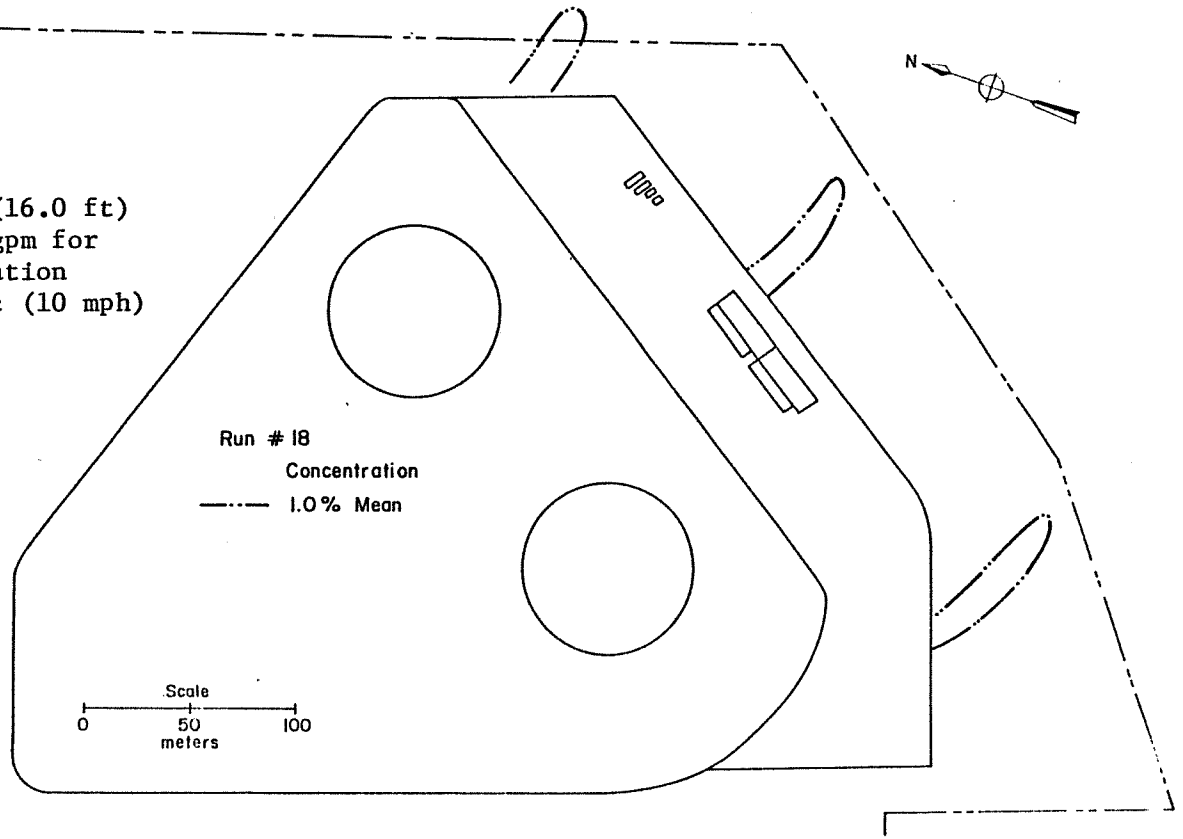

Figure 36. Concentration Isopleths

Run #19
Wind Direction 270°
LNG Boiloff Area D
Fence Height 2.44 m (8.0 ft)
LNG Spill Rate 7000 gpm for
Unlimited Time Duration
Wind Speed 6.69 m/sec (15 mph)
at 6.1 m Height

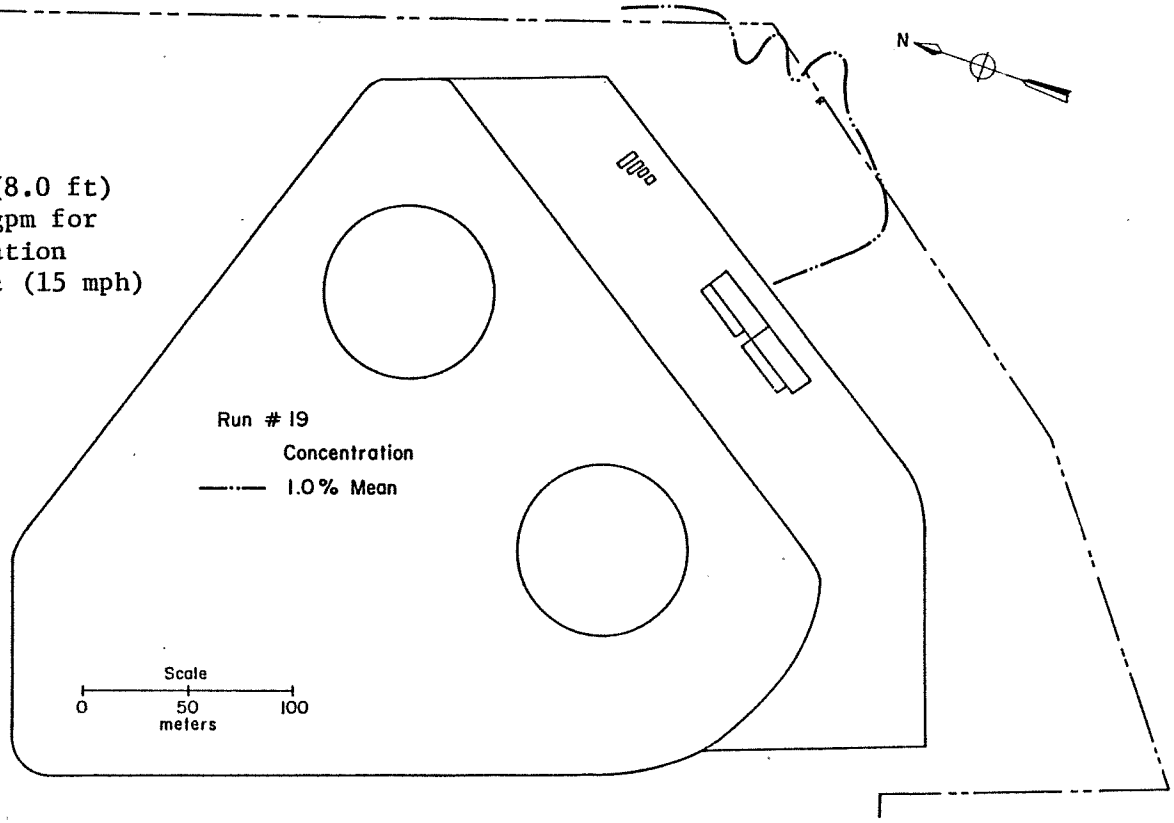

Figure 37. Concentration Isopleths

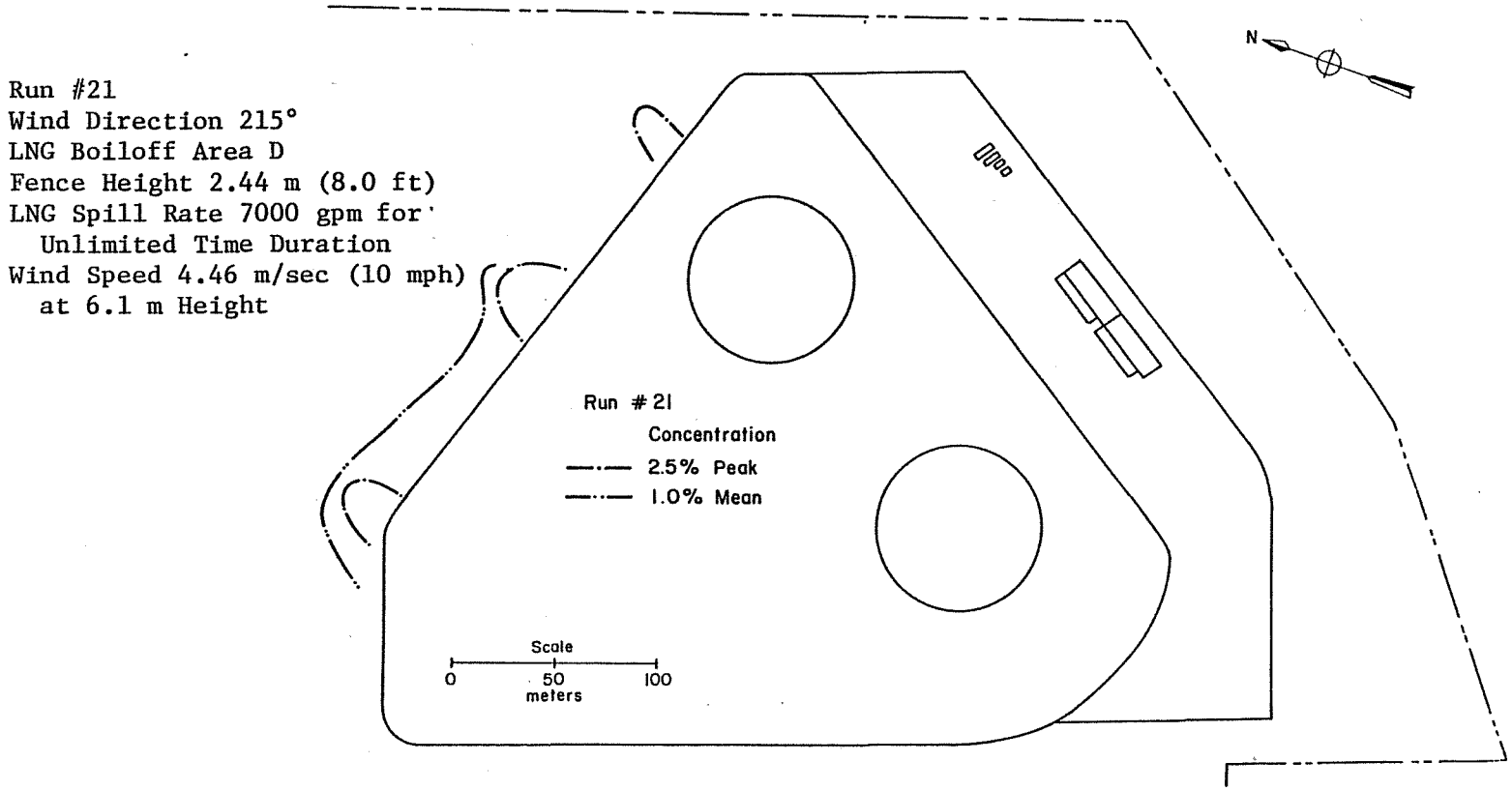

Figure 38. Concentration Isopleths

Run #23
Wind Direction 215°
LNG Boiloff Area D
Fence Height 2.44 m (8.0 ft)
LNG Spill Rate 7000 gpm for
Unlimited Time Duration
Wind Speed 6.69 m/sec (15 mph)
at 6.1 m Height

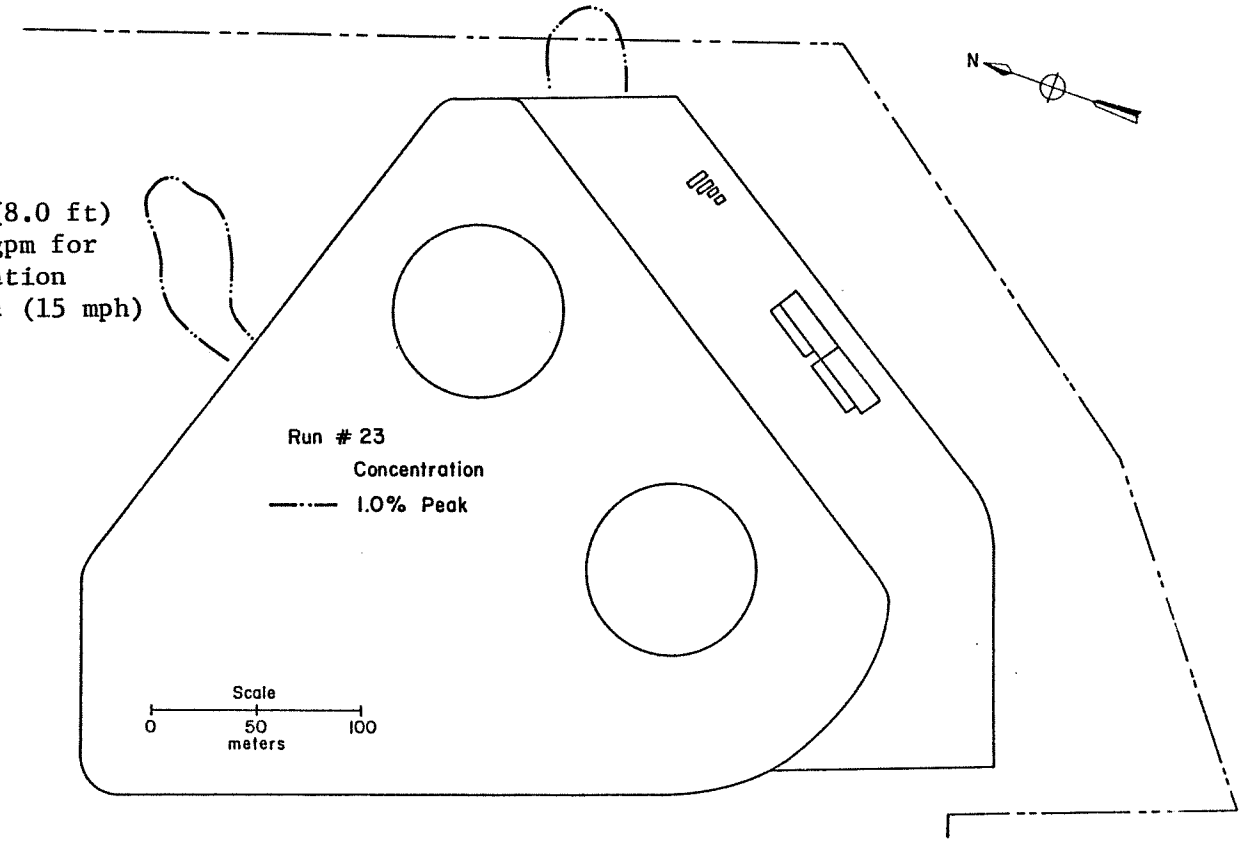

Figure 39. Concentration Isopleths

Run #31
Wind Direction 215°
LNG Boiloff Area P*
Fence Height 2.44 m (8.0 ft)
LNG Spill Rate 7000 gpm for
Unlimited Time Duration
Wind Speed 4.46 m/sec (10 mph)
at 6.1 m Height

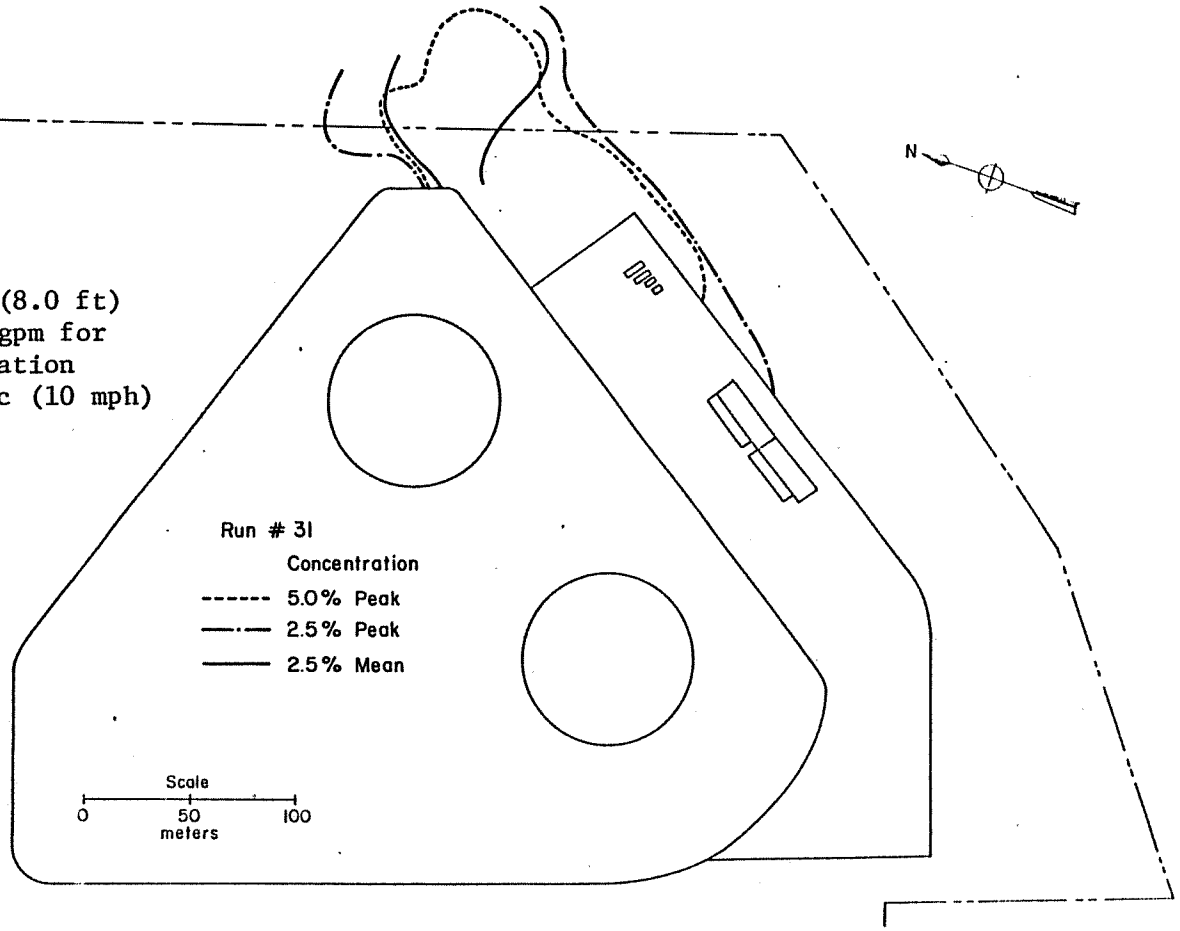

Figure 40. Concentration Isopleths

Run #32
Wind Direction 215°
LNG Boiloff Area P*
Fence Height 4.88 m (16.0 ft)
LNG Spill Rate 7000 gpm for
Unlimited Time Duration
Wind Speed 4.46 m/sec (10 mph)
at 6.1 m Height

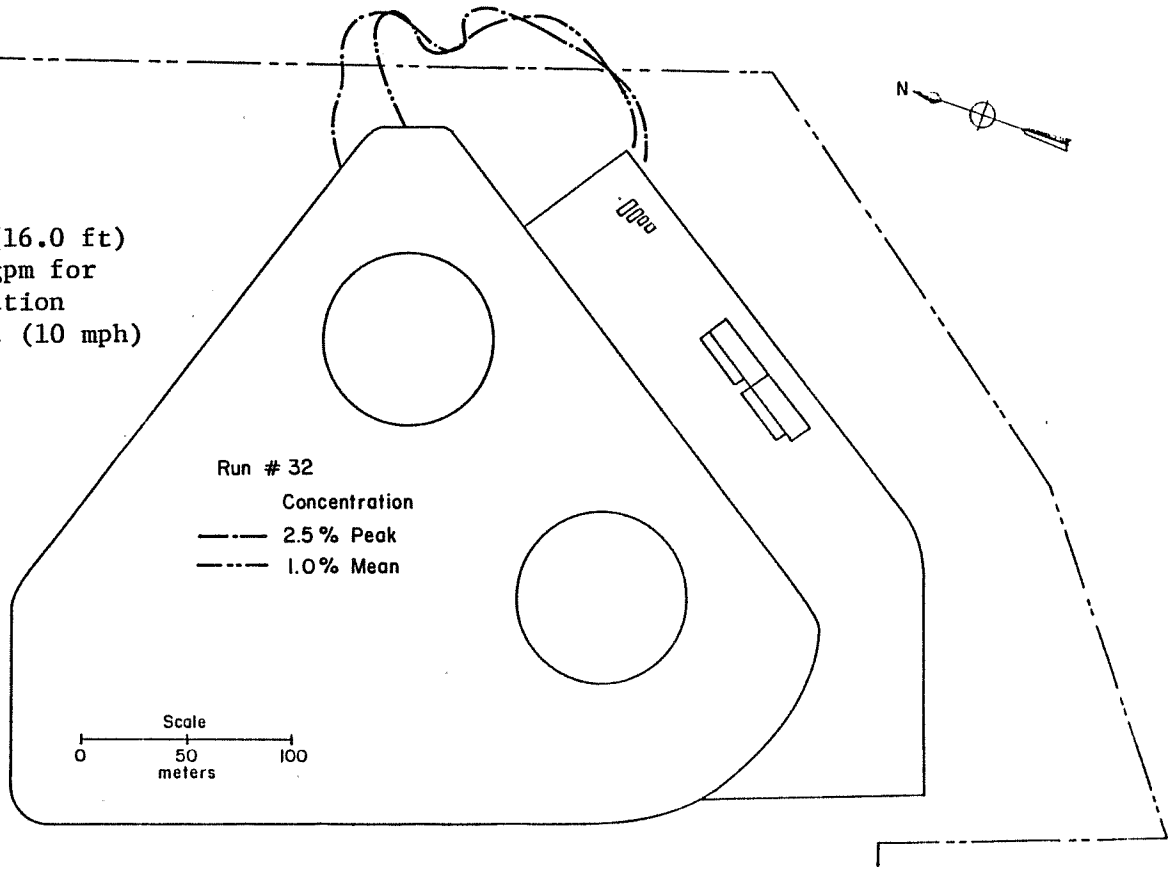

Figure 41. Concentration Isopleths

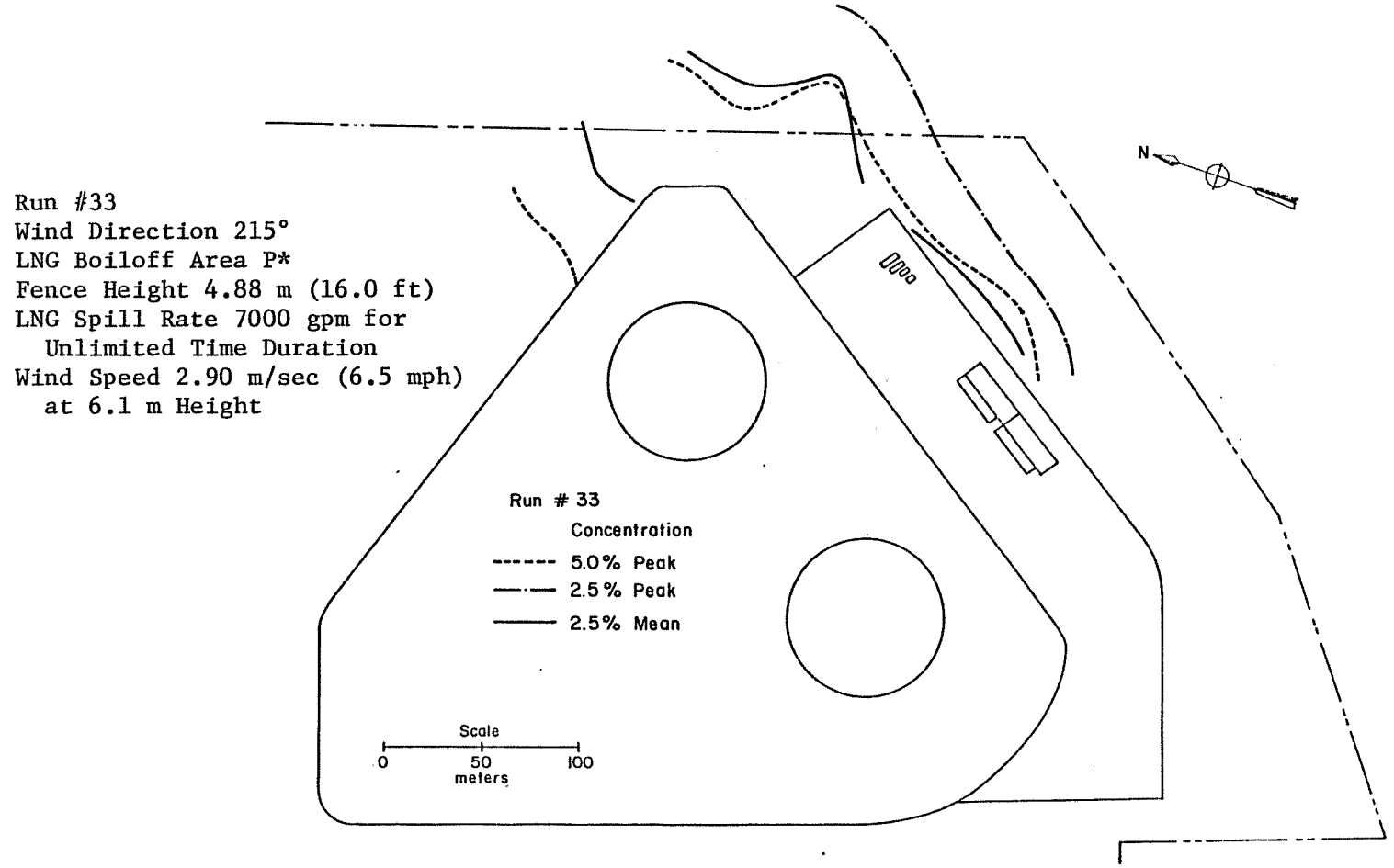

Figure 42. Concentration Isopleths

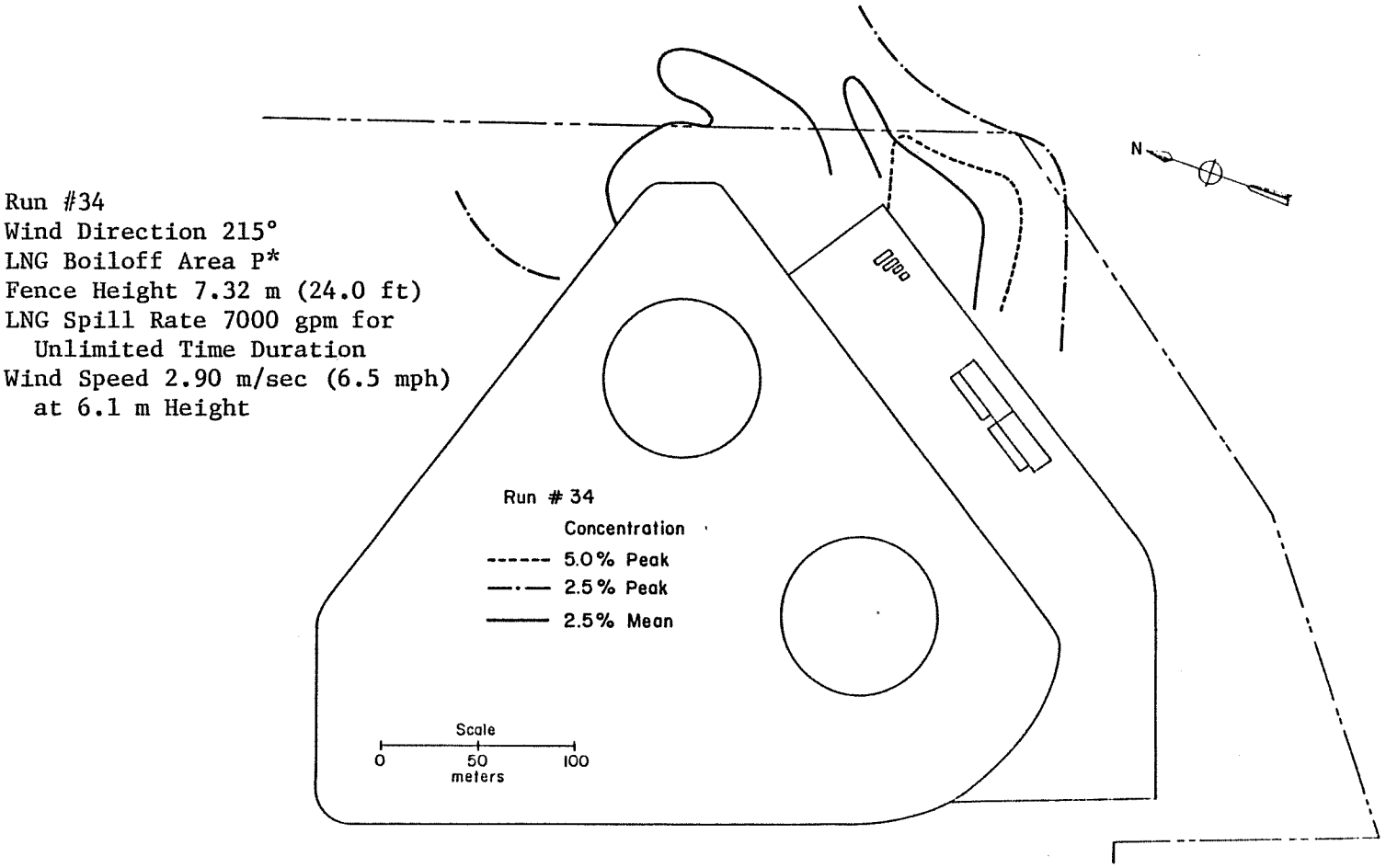

Figure 43. Concentration Isopleths

Run #39
Wind Direction 215°
LNG Boiloff Area P*/2
Fence Height 4.88 m (16.0 ft)
LNG Spill Rate 7000 gpm for
Unlimited Time Duration
Wind Speed 2.90 m/sec (6.5 mph)
at 6.1 m Height

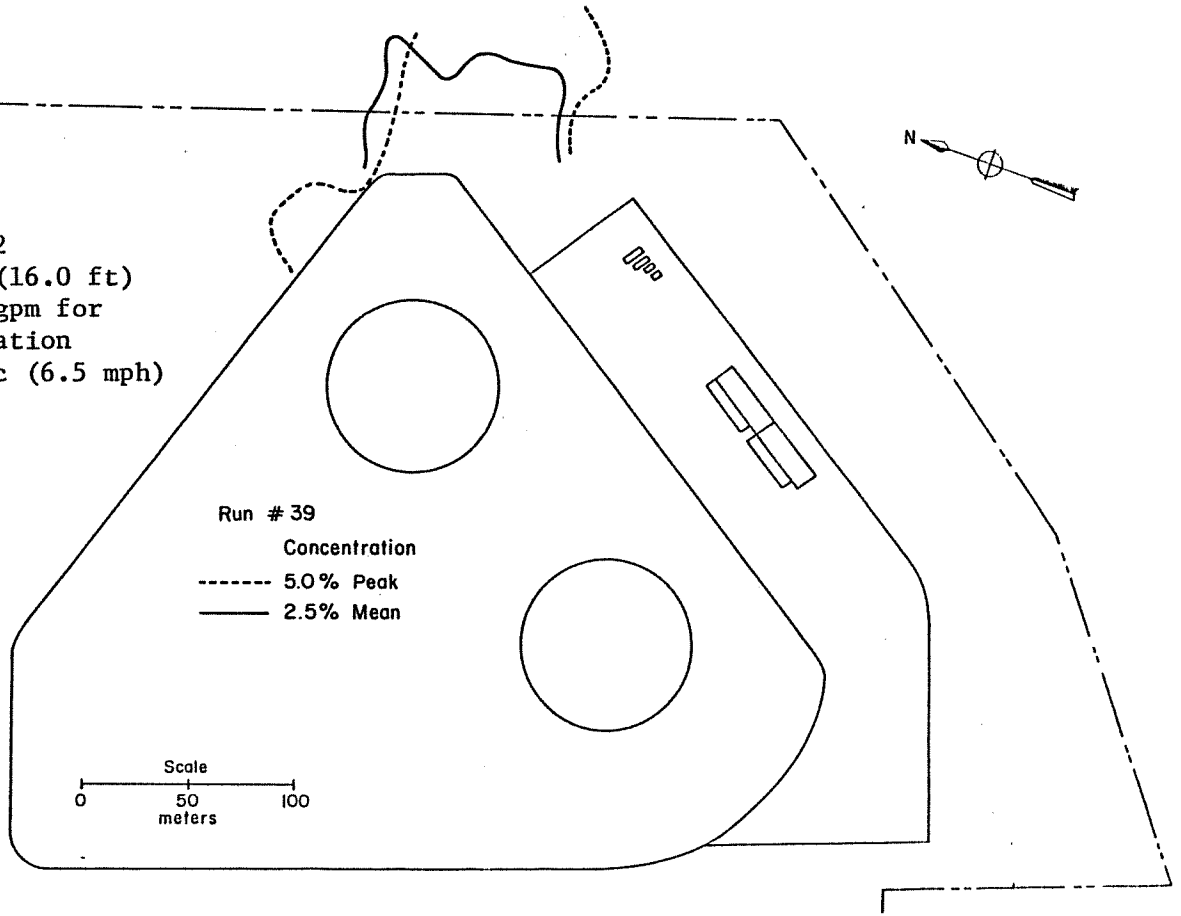

Figure 44. Concentration Isopleths

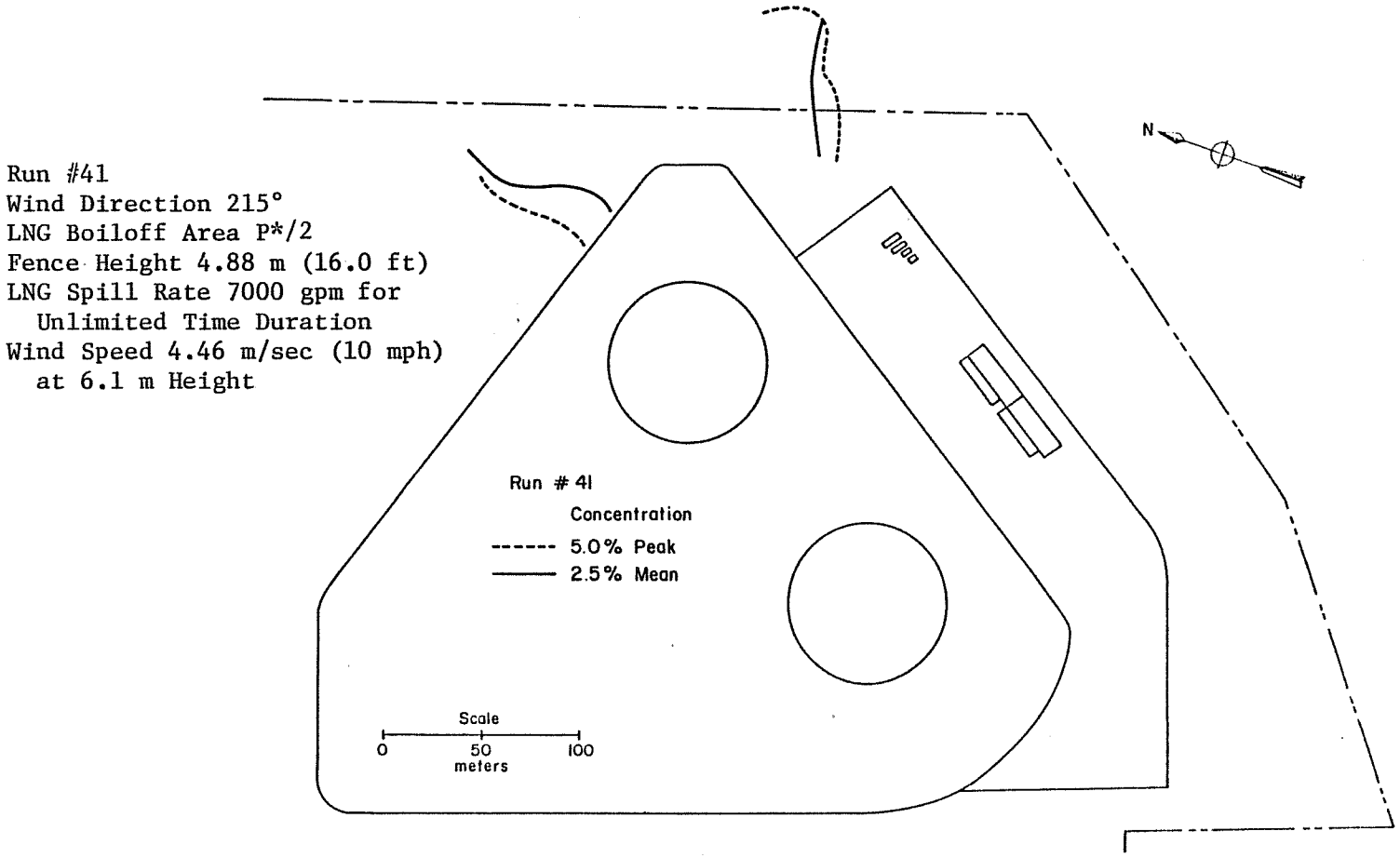

Figure 45. Concentration Isopleths

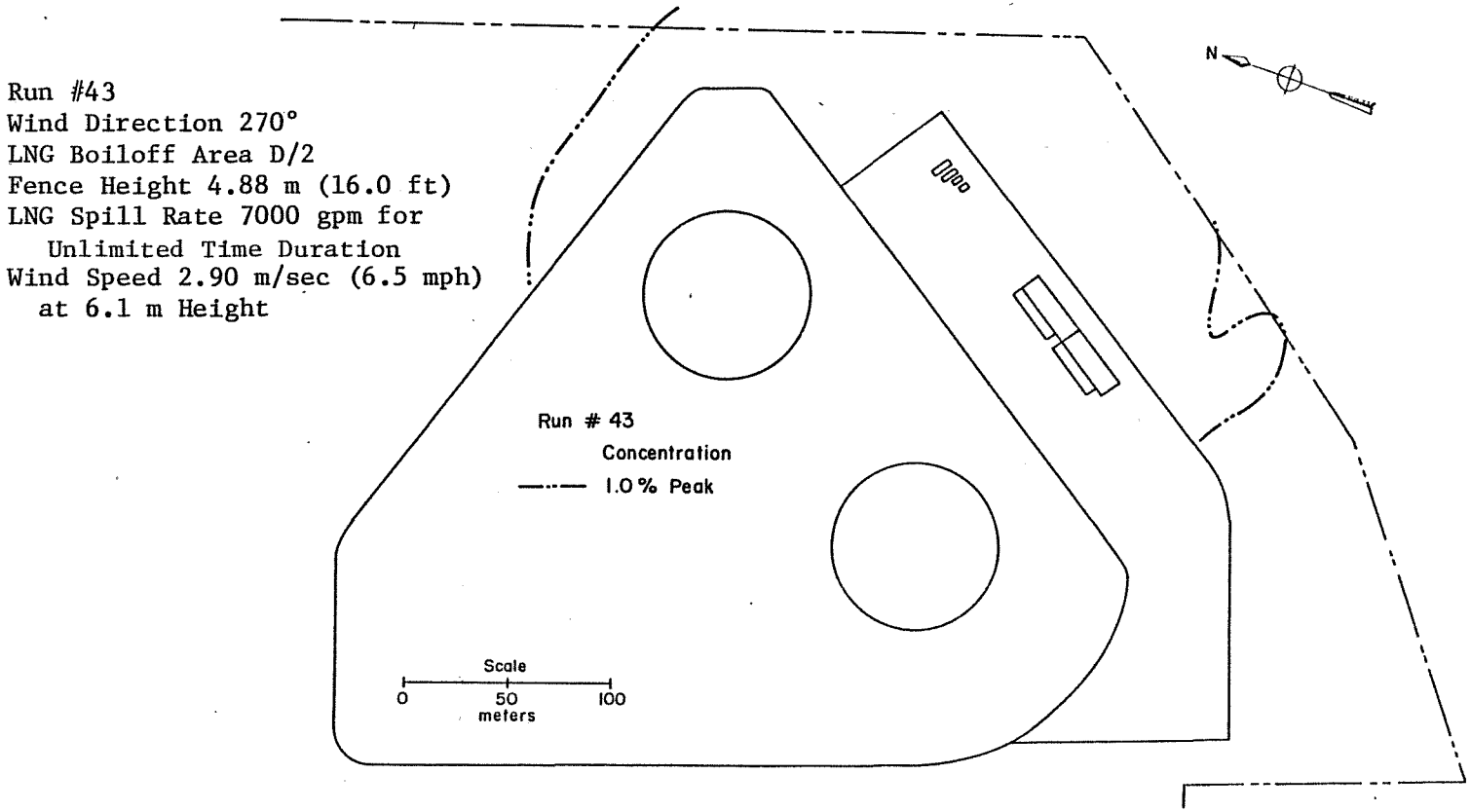

Figure 46. Concentration Isopleths

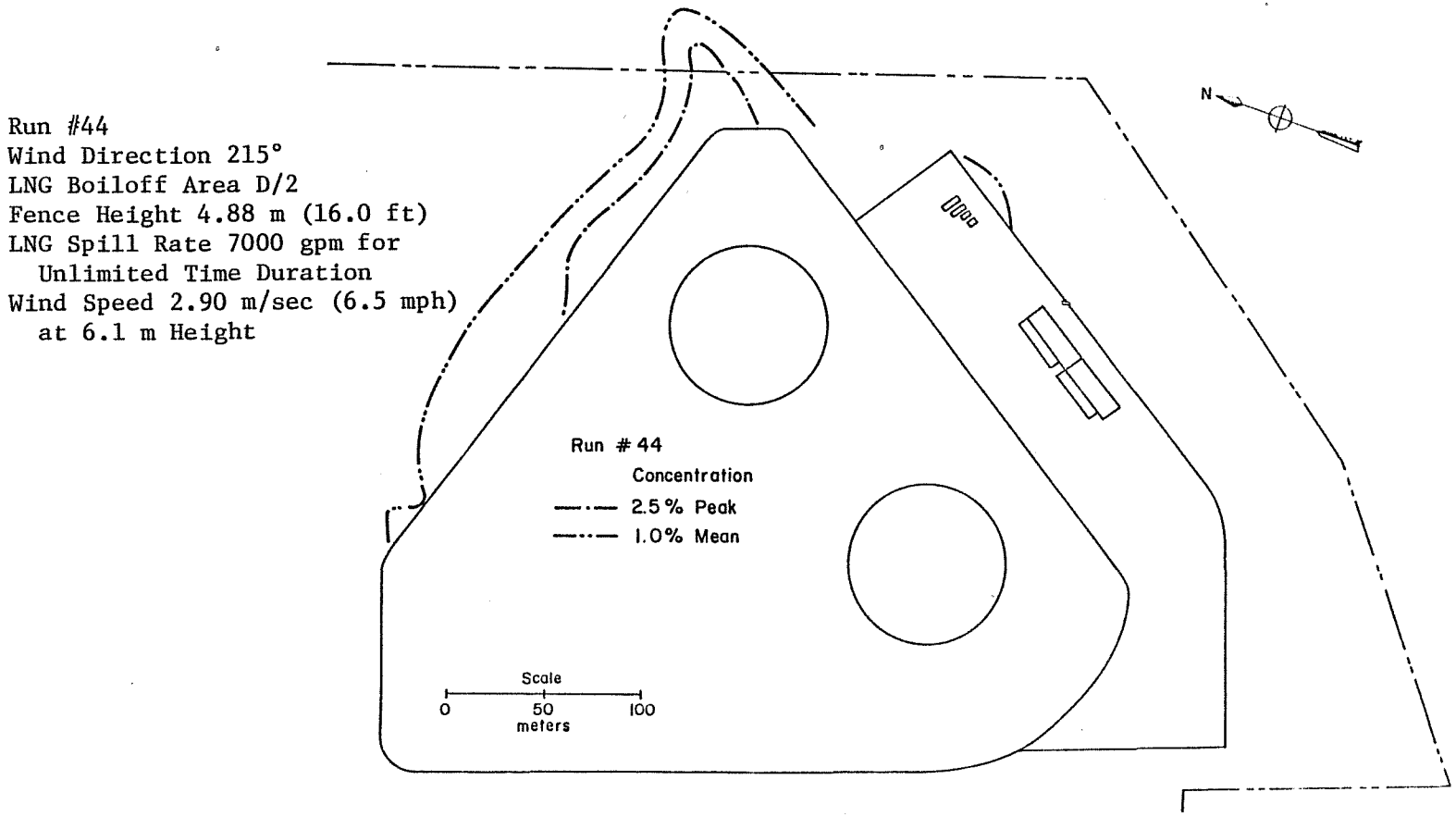

Figure 47. Concentration Isopleths

Run #45
Wind Direction 315°
LNG Boiloff Area P*/2
Fence Height 4.88 m (16.0 ft)
LNG Spill Rate 7000 gpm for
  Unlimited Time Duration
Wind Speed 2.90 m/sec (6.5 mph)
  at 6.1 m Height

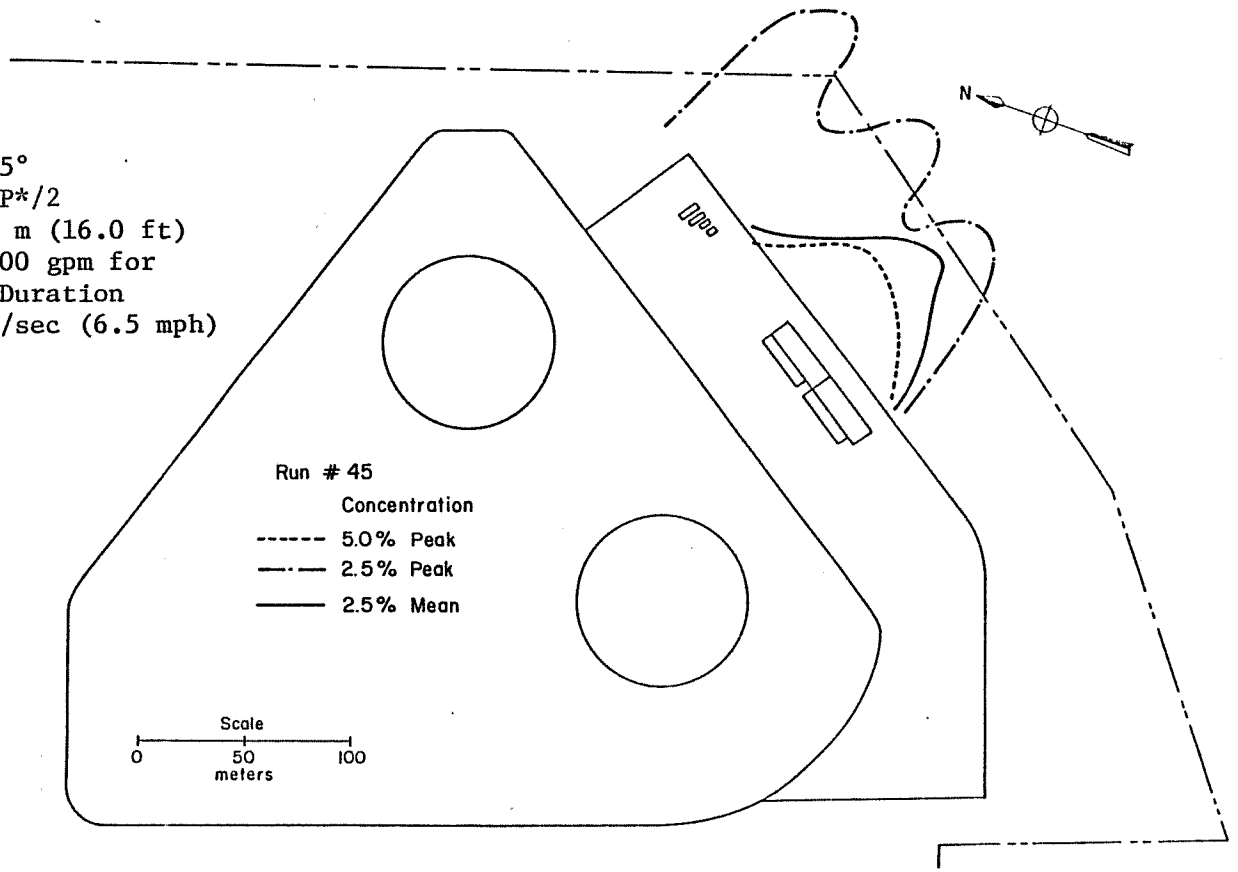

Figure 48. Concentration Isopleths

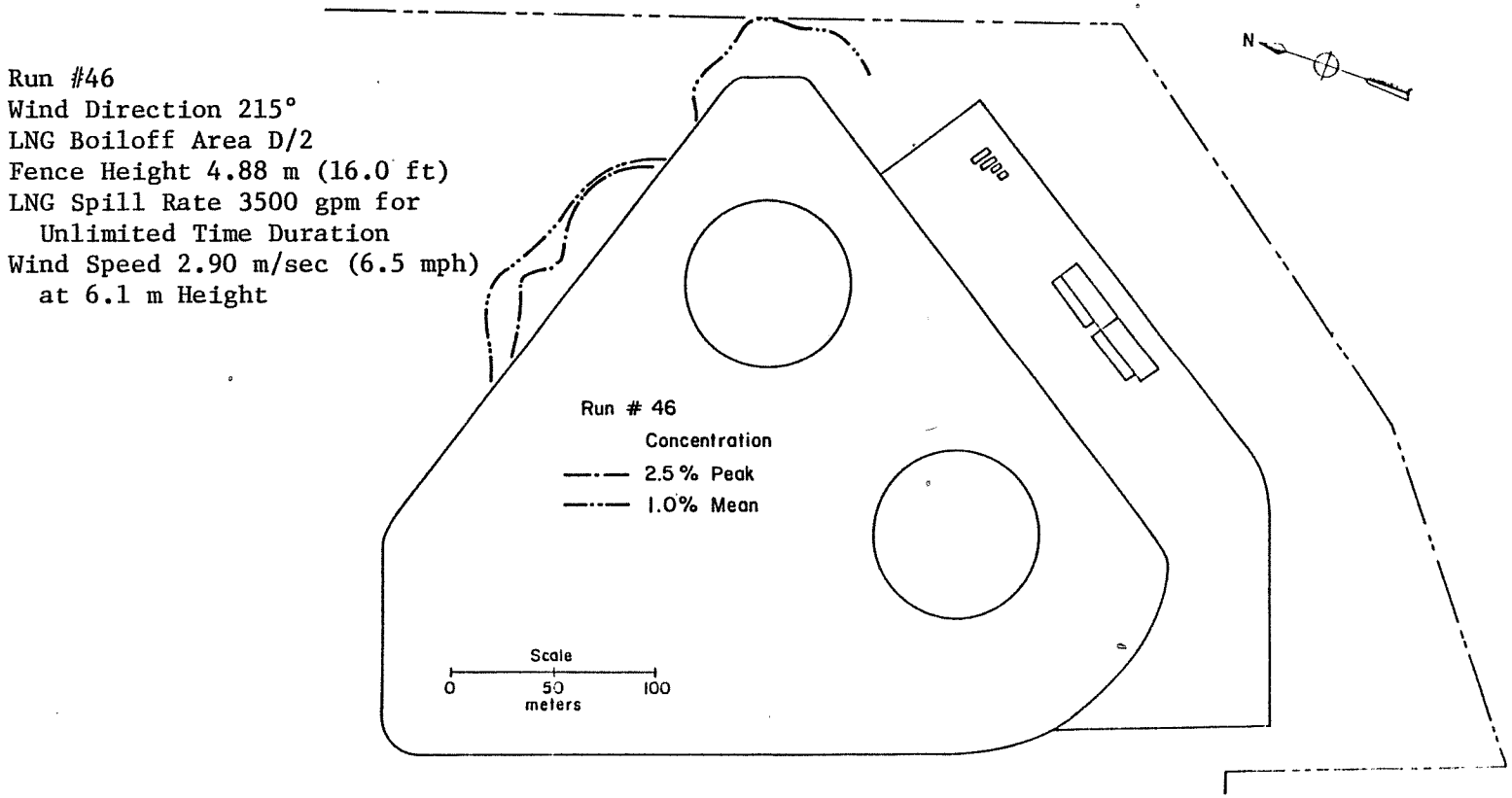

Figure 49. Concentration Isopleths

Run #47
Wind Direction 215°
LNG Boiloff Area P*/2
Fence Height 4.88 m (16.0 ft)
LNG Spill Rate 3500 gpm for
Unlimited Time Duration
Wind Speed 2.90 m/sec (6.5 mph)
at 6.1 m Height

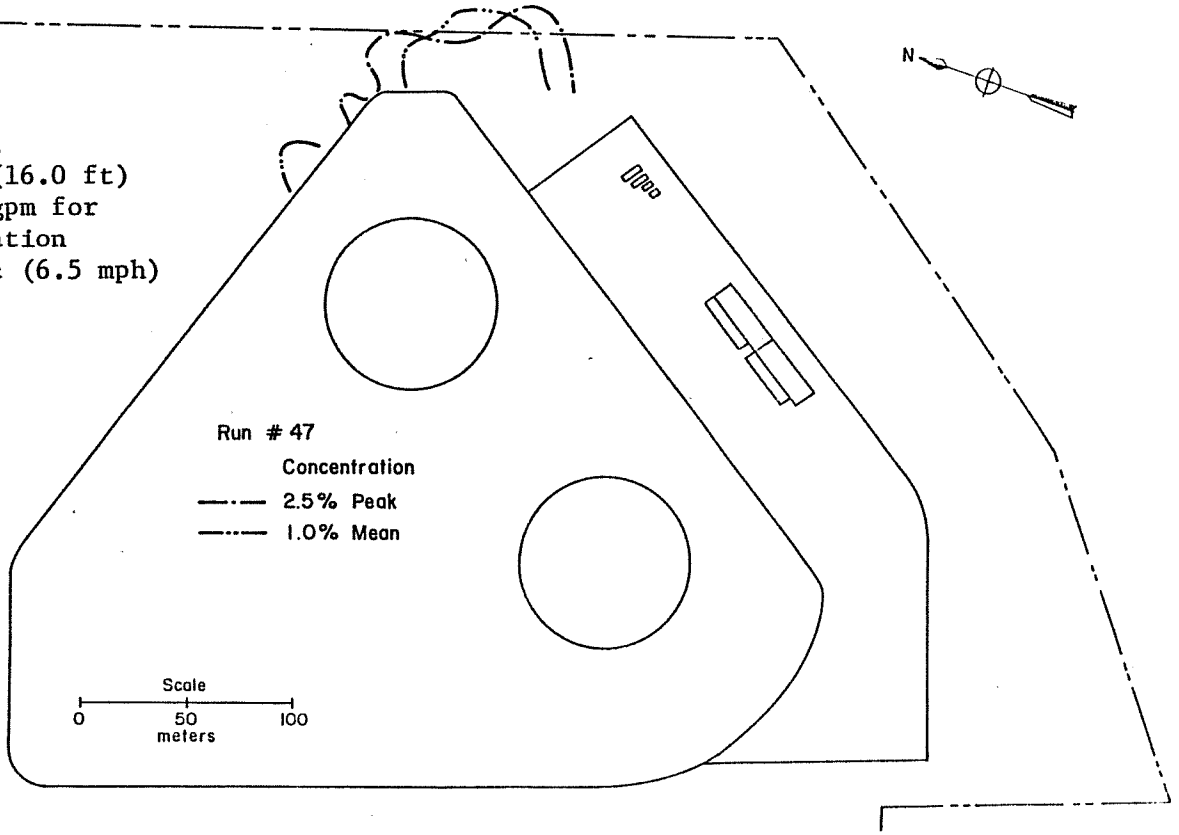

Figure 50. Concentration Isopleths

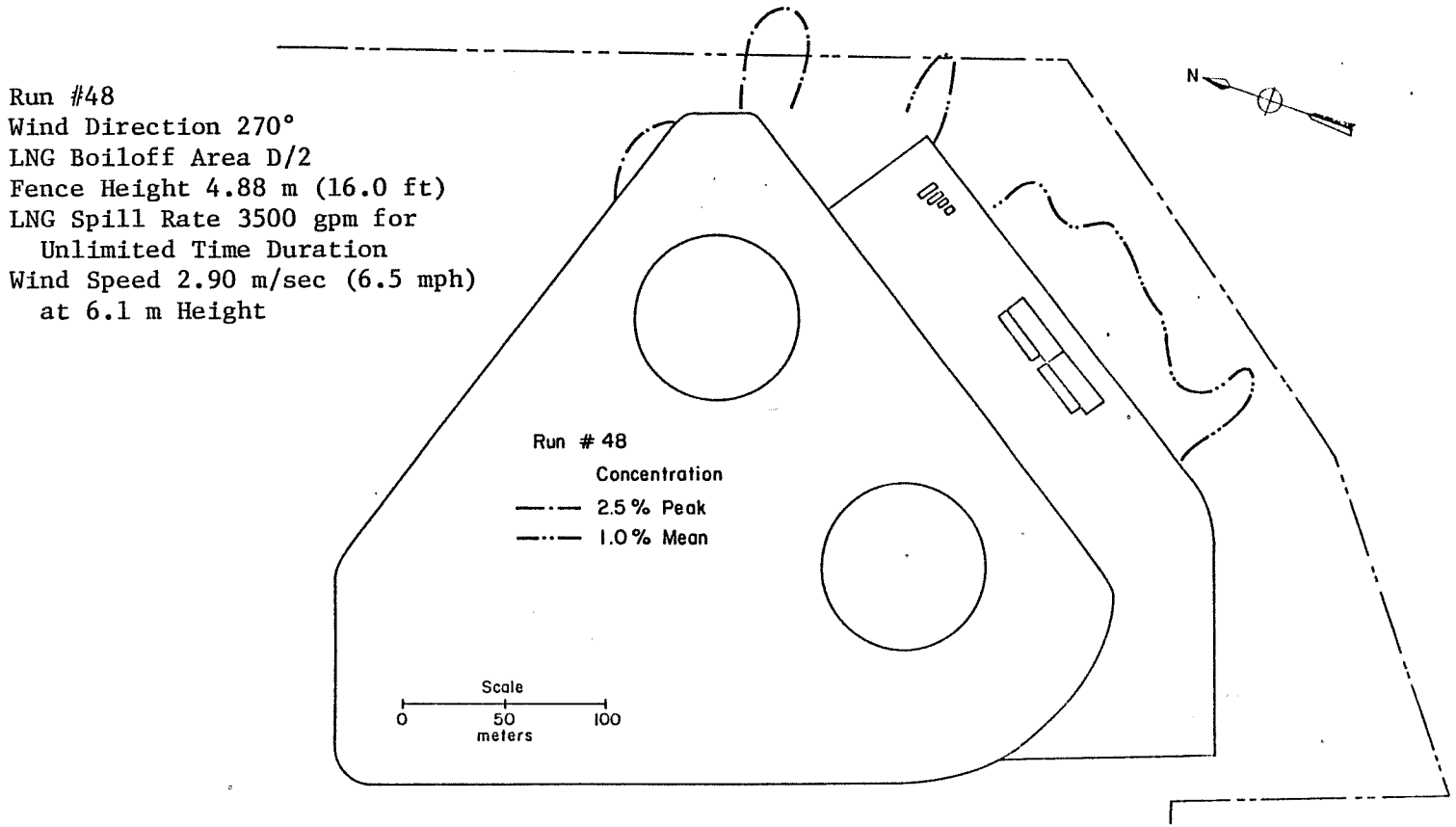

Figure 51. Concentration Isopleths

Run #49
Wind Direction 270°
LNG Boiloff Area P*/2
Fence Height 4.88 m (16.0 ft)
LNG Spill Rate 3500 gpm for
Unlimited Time Duration
Wind Speed 2.90 m/sec (6.5 mph)
at 6.1 m Height

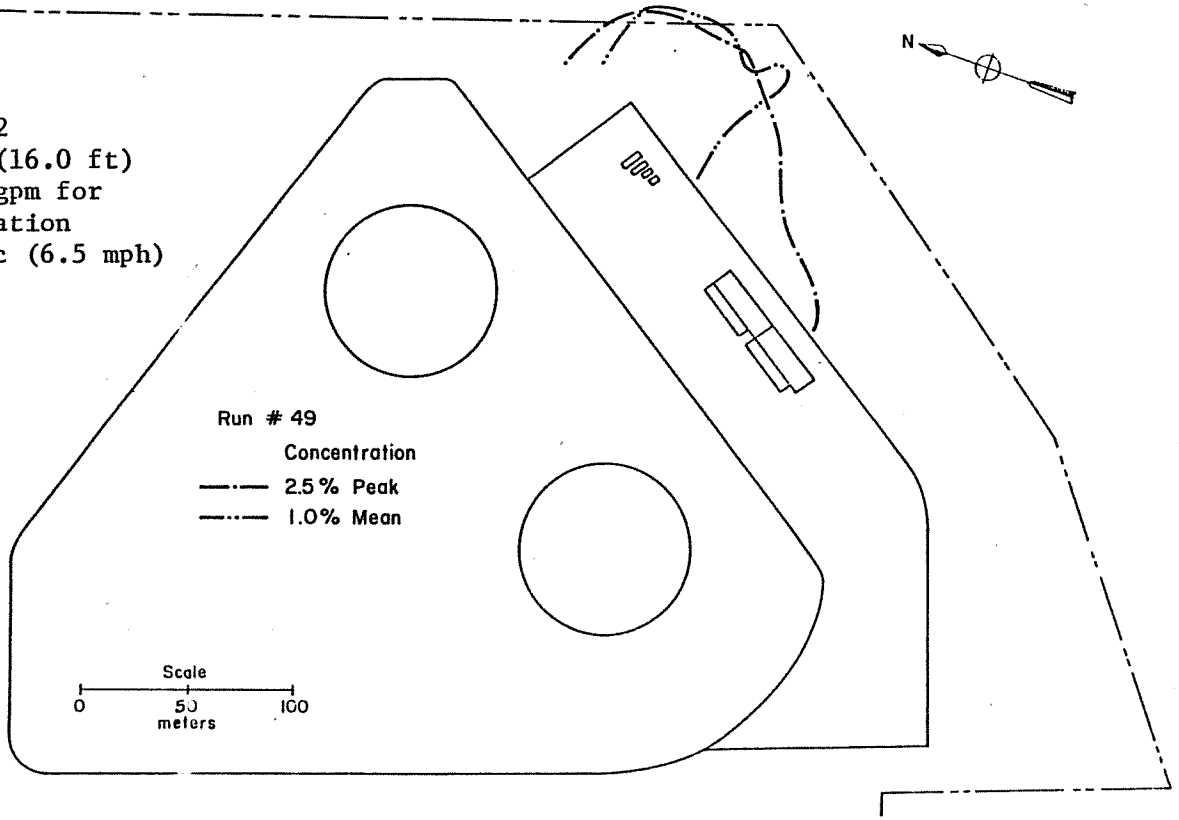

Figure 52. Concentration Isopleths

Run #50
Wind Direction 315°
LNG Boiloff Area D/2
Fence Height 4.88 m (16.0 ft)
LNG Spill Rate 3500 gpm for
Unlimited Time Duration
Wind Speed 2.90 m/sec (6.5 mph)
at 6.1 m Height

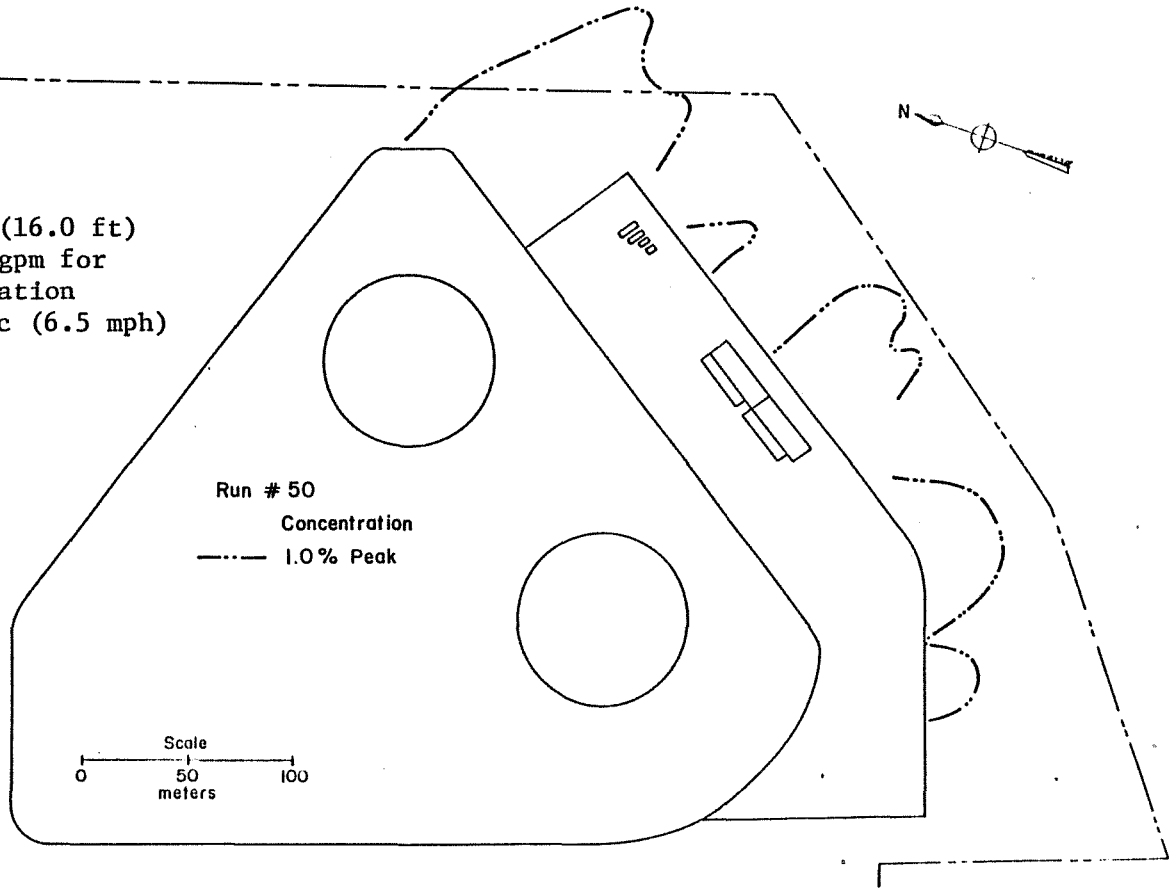

Figure 53. Concentration Isopleths

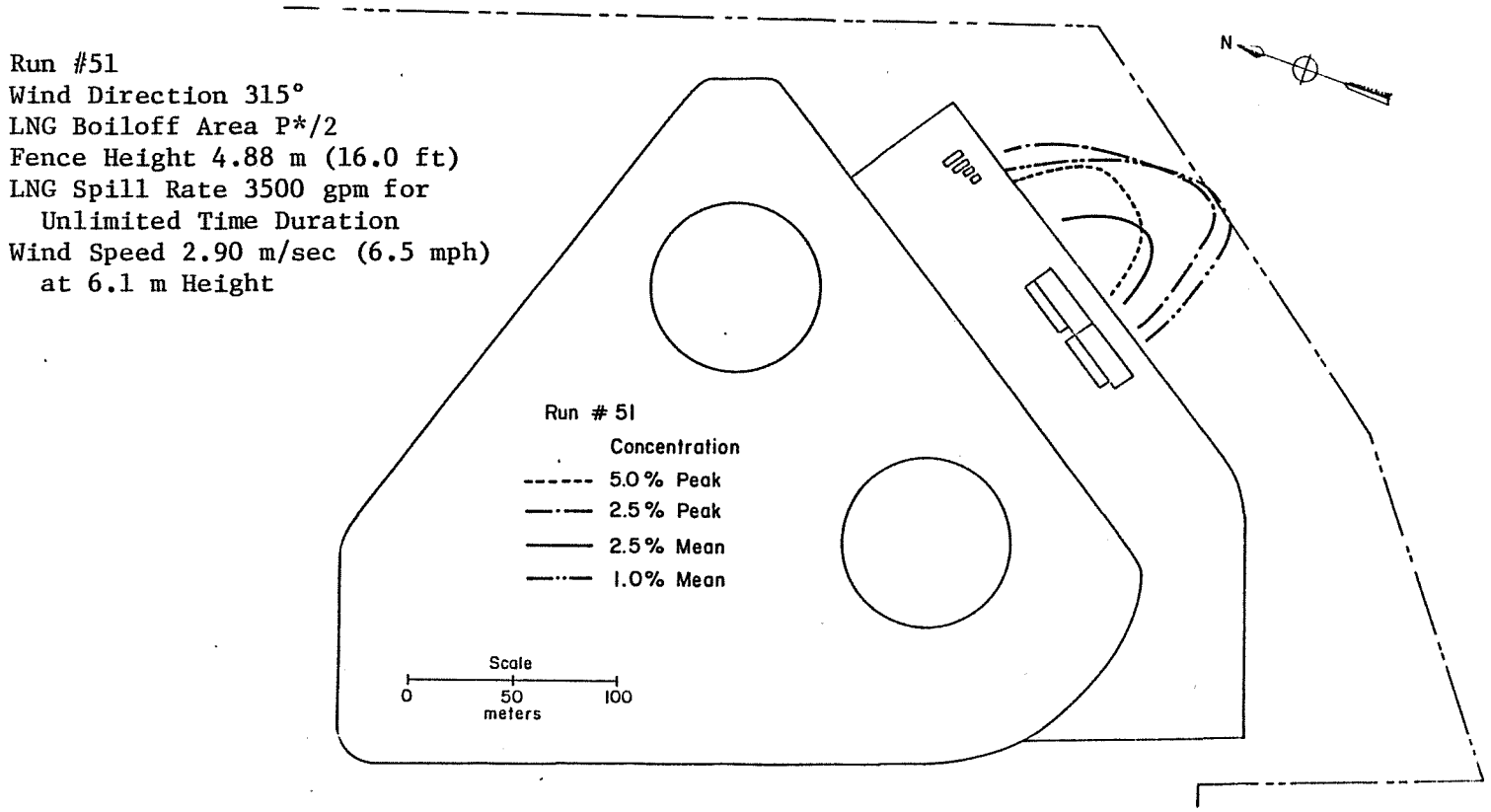

Figure 54. Concentration Isopleths

Run #36
Wind Direction 215°
LNG Boiloff Area P*
Fence Height 4.88 m (16.0 ft)
LNG Spill Rate 7000 gpm for
10 Minute Duration
Wind Speed 2.90 m/sec (6.5 mph)
at 6.1 m Height

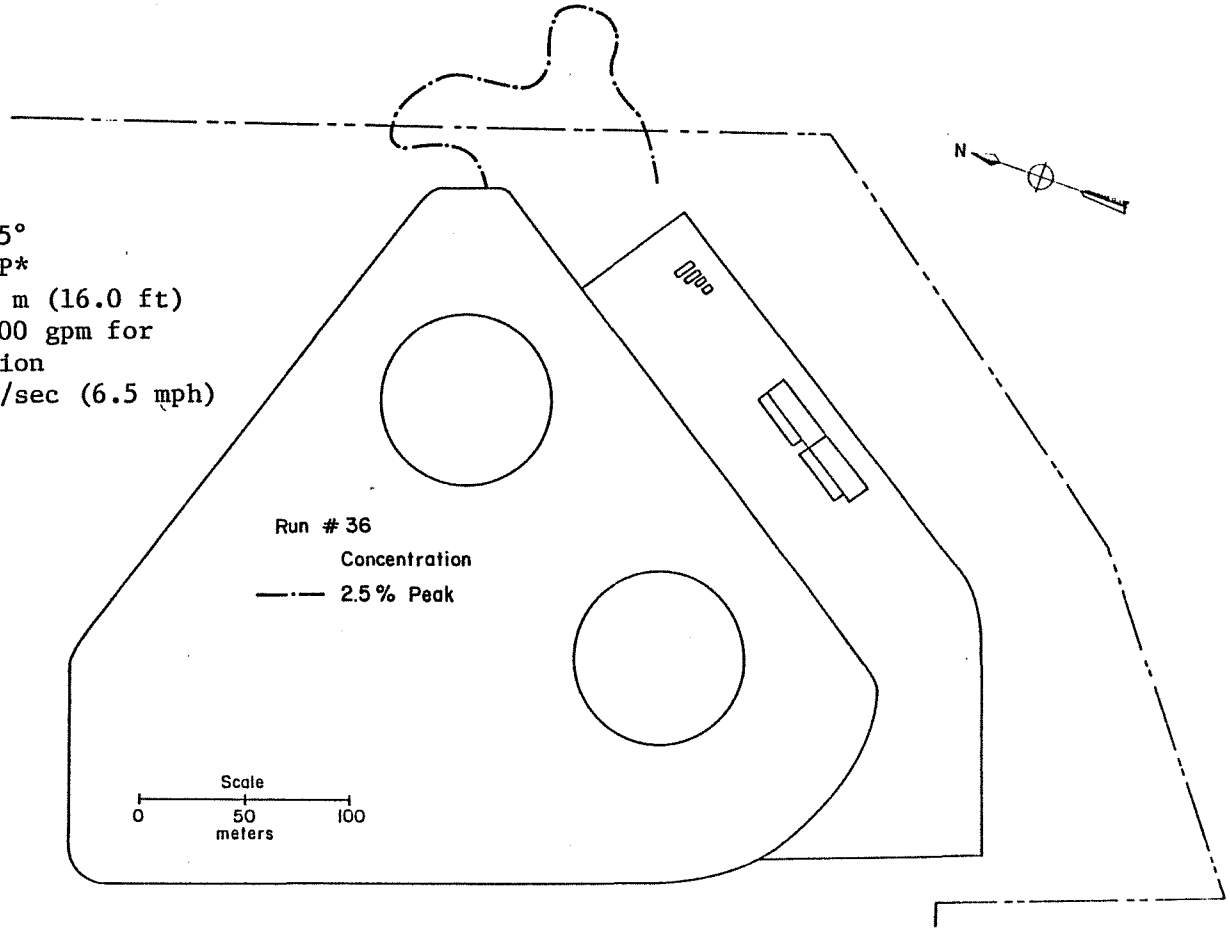

Figure 55. Concentration Isopleths

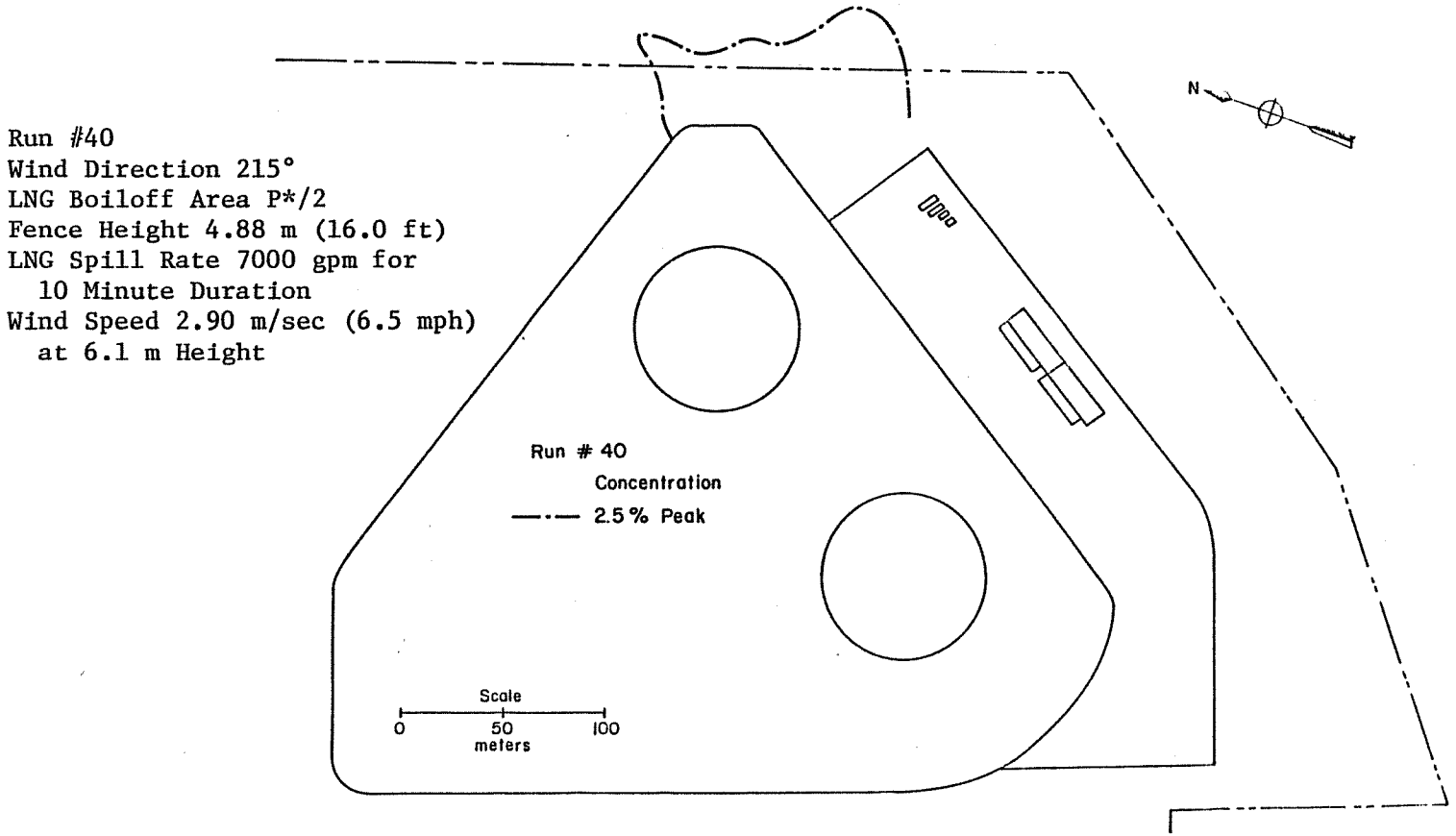

Figure 56. Concentration Isopleths

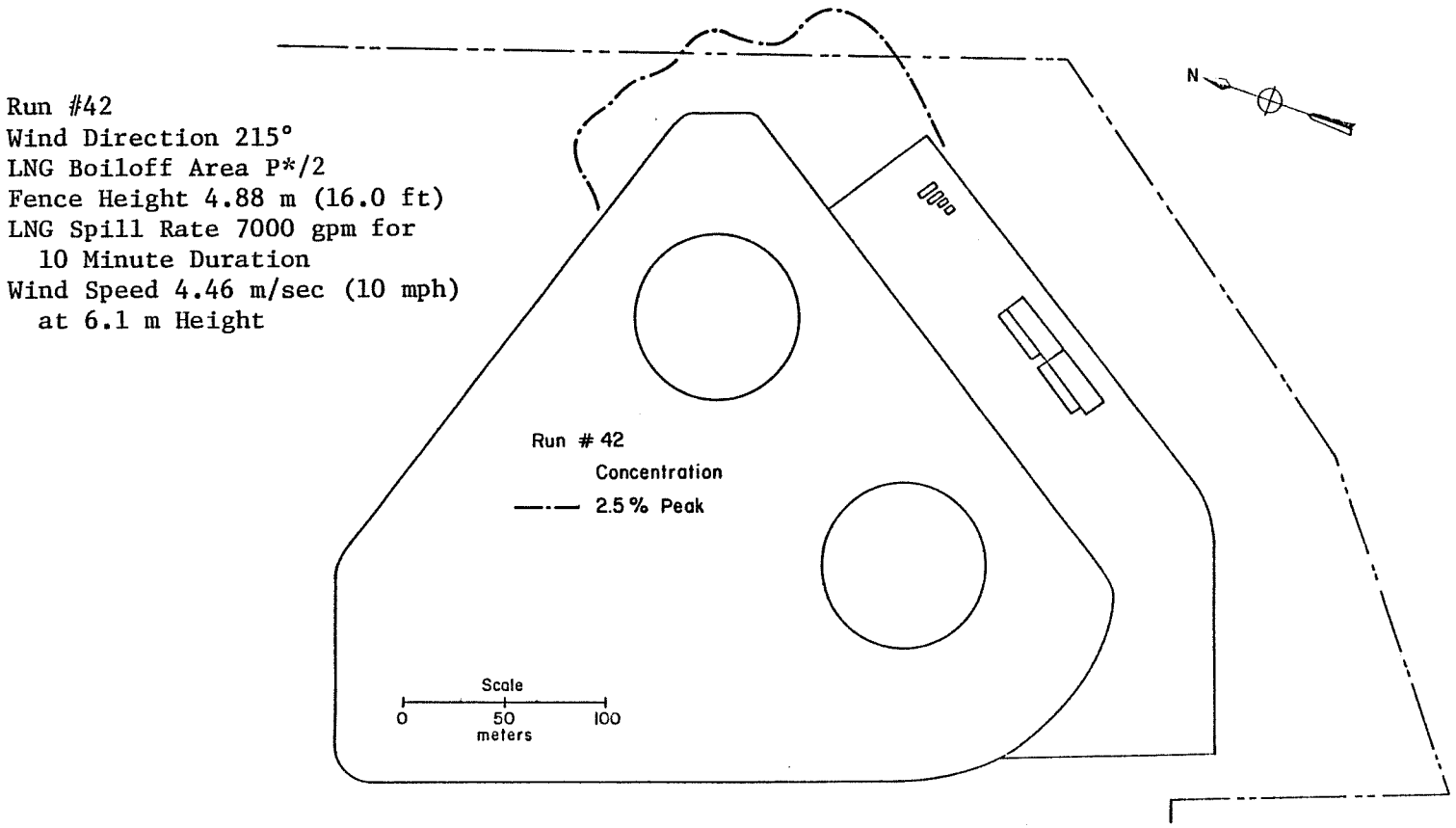

Figure 57. Concentration Isopleths

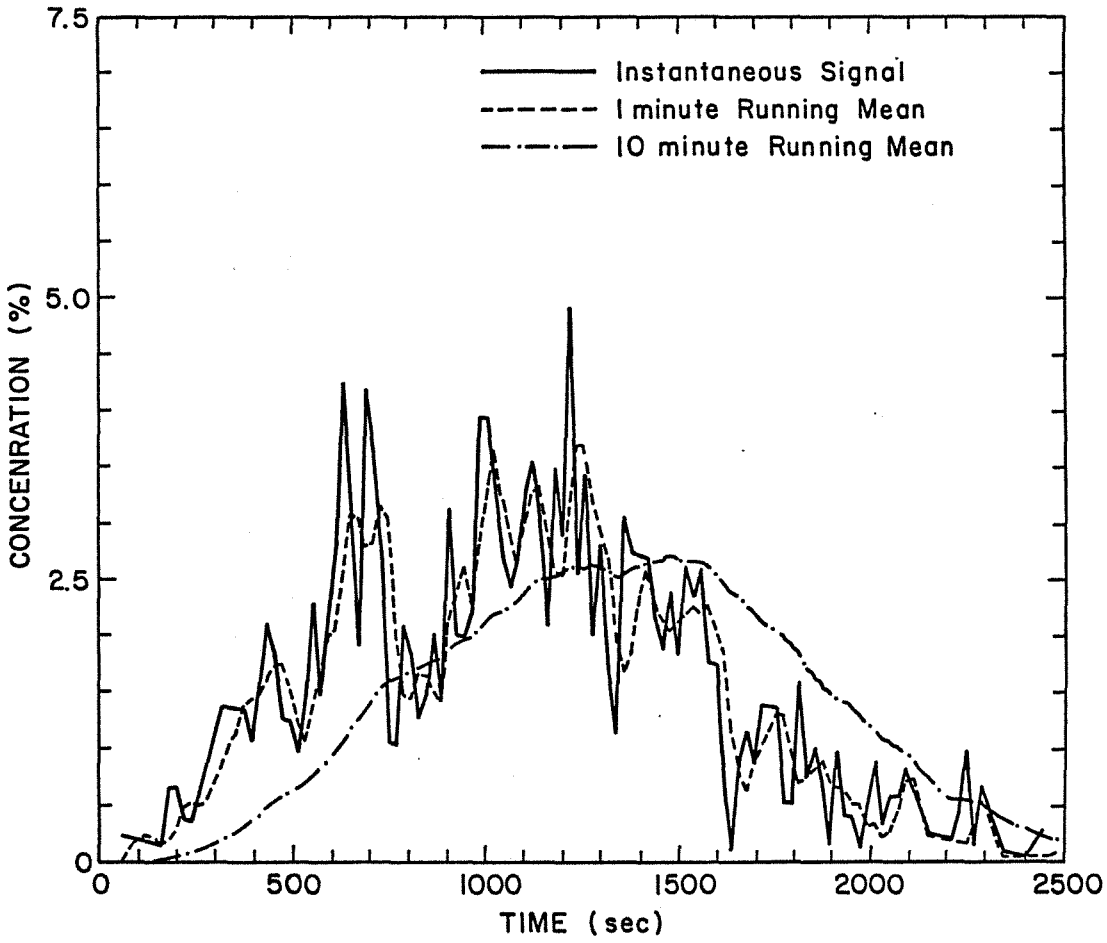

Figure 58. Various Time Average Mean Filters Applied to a Finite Duration Spill Signal (File E04210)

APPENDIX A

THE CALCULATION OF MODEL SCALE FACTORS

APPENDIX A

THE CALCULATION OF MODEL SCALE FACTORS

As discussed previously in Section 2.3, the dominant scaling criteria for the simulation of LNG vapor cloud physics are the Froude number and volume flux ratios. By setting these parameters equal for model and prototype the following relationships for the ETSC facility, length scale (L.S.) 1:250, and a model gas specific gravity, (S.G.) of 1.38 were derived:

$$
\begin{aligned}
U_m &= \left(\frac{S.G._m - 1}{S.G._p - 1}\right)^{1/2} \left(\frac{1}{L.S.}\right)^{1/2} U_p = 0.053\, U_p \,, \\
Q_m &= \left(\frac{S.G._m - 1}{S.G._p - 1}\right)^{1/2} \left(\frac{1}{L.S.}\right)^{2.5} Q_p = 8.411\times10^{-7}\, Q_p \,, \\
t_m &= \left(\frac{S.G._p - 1}{S.G._m - 1}\right)^{1/2} \left(\frac{1}{L.S.}\right)^{1/2} t_p = 0.076\, t_p \,, \\
L_m &= \left(\frac{1}{L.S.}\right) L_p = 4.0\times10^{-3}\, L_p \,.
\end{aligned}
\tag{A.1}
$$

In addition to these scaling parameters governing the flow, the mole fraction measured in the model should be scaled to its prototype value. This scaling is required since the number of moles released in thermal plumes are different than the number of moles being released in an isothermal plume. The relationship is derived by Neff and Meroney (1979) and given by

$$
\chi_p = \frac{\chi_m}{\chi_m + (1 - \chi_m)\left(\frac{T_p}{T_m}\right)_{\text{boiloff}}} \,. \tag{A.2}
$$

Prototype boiloff temperature is approximately 111°K and model release temperature is approximately 300°K, and hence,

$$\chi_p = \frac{\chi_m}{\chi_m + (1 - \chi_m)\ 0.37} \cdot \qquad (A.3)$$

This equation was used to convert the modeled Argon run measurements to those that would be observed in the field.

APPENDIX B

CONCENTRATION DATA WITH LNG SPILL RATES OF 7000 gpm AND 3500 gpm FOR UNLIMITED TIME DURATION

FILE NAME	MODEL CONDITIONS PEAK CONC (%)	MEAN CONC (%)	RMS CONC (%)	PROTOTYPE CONDITIONS POSITION X (M)	Y (M)	Z (M)	PEAK CONC (%)	MEAN CONC (%)	RMS CONC (%)
C001104	.3	0.0	.1	150.0	-225.0	0.0	.9	0.0	.2
C001105	1.1	.2	.2	150.0	-212.5	0.0	2.9	.5	.7
C001106	1.2	.5	.3	150.0	-200.0	0.0	3.2	1.3	.8
C001107	1.0	.4	.2	150.0	-187.5	0.0	2.8	1.1	.6
C001108	2.8	1.0	.4	150.0	-175.0	0.0	7.3	2.6	1.1
C001109	3.5	1.8	.5	150.0	-162.5	0.0	8.8	4.8	1.3
C001110	3.3	2.0	.5	150.0	-150.0	0.0	8.3	5.1	1.3
C001111	2.8	1.7	.4	150.0	-137.5	0.0	7.3	4.6	1.1
D001104	1.7	1.0	.2	200.0	-187.5	0.0	4.3	2.5	.6
D001105	1.5	.8	.2	200.0	-175.0	0.0	3.9	2.0	.6
D001106	1.8	1.1	.3	200.0	-162.5	0.0	4.7	3.0	.7
D001107	1.6	.7	.3	200.0	-150.0	0.0	4.2	1.9	.7
D001108	1.4	.4	.3	200.0	-137.5	0.0	3.6	1.1	.7
D001109	1.1	.3	.2	200.0	-125.0	0.0	2.8	.8	.6
D001110	1.1	.3	.2	200.0	-112.5	0.0	2.8	.8	.6
D001111	.8	.2	.1	200.0	-100.0	0.0	2.1	.7	.5
E001104	1.0	.4	.1	200.0	-87.5	0.0	2.7	1.2	.5
E001105	.7	.3	.1	200.0	-75.0	0.0	1.9	.8	.4
E001106	.5	.2	.1	200.0	-62.5	0.0	1.3	.5	.3
E001107	.3	.1	.1	200.0	-50.0	0.0	.9	.3	.2
E001108	.5	.2	.1	200.0	-37.5	0.0	1.4	.5	.3
E001109	.7	.2	.1	200.0	-25.0	0.0	1.9	.6	.4
E001110	1.0	.5	.1	200.0	-12.5	0.0	2.6	1.3	.4
E001111	.8	.3	.1	200.0	0.0	0.0	2.0	.9	.4
F001104	0.0	0.0	0.0	200.0	12.5	0.0	0.0	0.0	0.0
F001105	.4	0.0	.1	200.0	25.0	0.0	1.0	0.0	.2
F001106	.4	0.0	.1	200.0	37.5	0.0	1.0	0.0	.2
F001107	.1	0.0	.1	200.0	50.0	0.0	.4	0.0	.1
F001108	.1	0.0	.1	200.0	62.5	0.0	.4	0.0	.1
F001109	.3	0.0	.1	200.0	75.0	0.0	.7	0.0	.2
F001110	.5	.1	.1	200.0	87.5	0.0	1.2	.3	.3
F001111	.4	.1	.1	200.0	100.0	0.0	1.1	.3	.2
G001104	0.0	0.0	0.0	200.0	112.5	0.0	0.0	0.0	0.0
G001105	.4	.1	.1	200.0	125.0	0.0	1.0	.3	.2
G001106	.4	.1	.1	200.0	137.5	0.0	1.1	.3	.2
G001107	.3	0.0	.1	200.0	150.0	0.0	.7	0.0	.2
G001108	.3	0.0	.1	200.0	162.5	0.0	.7	0.0	.2
G001109	.1	0.0	.1	200.0	175.0	0.0	.3	0.0	.1
G001110	.3	.1	.1	200.0	187.5	0.0	.9	.1	.2
G001111	.2	0.0	.1	200.0	200.0	0.0	.5	0.0	.1
H001104	3.5	1.0	.4	150.0	0.0	0.0	9.0	2.1	1.0
H001105	3.1	.8	.4	150.0	12.5	0.0	8.1	2.0	1.0
H001106	2.7	.1	.4	150.0	25.0	0.0	7.2	.1	.9
H001107	.9	.1	.1	150.0	37.5	0.0	2.5	.1	.3
H001108	.6	0.0	.1	150.0	50.0	0.0	1.5	0.0	.2
H001109	.9	.1	.1	150.0	62.5	0.0	2.2	.1	.3
H001110	1.1	.5	.1	150.0	75.0	0.0	2.8	1.1	.3
H001111	.7	.2	.1	150.0	87.5	0.0	1.8	.4	.2
I001104	.8	.4	.1	150.0	100.0	0.0	2.1	1.0	.3
I001105	1.1	.5	.2	150.0	112.5	0.0	2.8	1.3	.4
I001106	1.3	.7	.2	150.0	125.0	0.0	3.5	1.9	.5
I001107	.9	.5	.2	150.0	137.5	0.0	2.2	1.1	.3
I001108	.7	.2	.2	150.0	150.0	0.0	1.9	.6	.4
I001109	.5	.2	.1	150.0	162.5	0.0	1.2	.4	.2
I001110	.3	.1	.1	150.0	175.0	0.0	.8	.2	.2
I001111	0.0	0.0	0.0	150.0	187.5	0.0	0.0	0.0	0.0
J001104	.4	0.0	.1	100.0	150.0	0.0	1.0	0.0	.2
J001105	.3	.1	0.0	100.0	162.5	0.0	.8	.2	.1
J001106	.2	.1	0.0	100.0	175.0	0.0	.5	.2	.1
J001107	.1	0.0	0.0	100.0	187.5	0.0	.3	0.0	.1
J001108	.1	0.0	0.0	100.0	200.0	0.0	.3	0.0	.1
J001109	.2	.1	0.0	100.0	212.5	0.0	.4	.1	.1
J001110	.2	.1	0.1	100.0	225.0	0.0	.5	.2	.1
J001111	.1	.1	0.0	100.0	237.5	0.0	.3	.2	.1

FILE NAME	MODEL CONDITIONS PEAK CONC (%)	MEAN CONC (%)	RMS CONC (%)	PROTOTYPE CONDITIONS POSITION X (M)	Y (M)	Z (M)	PEAK CONC (%)	MEAN CONC (%)	RMS CONC (%)
C002204	.2	0.0	.1	150.0	-225.0	0.0	.5	0.0	.3
C002205	1.0	.3	.2	150.0	-212.5	0.0	3.7	.9	.5
C002206	1.0	.4	.2	150.0	-200.0	0.0	3.7	.8	.4
C002207	1.0	.3	.1	150.0	-187.5	0.0	3.5	.8	.4
C002208	1.2	.4	.2	150.0	-175.0	0.0	3.1	1.2	.7
C002209	1.9	.8	.3	150.0	-162.5	0.0	5.1	1.2	.7
C002210	1.6	.6	.3	150.0	-150.0	0.0	4.3	1.1	.6
C002211	2.1	1.2	.2	150.0	-137.5	0.0	5.4	3.1	1.9
D002204	.8	.3	.1	200.0	-187.5	0.0	2.1	.9	.5
D002205	1.0	.4	.2	200.0	-175.0	0.0	2.7	1.1	.6
D002206	1.0	.4	.2	200.0	-162.5	0.0	2.6	1.1	.6
D002207	1.0	.4	.2	200.0	-150.0	0.0	2.9	1.1	.7
D002208	1.0	.3	.2	200.0	-137.5	0.0	2.9	.9	.5
D002209	.8	.3	.1	200.0	-125.0	0.0	2.9	.9	.4
D002210	.8	.2	.1	200.0	-112.5	0.0	2.9	.8	.4
D002211	.4	.1	.1	200.0	-100.0	0.0	1.4	.3	.2
E002204	.5	.2	.1	200.0	-87.5	0.0	1.4	.5	.3
E002205	.4	.1	.1	200.0	-75.0	0.0	1.4	.3	.2
E002206	.6	.2	.1	200.0	-62.5	0.0	1.6	.5	.3
E002207	.5	.2	.1	200.0	-50.0	0.0	1.6	.5	.3
E002208	.5	.2	.1	200.0	-37.5	0.0	1.4	.5	.3
E002209	.6	.3	.1	200.0	-25.0	0.0	1.6	.6	.3
E002210	.9	.3	.1	200.0	-12.5	0.0	2.5	1.1	.6
E002211	.6	.3	.1	200.0	0.0	0.0	1.6	.6	.3
F002204	.4	0.0	.1	200.0	12.5	0.0	1.4	0.0	.2
F002205	.5	.3	.1	200.0	25.0	0.0	1.5	.8	.4
F002206	.4	.2	0.0	200.0	37.5	0.0	1.1	.7	.3
F002207	.3	.1	0.0	200.0	50.0	0.0	.7	.3	.2
F002208	.1	0.0	0.0	200.0	62.5	0.0	.3	0.0	.1
F002209	.1	0.0	0.0	200.0	75.0	0.0	.3	0.0	.1
F002210	.1	0.0	.1	200.0	87.5	0.0	.3	0.0	.1
F002211	.3	.1	0.0	200.0	100.0	0.0	.8	.4	.2
G002204	.6	.3	.1	200.0	112.5	0.0	1.6	.9	.4
G002205	.6	.3	.1	200.0	125.0	0.0	1.6	.9	.4
G002206	.8	.4	.1	200.0	137.5	0.0	2.0	1.2	.5
G002207	.6	.2	.1	200.0	150.0	0.0	1.5	.6	.3
G002208	.2	.1	0.0	200.0	162.5	0.0	.5	.2	.1
G002209	.2	.1	.1	200.0	175.0	0.0	.5	.2	.1
G002210	.4	.1	.1	200.0	187.5	0.0	1.0	.3	.2
G002211	.1	0.0	.1	200.0	200.0	0.0	.3	0.0	.1
H002204	1.6	.6	.3	150.0	0.0	0.0	4.4	1.6	.8
H002205	1.5	.5	.2	150.0	12.5	0.0	4.0	1.5	.8
H002206	1.2	.5	.1	150.0	25.0	0.0	3.2	1.5	.7
H002207	.8	.2	.1	150.0	37.5	0.0	2.3	.7	.4
H002208	.5	.1	.1	150.0	50.0	0.0	1.5	.5	.3
H002209	.6	.2	.1	150.0	62.5	0.0	1.6	.5	.3
H002210	.7	0.0	.1	150.0	75.0	0.0	1.9	0.0	.4
H002211	.6	.2	.1	150.0	87.5	0.0	1.6	.6	.3
I002204	.7	.3	.1	150.0	100.0	0.0	1.8	.8	.4
I002205	.7	.1	.1	150.0	112.5	0.0	2.0	.4	.2
I002206	.9	.1	.2	150.0	125.0	0.0	2.3	.3	.3
I002207	.8	.1	.2	150.0	137.5	0.0	1.9	.3	.3
I002208	.6	.1	.1	150.0	150.0	0.0	1.7	.3	.2
I002209	.3	0.0	0.0	150.0	162.5	0.0	.8	0.0	.1
I002210	.4	.2	.1	150.0	175.0	0.0	1.1	.6	.2
I002211	.1	0.0	0.0	150.0	187.5	0.0	.3	0.0	.1
J002204	.6	0.0	.1	100.0	150.0	0.0	1.7	0.0	.2
J002205	.2	.1	0.0	100.0	162.5	0.0	.7	.3	.1
J002206	.4	.2	.1	100.0	175.0	0.0	1.0	.5	.2
J002207	.1	0.0	0.0	100.0	187.5	0.0	.4	0.0	.1
J002208	.1	0.0	0.0	100.0	200.0	0.0	.4	0.0	.1
J002209	.2	.1	0.0	100.0	212.5	0.0	.5	.2	.1
J002210	.4	.1	.1	100.0	225.0	0.0	1.0	.4	.2
J002211	.1	0.0	.1	100.0	237.5	0.0	.2	0.0	.1

MODEL CONDITIONS				PROTOTYPE CONDITIONS					
FILE NAME	PEAK CONC (%)	MEAN CONC (%)	RMS CONC (%)	POSITION X (M)	Y (M)	Z (M)	PEAK CONC (%)	MEAN CONC (%)	RMS CONC (%)
C00304	.7	.2	.1	150.0	-225.0	0.0	1.9	.6	.2
C00305	.9	.4	.1	150.0	-212.5	0.0	2.4	.8	.2
C00306	1.4	1.0	.1	150.0	-200.0	0.0	3.7	2.5	.1
C00307	1.9	.8	.1	150.0	-187.5	0.0	4.9	2.1	.1
C00308	1.5	.7	.2	150.0	-175.0	0.0	3.9	1.9	.1
C00309	1.2	1.2	.2	150.0	-162.5	0.0	3.1	3.1	.1
C00310	2.7	1.6	.2	150.0	-150.0	0.0	7.0	4.3	.1
C00311	2.2	1.3	.2	150.0	-137.5	0.0	5.8	3.5	.0
D00304	.2	0.0	.1	200.0	-187.5	0.0	.6	.0	.0
D00305	.5	.1	.1	200.0	-175.0	0.0	1.3	.3	.0
D00306	.7	.2	.2	200.0	-162.5	0.0	1.8	.5	.0
D00307	.7	.3	.1	200.0	-150.0	0.0	1.8	.8	.0
D00308	.7	.4	.1	200.0	-137.5	0.0	1.8	.9	.0
D00309	.9	.3	.2	200.0	-125.0	0.0	2.3	.8	.0
D00310	.8	.2	.1	200.0	-112.5	0.0	2.0	.7	.0
D00311	1.0	.6	.1	200.0	-100.0	0.0	2.7	1.5	.0
E00304	.2	0.0	.1	200.0	-87.5	0.0	.5	.0	.0
E00305	.2	0.0	.1	200.0	-75.0	0.0	.5	.0	.0
E00306	.2	0.0	.1	200.0	-62.5	0.0	.5	.0	.0
E00307	.3	0.0	.1	200.0	-50.0	0.0	.9	.0	.0
E00308	.5	.1	.1	200.0	-37.5	0.0	1.4	.3	.0
E00309	.5	.1	.1	200.0	-25.0	0.0	1.3	.3	.0
E00310	.6	.2	.1	200.0	-12.5	0.0	1.5	.5	.0
E00311	.6	.3	.1	200.0	0.0	0.0	1.6	.7	.0
F00304	.4	0.0	.1	200.0	12.5	0.0	1.1	.0	.0
F00305	.3	0.0	.1	200.0	25.0	0.0	.7	.0	.0
F00306	.3	0.0	.1	200.0	37.5	0.0	.7	.0	.0
F00307	.3	.1	.1	200.0	50.0	0.0	.7	.3	.0
F00308	.2	0.0	0.0	200.0	62.5	0.0	.5	.0	.0
F00309	.2	0.0	0.0	200.0	75.0	0.0	.5	.0	.0
F00310	.3	0.0	.1	200.0	87.5	0.0	.5	.0	.0
F00311	.2	0.0	.1	200.0	100.0	0.0	.5	.0	.0
G00304	.4	.1	.1	200.0	112.5	0.0	1.0	.3	.0
G00305	.3	.1	.1	200.0	125.0	0.0	.8	.3	.0
G00306	.3	.1	.1	200.0	137.5	0.0	.8	.3	.0
G00307	.3	.1	.1	200.0	150.0	0.0	.8	.3	.0
G00308	.2	0.0	.1	200.0	162.5	0.0	.6	.0	.0
G00309	.2	.1	0.0	200.0	175.0	0.0	.6	.3	.0
G00310	.2	.1	0.0	200.0	187.5	0.0	.6	.3	.0
G00311	.2	.1	0.0	200.0	200.0	0.0	.5	.2	.0
H00304	2.1	.5	.2	150.0	0.0	0.0	5.4	1.1	.5
H00305	1.8	.6	.2	150.0	12.5	0.0	4.6	1.6	.5
H00306	1.3	.4	.2	150.0	25.0	0.0	3.4	1.0	.5
H00307	.6	.2	.1	150.0	37.5	0.0	1.7	.6	.2
H00308	.4	.1	0.0	150.0	50.0	0.0	1.0	.4	.1
H00309	.5	.1	.1	150.0	62.5	0.0	1.1	.4	.1
H00310	.6	.1	.1	150.0	75.0	0.0	1.5	.4	.1
H00311	.5	.1	.1	150.0	87.5	0.0	1.4	.3	.1
I00304	.5	.1	.1	150.0	100.0	0.0	1.2	.3	.1
I00305	.6	.1	.1	150.0	112.5	0.0	1.5	.3	.1
I00306	.6	.2	.1	150.0	125.0	0.0	1.5	.5	.1
I00307	.6	.1	.1	150.0	137.5	0.0	1.5	.3	.1
I00308	.6	.1	.1	150.0	150.0	0.0	1.6	.3	.1
I00309	.3	0.0	.1	150.0	162.5	0.0	.8	.0	.0
I00310	.2	0.0	.1	150.0	175.0	0.0	.6	.0	.0
I00311	.1	0.0	0.0	150.0	187.5	0.0	.4	.0	.0
J00304	.5	.2	.1	100.0	150.0	0.0	1.4	.5	.2
J00305	.3	.1	0.0	100.0	162.5	0.0	.7	.2	.1
J00306	.3	.1	0.0	100.0	175.0	0.0	.7	.2	.1
J00307	.2	.1	0.0	100.0	187.5	0.0	.5	.2	.1
J00308	.2	.1	0.0	100.0	200.0	0.0	.5	.2	.1
J00309	.2	.1	0.0	100.0	212.5	0.0	.5	.2	.1
J00310	.4	.2	.1	100.0	225.0	0.0	1.0	.5	.2
J00311	.1	0.0	0.0	100.0	237.5	0.0	.2	0.0	.1

FILE NAME	MODEL CONDITIONS PEAK CONC (%)	MEAN CONC (%)	RMS CONC (%)	PROTOTYPE CONDITIONS POSITION X (M)	Y (M)	Z (M)	PEAK CONC (%)	MEAN CONC (%)	RMS CONC (%)
C00404	.4	.1	.1	150.0	-225.0	0.0	1.2	.2	.2
C00405	.8	.3	.1	150.0	-212.5	0.0	2.1	.8	.3
C00406	.7	.3	.1	150.0	-200.0	0.0	1.9	.8	.3
C00407	.5	.2	.1	150.0	-187.5	0.0	1.3	.6	.2
C00408	.5	.2	.1	150.0	-175.0	0.0	1.3	.5	.2
C00409	.8	.4	.1	150.0	-162.5	0.0	2.2	1.0	.4
C00410	.8	.2	.1	150.0	-150.0	0.0	2.2	.5	.4
C00411	1.0	.7	.1	150.0	-137.5	0.0	2.9	1.0	.3
D00404	0.0	0.0	0.0	200.0	-187.5	0.0	0.0	0.0	0.0
D00405	.5	.1	0.0	200.0	-175.0	0.0	1.3	.4	.2
D00406	.6	.0	0.0	200.0	-162.5	0.0	1.6	0.0	.4
D00407	.5	.2	0.0	200.0	-150.0	0.0	1.4	.5	.3
D00408	.6	.2	0.0	200.0	-137.5	0.0	1.6	.5	.3
D00409	.8	.2	0.0	200.0	-125.0	0.0	2.1	.5	.3
D00410	.4	.0	0.0	200.0	-112.5	0.0	1.0	0.0	.2
D00411	.6	0.0	0.0	200.0	-100.0	0.0	1.6	0.0	.2
E00404	.2	0.0	.1	200.0	-187.5	0.0	0.0	0.0	.1
E00405	.5	.2	0.0	200.0	-175.0	0.0	1.3	.6	.1
E00406	.6	.3	.1	200.0	-162.5	0.0	1.6	.8	.2
E00407	.4	.1	.1	200.0	-150.0	0.0	1.1	.3	.2
E00408	.6	.1	.1	200.0	-137.5	0.0	1.7	.3	.2
E00409	.5	.2	.1	200.0	-125.0	0.0	1.3	.6	.2
E00410	.6	.2	.1	200.0	-112.5	0.0	1.5	.5	.3
E00411	.5	.2	.1	200.0	-100.0	0.0	1.2	.6	.2
F00404	.4	.1	.1	200.0	-12.5	0.0	1.1	.4	.2
F00405	.2	0.0	0.0	200.0	25.0	0.0	0.0	0.0	.1
F00406	.5	.3	.1	200.0	37.5	0.0	1.3	.9	.2
F00407	.3	.2	0.0	200.0	50.0	0.0	.8	.5	.1
F00408	.3	.2	0.0	200.0	62.5	0.0	.8	.5	.1
F00409	.4	.3	0.0	200.0	75.0	0.0	1.1	.7	.1
F00410	.7	.4	.1	200.0	87.5	0.0	1.8	1.1	.2
F00411	.4	.3	.1	200.0	100.0	0.0	1.1	.8	.2
G00404	.5	.3	.1	200.0	112.5	0.0	1.3	.8	.2
G00405	.3	.1	.1	200.0	125.0	0.0	.8	.2	.1
G00406	.4	.2	.1	200.0	137.5	0.0	1.1	.6	.2
G00407	.3	.1	.1	200.0	150.0	0.0	.8	.2	.2
G00408	.3	.1	0.0	200.0	162.5	0.0	.8	.3	.1
G00409	.3	.1	.1	200.0	175.0	0.0	.8	.3	.1
G00410	.5	.4	.1	200.0	187.5	0.0	1.4	1.0	.2
G00411	.3	.2	0.0	200.0	200.0	0.0	.8	.4	.1
H00404	1.0	.6	.2	150.0	0.0	0.0	4.7	1.7	.5
H00405	1.5	.3	.2	150.0	12.5	0.0	3.9	.8	.5
H00406	1.1	.3	.1	150.0	25.0	0.0	3.2	.7	.3
H00407	.4	.1	.1	150.0	37.5	0.0	1.0	.2	.2
H00408	.4	.1	.1	150.0	50.0	0.0	1.0	.2	.1
H00409	.4	.1	.1	150.0	62.5	0.0	1.1	.2	.2
H00410	.2	0.0	.1	150.0	75.0	0.0	0.0	0.0	.2
H00411	.7	.3	.1	150.0	87.5	0.0	1.8	.8	.2
I00404	.4	.1	.1	150.0	100.0	0.0	1.1	.4	.2
I00405	.8	.2	.1	150.0	112.5	0.0	2.1	.5	.2
I00406	.7	.3	.1	150.0	125.0	0.0	1.8	.9	.2
I00407	.7	.2	.1	150.0	137.5	0.0	1.8	.6	.2
I00408	.6	.2	.1	150.0	150.0	0.0	1.5	.6	.2
I00409	.4	.1	0.0	150.0	162.5	0.0	1.1	.4	.1
I00410	.4	.2	.1	150.0	175.0	0.0	1.1	.4	.2
I00411	.2	.1	0.0	150.0	187.5	0.0	.4	.2	.1
J00404	.1	0.0	0.0	100.0	150.0	0.0	.4	0.0	.1
J00405	.1	0.0	0.0	100.0	162.5	0.0	.4	0.0	.1
J00406	.1	0.0	.1	100.0	175.0	0.0	.4	0.0	.2
J00407	0.0	0.0	0.0	100.0	187.5	0.0	0.0	0.0	0.0
J00408	.1	0.0	0.0	100.0	200.0	0.0	.4	0.0	.1
J00409	0.0	0.0	0.0	100.0	212.5	0.0	0.0	0.0	0.0
J00410	.1	0.0	.1	100.0	225.0	0.0	.4	0.0	.1
J00411	0.0	0.0	0.0	100.0	237.5	0.0	0.0	0.0	0.0

MODEL CONDITIONS				PROTOTYPE CONDITIONS					
				POSITION					
FILE NAME	PEAK CONC (%)	MEAN CONC (%)	RMS CONC (%)	X (M)	Y (M)	Z (M)	PEAK CONC (%)	MEAN CONC (%)	RMS CONC (%)
A00504	.1	0.0	0.0	0.0	-300.0	0.0	.4	0.0	.2
A00505	.1	0.0	0.0	0.0	-287.5	0.0	.2	0.0	.1
A00506	.1	0.0	0.0	0.0	-275.0	0.0	.3	0.0	.1
A00507	.3	.1	0.0	0.0	-262.5	0.0	.7	.3	.2
A00508	.2	0.0	0.0	0.0	-250.0	0.0	.4	0.0	.1
A00509	.5	.3	0.0	0.0	-237.5	0.0	1.4	.8	.2
A00510	.9	.4	.1	0.0	-225.0	0.0	2.5	1.0	.4
A00511	1.9	.6	.2	0.0	-212.5	0.0	5.0	1.5	.6
B00504	.1	0.0	.1	50.0	-275.0	0.0	.3	0.0	.3
B00505	.2	.1	.1	50.0	-262.5	0.0	.5	.1	.3
B00506	0.0	0.0	0.0	50.0	-250.0	0.0	0.0	0.0	0.0
B00507	.5	.1	.1	50.0	-237.5	0.0	1.4	.2	.4
B00508	.3	0.0	.1	50.0	-225.0	0.0	.8	0.0	.5
B00509	1.1	.4	.2	50.0	-212.5	0.0	2.9	1.1	.5
B00510	1.4	.5	.2	50.0	-200.0	0.0	3.7	1.3	.7
B00511	2.8	1.3	.4	50.0	-187.5	0.0	7.2	3.3	1.1
C00504	.9	.3	.1	100.0	-200.0	0.0	2.3	.8	.5
C00505	1.2	.6	.2	100.0	-187.5	0.0	3.1	1.5	.6
C00506	1.5	.7	.2	100.0	-175.0	0.0	4.1	1.9	.7
C00507	1.8	.9	.2	100.0	-162.5	0.0	4.7	2.4	.7
C00508	1.8	1.0	.2	100.0	-150.0	0.0	4.7	2.5	.8
C00509	2.1	1.1	.3	100.0	-137.5	0.0	5.5	3.0	.8
C00510	1.7	.8	.2	100.0	-125.0	0.0	5.4	2.1	.6
C00511	1.3	.6	.2	100.0	-112.5	0.0	3.5	1.7	.6
D00504	.6	.1	.1	150.0	-125.0	0.0	1.7	.2	.4
D00505	.6	.2	.1	150.0	-112.5	0.0	1.7	.5	.3
D00506	.3	.1	.1	150.0	-100.0	0.0	.9	.2	.2
D00507	.7	.3	.1	150.0	-87.5	0.0	1.7	.7	.3
D00508	.5	.2	.1	150.0	-75.0	0.0	1.2	.4	.2
D00509	.8	.3	.1	150.0	-62.5	0.0	2.2	.8	.4
D00510	1.1	.3	.2	150.0	-50.0	0.0	2.9	.8	.6
D00511	1.8	.6	.2	150.0	-37.5	0.0	4.6	1.6	.8
E00504	.3	0.0	.1	200.0	-87.5	0.0	.7	0.0	.3
E00505	.3	.1	.1	200.0	-75.0	0.0	.9	.3	.3
E00506	.1	0.0	.1	200.0	-62.5	0.0	.4	0.0	.1
E00507	.1	0.0	.1	200.0	-50.0	0.0	.4	0.0	.2
E00508	.5	0.0	.1	200.0	-37.5	0.0	1.4	0.0	.3
E00509	.4	0.0	.1	200.0	-25.0	0.0	1.1	0.0	.4
E00510	.5	0.0	.2	200.0	-12.5	0.0	1.2	0.0	.4
E00511	.9	.2	.2	200.0	0.0	0.0	2.3	.5	.5
F00504	.8	.2	.2	200.0	12.5	0.0	2.1	.5	.4
F00505	.8	.3	.2	200.0	25.0	0.0	2.1	.7	.4
F00506	1.1	.1	.1	200.0	37.5	0.0	2.8	.4	.4
F00507	.8	.2	.1	200.0	50.0	0.0	2.1	.6	.4
F00508	.7	.2	.1	200.0	62.5	0.0	1.8	.5	.2
F00509	.2	0.0	.1	200.0	75.0	0.0	.6	0.0	.2
F00510	.2	0.0	.1	200.0	87.5	0.0	.5	0.0	.2
F00511	.3	0.0	.1	200.0	100.0	0.0	.7	0.0	.1

MODEL CONDITIONS				PROTOTYPE CONDITIONS					
FILE NAME	PEAK CONC (%)	MEAN CONC (%)	RMS CONC (%)	POSITION X (M)	Y (M)	Z (M)	PEAK CONC (%)	MEAN CONC (%)	RMS CONC (%)
A006604	.3	.1	.1	0.0	-300.0	0.0	.8	.4	.1
A006605	.2	.1	.1	0.0	-287.5	0.0	.5	.3	.1
A006606	.6	.4	.1	0.0	-275.0	0.0	1.7	1.2	.3
A006607	.6	.3	.2	0.0	-262.5	0.0	1.7	.8	.5
A006608	1.9	1.4	.2	0.0	-250.0	0.0	4.8	3.8	.6
A006609	.8	.3	.1	0.0	-237.5	0.0	2.1	.7	.4
A006610	.6	.2	.1	0.0	-225.0	0.0	1.6	.5	.4
A006611	1.0	.3	.1	0.0	-212.5	0.0	2.5	.8	.4
B006604	.1	0.0	.2	50.0	-275.0	0.0	.2	0.0	.1
B006605	.2	0.0	.1	50.0	-262.5	0.0	.6	0.0	.1
B006606	0.0	0.0	0.0	50.0	-250.0	0.0	0.0	0.0	0.0
B006607	.5	0.0	.1	50.0	-237.5	0.0	1.4	0.0	.3
B006608	.7	.2	.1	50.0	-225.0	0.0	1.8	.5	.3
B006609	.9	.3	.2	50.0	-212.5	0.0	2.5	.7	.5
B006610	1.1	.3	.2	50.0	-200.0	0.0	3.0	.8	.6
B006611	2	.4	.3	50.0	-187.5	0.0	5.6	1.2	.7
C006604	.2	.2	.1	100.0	-200.0	0.0	1.4	.5	.4
C006605	.2	.1	.1	100.0	-187.5	0.0	2.0	.2	.4
C006606	.6	.1	.1	100.0	-175.0	0.0	1.5	.3	.3
C006607	.6	.3	.1	100.0	-162.5	0.0	2.0	.9	.3
C006608	2.9	2.7	.3	100.0	-150.0	0.0	9.9	8.9	.7
C006609	1.5	.6	.2	100.0	-137.5	0.0	4.0	1.6	.5
C006610	1.4	.6	.2	100.0	-125.0	0.0	3.6	1.6	.4
C006611	1.2	.6	.2	100.0	-112.5	0.0	3.3	1.7	.4
D006604	.2	0.0	.1	150.0	-125.0	0.0	.9	0.0	.3
D006605	.3	0.0	.1	150.0	-112.5	0.0	1.3	0.0	.2
D006606	.3	0.0	.1	150.0	-100.0	0.0	.7	0.0	.2
D006607	.3	0.0	.1	150.0	-87.5	0.0	.8	0.0	.3
D006608	.6	.1	.1	150.0	-75.0	0.0	1.5	.3	.3
D006609	.7	0.0	.1	150.0	-62.5	0.0	1.8	0.0	.4
D006610	.6	0.0	.1	150.0	-37.5	0.0	1.7	0.0	.4
D006611	1.1	.2	.1	150.0	-37.5	0.0	2.9	.5	.5
E006604	.5	.2	.1	200.0	-87.5	0.0	1.5	.7	.3
E006605	.6	.3	.1	200.0	-75.0	0.0	1.7	.7	.3
E006606	.6	.4	.1	200.0	-62.5	0.0	1.6	1.0	.2
E006607	.8	.5	.1	200.0	-50.0	0.0	2.2	1.3	.3
E006608	.9	.4	.1	200.0	-37.5	0.0	2.3	1.1	.3
E006609	.9	.5	.1	200.0	-25.0	0.0	2.5	1.3	.3
E006610	.7	.3	.1	200.0	-12.5	0.0	1.9	.8	.3
E006611	1.0	.3	.2	200.0	0.0	0.0	2.8	.9	.4
F006604	.9	.4	.1	200.0	12.5	0.0	2.3	1.2	.3
F006605	.8	.3	.1	200.0	25.0	0.0	2.1	.8	.3
F006606	.8	.5	.1	200.0	37.5	0.0	2.1	1.4	.2
F006607	.7	.5	.1	200.0	50.0	0.0	1.9	1.3	.2
F006608	.8	.4	.1	200.0	62.5	0.0	2.2	1.1	.2
F006609	.6	.1	.6	200.0	75.0	0.0	1.6	.2	1.6
F006610	.4	.2	.1	200.0	87.5	0.0	1.1	.5	.2
F006611	.3	.1	0.0	200.0	100.0	0.0	.7	0.0	0.0
G006604	0.0	0.0	0.0	150.0	112.5	0.0	0.0	0.0	0.0
G006605	0.0	0.0	0.0	150.0	125.0	0.0	0.0	0.0	0.0
G006606	.1	0.0	.1	150.0	137.5	0.0	.3	0.0	.2
G006607	0.0	0.0	0.0	150.0	150.0	0.0	0.0	0.0	0.0
G006608	.6	.5	.1	150.0	162.5	0.0	1.6	1.3	.1
G006609	0.0	0.0	0.0	150.0	175.0	0.0	0.0	0.0	0.0
G006610	0.0	0.0	0.0	150.0	187.5	0.0	0.0	0.0	0.0
G006611	0.0	0.0	0.0	150.0	200.0	0.0	0.0	0.0	0.0

MODEL CONDITIONS				PROTOTYPE CONDITIONS					
FILE NAME	PEAK CONC (%)	MEAN CONC (%)	RMS CONC (%)	POSITION X (M)	Y (M)	Z (M)	PEAK CONC (%)	MEAN CONC (%)	RMS CONC (%)
A007O4	.2	.1	.1	0.0	-300.0	0.0	.6	.2	
A007O5	.1	0.0	.1	0.0	-287.5	0.0	.3	0.0	
A007O6	.5	.3	.1	0.0	-275.0	0.0	1.3	.7	
A007O7	.2	.2	0.0	0.0	-262.5	0.0	.9	.4	
A007O8	.2	.1	0.0	0.0	-250.0	0.0	.8	.3	
A007O9	.5	.2	.1	0.0	-237.5	0.0	1.3	.5	
A007I0	.5	.1	.1	0.0	-225.0	0.0	1.4	.2	
A007I1	.8	.4	.1	0.0	-212.5	0.0	2.1	.9	
B007O4	.3	.2	.1	50.0	-275.0	0.0	.7	.4	
B007O5	.5	.1	.1	50.0	-262.5	0.0	.9	.4	
B007O6	.5	.3	.1	50.0	-250.0	0.0	1.1	.5	
B007O7	.5	.3	.1	50.0	-237.5	0.0	1.1	.5	
B007O8	.7	.3	.1	50.0	-225.0	0.0	1.8	.8	
B007O9	.9	.5	.1	50.0	-212.5	0.0	2.4	1.1	
B007I0	.6	0.0	.2	50.0	-200.0	0.0	1.5	.6	
B007I1	1.9	.7	.2	50.0	-187.5	0.0	4.4	1.6	
C007O4	1.6	.7	.1	100.0	-262.5	0.0	3.9	1.6	
C007O5	1.5	.6	.2	100.0	-250.0	0.0	3.6	1.5	
C007O6	1.5	.9	.2	100.0	-237.5	0.0	3.6	2.1	
C007O7	1.9	.9	.1	100.0	-225.0	0.0	4.6	2.1	
C007O8	1.7	.5	.1	100.0	-212.5	0.0	4.2	1.3	
C007O9	1.7	.5	.1	100.0	-200.0	0.0	4.2	1.3	
C007I0	2.0	1.3	.2	100.0	-187.5	0.0	4.7	3.0	
C007I1	1.6	.5	.1	100.0	-175.0	0.0	3.8	1.2	
D007O4	.7	.5	.1	150.0	-262.5	0.0	1.9	1.2	
D007O5	.4	.3	.1	150.0	-250.0	0.0	1.0	.7	
D007O6	.5	.3	.1	150.0	-237.5	0.0	1.2	.7	
D007O7	.4	.1	.1	150.0	-225.0	0.0	1.0	.3	
D007O8	.4	.1	.1	150.0	-212.5	0.0	1.0	.3	
D007O9	.6	.3	.1	150.0	-200.0	0.0	1.5	.8	
D007I0	.5	0.0	.1	150.0	-187.5	0.0	1.3	0.0	
D007I1	1.0	.4	.1	150.0	-175.0	0.0	2.6	1.0	
E007O4	.4	.2	.1	200.0	-187.5	0.0	1.1	.5	
E007O5	.9	.4	.1	200.0	-175.0	0.0	2.2	1.1	
E007O6	.4	.1	.1	200.0	-162.5	0.0	1.0	.3	
E007O7	.7	.3	.1	200.0	-150.0	0.0	1.7	.8	
E007O8	.9	.4	.1	200.0	-137.5	0.0	2.3	1.0	
E007O9	1.1	.6	.1	200.0	-125.0	0.0	2.8	1.5	
E007I0	1.3	.8	.2	200.0	-112.5	0.0	3.3	2.0	
E007I1	1.0	.5	.1	200.0	-100.0	0.0	2.6	1.3	
C207O4	1.2	.7	.1	150.0	-125.0	0.0	3.1	1.7	
C207O5	1.0	.6	.1	150.0	-112.5	0.0	2.6	1.5	
C207O6	1.5	.8	.1	150.0	-100.0	0.0	3.9	2.1	
C207O7	1.1	.6	.1	150.0	-87.5	0.0	2.8	1.5	
C207O8	1.2	.5	.1	150.0	-75.0	0.0	3.1	1.3	
C207O9	1.0	.5	.1	150.0	-62.5	0.0	2.6	1.3	
C207I0	1.4	.7	.1	150.0	-50.0	0.0	3.6	1.9	
C207I1	.9	.4	.1	150.0	-37.5	0.0	2.4	1.0	
F007O4	.2	.2	.1	200.0	-112.5	0.0	.5	.5	
F007O5	.2	.2	.1	200.0	-100.0	0.0	.5	.5	
F007O8	.2	.2	.1	200.0	-37.5	0.0	.5	.5	
F007O7	.4	.1	.1	200.0	-50.0	0.0	1.0	.3	
F007O8	.2	.1	0.0	200.0	-62.5	0.0	.5	.3	
F007O9	.1	0.0	0.0	200.0	-75.0	0.0	0.0	0.0	
F007I0	0.0	0.0	0.0	200.0	-87.5	0.0	0.0	0.0	
F007I1	0.0	0.0	0.0	200.0	100.0	0.0	0.0	0.0	0.0
G007O4	.4	.2	.1	150.0	112.5	0.0	1.1	.5	
G007O5	.3	.2	.1	150.0	125.0	0.0	.8	.5	
G007O6	.5	.4	.1	150.0	137.5	0.0	1.3	1.0	
G007O7	.3	.1	.1	150.0	150.0	0.0	.8	.3	
G007O8	.2	.1	0.0	150.0	162.5	0.0	.5	.3	
G007O9	.5	.3	.1	150.0	175.0	0.0	1.4	.8	
G007I0	.5	.3	.1	150.0	187.5	0.0	1.4	.8	
G007I1	.3	.2	0.0	150.0	200.0	0.0	.9	.5	

MODEL CONDITIONS				PROTOTYPE CONDITIONS					
FILE NAME	PEAK CONC (%)	MEAN CONC (%)	RMS CONC (%)	POSITION X (M)	Y (M)	Z (M)	PEAK CONC (%)	MEAN CONC (%)	RMS CONC (%)
A006804	.6	.4	.1	0.0	-300.0	0.0	1.5	1.0	.2
A006805	.7	.5	.1	0.0	-287.5	0.0	1.8	1.3	.2
A006806	1.1	.8	.1	0.0	-275.0	0.0	3.0	2.2	.3
A006807	.8	.6	.1	0.0	-262.5	0.0	2.1	1.6	.2
A006808	.8	.5	.1	0.0	-250.0	0.0	2.0	1.3	.2
A006809	1.2	.8	.1	0.0	-237.5	0.0	3.3	2.2	.3
A006810	1.6	1.0	.1	0.0	-225.0	0.0	4.2	2.8	.4
A006811	1.3	.7	.1	0.0	-212.5	0.0	3.5	1.9	.3
B006804	.4	.3	0.0	50.0	-275.0	0.0	1.1	.8	.1
B006805	.4	.1	.1	50.0	-262.5	0.0	1.0	.4	.2
B006806	1.0	.7	.1	50.0	-250.0	0.0	2.6	1.8	.2
B006807	.7	.5	.1	50.0	-237.5	0.0	1.8	1.2	.2
B006808	.1	0.0	.1	50.0	-225.0	0.0	.2	0.0	.2
B006809	.8	.5	.1	50.0	-212.5	0.0	2.0	1.3	.2
B006810	1.2	.6	.1	50.0	-200.0	0.0	3.1	1.7	.3
B006811	1.0	.5	.1	50.0	-187.5	0.0	2.7	1.4	.2
C006804	.9	.7	.1	100.0	-200.0	0.0	2.5	1.8	.2
C006805	1.2	.8	.1	100.0	-187.5	0.0	3.1	2.0	.3
C006806	1.5	.9	.1	100.0	-175.0	0.0	4.0	2.5	.4
C006807	1.2	.8	.1	100.0	-162.5	0.0	3.1	2.1	.3
C006808	2.1	1.1	.6	100.0	-150.0	0.0	5.4	2.8	1.7
C006809	1.6	1.0	.2	100.0	-137.5	0.0	4.2	2.6	.4
C006810	1.4	1.0	.1	100.0	-125.0	0.0	3.7	2.6	.3
C006811	1.0	.6	.1	100.0	-112.5	0.0	2.5	1.5	.2
D006804	.8	.6	.1	150.0	-125.0	0.0	2.1	1.5	.2
D006805	.8	.5	.1	150.0	-112.5	0.0	2.2	1.4	.2
D006806	.9	.7	.1	150.0	-100.0	0.0	2.5	1.8	.3
D006807	.7	.4	.1	150.0	-87.5	0.0	1.9	1.2	.2
D006808	.5	.3	.1	150.0	-75.0	0.0	1.4	.8	.2
D006809	.8	.5	.1	150.0	-62.5	0.0	2.1	1.4	.2
D006810	1.0	.7	.1	150.0	-50.0	0.0	2.6	1.7	.2
D006811	.6	.4	.1	150.0	-37.5	0.0	1.7	1.1	.2
E006804	.5	.2	.1	200.0	-87.5	0.0	1.3	.5	.2
E006805	.5	.1	.1	200.0	-75.0	0.0	1.4	.4	.3
E006806	.7	.2	.2	200.0	-62.5	0.0	2.0	.5	.5
E006807	.6	.1	.1	200.0	-50.0	0.0	1.6	.4	.4
E006808	.9	.3	.1	200.0	-37.5	0.0	2.3	.7	.3
E006809	.8	.3	.2	200.0	-25.0	0.0	2.1	.7	.5
E006810	.9	.3	.2	200.0	-12.5	0.0	2.5	.8	.5
E006811	.8	.3	.1	200.0	0.0	0.0	2.2	.7	.4
F006804	.5	.2	.1	200.0	12.5	0.0	1.2	.5	.4
F006805	.1	0.0	.1	200.0	25.0	0.0	.3	0.0	.1
F006806	.6	.2	.1	200.0	37.5	0.0	.9	.4	.2
F006807	.2	.1	0.0	200.0	50.0	0.0	.5	.2	.1
F006808	.2	0.0	0.0	200.0	62.5	0.0	.5	0.0	.1
F006809	.3	.1	.1	200.0	75.0	0.0	.7	.2	.2
F006810	.1	0.0	.1	200.0	87.5	0.0	.3	0.0	.2
F006811	0.0	0.0	0.0	200.0	100.0	0.0	0.0	0.0	0.0
G006804	.4	.3	0.0	150.0	112.5	0.0	1.1	.8	.1
G006805	.3	.2	.1	150.0	125.0	0.0	.9	.5	.2
G006806	.7	.6	.1	150.0	137.5	0.0	1.9	1.6	.2
G006807	.6	.4	.1	150.0	150.0	0.0	1.5	1.1	.3
G006808	.2	.1	0.0	150.0	162.5	0.0	.5	.3	.1
G006809	.5	.4	.1	150.0	175.0	0.0	1.3	1.0	.2
G006810	.4	.2	.1	150.0	187.5	0.0	.9	.6	.2
G006811	.2	.2	0.0	150.0	200.0	0.0	.6	.5	.1

FILE NAME	MODEL PEAK CONC (%)	MODEL MEAN CONC (%)	MODEL RMS CONC (%)	PROTOTYPE POSITION X (M)	PROTOTYPE POSITION Y (M)	PROTOTYPE POSITION Z (M)	PROTOTYPE PEAK CONC (%)	PROTOTYPE MEAN CONC (%)	PROTOTYPE RMS CONC (%)
A00904	0.0	0.0	0.0	-125.0	-230.0	0.0	0.0	0.0	0.0
A00905	.3	.2	0.0	-125.0	-217.5	0.0	.8	.5	.1
A00906	.1	0.0	.1	-125.0	-205.0	0.0	.3	0.0	.2
A00907	.1	0.0	0.0	-125.0	-192.5	0.0	.4	0.0	.1
A00908	0.0	0.0	0.0	-125.0	-180.0	0.0	0.0	0.0	0.0
A00909	.1	0.0	0.0	-125.0	-167.5	0.0	.3	0.0	.1
A00910	.3	.1	.1	-125.0	-155.0	0.0	.9		.2
A00911	.5	.1	.1	-125.0	-142.5	0.0	1.3		.2
B00904	0.0	0.0	0.0	0.0	-230.0	0.0	0.0	0.0	0.0
B00905	.2	.1	.1	0.0	-217.5	0.0	.6		.2
B00906	.3	0.0	.1	0.0	-205.0	0.0	.9	0.0	.2
B00907	.3	0.0	.1	0.0	-192.5	0.0	.7	0.0	.2
B00908	.5	.3	.1	0.0	-180.0	0.0	1.4		.3
B00909	.5	0.0	.1	0.0	-167.5	0.0	1.4	0.0	.3
B00910	.8	.1	.2	0.0	-155.0	0.0	2.3		.5
B00911	.8	.3	.2	0.0	-142.5	0.0	2.2		.5
C00904	0.0	0.0	0.0	50.0	-230.0	0.0	0.0	0.0	0.0
C00905	.3	.2	0.0	50.0	-217.5	0.0	.8		.1
C00906	.4	.3	.1	50.0	-205.0	0.0	1.2		.2
C00907	.4	.2	.1	50.0	-192.5	0.0	1.0		.2
C00908	1.0	.8	.1	50.0	-180.0	0.0	2.5	2.0	.3
C00909	.6	.2	.1	50.0	-167.5	0.0	1.7		.3
C00910	.6	.2	.1	50.0	-155.0	0.0	1.7		.3
C00911	.8	.2	.1	50.0	-142.5	0.0	2.1		.3
D00904	0.0	0.0	0.0	100.0	-230.0	0.0	0.0	0.0	0.0
D00905	.2	.1	.1	100.0	-217.5	0.0	.5		.1
D00906	.5	.3	.1	100.0	-205.0	0.0	1.4		.2
D00907	.4	.2	.1	100.0	-192.5	0.0	1.1		.2
D00908	.8	.5	.1	100.0	-180.0	0.0	2.1	1.3	.3
D00909	.6	.3	.1	100.0	-167.5	0.0	1.5		.3
D00910	1.1	.4	.2	100.0	-155.0	0.0	2.9	1.1	.4
D00911	1.1	.4	.2	100.0	-142.5	0.0	2.9	1.1	.4
F00904	0.0	0.0	0.0	200.0	-87.5	0.0	0.0	0.0	0.0
F00905	1.8	.5	.3	200.0	-75.0	0.0	4.6	1.3	.8
F00906	2.4	1.2	.4	200.0	-62.5	0.0	5.5	2.5	1.1
F00907	2.1	.8	.4	200.0	-50.0	0.0	5.2	1.1	1.1
F00908	1.0	0.0	.2	200.0	-37.5	0.0	2.6	0.0	.5
F00909	.6	.3	.1	200.0	-25.0	0.0	1.7		.2
F00910	.5	.3	.1	200.0	-12.5	0.0	1.4		.2
F00911	.3	.2	0.0	200.0	0.0	0.0	.8		.1
E00904	.2	0.0	.1	150.0	-177.5	0.0	0.0	0.0	.1
E00905	.4	.2	.1	150.0	-165.0	0.0	1.0		.2
E00906	.9	.3	.1	150.0	-152.5	0.0	2.4		.3
E00907	1.5	.5	.2	150.0	-140.0	0.0	4.0	1.2	.5
E00908	2.3	1.0	.4	150.0	-127.5	0.0	6.0	2.6	.9
E00909	2.7	1.4	.4	150.0	-115.0	0.0	7.0	3.6	1.0
E00910	3.5	1.8	.4	150.0	-102.5	0.0	8.7	4.8	1.0
E00911	3.0	1.9	.4	150.0	-90.0	0.0	7.0	4.8	1.0
J00904	0.0	0.0	0.0	175.0	-177.5	0.0	0.0	0.0	0.0
J00905	.7	.3	.1	175.0	-165.0	0.0	1.8		.2
J00906	.4	0.0	.1	175.0	-152.5	0.0	1.1	0.0	.2
J00907	1.2	.4	.2	175.0	-140.0	0.0	3.1	1.1	.4
J00908	1.3	.5	.2	175.0	-127.5	0.0	3.4	1.2	.5
J00909	1.8	.8	.3	175.0	-115.0	0.0	4.6	2.2	.6
J00910	2.4	1.4	.3	175.0	-102.5	0.0	6.5	3.6	.8
J00911	2.0	.7	.3	175.0	-90.0	0.0	5.0	1.5	.8
K00904	3.2	2.0	.4	175.0	-77.5	0.0	8.1	5.1	1.1
K00905	2.8	1.5	.4	175.0	-65.0	0.0	7.3	4.1	1.1
K00906	1.4	.3	.3	175.0	-52.5	0.0	3.6		.7
K00907	.4	.1	.1	175.0	-40.0	0.0	1.1		.2
K00908	0.0	0.0	0.0	175.0	-27.5	0.0	0.0	0.0	0.0
K00909	.1	0.0	0.0	175.0	-15.0	0.0	.4	0.0	.1
K00910	.2	0.0	.1	175.0	-2.5	0.0	.5	0.0	.2
K00911	0.0	0.0	0.0	175.0	10.0	0.0	0.0	0.0	0.0

FILE NAME	MODEL CONDITIONS PEAK CONC (%)	MEAN CONC (%)	RMS CONC (%)	PROTOTYPE CONDITIONS POSITION X (M)	Y (M)	Z (M)	PEAK CONC (%)	MEAN CONC (%)	RMS CONC (%)
D01004	0.0	0.0	0.0	100.0	-230.0	0.0	0.0	0.0	0.0
D01005	0.0	0.0	0.0	100.0	-217.5	0.0	0.0	0.0	0.0
D01006	0.0	0.0	0.0	100.0	-205.0	0.0	0.0	0.0	0.0
D01007	0.0	0.0	0.0	100.0	-192.5	0.0	0.0	0.0	0.0
D01008	.1	0.0	.1	100.0	-180.0	0.0	.3	0.0	.2
D01009	.3	0.0	.1	100.0	-167.5	0.0	.9	0.0	.3
D01010	.5	0.0	.1	100.0	-155.0	0.0	1.3	0.0	.3
D01011	.4	0.0	.1	100.0	-142.5	0.0	1.1	0.0	.3
E01004	0.0	0.0	0.0	150.0	-177.5	0.0	0.0	0.0	0.0
E01005	0.0	0.0	0.0	150.0	-165.0	0.0	0.0	0.0	0.0
E01006	.2	0.0	.1	150.0	-152.5	0.0	.5	0.0	.3
E01007	.6	0.0	.2	150.0	-140.0	0.0	1.5	0.0	.5
E01008	1.8	.5	.2	150.0	-127.5	0.0	4.6	1.4	.7
E01009	1.8	.8	.3	150.0	-115.0	0.0	4.8	2.2	.8
E01010	1.7	.9	.2	150.0	-102.5	0.0	4.5	2.3	.6
E01011	1.2	.7	.1	150.0	-90.0	0.0	3.2	2.0	.4
A01004	.3	0.0	.1	-125.0	-230.0	0.0	.8	0.0	.3
A01005	.2	0.0	.1	-125.0	-217.5	0.0	.6	0.0	.3
A01006	.3	0.0	.1	-125.0	-205.0	0.0	.9	0.0	.4
A01007	.1	0.0	.1	-125.0	-192.5	0.0	.4	0.0	.2
A01008	0.0	0.0	0.0	-125.0	-180.0	0.0	0.0	0.0	0.0
A01009	0.0	0.0	0.0	-125.0	-167.5	0.0	0.0	0.0	0.0
A01010	0.0	0.0	0.0	-125.0	-155.0	0.0	0.0	0.0	0.0
A01011	.3	0.0	.1	-125.0	-142.5	0.0	.8	0.0	.1
B01004	.2	0.0	0.0	0.0	-230.0	0.0	.5	0.0	.1
B01005	.2	.1	0.0	0.0	-217.5	0.0	.5	.1	.1
B01006	.4	.2	.1	0.0	-205.0	0.0	1.0	.5	.2
B01007	.3	.2	.1	0.0	-192.5	0.0	.8	.5	.2
B01008	.4	.1	.1	0.0	-180.0	0.0	1.1	.4	.2
B01009	.8	.2	.1	0.0	-167.5	0.0	2.2	.6	.4
B01010	1.2	.4	.2	0.0	-155.0	0.0	3.1	1.2	.6
B01011	1.1	.4	.2	0.0	-142.5	0.0	3.0	1.0	.5
C01004	.2	.1	.1	50.0	-230.0	0.0	.5	.2	.1
C01005	.1	0.0	.1	50.0	-217.5	0.0	.2	0.0	.1
C01006	.1	0.0	.1	50.0	-205.0	0.0	.3	0.0	.1
C01007	.2	0.0	.1	50.0	-192.5	0.0	.4	0.0	.2
C01008	.2	0.0	.1	50.0	-180.0	0.0	.5	0.0	.2
C01009	.5	0.0	.1	50.0	-167.5	0.0	1.2	0.0	.3
C01010	.7	.2	.2	50.0	-155.0	0.0	1.9	.5	.4
C01011	.5	.2	.1	50.0	-142.5	0.0	1.4	.5	.3
F01004	1.4	.6	.2	200.0	-87.5	0.0	3.7	1.5	.6
F01005	.4	0.0	.2	200.0	-75.0	0.0	1.2	0.0	.5
F01006	1.3	.2	.3	200.0	-62.5	0.0	3.5	.6	.8
F01007	1.6	0.0	.4	200.0	-50.0	0.0	4.2	0.0	1.1
F01008	.8	0.0	.2	200.0	-37.5	0.0	2.2	0.0	.5
F01009	0.0	0.0	0.0	200.0	-25.0	0.0	0.0	0.0	0.0
F01010	.1	0.0	.1	200.0	-12.5	0.0	.4	0.0	.2
F01011	0.0	0.0	0.0	200.0	0.0	0.0	0.0	0.0	0.0
J01004	.6	.3	.1	175.0	-177.5	0.0	1.5	.8	.2
J01005	.4	0.0	.1	175.0	-165.0	0.0	1.1	0.0	.3
J01006	.4	0.0	.1	175.0	-152.5	0.0	1.1	0.0	.4
J01007	1.1	.2	.2	175.0	-140.0	0.0	3.0	.4	.6
J01008	1.2	.2	.2	175.0	-127.5	0.0	3.1	.7	.6
J01009	2.0	.6	.3	175.0	-115.0	0.0	5.2	1.7	.8
J01010	1.6	.5	.3	175.0	-102.5	0.0	4.1	1.4	.7
J01011	1.7	.8	.2	175.0	-90.0	0.0	4.6	2.1	.6
K01004	2.9	1.8	.3	175.0	-77.5	0.0	7.4	4.7	.8
K01005	2.7	1.4	.3	175.0	-65.0	0.0	7.0	3.6	.9
K01006	2.3	.5	.4	175.0	-52.5	0.0	5.9	1.3	1.1
K01007	1.0	.4	.2	175.0	-40.0	0.0	2.7	1.0	.5
K01008	.8	.3	.1	175.0	-27.5	0.0	2.1	.8	.2
K01009	.6	.3	.1	175.0	-15.0	0.0	1.7	.7	.2
K01010	.5	.2	.1	175.0	-2.5	0.0	1.4	.5	.4
K01011	.3	.1	.1	175.0	10.0	0.0	.8	.2	.3

FILE NAME	MODEL CONDITIONS PEAK CONC (%)	MEAN CONC (%)	RMS CONC (%)	PROTOTYPE CONDITIONS POSITION X (M)	Y (M)	Z (M)	PEAK CONC (%)	MEAN CONC (%)	RMS CONC (%)
A01104	.3	.2	.1	-125.0	-230.0	0.0	.8	.5	1.0
A01105	0.0	0.0	0.0	-125.0	-217.5	0.0	0.0	0.0	0.0
A01106	.4	.2	.1	-125.0	-205.0	0.0	1.2	.6	1.3
A01107	.3	.1	.1	-125.0	-192.5	0.0	.7	.3	.9
A01108	0.0	0.0	0.0	-125.0	-180.0	0.0	0.0	0.0	0.0
A01109	.1	.1	.1	-125.0	-167.5	0.0	.4	.1	.2
A01110	.4	.1	.1	-125.0	-155.0	0.0	1.1	.4	.9
A01111	.6	0.0	.1	-125.0	-142.5	0.0	1.6	0.0	.2
B01104	.3	.2	.1	0.0	-230.0	0.0	.8	.5	1.0
B01105	.3	.2	.1	0.0	-217.5	0.0	.9	.6	1.0
B01106	.6	.4	.1	0.0	-205.0	0.0	1.6	1.0	1.3
B01107	.5	.2	.1	0.0	-192.5	0.0	1.2	.6	1.3
B01108	.5	0.0	.1	0.0	-180.0	0.0	1.4	0.0	.2
B01109	1.1	.5	.2	0.0	-167.5	0.0	3.0	1.4	1.8
B01110	1.6	.9	.2	0.0	-155.0	0.0	4.3	2.3	1.8
B01111	1.4	.7	.2	0.0	-142.5	0.0	3.6	1.9	.4
C01104	.4	.3	0.0	50.0	-230.0	0.0	1.2	.9	1.2
C01105	.4	.2	.1	50.0	-217.5	0.0	1.0	.6	1.2
C01106	.8	.5	.1	50.0	-205.0	0.0	2.1	1.2	1.3
C01107	.8	.4	.1	50.0	-192.5	0.0	2.2	1.0	1.3
C01108	1.3	.7	.1	50.0	-180.0	0.0	3.3	1.9	1.3
C01109	1.1	.6	.2	50.0	-167.5	0.0	2.9	1.7	1.4
C01110	1.2	.7	.1	50.0	-155.0	0.0	3.2	1.9	1.4
C01111	.6	.5	.1	50.0	-142.5	0.0	2.2	1.3	1.3
D01104	.4	.2	.1	100.0	-230.0	0.0	1.0	.5	1.2
D01105	.4	.2	.1	100.0	-217.5	0.0	1.1	.5	1.2
D01106	.6	.2	.1	100.0	-205.0	0.0	1.5	.6	1.3
D01107	.5	.2	.1	100.0	-192.5	0.0	1.2	.4	1.3
D01108	.5	.2	.1	100.0	-180.0	0.0	1.3	.6	1.3
D01109	.6	.3	.1	100.0	-167.5	0.0	1.5	.8	1.3
D01110	.8	.4	.1	100.0	-155.0	0.0	2.0	1.0	1.3
D01111	.7	.3	.1	100.0	-142.5	0.0	1.9	.8	1.3
E01104	.8	.4	.1	150.0	-177.5	0.0	2.2	1.1	1.3
E01105	.7	.4	.1	150.0	-165.0	0.0	1.9	1.1	1.3
E01106	1.1	.6	.2	150.0	-152.5	0.0	2.9	1.6	1.4
E01107	1.1	.5	.2	150.0	-140.0	0.0	3.0	1.4	1.4
E01108	.9	.2	.2	150.0	-127.5	0.0	2.3	.7	1.5
E01109	1.9	.9	.2	150.0	-115.0	0.0	5.4	2.6	1.5
E01110	1.9	.8	.3	150.0	-102.5	0.0	4.9	2.2	1.6
E01111	1.2	.5	.2	150.0	-90.0	0.0	3.2	1.3	1.5
F01104	.5	.1	.1	200.0	-87.5	0.0	1.3	.3	1.2
F01105	.4	0.0	.1	200.0	-75.0	0.0	1.1	0.0	.2
F01106	.4	.1	.1	200.0	-62.5	0.0	1.0	.3	.8
F01107	.1	0.0	.1	200.0	-50.0	0.0	.4	0.0	.1
F01108	.3	.1	.1	200.0	-37.5	0.0	.7	.3	.8
F01109	.1	0.0	0.0	200.0	-25.0	0.0	.3	0.0	.1
F01110	.2	0.0	.1	200.0	-12.5	0.0	.4	0.0	.2
F01111	0.0	0.0	0.0	200.0	0.0	0.0	0.0	0.0	0.0
J01104	.6	.4	.1	175.0	-177.5	0.0	1.6	1.1	1.2
J01105	.6	.3	.1	175.0	-165.0	0.0	1.6	.9	1.2
J01106	1.1	.6	.1	175.0	-152.5	0.0	2.8	1.5	1.3
J01107	1.1	.6	.1	175.0	-140.0	0.0	2.9	1.5	1.4
J01108	2.1	1.2	.4	175.0	-127.5	0.0	5.4	3.2	1.0
J01109	1.5	.9	.2	175.0	-115.0	0.0	4.0	2.5	1.4
J01110	2.1	1.2	.2	175.0	-102.5	0.0	5.4	3.2	1.4
J01111	1.8	.9	.2	175.0	-90.0	0.0	4.6	2.4	1.4
K01104	.8	.2	.1	175.0	-77.5	0.0	2.1	.6	1.4
K01105	.4	.1	.1	175.0	-65.0	0.0	1.1	.3	1.4
K01106	.3	.2	.1	175.0	-52.5	0.0	.7	.4	1.1
K01107	.3	.2	.1	175.0	-40.0	0.0	.7	.4	1.1
K01108	0.0	0.0	0.0	175.0	-27.5	0.0	0.0	0.0	0.0
K01109	.3	.1	.1	175.0	-15.0	0.0	.7	.4	1.1
K01110	.3	.1	.1	175.0	-2.5	0.0	.8	.3	1.3
K01111	.2	.1	0.0	175.0	10.0	0.0	.4	.1	1.1

FILE NAME	MODEL CONDITIONS PEAK CONC (%)	MEAN CONC (%)	RMS CONC (%)	PROTOTYPE CONDITIONS POSITION X (M)	Y (M)	Z (M)	PEAK CONC (%)	MEAN CONC (%)	RMS CONC (%)
A01204	.2	.1	0.0	-125.0	-230.0	0.0	.5	.3	.1
A01205	.2	.1	0.0	-125.0	-217.5	0.0	.6	.4	.1
A01206	.4	.3	.1	-125.0	-205.0	0.0	1.0	.7	.1
A01207	.3	.2	0.0	-125.0	-192.5	0.0	.7	.4	.1
A01208	.3	.1	0.0	-125.0	-180.0	0.0	.7	.3	.1
A01209	.3	.1	0.0	-125.0	-167.5	0.0	.7	.4	.1
A01210	.5	.2	.1	-125.0	-155.0	0.0	1.3	.6	.2
A01211	1.1	.3	.1	-125.0	-142.5	0.0	2.9	.8	.3
B01204	.3	.2	.1	0.0	-230.0	0.0	.9	.4	.2
B01205	.1	0.0	.1	0.0	-217.5	0.0	.4	0.0	.2
B01206	.2	0.0	.1	0.0	-205.0	0.0	.6	0.0	.2
B01207	.3	0.0	.1	0.0	-192.5	0.0	.8	0.0	.2
B01208	.9	.4	.1	0.0	-180.0	0.0	2.3	1.0	.3
B01209	.7	.2	.1	0.0	-167.5	0.0	1.8	.6	.4
B01210	1.0	.5	.1	0.0	-155.0	0.0	2.7	1.3	.4
B01211	.6	.2	.1	0.0	-142.5	0.0	1.6	.6	.2
C01204	0.0	0.0	0.0	50.0	-230.0	0.0	0.0	0.0	0.0
C01205	0.0	0.0	0.0	50.0	-217.5	0.0	0.0	0.0	0.0
C01206	.2	0.0	.1	50.0	-205.0	0.0	.6	0.0	.3
C01207	.1	0.0	.1	50.0	-192.5	0.0	.4	0.0	.2
C01208	.7	.4	.1	50.0	-180.0	0.0	2.0	1.1	.3
C01209	.5	.1	.1	50.0	-167.5	0.0	1.4	.4	.3
C01210	1.3	.9	.2	50.0	-155.0	0.0	3.5	2.4	.4
C01211	.8	.4	.1	50.0	-142.5	0.0	2.0	1.2	.3
D01204	0.0	0.0	0.0	100.0	-230.0	0.0	0.0	0.0	0.0
D01205	.1	0.0	0.0	100.0	-217.5	0.0	.3	0.0	.1
D01206	.3	.1	.1	100.0	-205.0	0.0	.9	.2	.2
D01207	.3	.1	.1	100.0	-192.5	0.0	.9	.2	.2
D01208	.5	.3	.1	100.0	-180.0	0.0	1.4	.7	.2
D01209	.4	.2	.1	100.0	-167.5	0.0	1.1	.4	.2
D01210	.6	.1	.1	100.0	-155.0	0.0	1.6	.2	.3
D01211	.3	.1	.1	100.0	-142.5	0.0	.8	.2	.2
E01204	.3	.1	.1	150.0	-177.5	0.0	.8	.2	.2
E01205	.5	.2	.1	150.0	-165.0	0.0	1.3	.3	.2
E01206	.5	.1	.1	150.0	-152.5	0.0	1.3	.3	.2
E01207	.7	.2	.1	150.0	-140.0	0.0	1.8	.5	.3
E01208	.7	.1	.2	150.0	-127.5	0.0	2.0	.2	.4
E01209	1.3	.6	.2	150.0	-115.0	0.0	3.4	1.5	.5
E01210	1.3	.7	.2	150.0	-102.5	0.0	3.5	1.8	.5
E01211	.9	.5	.1	150.0	-90.0	0.0	2.4	1.4	.3
J01204	.2	0.0	.1	175.0	-177.5	0.0	.5	0.0	.2
J01205	.4	0.0	.1	175.0	-165.0	0.0	1.0	0.0	.2
J01206	.2	0.0	.1	175.0	-152.5	0.0	.6	0.0	.3
J01207	.5	.1	.1	175.0	-140.0	0.0	1.3	.2	.3
J01208	.7	.3	.1	175.0	-127.5	0.0	1.9	.8	.4
J01209	.8	.4	.1	175.0	-115.0	0.0	2.2	1.0	.4
J01210	.9	.4	.2	175.0	-102.5	0.0	2.4	1.0	.4
J01211	.8	.3	.1	175.0	-90.0	0.0	2.1	.7	.4
K01204	0.0	0.0	0.0	175.0	-77.5	0.0	0.0	0.0	0.0
K01205	.6	.1	.1	175.0	-65.0	0.0	1.6	.2	.3
K01206	.3	.1	.1	175.0	-52.5	0.0	.9	.1	.4
K01207	.4	.2	.1	175.0	-40.0	0.0	1.0	.5	.1
K01208	0.0	0.0	0.0	175.0	-27.5	0.0	0.0	0.0	0.0
K01209	.3	.1	.1	175.0	-15.0	0.0	.7	.3	.2
K01210	.8	.5	.1	175.0	-2.5	0.0	2.0	1.3	.2
K01211	.1	0.0	.1	175.0	10.0	0.0	.4	0.0	.2
F01204	0.0	0.0	0.0	200.0	-87.5	0.0	0.0	0.0	0.0
F01205	.3	0.0	.1	200.0	-75.0	0.0	.8	0.0	.2
F01206	.7	.3	.1	200.0	-62.5	0.0	1.8	.9	.2
F01207	.4	.2	.1	200.0	-50.0	0.0	1.1	.4	.2
F01208	.5	.3	.1	200.0	-37.5	0.0	1.2	.7	.2
F01209	.3	.1	0.0	200.0	-25.0	0.0	.7	.3	.1
F01210	.4	.2	.1	200.0	-12.5	0.0	1.1	.4	.3
F01211	.2	.1	.1	200.0	0.0	0.0	.7	.2	.2

FILE NAME	MODEL CONDITIONS PEAK CONC (%)	MEAN CONC (%)	RMS CONC (%)	PROTOTYPE CONDITIONS POSITION X (M)	Y (M)	Z (M)	PEAK CONC (%)	MEAN CONC (%)	RMS CONC (%)
A013304	0.0	0.0	0.0	0.0	-262.5	0.0	0.0	0.0	0.0
A013305	.4	.3	0.0	0.0	-250.0	0.0	1.1	.7	1
A013306	.1	0.0	.1	0.0	-237.5	0.0	.3	0.0	3
A013307	.2	0.0	.1	0.0	-225.0	0.0	.5	0.0	2
A013308	.1	0.0	0.0	0.0	-212.5	0.0	.2	0.0	1
A013309	.1	0.0	0.0	0.0	-200.0	0.0	.4	0.0	1
A013310	.3	.1	.1	0.0	-187.5	0.0	.7	.3	2
A013311	.2	.1	0.0	0.0	-175.0	0.0	.6	.3	1
B013304	.3	.3	0.0	50.0	-287.5	0.0	.9	.7	1
B013305	.4	.3	0.0	50.0	-275.0	0.0	1.0	.7	1
B013306	.1	0.0	.1	50.0	-262.5	0.0	.3	0.0	2
B013307	0.0	0.0	0.0	50.0	-250.0	0.0	0.0	0.0	0
B013308	0.0	0.0	0.0	50.0	-237.5	0.0	0.0	0.0	0
B013309	0.0	0.0	0.0	50.0	-225.0	0.0	0.0	0.0	0
B013310	0.0	0.0	0.0	50.0	-212.5	0.0	0.0	0.0	0
B013311	0.0	0.0	0.0	50.0	-200.0	0.0	0.0	0.0	0
C013304	0.0	0.0	0.0	150.0	-225.0	0.0	0.0	0.0	0
C013305	.3	0.0	.1	150.0	-212.5	0.0	.7	0.0	2
C013306	.3	0.0	.1	150.0	-200.0	0.0	.8	0.0	3
C013307	.3	0.0	.1	150.0	-187.5	0.0	.8	0.0	3
C013308	.4	.1	.1	150.0	-175.0	0.0	1.0	.4	3
C013309	.4	.1	.1	150.0	-162.5	0.0	1.2	.4	3
C013310	.5	.1	.1	150.0	-150.0	0.0	1.4	.4	3
C013311	.5	.2	.1	150.0	-137.5	0.0	1.3	.6	2
D013304	.1	0.0	.1	200.0	-187.5	0.0	.2	0.0	3
D013305	0.0	0.0	0.0	200.0	-175.0	0.0	0.0	0.0	0
D013306	.4	.2	.1	200.0	-162.5	0.0	1.1	.5	2
D013307	.4	.1	.1	200.0	-150.0	0.0	1.1	.4	2
D013308	.3	.1	.1	200.0	-137.5	0.0	.9	.3	2
D013309	.3	.1	.1	200.0	-125.0	0.0	.8	.2	2
D013310	.2	0.0	.1	200.0	-112.5	0.0	.6	0.0	2
D013311	.3	.1	.1	200.0	-100.0	0.0	.9	.4	1
E013304	0.0	0.0	0.0	200.0	-87.5	0.0	0.0	0.0	0
E013305	.1	0.0	.1	200.0	-75.0	0.0	.3	0.0	2
E013306	.2	0.0	.1	200.0	-62.5	0.0	.5	0.0	2
E013307	.2	0.0	.1	200.0	-50.0	0.0	.5	0.0	2
E013308	.3	.2	.1	200.0	-37.5	0.0	.9	.5	1
E013309	.5	.3	.1	200.0	-25.0	0.0	1.3	.8	2
E013310	.6	.3	.1	200.0	-12.5	0.0	1.7	.9	3
E013311	.4	.3	.1	200.0	0.0	0.0	1.2	.7	2
F013304	.2	0.0	.1	200.0	12.5	0.0	.6	0.0	2
F013305	0.0	0.0	0.0	200.0	25.0	0.0	0.0	0.0	0
F013306	0.0	0.0	0.0	200.0	37.5	0.0	0.0	0.0	0
F013307	0.0	0.0	0.0	200.0	50.0	0.0	0.0	0.0	0
F013308	0.0	0.0	0.0	200.0	62.5	0.0	0.0	0.0	0
F013309	0.0	0.0	0.0	200.0	75.0	0.0	0.0	0.0	0
F013310	0.0	0.0	0.0	200.0	87.5	0.0	0.0	0.0	0
F013311	0.0	0.0	0.0	200.0	100.0	0.0	0.0	0.0	0
G013304	.2	.1	0.0	200.0	112.5	0.0	.7	.2	1
G013305	.4	.2	.1	200.0	125.0	0.0	1.2	.5	2
G013306	.5	.2	.1	200.0	137.5	0.0	1.5	.4	3
G013307	.2	0.0	.1	200.0	150.0	0.0	.5	0.0	1
G013308	.2	0.0	.1	200.0	162.5	0.0	.5	0.0	1
G013309	0.0	0.0	0.0	200.0	175.0	0.0	0.0	0.0	0
G013310	0.0	0.0	0.0	200.0	187.5	0.0	0.0	0.0	0
G013311	0.0	0.0	0.0	200.0	200.0	0.0	0.0	0.0	0
H013304	0.0	0.0	0.0	150.0	0.0	0.0	0.0	0.0	0
H013305	.4	0.0	.1	150.0	12.5	0.0	1.1	0.0	3
H013306	.2	0.0	.1	150.0	25.0	0.0	.5	0.0	2
H013307	.2	0.0	0.0	150.0	37.5	0.0	.5	0.0	1
H013308	.2	0.0	0.0	150.0	50.0	0.0	.5	0.0	1
H013309	.2	0.0	0.0	150.0	62.5	0.0	.5	0.0	1
H013310	.2	0.0	.1	150.0	75.0	0.0	.5	0.0	2
H013311	.2	0.0	0.0	150.0	87.5	0.0	.6	0.0	1
I013304	0.0	0.0	0.0	150.0	100.0	0.0	0.0	0.0	0
I013305	0.0	0.0	0.0	150.0	112.5	0.0	0.0	0.0	0
I013306	0.0	0.0	0.0	150.0	125.0	0.0	0.0	0.0	0
I013307	0.0	0.0	0.0	150.0	137.5	0.0	0.0	0.0	0
I013308	.2	0.0	.1	150.0	150.0	0.0	.5	0.0	2
I013309	.2	0.0	.1	150.0	162.5	0.0	.6	0.0	2
I013310	.3	.1	.1	150.0	175.0	0.0	.8	.2	2
I013311	.2	.1	0.0	150.0	187.5	0.0	.6	.2	1
J013304	0.0	0.0	0.0	100.0	150.0	0.0	0.0	0.0	0
J013305	.2	0.0	.1	100.0	162.5	0.0	.6	0.0	2
J013306	0.0	0.0	0.0	100.0	175.0	0.0	0.0	0.0	0
J013307	0.0	0.0	0.0	100.0	187.5	0.0	0.0	0.0	0
J013308	0.0	0.0	0.0	100.0	200.0	0.0	0.0	0.0	0
J013309	0.0	0.0	0.0	100.0	212.5	0.0	0.0	0.0	0
J013310	0.0	0.0	0.0	100.0	225.0	0.0	0.0	0.0	0
J013311	0.0	0.0	0.0	100.0	237.5	0.0	0.0	0.0	0
K013304	.4	0.0	.1	50.0	175.0	0.0	1.1	0.0	3
K013305	.2	0.0	0.0	50.0	187.5	0.0	.5	0.0	1
K013306	0.0	0.0	0.0	50.0	200.0	0.0	0.0	0.0	0
K013307	.1	0.0	0.0	50.0	212.5	0.0	.2	0.0	1
K013308	.1	0.0	0.0	50.0	225.0	0.0	.2	0.0	1
K013309	0.0	0.0	0.0	50.0	237.5	0.0	0.0	0.0	0
K013310	.3	.1	.1	50.0	250.0	0.0	.8	.2	2
K013311	.1	0.0	.1	50.0	262.5	0.0	.3	0.0	2
L013304	.6	.5	0.0	0.0	187.5	0.0	1.7	1.4	1
L013305	.2	.1	.1	0.0	200.0	0.0	.5	.2	1
L013306	.2	0.0	.1	0.0	212.5	0.0	.5	0.0	2
L013307	.1	0.0	.1	0.0	225.0	0.0	.3	0.0	2
L013308	.1	0.0	0.0	0.0	237.5	0.0	.3	0.0	1
L013309	.1	0.0	.1	0.0	250.0	0.0	.3	0.0	1
L013310	.1	0.0	.1	0.0	262.5	0.0	.3	0.0	2
L013311	.1	0.0	0.0	0.0	275.0	0.0	.2	0.0	1

FILE NAME	MODEL CONDITIONS PEAK CONC (%)	MEAN CONC (%)	RMS CONC (%)	PROTOTYPE CONDITIONS POSITION X (M)	Y (M)	Z (M)	PEAK CONC (%)	MEAN CONC (%)	RMS CONC (%)
B01404	0.0	0.0	0.0	50.0	-287.5	0.0	0.0	0.0	0.0
B01405	.2	0.0	.1	50.0	-275.0	0.0	.4	0.0	.2
B01406	0.0	0.0	0.0	50.0	-262.5	0.0	0.0	0.0	0.0
B01407	0.0	0.0	0.0	50.0	-250.0	0.0	0.0	0.0	0.0
B01408	.1	0.0	0.0	50.0	-237.5	0.0	.2	0.0	.1
B01409	0.0	0.0	0.0	50.0	-225.0	0.0	0.0	0.0	0.0
B01410	.1	0.0	.1	50.0	-212.5	0.0	.3	0.0	.2
B01411	.1	0.0	0.0	50.0	-200.0	0.0	.3	0.0	.1
C01404	0.0	0.0	0.0	150.0	-225.0	0.0	0.0	0.0	0.0
C01405	0.0	0.0	0.0	150.0	-212.5	0.0	0.0	0.0	0.0
C01406	0.0	0.0	0.0	150.0	-200.0	0.0	0.0	0.0	0.0
C01407	0.0	0.0	0.0	150.0	-187.5	0.0	0.0	0.0	0.0
C01408	.2	0.0	.1	150.0	-175.0	0.0	.7	0.0	.2
C01409	.2	0.0	.1	150.0	-162.5	0.0	.5	0.0	.2
C01410	.5	.3	.1	150.0	-150.0	0.0	1.6	.9	.2
C01411	.4	.2	.1	150.0	-137.5	0.0	1.1	.4	.2
D01404	0.0	0.0	0.0	200.0	-187.5	0.0	0.0	0.0	0.0
D01405	.2	0.0	.1	200.0	-175.0	0.0	.6	0.0	.2
D01406	.3	0.0	.1	200.0	-162.5	0.0	.7	0.0	.2
D01407	.3	.1	.1	200.0	-150.0	0.0	.8	.2	.2
D01408	.2	.1	.1	200.0	-137.5	0.0	.6	.2	.2
D01409	.3	0.0	.1	200.0	-125.0	0.0	.7	0.0	.2
D01410	0.0	0.0	0.0	200.0	-112.5	0.0	0.0	0.0	0.0
D01411	.2	.1	.1	200.0	-100.0	0.0	.5	.2	.1
E01404	0.0	0.0	0.0	200.0	-87.5	0.0	0.0	0.0	0.0
E01405	0.0	0.0	0.0	200.0	-75.0	0.0	0.0	0.0	0.0
E01406	0.0	0.0	0.0	200.0	-62.5	0.0	0.0	0.0	0.0
E01407	.2	0.0	.1	200.0	-50.0	0.0	.5	0.0	.2
E01408	.5	.1	0.0	200.0	-37.5	0.0	.8	.3	.1
E01409	.2	0.0	.1	200.0	-25.0	0.0	.7	0.0	.2
E01410	.4	.1	.1	200.0	-12.5	0.0	1.2	.3	.3
E01411	.3	.1	.1	200.0	0.0	0.0	.9	.3	.2
F01404	0.0	0.0	0.0	200.0	12.5	0.0	0.0	0.0	0.0
F01405	.1	0.0	0.0	200.0	25.0	0.0	.2	0.0	.1
F01406	0.0	0.0	0.0	200.0	37.5	0.0	0.0	0.0	0.0
F01407	0.0	0.0	0.0	200.0	50.0	0.0	0.0	0.0	0.0
F01408	0.0	0.0	0.0	200.0	62.5	0.0	0.0	0.0	0.0
F01409	0.0	0.0	0.0	200.0	75.0	0.0	0.0	0.0	0.0
F01410	0.0	0.0	0.0	200.0	87.5	0.0	0.0	0.0	0.0
F01411	0.0	0.0	0.0	200.0	100.0	0.0	0.0	0.0	0.0
G01404	0.0	0.0	0.0	200.0	112.5	0.0	0.0	0.0	0.0
G01405	.2	0.0	0.0	200.0	125.0	0.0	.5	0.0	.1
G01406	.1	0.0	.1	200.0	137.5	0.0	.3	0.0	.2
G01407	.2	0.0	.1	200.0	150.0	0.0	.5	0.0	.1
G01408	.2	0.0	0.0	200.0	162.5	0.0	.5	0.0	.1
G01409	.1	0.0	.1	200.0	175.0	0.0	.2	0.0	.1
G01410	.1	0.0	.1	200.0	187.5	0.0	.3	0.0	.1
G01411	.1	0.0	.1	200.0	20	0.0	.3	0.0	.1
H01404	.1	0.0	.1	150.0	0.0	0.0	.3	0.0	.2
H01405	.4	.1	.1	150.0	12.5	0.0	1.0	.3	.2
H01406	.2	0.0	.1	150.0	25.0	0.0	.6	.2	.2
H01407	.2	.1	.1	150.0	37.5	0.0	.6	.2	.1
H01408	.3	.2	0.0	150.0	50.0	0.0	.8	.2	.1
H01409	.2	.1	0.0	150.0	62.5	0.0	.6	.2	.1
H01410	.2	.1	.1	150.0	75.0	0.0	.6	.2	.2
H01411	.3	.1	0.0	150.0	87.5	0.0	.8	.3	.1
I01404	0.0	0.0	0.0	150.0	100.0	0.0	0.0	0.0	0.0
I01405	.1	0.0	.1	150.0	112.5	0.0	.4	0.0	.2
I01406	.2	0.0	.1	150.0	125.0	0.0	.7	0.0	.2
I01407	.3	.1	.1	150.0	137.5	0.0	.8	.3	.2
I01408	.3	.1	.1	150.0	150.0	0.0	.8	.3	.2
I01409	.3	.1	.1	150.0	162.5	0.0	.9	.3	.2
I01410	.4	.1	.1	150.0	175.0	0.0	1.1	.3	.2
I01411	.1	0.0	0.0	150.0	187.5	0.0	.3	0.0	.1
J01404	0.0	0.0	0.0	100.0	150.0	0.0	0.0	0.0	0.0
J01405	.2	0.0	.1	100.0	162.5	0.0	.6	0.0	.2
J01406	.3	0.0	.1	100.0	175.0	0.0	.8	0.0	.2
J01407	0.0	0.0	0.0	100.0	187.5	0.0	0.0	0.0	0.0
J01408	0.0	0.0	0.0	100.0	200.0	0.0	0.0	0.0	0.0
J01409	.1	0.0	0.0	100.0	212.5	0.0	.2	0.0	.1
J01410	.4	.2	.1	100.0	225.0	0.0	1.2	.6	.2
J01411	.3	.2	0.0	100.0	237.5	0.0	.9	.5	.1
K01404	.5	.2	.1	50.0	175.0	0.0	1.2	.4	.2
K01405	0.0	0.0	0.0	50.0	187.5	0.0	0.0	0.0	0.0
K01406	0.0	0.0	0.0	50.0	200.0	0.0	0.0	0.0	0.0
K01407	0.0	0.0	0.0	50.0	212.5	0.0	0.0	0.0	0.0
K01408	0.0	0.0	0.0	50.0	225.0	0.0	0.0	0.0	0.0
K01409	0.0	0.0	0.0	50.0	237.5	0.0	0.0	0.0	0.0
K01410	.2	0.0	.1	50.0	250.0	0.0	.4	0.0	.2
K01411	0.0	0.0	0.0	50.0	262.5	0.0	0.0	0.0	0.0
L01404	0.0	0.0	0.0	0.0	187.5	0.0	0.0	0.0	0.0
L01405	0.0	0.0	0.0	0.0	200.0	0.0	0.0	0.0	0.0
L01406	0.0	0.0	0.0	0.0	212.5	0.0	0.0	0.0	0.0
L01407	.1	0.0	0.0	0.0	225.0	0.0	.2	0.0	.1
L01408	.2	0.0	0.0	0.0	237.5	0.0	.4	0.0	.1
L01409	.1	0.0	.1	0.0	250.0	0.0	.2	0.0	.2
L01410	.1	0.0	.1	0.0	262.5	0.0	.3	0.0	.2
L01411	.1	0.0	.1	0.0	275.0	0.0	.3	0.0	.2

FILE NAME	MODEL CONDITIONS PEAK CONC (%)	MEAN CONC (%)	RMS CONC (%)	PROTOTYPE CONDITIONS POSITION X (M)	Y (M)	Z (M)	PEAK CONC (%)	MEAN CONC (%)	RMS CONC (%)
A01504	0.0	0.0	0.0	0.0	-262.5	0.0	0.0	0.0	0.0
A01505	.1	0.0	0.0	0.0	-250.0	0.0	.3	0.0	.1
A01506	.1	0.0	0.0	0.0	-237.5	0.0	.3	0.0	.1
A01507	.3	.2	0.0	0.0	-225.0	0.0	.9	.5	.1
A01508	.1	.1	0.0	0.0	-212.5	0.0	.3	.2	.1
A01509	.1	.1	0.0	0.0	-200.0	0.0	.3	.2	0
A01510	.1	0.0	.1	0.0	-187.5	0.0	.2	0	.2
A01511	.3	.2	0.0	0.0	-175.0	0.0	.7	.5	.1
B01504	.1	0.0	0.0	50.0	-287.5	0.0	.2	0	.1
B01505	.2	.1	0.0	50.0	-275.0	0.0	.7	.3	.1
B01506	.3	.2	0.0	50.0	-262.5	0.0	.9	.5	.1
B01507	.1	.1	0.0	50.0	-250.0	0.0	.4	.2	.1
B01508	.1	0.0	0.0	50.0	-237.5	0.0	.1	0	.1
B01509	.1	0.0	0.0	50.0	-225.0	0.0	.3	0	0
B01510	.1	0.0	.1	50.0	-212.5	0.0	.1	0	0
B01511	.1	0.0	0.0	50.0	-200.0	0.0	.1	0	0
C01504	.1	0.0	0.0	150.0	-225.0	0.0	.3	0	0
C01505	0.0	0.0	0.0	150.0	-212.5	0.0	0	0	0
C01506	.3	0.0	.1	150.0	-200.0	0.0	.8	0	.2
C01507	.3	.1	.1	150.0	-187.5	0.0	.8	.2	.2
C01508	.2	0.0	.1	150.0	-175.0	0.0	.8	0	.2
C01509	.2	0.0	.1	150.0	-162.5	0.0	.6	0	.2
C01510	.2	0.0	.1	150.0	-150.0	0.0	.6	0	.2
C01511	.3	.1	.1	150.0	-137.5	0.0	.8	0	.2
D01504	0.0	0.0	0.0	200.0	-187.5	0.0	0	0	0
D01505	0.0	0.0	0.0	200.0	-175.0	0.0	0	0	0
D01506	0.0	0.0	0.0	200.0	-162.5	0.0	0	0	0
D01507	0.0	0.0	0.0	200.0	-150.0	0.0	0	0	0
D01508	.1	0.0	.1	200.0	-137.5	0.0	.4	0	.2
D01509	0.0	0.0	0.0	200.0	-125.0	0.0	0	0	0
D01510	0.0	0.0	0.0	200.0	-112.5	0.0	0	0	0
D01511	0.0	0.0	0.0	200.0	-100.0	0.0	0	0	0
E01504	0.0	0.0	0.0	200.0	-87.5	0.0	0	0	0
E01505	.3	.1	.1	200.0	-75.0	0.0	.8	.4	.1
E01506	.6	.4	.1	200.0	-62.5	0.0	1.6	1	.1
E01507	.3	.2	0.0	200.0	-50.0	0.0	.9	.5	.1
E01508	.3	.2	0.0	200.0	-37.5	0.0	.9	.5	.1
E01509	.5	.3	.1	200.0	-25.0	0.0	1.2	.8	.2
E01510	.7	.4	.1	200.0	-12.5	0.0	1.8	1	.2
E01511	.5	.3	.1	200.0	0.0	0.0	1.4	.9	.1
F01504	0.0	0.0	0.0	200.0	12.5	0.0	0	0	0
F01505	.2	0.0	0.0	200.0	25.0	0.0	.5	0	.1
F01506	.2	0.0	.1	200.0	37.5	0.0	.4	0	.1
F01507	.1	0.0	0.0	200.0	50.0	0.0	.4	0	.1
F01508	.1	0.0	0.0	200.0	62.5	0.0	.4	0	.1
F01509	.1	0.0	0.0	200.0	75.0	0.0	.2	0	0
F01510	.2	0.0	.1	200.0	87.5	0.0	.5	0	.1
F01511	.2	.1	0.0	200.0	100.0	0.0	.5	0	.1
G01504	0.0	0.0	0.0	200.0	112.5	0.0	0	0	0
G01505	.3	.2	0.0	200.0	125.0	0.0	.8	.4	.1
G01506	.4	.3	.1	200.0	137.5	0.0	1.1	.7	.2
G01507	.3	.1	0.0	200.0	150.0	0.0	.7	.4	.1
G01508	.3	.2	0.0	200.0	162.5	0.0	.9	.5	.1
G01509	.5	.3	.1	200.0	175.0	0.0	1.2	.8	.2
G01510	.8	.5	.1	200.0	187.5	0.0	1.8	1	.4
G01511	.3	.1	.1	200.0	200.0	0.0	.7	.4	.2
H01504	.6	.5	.1	150.0	0.0	0.0	1.7	1	.3
H01505	.5	.3	.1	150.0	12.5	0.0	1.2	.8	.2
H01506	.7	.5	.1	150.0	25.0	0.0	1.6	1	.3
H01507	.5	.3	.1	150.0	37.5	0.0	1.1	.8	.2
H01508	.3	.1	0.0	150.0	50.0	0.0	.7	.4	.1
H01509	.3	.2	.1	150.0	62.5	0.0	.9	.5	.1
H01510	.4	.2	.1	150.0	75.0	0.0	1.0	.6	.3
H01511	.4	.2	0.0	150.0	87.5	0.0	1.0	.6	.1
I01504	.5	.4	0.0	150.0	100.0	0.0	1.1	.8	.1
I01505	.4	.1	.1	150.0	112.5	0.0	1.0	.4	.2
I01506	.5	.3	.1	150.0	125.0	0.0	1.5	.8	.2
I01507	.4	.3	.1	150.0	137.5	0.0	1.1	.7	.2
I01508	.3	.1	.1	150.0	150.0	0.0	.9	.3	.2
I01509	.3	.1	.1	150.0	162.5	0.0	.8	.3	.2
I01510	.4	.1	.1	150.0	175.0	0.0	1.0	.4	.2
I01511	.3	.1	0.0	150.0	187.5	0.0	.8	.3	.1
J01504	0.0	0.0	0.0	100.0	150.0	0.0	0	0	0
J01505	.1	0.0	.1	100.0	162.5	0.0	.2	0	.2
J01506	0.0	0.0	0.0	100.0	175.0	0.0	0	0	0
J01507	0.0	0.0	0.0	100.0	187.5	0.0	0	0	0
J01508	.1	0.0	0.0	100.0	200.0	0.0	.4	0	.1
J01509	.1	0.0	0.0	100.0	212.5	0.0	.3	0	.1
J01510	.5	.3	.1	100.0	225.0	0.0	1.3	.7	.2
J01511	0.0	0.0	0.0	100.0	237.5	0.0	0	0	0
K01504	.5	.1	.1	50.0	175.0	0.0	1.1	.2	.3
K01505	.3	.1	0.0	50.0	187.5	0.0	.8	.2	.1
K01506	.4	.2	.1	50.0	200.0	0.0	1.1	.5	.3
K01507	.3	.1	.1	50.0	212.5	0.0	.7	.3	.1
K01508	.3	.2	0.0	50.0	225.0	0.0	.7	.5	.1
K01509	.3	.1	.1	50.0	237.5	0.0	.9	.3	.2
K01510	.4	0.0	.1	50.0	250.0	0.0	1.1	0	.3
K01511	.3	.1	.1	50.0	262.5	0.0	.7	.3	.1
L01504	0.0	0.0	0.0	0.0	187.5	0.0	0	0	0
L01505	.3	.2	0.0	0.0	200.0	0.0	.7	.4	.1
L01506	.6	.5	.1	0.0	212.5	0.0	1.7	1	.2
L01507	.5	.4	0.0	0.0	225.0	0.0	1.2	1	.1
L01508	.1	0.0	0.0	0.0	237.5	0.0	.3	0	.1
L01509	.6	.5	.1	0.0	250.0	0.0	1.6	1	.2
L01510	.8	.7	.1	0.0	262.5	0.0	2.3	1	.2
L01511	.6	.4	.1	0.0	275.0	0.0	1.5	1	.2

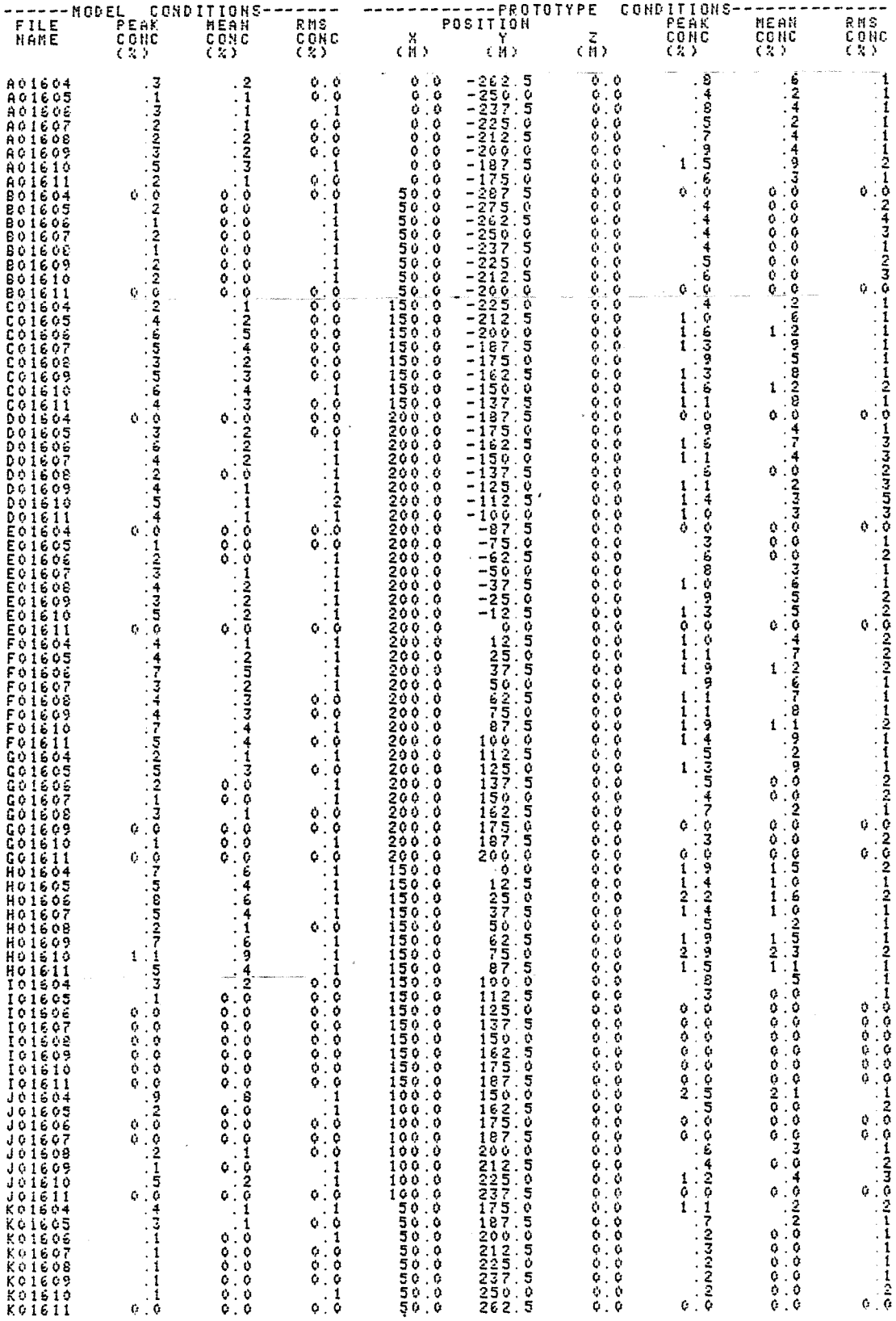

FILE NAME	MODEL CONDITIONS PEAK CONC (%)	MEAN CONC (%)	RMS CONC (%)	PROTOTYPE CONDITIONS POSITION X (M)	Y (M)	Z (M)	PEAK CONC (%)	MEAN CONC (%)	RMS CONC (%)
A01704	0.0	0.0	0.0	0.0	-300.0	0.0	0.0	0.0	0.0
A01705	.4	.3	.1	0.0	-287.5	0.0	1.1	.7	.1
A01706	.2	0.0	.1	0.0	-275.0	0.0	.5	0.0	.2
A01707	.2	.1	.1	0.0	-262.5	0.0	.6	.3	.1
A01708	0.0	0.0	0.0	0.0	-250.0	0.0	0.0	0.0	0.0
A01709	.1	0.0	.1	0.0	-237.5	0.0	.3	0.0	.1
A01710	.2	0.0	.1	0.0	-225.0	0.0	.4	0.0	.2
A01711	0.0	0.0	0.0	0.0	-212.5	0.0	0.0	0.0	0.0
B01704	0.0	0.0	0.0	.5	-275.0	0.0	0.0	0.0	0.0
B01705	.2	.1	.1	.5	-262.5	0.0	.7	.2	.2
B01706	.5	.4	.1	.5	-250.0	0.0	1.4	.9	.2
B01707	.8	.3	.1	.5	-237.5	0.0	2.2	.7	.2
B01708	2.1	1.7	.2	.5	-225.0	0.0	5.4	4.4	.6
B01709	.9	.5	.1	.5	-212.5	0.0	2.4	1.2	.3
B01710	1.0	.5	.2	.5	-200.0	0.0	2.6	1.2	.5
B01711	.5	.2	.2	.5	-187.5	0.0	1.4	.5	.4
C01704	0.0	0.0	0.0	100.0	-200.0	0.0	0.0	0.0	0.0
C01705	.4	.2	.1	100.0	-187.5	0.0	1.1	.6	.2
C01706	.5	.3	.1	100.0	-175.0	0.0	1.3	.8	.3
C01707	.4	.1	.1	100.0	-162.5	0.0	.9	.3	.2
C01708	1.4	.3	.3	100.0	-150.0	0.0	3.8	.8	.8
C01709	.1	0.0	.1	100.0	-137.5	0.0	.4	0.0	.2
C01710	.1	0.0	.1	100.0	-125.0	0.0	.4	0.0	.2
C01711	.2	0.0	0.0	100.0	-112.5	0.0	.4	0.0	0.0
D01704	0.0	0.0	0.0	150.0	-125.0	0.0	0.0	0.0	0.0
D01705	.3	.2	.1	150.0	-112.5	0.0	.9	.6	.2
D01706	.2	0.0	.1	150.0	-100.0	0.0	.5	0.0	.2
D01707	1.1	.9	.1	150.0	-87.5	0.0	2.9	2.5	.3
D01708	.5	.4	0.0	150.0	-75.0	0.0	1.3	1.0	.1
D01709	.4	.2	.1	150.0	-62.5	0.0	1.1	.6	.2
D01710	.8	.5	.1	150.0	-50.0	0.0	2.0	1.2	.2
D01711	0.0	0.0	0.0	150.0	-37.5	0.0	0.0	0.0	0.0
E01704	0.0	0.0	0.0	200.0	-87.5	0.0	0.0	0.0	0.0
E01705	.4	.3	0.0	200.0	-75.0	0.0	1.1	.7	.1
E01706	.8	.5	.1	200.0	-62.5	0.0	2.1	1.6	.2
E01707	.5	.3	.1	200.0	-50.0	0.0	1.5	.9	.2
E01708	.1	0.0	0.0	200.0	-37.5	0.0	.2	0.0	.1
E01709	.3	.2	.1	200.0	-25.0	0.0	.9	.4	.2
E01710	.3	.1	.1	200.0	-12.5	0.0	.8	.2	.2
E01711	.3	.1	.1	200.0	0.0	0.0	.7	.3	.2
F01704	0.0	0.0	0.0	200.0	12.5	0.0	0.0	0.0	0.0
F01705	.3	.1	.1	200.0	25.0	0.0	.8	.2	.2
F01706	.7	.4	.2	200.0	37.5	0.0	1.8	1.0	.3
F01707	.4	.1	.1	200.0	50.0	0.0	1.0	.3	.2
F01708	0.0	0.0	0.0	200.0	62.5	0.0	0.0	0.0	0.0
F01709	.2	0.0	.1	200.0	75.0	0.0	.5	0.0	.2
F01710	.2	0.0	.1	200.0	87.5	0.0	.6	0.0	.2
F01711	.2	0.0	.1	200.0	100.0	0.0	.7	0.0	.2
G01704	0.0	0.0	0.0	150.0	112.5	0.0	0.0	0.0	0.0
G01705	.4	.1	.1	150.0	125.0	0.0	1.1	.4	.2
G01706	.5	.3	.1	150.0	137.5	0.0	1.2	.5	.2
G01707	.4	.2	.1	150.0	150.0	0.0	1.1	.6	.2
G01708	.4	.2	.1	150.0	162.5	0.0	1.1	.5	.2
G01709	.3	.1	.1	150.0	175.0	0.0	.7	.2	.2
G01710	.2	0.0	.1	150.0	187.5	0.0	.5	0.0	.2
G01711	.2	0.0	.1	150.0	200.0	0.0	.6	0.0	.2
H01704	0.0	0.0	0.0	100.0	125.0	0.0	0.0	0.0	0.0
H01705	.5	.2	.1	100.0	137.5	0.0	1.4	.6	.2
H01706	.5	.2	.1	100.0	150.0	0.0	1.4	.6	.2
H01707	.4	.1	.1	100.0	162.5	0.0	.9	.2	.2
H01708	.2	0.0	0.0	100.0	175.0	0.0	.6	0.0	.2
H01709	.2	0.0	.1	100.0	187.5	0.0	.5	0.0	.2
H01710	.4	.1	.1	100.0	200.0	0.0	1.0	.2	.2
H01711	.2	.1	.1	100.0	212.5	0.0	.5	.2	.2
I01704	0.0	0.0	0.0	50.0	150.0	0.0	0.0	0.0	0.0
I01705	1.1	.5	.1	50.0	162.5	0.0	2.9	1.3	.2
I01706	.5	.2	.1	50.0	175.0	0.0	1.2	.5	.2
I01707	.4	.2	.1	50.0	187.5	0.0	1.0	.5	.2
I01708	.5	.3	.1	50.0	200.0	0.0	1.3	.7	.2
I01709	.4	.2	0.0	50.0	212.5	0.0	1.0	.5	.2
I01710	.7	.3	.1	50.0	225.0	0.0	1.8	.8	.2
I01711	.4	.2	.1	50.0	237.5	0.0	1.1	.5	.2
J01704	0.0	0.0	0.0	0.0	162.5	0.0	0.0	0.0	0.0
J01705	.5	.1	.1	0.0	175.0	0.0	1.3	.3	.2
J01706	.3	.1	.1	0.0	187.5	0.0	.9	.3	.2
J01707	.2	0.0	.1	0.0	200.0	0.0	.6	0.0	.2
J01708	.3	.1	0.0	0.0	212.5	0.0	.7	.4	.2
J01709	.2	0.0	.1	0.0	225.0	0.0	.4	0.0	.2
J01710	.2	0.0	.1	0.0	237.5	0.0	.4	0.0	.2
J01711	.1	0.0	0.0	0.0	250.0	0.0	.3	0.0	.1
K01704	0.0	0.0	0.0	-50.0	175.0	0.0	0.0	0.0	0.0
K01705	.6	.1	.1	-50.0	187.5	0.0	1.5	.4	.2
K01706	.3	.1	.1	-50.0	200.0	0.0	.9	.4	.2
K01707	.1	0.0	.1	-50.0	212.5	0.0	.2	0.0	.1
K01708	.2	0.0	.1	-50.0	225.0	0.0	.6	0.0	.2
K01709	0.0	0.0	0.0	-50.0	237.5	0.0	0.0	0.0	0.0
K01710	0.0	0.0	0.0	-50.0	250.0	0.0	0.0	0.0	0.0
K01711	0.0	0.0	0.0	-50.0	262.5	0.0	0.0	0.0	0.0

FILE NAME	MODEL CONDITIONS PEAK CONC (%)	MEAN CONC (%)	RMS CONC (%)	PROTOTYPE CONDITIONS POSITION X (M)	Y (M)	Z (M)	PEAK CONC (%)	MEAN CONC (%)	RMS CONC (%)
B01804	0.0	0.0	0.0	50.0	-275.0	0.0	0.0	0.0	0.0
B01805	.3	.2	.1	50.0	-262.5	0.0	.9	.7	.2
B01806	.5	.4	.1	50.0	-250.0	0.0	1.5	1.0	.3
B01807	.5	.3	.1	50.0	-237.5	0.0	1.5	.9	.3
B01808	.3	.1	0.0	50.0	-225.0	0.0	.8	.3	.1
B01809	.3	.1	.1	50.0	-212.5	0.0	.8	.3	.2
B01810	.4	.2	.1	50.0	-200.0	0.0	1.0	.4	.2
B01811	.3	.2	.1	50.0	-187.5	0.0	.8	.4	.2
A01804	0.0	0.0	0.0	0.0	-300.0	0.0	0.0	0.0	0.0
A01805	.1	0.0	0.0	0.0	-287.5	0.0	.3	0.0	.1
A01806	.2	.1	.1	0.0	-275.0	0.0	.7	.2	.2
A01807	.2	.1	.1	0.0	-262.5	0.0	.7	.2	.1
A01808	.1	.1	0.0	0.0	-250.0	0.0	.3	.1	.1
A01809	.4	.3	.1	0.0	-237.5	0.0	1.0	.7	.2
A01810	.6	.4	.1	0.0	-225.0	0.0	1.6	1.1	.2
A01811	.4	.3	.1	0.0	-212.5	0.0	1.1	.9	.1
C01804	0.0	0.0	0.0	100.0	-200.0	0.0	0.0	0.0	0.0
C01805	.3	.1	.2	100.0	-187.5	0.0	.9	.2	.4
C01806	.5	.2	.2	100.0	-175.0	0.0	1.3	.6	.5
C01807	.3	.1	.1	100.0	-162.5	0.0	.8	.3	.3
C01808	.1	0.0	.1	100.0	-150.0	0.0	.3	0.0	.1
C01809	0.0	0.0	0.0	100.0	-137.5	0.0	0.0	0.0	0.0
C01810	0.0	0.0	0.0	100.0	-125.0	0.0	0.0	0.0	0.0
C01811	.1	0.0	.1	100.0	-112.5	0.0	.2	0.0	.1
D01804	0.0	0.0	0.0	150.0	-125.0	0.0	0.0	0.0	0.0
D01805	.2	.1	0.0	150.0	-112.5	0.0	.6	.3	.1
D01806	.6	.4	.1	150.0	-100.0	0.0	2.1	1.3	.2
D01807	.5	.4	.1	150.0	-87.5	0.0	1.3	.9	.2
D01808	.1	0.0	0.0	150.0	-75.0	0.0	.4	0.0	.1
D01809	.2	.1	.1	150.0	-62.5	0.0	.6	.4	.2
D01810	.3	.1	.1	150.0	-50.0	0.0	.7	.4	.2
D01811	.2	.1	.1	150.0	-37.5	0.0	.6	.3	.2
E01804	0.0	0.0	0.0	200.0	-87.5	0.0	0.0	0.0	0.0
E01805	.6	.2	.2	200.0	-75.0	0.0	1.5	.7	.5
E01806	.4	.2	.2	200.0	-62.5	0.0	1.1	.6	.4
E01807	.5	.1	.2	200.0	-50.0	0.0	1.3	.4	.5
E01808	.3	.1	.1	200.0	-37.5	0.0	.8	.3	.3
E01809	.4	.2	.1	200.0	-25.0	0.0	1.1	.7	.3
E01810	.5	.2	.1	200.0	-12.5	0.0	1.3	.7	.2
E01811	.3	.2	0.0	200.0	0.0	0.0	.9	.5	.2
F01804	0.0	0.0	0.0	200.0	12.5	0.0	0.0	0.0	0.0
F01805	.4	.2	.1	200.0	25.0	0.0	1.0	.7	.2
F01806	.7	.4	.1	200.0	37.5	0.0	1.8	1.2	.2
F01807	.5	.3	.1	200.0	50.0	0.0	1.3	.8	.1
F01808	.3	.2	.1	200.0	62.5	0.0	.8	.4	.1
F01809	.6	.3	.1	200.0	75.0	0.0	1.6	.9	.2
F01810	.8	.4	.1	200.0	87.5	0.0	2.0	1.1	.3
F01811	.7	.4	.1	200.0	100.0	0.0	1.9	1.0	.2
G01804	0.0	0.0	0.0	150.0	112.5	0.0	0.0	0.0	0.0
G01805	.2	0.0	.1	150.0	125.0	0.0	.6	0.0	.2
G01806	.4	.3	.1	150.0	137.5	0.0	1.0	.7	.3
G01807	.3	.1	.1	150.0	150.0	0.0	.8	.2	.2
G01808	.9	.5	.1	150.0	162.5	0.0	2.4	1.4	.3
G01809	.5	.2	.1	150.0	175.0	0.0	1.4	.6	.2
G01810	.5	.2	.1	150.0	187.5	0.0	1.3	.5	.2
G01811	.3	.2	.1	150.0	200.0	0.0	.9	.4	.2
H01804	0.0	0.0	0.0	100.0	125.0	0.0	0.0	0.0	0.0
H01805	.5	.2	.1	100.0	137.5	0.0	1.4	.6	.3
H01806	.6	.3	.1	100.0	150.0	0.0	1.6	.7	.3
H01807	.5	.1	.1	100.0	162.5	0.0	1.4	.3	.4
H01808	.8	.5	.1	100.0	175.0	0.0	2.1	1.3	.3
H01809	.5	.1	.2	100.0	187.5	0.0	1.4	.3	.5
H01810	.5	.2	.2	100.0	200.0	0.0	1.4	.5	.5
H01811	.5	.3	.1	100.0	212.5	0.0	1.3	.7	.4
I01804	0.0	0.0	0.0	50.0	150.0	0.0	0.0	0.0	0.0
I01805	.8	.3	.1	50.0	162.5	0.0	2.2	.7	.2
I01806	.4	0.0	.1	50.0	175.0	0.0	1.0	0.0	.2
I01807	.2	.1	0.0	50.0	187.5	0.0	.6	.2	.1
I01808	.2	.1	0.0	50.0	200.0	0.0	.6	.3	.1
I01809	.2	.1	0.0	50.0	212.5	0.0	.5	.2	.1
I01810	.2	0.0	.1	50.0	225.0	0.0	.4	0.0	.1
I01811	.2	0.0	.1	50.0	237.5	0.0	.4	0.0	.1
J01804	0.0	0.0	0.0	0.0	162.5	0.0	0.0	0.0	0.0
J01805	.6	.2	.1	0.0	175.0	0.0	1.5	.6	.2
J01806	.3	0.0	.1	0.0	187.5	0.0	.8	0.0	.2
J01807	.3	0.0	.1	0.0	200.0	0.0	.8	0.0	.2
J01808	.2	.1	0.0	0.0	212.5	0.0	.5	.2	.1
J01809	.1	0.0	0.0	0.0	225.0	0.0	.2	0.0	.1
J01810	.2	0.0	.1	0.0	237.5	0.0	.4	0.0	.1
J01811	.2	.1	.1	0.0	250.0	0.0	.4	.2	.1
K01804	0.0	0.0	0.0	-50.0	175.0	0.0	0.0	0.0	0.0
K01805	.4	.2	.1	-50.0	187.5	0.0	1.1	.5	.2
K01806	.4	.2	.1	-50.0	200.0	0.0	1.1	.5	.2
K01807	.3	.2	.1	-50.0	212.5	0.0	.8	.4	.2
K01808	.3	.2	0.0	-50.0	225.0	0.0	.8	.4	.1
K01809	.4	.2	.1	-50.0	237.5	0.0	1.0	.6	.2
K01810	.4	.3	.1	-50.0	250.0	0.0	1.1	.8	.1
K01811	.3	.2	0.0	-50.0	262.5	0.0	.7	.5	.1

MODEL CONDITIONS				PROTOTYPE CONDITIONS					
FILE NAME	PEAK CONC (%)	MEAN CONC (%)	RMS CONC (%)	POSITION X (M)	Y (M)	Z (M)	PEAK CONC (%)	MEAN CONC (%)	RMS CONC (%)
A01904	.4	.3	.1	0.0	-300.0	0.0	1.2	.8	.1
A01905	.4	.2	0.0	0.0	-287.5	0.0	1.0	.6	.1
A01906	.7	.5	.1	0.0	-275.0	0.0	1.7	1.1	.2
A01907	.5	.3	0.0	0.0	-262.5	0.0	1.1	.6	.1
A01908	.2	.1	0.0	0.0	-250.0	0.0	.5	.3	.1
A01909	.5	.3	.1	0.0	-237.5	0.0	1.1	.7	.2
A01910	.3	.1	.1	0.0	-225.0	0.0	.6	.3	.2
A01911	.3	.2	0.0	0.0	-212.5	0.0	.7	.4	.1
B01904	.3	0.0	.1	50.0	-275.0	0.0	.8	0.0	.2
B01905	.2	0.0	.1	50.0	-262.5	0.0	.5	0.0	.2
B01906	.3	.1	.1	50.0	-250.0	0.0	.8	.2	.2
B01907	.2	0.0	.1	50.0	-237.5	0.0	.5	0.0	.2
B01908	.6	.5	.1	50.0	-225.0	0.0	1.5	1.1	.2
B01909	.2	0.0	.1	50.0	-212.5	0.0	.6	0.0	.2
B01910	0.0	0.0	0.0	50.0	-200.0	0.0	0.0	0.0	0.0
B01911	.1	0.0	0.0	50.0	-187.5	0.0	.3	0.0	.1
C01904	.2	.1	0.0	100.0	-200.0	0.0	.5	.2	.1
C01905	.1	0.0	0.0	100.0	-187.5	0.0	.3	0.0	.1
C01906	.4	.3	0.0	100.0	-175.0	0.0	1.0	.7	.1
C01907	.2	.1	0.0	100.0	-162.5	0.0	.6	.4	.1
C01908	.4	.3	0.0	100.0	-150.0	0.0	1.0	.8	.1
C01909	.3	.2	0.0	100.0	-137.5	0.0	.7	.5	.1
C01910	.2	.1	.1	100.0	-125.0	0.0	.5	.2	.1
C01911	.3	.1	0.0	100.0	-112.5	0.0	.7	.3	.1
D01904	.8	.6	.1	150.0	-125.0	0.0	2.1	1.5	.2
D01905	.9	.7	.1	150.0	-112.5	0.0	2.3	1.7	.2
D01906	.8	.6	.1	150.0	-100.0	0.0	2.0	1.5	.2
D01907	.7	.6	0.0	150.0	-87.5	0.0	1.8	1.4	.1
D01908	.7	.6	0.0	150.0	-75.0	0.0	1.8	1.4	.1
D01909	.9	.8	0.0	150.0	-62.5	0.0	2.4	2.0	.1
D01910	3.7	3.4	.2	150.0	-50.0	0.0	9.8	8.6	.4
D01911	.7	.6	0.0	150.0	-37.5	0.0	1.8	1.5	.1
E01904	.8	.5	.1	200.0	-87.5	0.0	2.1	1.5	.3
E01905	.6	.4	.1	200.0	-75.0	0.0	1.5	1.1	.2
E01906	.9	.7	.1	200.0	-62.5	0.0	2.2	1.7	.2
E01907	.6	.4	.1	200.0	-50.0	0.0	1.5	1.1	.2
E01908	.8	.7	.1	200.0	-37.5	0.0	2.0	1.6	.2
E01909	.7	.6	.1	200.0	-25.0	0.0	1.8	1.4	.2
E01910	.1	0.0	.1	200.0	-12.5	0.0	.3	.1	.2
E01911	.5	.4	0.0	200.0	0.0	0.0	1.3	1.0	.1
F01904	.1	0.0	.1	200.0	12.5	0.0	.3	.1	.3
F01905	.2	0.0	.1	200.0	25.0	0.0	.5	.1	.3
F01906	.1	0.0	.1	200.0	37.5	0.0	.3	.1	.3
F01907	0.0	0.0	.1	200.0	50.0	0.0	0.0	0.0	.2
F01908	.1	.1	.1	200.0	62.5	0.0	.3	.2	.2
F01909	.4	.1	.1	200.0	75.0	0.0	1.0	.3	.2
F01910	1.0	.7	.1	200.0	87.5	0.0	2.7	1.9	.2
F01911	.4	.2	0.0	200.0	100.0	0.0	1.1	.6	.2
G01904	.4	.1	.1	150.0	112.5	0.0	1.1	.3	.2
G01905	.3	.2	.1	150.0	125.0	0.0	.8	.5	.2
G01906	.3	.2	.1	150.0	137.5	0.0	.8	.5	.2
G01907	.3	.1	.1	150.0	150.0	0.0	.8	.4	.2
G01908	.7	.6	0.0	150.0	162.5	0.0	1.9	1.6	.2
G01909	.4	.2	.1	150.0	175.0	0.0	1.1	.6	.2
G01910	.1	0.0	.1	150.0	187.5	0.0	.3	.1	.2
G01911	.3	.2	0.0	150.0	200.0	0.0	.8	.5	.2
H01904	.3	.1	.1	100.0	125.0	0.0	.7	.4	.2
H01905	.1	0.0	.1	100.0	137.5	0.0	.3	0.0	.2
H01906	.6	.3	.1	100.0	150.0	0.0	1.5	.8	.2
H01907	.2	0.0	.1	100.0	162.5	0.0	.6	0.0	.2
H01908	0.0	0.0	0.0	100.0	175.0	0.0	0.0	0.0	0.0
H01909	.3	.1	.1	100.0	187.5	0.0	.8	.2	.2
H01910	0.0	0.0	0.0	100.0	200.0	0.0	0.0	0.0	0.0
H01911	0.0	0.0	0.0	100.0	212.5	0.0	0.0	0.0	0.0
I01904	.6	.2	.1	50.0	150.0	0.0	1.7	.6	.2
I01905	.3	0.0	.1	50.0	162.5	0.0	.8	0.0	.2
I01906	.3	0.0	.1	50.0	175.0	0.0	.8	0.0	.2
I01907	0.0	0.0	0.0	50.0	187.5	0.0	0.0	0.0	0.0
I01908	0.0	0.0	0.0	50.0	200.0	0.0	0.0	0.0	0.0
I01909	.1	0.0	.1	50.0	212.5	0.0	.3	0.0	.2
I01910	0.0	0.0	0.0	50.0	225.0	0.0	0.0	0.0	0.0
I01911	.1	0.0	0.0	50.0	237.5	0.0	.3	0.0	.1
J01904	.6	.3	.1	0.0	162.5	0.0	1.7	.8	.2
J01905	.5	.3	.1	0.0	175.0	0.0	1.4	.8	.2
J01906	.7	.4	.1	0.0	187.5	0.0	1.9	1.1	.2
J01907	.6	.4	.1	0.0	200.0	0.0	1.7	1.1	.2
J01908	.2	.1	0.0	0.0	212.5	0.0	.6	.3	.1
J01909	.5	.2	.1	0.0	225.0	0.0	1.4	.7	.2
J01910	1.1	.8	.3	0.0	237.5	0.0	3.0	2.0	.9
J01911	.1	0.0	0.0	0.0	250.0	0.0	.4	0.0	.1

FILE NAME	MODEL CONDITIONS PEAK CONC (%)	MEAN CONC (%)	RMS CONC (%)	PROTOTYPE CONDITIONS POSITION X (M)	Y (M)	Z (M)	PEAK CONC (%)	MEAN CONC (%)	RMS CONC (%)
B02004	0.0	0.0	0.0	50.0	-275.0	0.0	0.0	0.0	0.0
B02005	.2	.2	0.0	50.0	-262.5	0.0	.7	.4	.1
B02006	.2	.1	.1	50.0	-250.0	0.0	2.1	2.1	.1
B02007	.5	.1	.1	50.0	-237.5	0.0	2.4	1.5	.2
B02008	.4	.3	0.0	50.0	-225.0	0.0	1.1	1.0	.1
B02009	.6	.1	.1	50.0	-212.5	0.0	2.3	1.7	.3
B02010	1.0	.7	.1	50.0	-200.0	0.0	2.5	1.9	.3
B02011	.5	.1	0.0	50.0	-187.5	0.0	1.5	1.3	.2
A02004	.5	.1	.2	0.0	-300.0	0.0	1.5	.4	.5
A02005	.4	.3	0.0	0.0	-287.5	0.0	1.1	.7	.1
A02006	1.1	.8	.1	0.0	-275.0	0.0	2.1	2.0	.2
A02007	.7	.5	.1	0.0	-262.5	0.0	2.1	1.9	.2
A02008	.3	.2	0.0	0.0	-250.0	0.0	.7	.5	.1
A02009	.7	.5	.1	0.0	-237.5	0.0	1.7	1.5	.2
A02010	.7	.6	.1	0.0	-225.0	0.0	1.2	1.1	.2
A02011	.5	.4	.1	0.0	-212.5	0.0	1.1	1.0	.2
C02004	0.0	0.0	0.0	100.0	-200.0	0.0	1.0	1.0	0.0
C02005	.1	0.0	0.0	100.0	-187.5	0.0	.2	.2	.0
C02006	1.1	1.1	.1	100.0	-175.0	0.0	3.2	2.1	.9
C02007	.6	.2	.1	100.0	-162.5	0.0	3.2	1.6	.5
C02008	.3	.2	0.0	100.0	-150.0	0.0	.2	.2	.0
C02009	1.0	.9	.1	100.0	-137.5	0.0	2.8	2.3	.4
C02010	1.1	.9	.1	100.0	-125.0	0.0	3.7	2.4	.3
C02011	.5	.5	.1	100.0	-112.5	0.0	1.7	1.3	.2
D02004	0.0	0.0	0.0	150.0	-125.0	0.0	1.0	1.0	0.0
D02005	.9	.8	.1	150.0	-112.5	0.0	2.3	2.2	.2
D02006	1.2	1.1	.1	150.0	-100.0	0.0	2.5	2.2	.2
D02007	.8	.7	.1	150.0	-87.5	0.0	2.1	1.9	.2
D02008	.6	.5	0.0	150.0	-75.0	0.0	1.5	1.3	.2
D02009	.8	.7	.1	150.0	-62.5	0.0	2.2	1.9	.2
D02010	.9	.7	.1	150.0	-50.0	0.0	2.4	2.0	.2
D02011	.7	.6	0.0	150.0	-37.5	0.0	1.5	1.3	.1
E02004	0.0	0.0	0.0	200.0	-87.5	0.0	0.0	0.0	0.0
E02005	.1	0.0	0.0	200.0	-75.0	0.0	.2	.2	.0
E02006	.7	.4	.1	200.0	-62.5	0.0	1.8	1.2	.3
E02007	.3	.1	.1	200.0	-50.0	0.0	.8	.3	.2
E02008	.1	0.0	0.0	200.0	-37.5	0.0	.3	.1	.1
E02009	.4	.2	.1	200.0	-25.0	0.0	1.1	.5	.2
E02010	.5	.2	.1	200.0	-12.5	0.0	1.3	.6	.2
E02011	.2	.2	0.0	200.0	0.0	0.0	.7	.4	.1
F02004	0.0	0.0	0.0	200.0	12.5	0.0	0.0	0.0	0.0
F02005	.4	.2	.1	200.0	25.0	0.0	1.2	.5	.2
F02006	.9	.7	.1	200.0	37.5	0.0	2.1	1.5	.3
F02007	.6	.4	.1	200.0	50.0	0.0	1.6	1.1	.2
F02008	.1	0.0	0.0	200.0	62.5	0.0	.4	.1	.1
F02009	.5	.3	.1	200.0	75.0	0.0	1.3	.8	.2
F02010	.8	.6	.1	200.0	87.5	0.0	2.1	1.6	.2
F02011	.4	.3	.1	200.0	100.0	0.0	1.1	.8	.2
G02004	0.0	0.0	0.0	150.0	112.5	0.0	0.0	0.0	0.0
G02005	.4	.3	0.0	150.0	125.0	0.0	1.0	.6	.2
G02006	.5	.4	.1	150.0	137.5	0.0	1.1	.8	.2
G02007	.5	.4	0.0	150.0	150.0	0.0	1.1	.8	.2
G02008	.1	0.0	0.0	150.0	162.5	0.0	.3	.1	.1
G02009	.4	.3	.1	150.0	175.0	0.0	1.0	.7	.2
G02010	.5	.3	.1	150.0	187.5	0.0	1.1	.8	.2
G02011	.5	.4	.1	150.0	200.0	0.0	1.0	.9	.1
H02004	0.0	0.0	0.0	100.0	125.0	0.0	0.0	0.0	0.0
H02005	.2	0.0	.1	100.0	137.5	0.0	.5	.2	.1
H02006	.7	.5	.1	100.0	150.0	0.0	1.5	.5	.2
H02007	.5	.4	.1	100.0	162.5	0.0	1.1	.8	.2
H02008	.2	0.0	0.0	100.0	175.0	0.0	.5	.2	.1
H02009	.4	.3	.1	100.0	187.5	0.0	1.1	.8	.2
H02010	.6	.4	.1	100.0	200.0	0.0	1.1	.8	.2
H02011	.4	.2	.1	100.0	212.5	0.0	.9	.6	.2
I02004	0.0	0.0	0.0	50.0	150.0	0.0	0.0	0.0	0.0
I02005	.9	.6	.1	50.0	162.5	0.0	2.1	.7	.2
I02006	.7	.4	.1	50.0	175.0	0.0	1.5	.8	.2
I02007	.5	.4	0.0	50.0	187.5	0.0	1.1	.9	.1
I02008	.5	.4	0.0	50.0	200.0	0.0	1.1	.9	.1
I02009	.4	.3	0.0	50.0	212.5	0.0	1.1	.9	.1
I02010	.6	.4	.1	50.0	225.0	0.0	1.1	.8	.2
I02011	.4	.3	0.0	50.0	237.5	0.0	1.1	.8	.1
J02004	0.0	0.0	0.0	0.0	162.5	0.0	0.0	0.0	0.0
J02005	.5	.2	.1	0.0	175.0	0.0	1.1	.4	.1
J02006	.5	.3	0.0	0.0	187.5	0.0	1.1	.7	.1
J02007	.5	.3	.1	0.0	200.0	0.0	1.1	.7	.2
J02008	.5	.4	0.0	0.0	212.5	0.0	1.1	.9	.1
J02009	.5	.3	.1	0.0	225.0	0.0	1.1	.7	.2
J02010	.6	.3	.1	0.0	237.5	0.0	1.1	.8	.2
J02011	.4	.2	.1	0.0	250.0	0.0	1.1	.6	.2
K02004	0.0	0.0	0.0	-50.0	175.0	0.0	0.0	0.0	0.0
K02005	.6	.4	.1	-50.0	187.5	0.0	1.1	.6	.2
K02006	.4	.2	.1	-50.0	200.0	0.0	1.1	.6	.2
K02007	.2	.1	.1	-50.0	212.5	0.0	.6	.1	.2
K02008	0.0	0.0	0.0	-50.0	225.0	0.0	0.0	0.0	0.0
K02009	.3	.1	.1	-50.0	237.5	0.0	.8	.3	.2
K02010	.3	.1	.1	-50.0	250.0	0.0	.9	.3	.2
K02011	.2	.1	0.0	-50.0	262.5	0.0	.6	.3	.1

FILE NAME	MODEL CONDITIONS PEAK CONC (%)	MEAN CONC (%)	RMS CONC (%)	PROTOTYPE CONDITIONS POSITION X (M)	Y (M)	Z (M)	PEAK CONC (%)	MEAN CONC (%)	RMS CONC (%)
D02104	0.0	0.0	0.0	150.0	-177.5	0.0	0.0	0.0	0.0
D02105	0.0	0.0	0.0	150.0	-165.0	0.0	0.0	0.0	0.0
D02106	0.0	0.0	0.0	150.0	-152.5	0.0	0.0	0.0	0.0
D02107	0.0	0.0	0.0	150.0	-140.0	0.0	0.0	0.0	0.0
D02108	0.0	0.0	0.0	150.0	-127.5	0.0	0.0	0.0	0.0
D02109	0.0	0.0	0.0	150.0	-115.0	0.0	0.0	0.0	0.0
D02110	.1	0.0	.2	150.0	-102.5	0.0	.2	0.0	.4
D02111	0.0	0.0	0.0	150.0	-90.0	0.0	0.0	0.0	0.0
E02104	.4	.2	.1	150.0	-177.5	0.0	1.0	.5	.2
E02105	.2	.1	.1	150.0	-165.0	0.0	.6	.2	.2
E02106	.2	.1	.1	150.0	-152.5	0.0	.7	.2	.3
E02107	.2	0.0	.1	150.0	-140.0	0.0	.4	0.0	.2
E02108	.1	0.0	.1	150.0	-127.5	0.0	.4	0.0	.1
E02109	.2	0.0	.1	150.0	-115.0	0.0	.6	0.0	.2
E02110	.5	.2	.1	150.0	-102.5	0.0	1.4	.5	.3
E02111	.3	.2	.1	150.0	-90.0	0.0	.8	.4	.2
F02104	.3	.2	.1	150.0	-177.5	0.0	.9	.4	.2
F02105	.3	0.0	.1	150.0	-165.0	0.0	.6	0.0	.2
F02106	.3	.1	.1	150.0	-152.5	0.0	.8	.3	.2
F02107	.4	.1	.1	150.0	-140.0	0.0	1.1	.2	.2
F02108	.4	.1	.1	150.0	-127.5	0.0	1.0	.2	.2
F02109	.5	.2	.1	150.0	-115.0	0.0	1.5	.4	.2
F02110	.7	.3	.1	150.0	-102.5	0.0	1.9	.7	.2
F02111	.3	.1	0.0	150.0	-90.0	0.0	.8	.2	.1
G02104	.2	0.0	.1	200.0	12.5	0.0	.6	0.0	.1
G02105	0.0	0.0	0.0	200.0	25.0	0.0	0.0	0.0	0.0
G02106	.1	0.0	.1	200.0	37.5	0.0	.3	0.0	.2
G02107	.1	0.0	0.0	200.0	50.0	0.0	.2	0.0	.1
G02108	.2	0.0	0.0	200.0	62.5	0.0	.5	0.0	.1
G02109	.4	.1	.1	200.0	75.0	0.0	1.0	.3	.1
G02110	.7	.3	.1	200.0	87.5	0.0	2.0	.8	.3
G02111	.4	.2	.1	200.0	100.0	0.0	1.1	.5	.2
H02104	.1	0.0	.1	150.0	25.0	0.0	.3	0.0	.2
H02105	.1	0.0	.1	150.0	37.5	0.0	.3	0.0	.1
H02106	.2	0.0	.1	150.0	50.0	0.0	.6	0.0	.2
H02107	.6	0.0	.1	150.0	62.5	0.0	1.6	0.0	.3
H02108	.8	.1	.1	150.0	75.0	0.0	2.2	.2	.3
H02109	1.0	.3	.2	150.0	87.5	0.0	2.7	.8	.4
H02110	1.0	.5	.2	150.0	100.0	0.0	2.6	1.3	.4
H02111	.8	.4	.1	150.0	112.5	0.0	2.1	1.0	.3
I02104	.6	.4	.1	105.0	175.0	0.0	1.5	1.1	.2
I02105	.7	.4	.1	105.0	187.5	0.0	1.8	1.2	.2
I02106	.8	.5	.1	105.0	200.0	0.0	2.3	1.4	.3
I02107	.9	.5	.1	105.0	212.5	0.0	2.4	1.4	.4
I02108	.8	.3	.1	105.0	225.0	0.0	2.0	.9	.3
I02109	.9	.5	.2	105.0	237.5	0.0	2.5	1.3	.4
I02110	.8	.5	.1	105.0	250.0	0.0	2.1	1.3	.3
I02111	.5	.2	.1	105.0	262.5	0.0	1.4	.6	.2
J02104	.1	0.0	.1	175.0	-177.5	0.0	.3	0.0	.2
J02105	.1	0.0	.1	175.0	-165.0	0.0	.3	0.0	.1
J02106	.2	.1	.1	175.0	-152.5	0.0	.5	.1	.2
J02107	.2	.1	0.0	175.0	-140.0	0.0	.6	.3	.1
J02108	.2	.1	0.0	175.0	-127.5	0.0	.5	.2	.1
J02109	.3	.1	.1	175.0	-115.0	0.0	.7	.3	.1
J02110	.6	.4	.1	175.0	-102.5	0.0	1.6	1.0	.2
J02111	.4	.2	.1	175.0	-90.0	0.0	1.0	.5	.1
K02104	.4	.1	.1	175.0	-77.5	0.0	1.0	.4	.3
K02105	.5	.3	.1	175.0	-65.0	0.0	1.3	.7	.2
K02106	.5	.2	.1	175.0	-52.5	0.0	1.5	.7	.2
K02107	.6	.3	.1	175.0	-40.0	0.0	1.7	.8	.3
K02108	.7	.3	.1	175.0	-27.5	0.0	1.8	.8	.3
K02109	.7	.3	.1	175.0	-15.0	0.0	1.9	.8	.3
K02110	1.0	.3	.2	175.0	-2.5	0.0	2.6	.8	.4
K02111	.6	.1	.1	175.0	10.0	0.0	1.5	.1	.3

FILE NAME	MODEL CONDITIONS PEAK CONC (%)	MEAN CONC (%)	RMS CONC (%)	PROTOTYPE CONDITIONS POSITION X (M)	Y (M)	Z (M)	PEAK CONC (%)	MEAN CONC (%)	RMS CONC (%)
E02304	0.0	0.0	0.0	150.0	-177.5	0.0	0.0	0.0	0.0
E02305	.3	.1	0.0	150.0	-165.0	0.0	.7	.2	.1
E02306	.3	.1	.1	150.0	-152.5	0.0	.7	.2	.2
E02307	.3	.1	.1	150.0	-140.0	0.0	.7	.3	.2
E02308	.8	.6	.1	150.0	-127.5	0.0	2.1	1.7	.2
E02309	.3	.2	.1	150.0	-115.0	0.0	.9	.6	.1
E02310	.7	.4	.1	150.0	-102.5	0.0	1.8	1.1	.3
E02311	.1	0.0	.1	150.0	-90.0	0.0	.2	0.0	.1
J02304	0.0	0.0	0.0	175.0	-177.5	0.0	0.0	0.0	0.0
J02305	.2	.1	0.0	175.0	-165.0	0.0	.5	.2	.1
J02306	.5	.4	0.0	175.0	-152.5	0.0	1.4	1.0	.2
J02307	.4	.2	.1	175.0	-140.0	0.0	1.1	.6	.2
J02308	.1	0.0	.1	175.0	-127.5	0.0	.4	0.0	.1
J02309	.1	0.0	0.0	175.0	-115.0	0.0	.4	0.0	.1
J02310	.3	.1	.1	175.0	-102.5	0.0	.7	.1	.2
J02311	.3	.2	0.0	175.0	-90.0	0.0	.8	.4	.1
F02304	0.0	0.0	0.0	200.0	-177.5	0.0	0.0	0.0	0.0
F02305	.2	0.0	.1	200.0	-165.0	0.0	.4	0.0	.1
F02306	.3	0.0	.1	200.0	-152.5	0.0	.7	0.0	.2
F02307	.3	0.0	.1	200.0	-140.0	0.0	.7	0.0	.1
F02308	.7	.5	0.0	200.0	-127.5	0.0	1.6	1.4	.1
F02309	.5	.2	0.0	200.0	-115.0	0.0	1.2	.4	.1
F02310	.5	.2	.1	200.0	-102.5	0.0	1.2	.6	.2
F02311	.2	0.0	0.0	200.0	-90.0	0.0	.6	0.0	.1
G02304	.3	.1	0.0	200.0	125.0	0.0	.8	.3	.1
G02305	.4	.2	.1	200.0	137.5	0.0	1.1	.6	.2
G02306	.5	.3	.1	200.0	150.0	0.0	1.4	.7	.3
G02307	.5	.2	.1	200.0	162.5	0.0	1.5	.6	.2
G02308	.4	.2	.1	200.0	175.0	0.0	1.1	.5	.2
G02309	.6	.4	.1	200.0	187.5	0.0	1.5	1.1	.2
G02310	.9	.6	.1	200.0	200.0	0.0	2.3	1.5	.2
G02311	.4	.3	.1	200.0	212.5	0.0	1.2	.8	.1
K02304	.3	.1	.1	175.0	-77.5	0.0	.9	.3	.1
K02305	.4	.2	.1	175.0	-65.0	0.0	1.0	.3	.2
K02306	.5	.1	.1	175.0	-52.5	0.0	.7	.3	.2
K02307	.5	.2	.1	175.0	-40.0	0.0	1.3	.5	.2
K02308	.3	.1	.1	175.0	-27.5	0.0	.8	.2	.1
K02309	.3	.1	.1	175.0	-15.0	0.0	.8	.3	.2
K02310	.5	.1	.1	175.0	-2.5	0.0	1.3	.4	.2
K02311	.3	.1	.1	175.0	10.0	0.0	.8	.2	.2
H02304	.5	0.0	.1	150.0	25.0	0.0	1.4	0.0	.2
H02305	.3	0.0	.1	150.0	37.5	0.0	.7	0.0	.2
H02306	0.0	0.0	0.0	150.0	50.0	0.0	0.0	0.0	0.0
H02307	.5	.1	.1	150.0	62.5	0.0	1.2	.4	.2
H02308	.5	.2	.1	150.0	75.0	0.0	1.3	.5	.2
H02309	.6	.3	.1	150.0	87.5	0.0	1.6	.7	.2
H02310	.8	.5	.1	150.0	100.0	0.0	2.1	1.3	.3
H02311	.3	.1	.1	150.0	112.5	0.0	.7	.4	.2
I02304	.3	.1	0.0	105.0	175.0	0.0	.8	.4	.1
I02305	.4	.2	.1	105.0	187.5	0.0	.9	.5	.2
I02306	.4	.2	.1	105.0	200.0	0.0	1.2	.5	.2
I02307	.4	.2	.1	105.0	212.5	0.0	1.1	.6	.2
I02308	.2	0.0	.1	105.0	225.0	0.0	.6	0.0	.2
I02309	.5	.2	.1	105.0	237.5	0.0	1.2	.6	.2
I02310	.4	.1	.1	105.0	250.0	0.0	1.0	.2	.2
I02311	.4	.1	.1	105.0	262.5	0.0	1.0	.4	.1

FILE NAME	MODEL CONDITIONS PEAK CONC (%)	MEAN CONC (%)	RMS CONC (%)	PROTOTYPE POSITION X (M)	Y (M)	Z (M)	PROTOTYPE CONDITIONS PEAK CONC (%)	MEAN CONC (%)	RMS CONC (%)
A03104	.2	.2	0.0	-125.0	-230.0	0.0	.6	.4	.1
A03105	.2	.1	0.0	-125.0	-217.5	0.0	.4	.2	.1
A03106	.4	.2	0.0	-125.0	-205.0	0.0	1.0	.6	.1
A03107	.2	.1	0.0	-125.0	-192.5	0.0	.4	.3	.1
A03108	.1	0.0	0.0	-125.0	-180.0	0.0	.2	0.0	.1
A03109	.3	.2	.1	-125.0	-167.5	0.0	.7	.4	.2
A03110	.4	.2	.1	-125.0	-155.0	0.0	1.0	.4	.3
A03111	.4	.2	.1	-125.0	-142.5	0.0	1.2	.5	.3
B03104	.1	0.0	0.0	0.0	-230.0	0.0	.4	0.0	.1
B03105	.1	0.0	0.0	0.0	-217.5	0.0	.2	0.0	.1
B03106	.2	.1	.1	0.0	-205.0	0.0	.5	.2	.1
B03107	.2	.1	0.0	0.0	-192.5	0.0	.4	.2	.1
B03108	.1	0.0	0.0	0.0	-180.0	0.0	.2	0.0	.1
B03109	.2	0.0	0.0	0.0	-167.5	0.0	.6	0.0	.1
B03110	.2	.1	.1	0.0	-155.0	0.0	.8	.2	.1
B03111	1.2	.3	.2	0.0	-142.5	0.0	1.2	.3	.2
C03104	0.0	0.0	0.0	50.0	-230.0	0.0	0.0	0.0	0.0
C03105	.2	.1	.1	50.0	-217.5	0.0	.6	.2	.1
C03106	.3	.2	.1	50.0	-205.0	0.0	.8	.4	.2
C03107	.2	.1	.1	50.0	-192.5	0.0	.6	.3	.2
C03108	.1	0.0	0.0	50.0	-180.0	0.0	.3	0.0	.1
C03109	.4	.1	.1	50.0	-167.5	0.0	.9	.4	.2
C03110	.7	.2	.2	50.0	-155.0	0.0	1.0	.6	.4
C03111	2.1	.5	.3	50.0	-142.5	0.0	1.5	.6	.3
D03104	.2	0.0	.1	100.0	-230.0	0.0	.5	0.0	.2
D03105	.2	.1	0.0	100.0	-217.5	0.0	.6	.3	.1
D03106	.2	.1	0.0	100.0	-205.0	0.0	.4	.2	.1
D03107	.1	0.0	0.0	100.0	-192.5	0.0	.4	.2	.1
D03108	.2	0.0	0.0	100.0	-180.0	0.0	.4	0.0	.1
D03109	.5	.1	.1	100.0	-167.5	0.0	1.0	.3	.2
D03110	.9	.1	.2	100.0	-155.0	0.0	1.3	.4	.2
D03111	2.3	.6	.4	100.0	-142.5	0.0	1.9	.5	.3
E03104	.2	0.0	.1	150.0	-177.5	0.0	.5	0.0	.2
E03105	.5	0.0	.1	150.0	-165.0	0.0	1.4	0.0	.2
E03106	.7	0.0	.2	150.0	-152.5	0.0	1.9	0.0	.3
E03107	1.4	.3	.4	150.0	-140.0	0.0	3.8	.8	.6
E03108	2.1	.9	.3	150.0	-127.5	0.0	5.4	2.2	.5
E03109	2.1	.9	.3	150.0	-115.0	0.0	5.5	2.3	.5
E03110	2.1	.9	.4	150.0	-102.5	0.0	5.6	2.3	.6
E03111	2.1	1.0	.3	150.0	-90.0	0.0	5.4	2.6	.5
J03104	.9	.2	.2	175.0	-177.5	0.0	2.5	.4	.3
J03105	4.0	.9	.4	175.0	-165.0	0.0	1.0	.6	.4
J03106	1.7	.9	.4	175.0	-152.5	0.0	4.6	1.8	.6
J03107	1.9	1.0	.3	175.0	-140.0	0.0	5.1	2.7	.5
J03108	2.0	1.1	.4	175.0	-127.5	0.0	6.0	3.0	.6
J03109	2.5	1.2	.4	175.0	-115.0	0.0	6.6	3.3	.6
J03110	2.6	1.1	.4	175.0	-102.5	0.0	5.5	2.7	.6
J03111	2.6	1.2	.4	175.0	-90.0	0.0	5.5	3.1	.6
F03104	1.8	1.0	.3	200.0	-167.5	0.0	4.4	2.2	.5
F03105	1.9	.9	.3	200.0	-155.0	0.0	5.1	2.4	.5
F03106	1.9	1.2	.4	200.0	-142.5	0.0	3.3	1.6	.6
F03107	1.2	.7	.3	200.0	-130.0	0.0	3.3	1.5	.5
F03108	.7	0.0	.1	200.0	-117.5	0.0	1.8	0.0	.2
F03109	.1	0.0	.1	200.0	-105.0	0.0	.4	0.0	.2
F03110	.1	0.0	.1	200.0	-92.5	0.0	.4	0.0	.2
F03111	.2	0.0	.1	200.0	-80.0	0.0	.4	0.0	.2
K03104	2.1	1.1	.4	175.0	-77.5	0.0	5.2	2.3	.6
K03105	.7	.1	.2	175.0	-65.0	0.0	2.0	.3	.4
K03106	.5	.2	.1	175.0	-52.5	0.0	1.3	.6	.2
K03107	.3	.1	0.0	175.0	-40.0	0.0	.7	.2	.1
K03108	.3	0.0	0.0	175.0	-27.5	0.0	.7	0.0	.1
K03109	.1	0.0	0.0	175.0	-15.0	0.0	.3	0.0	.1
K03110	.1	0.0	0.0	175.0	-2.5	0.0	.3	0.0	.1
K03111	0.0	0.0	0.0	175.0	10.0	0.0	0.0	0.0	0.0

FILE NAME	MODEL CONDITIONS PEAK CONC (%)	MEAN CONC (%)	RMS CONC (%)	PROTOTYPE CONDITIONS POSITION X (M)	Y (M)	Z (M)	PEAK CONC (%)	MEAN CONC (%)	RMS CONC (%)
A032C4	.1	0.0	0.0	-125.0	-230.0	0.0	.3	0.0	.1
A032C5	.1	0.0	0.0	-125.0	-217.5	0.0	.3	0.0	.1
A032C6	.3	.1	.1	-125.0	-205.0	0.0	.3		.2
A032C7	.3	.1	.1	-125.0	-192.5	0.0	.7		.2
A032C8	.2	.1	0.0	-125.0	-180.0	0.0	.5		.1
A032C9	.3	.1	.1	-125.0	-167.5	0.0	.8		.2
A032C10	.4	.2	.1	-125.0	-155.0	0.0	1.2		.3
A032C11	1.4	.3	.1	-125.0	-142.5	0.0	3.8		.4
B032C4	.1	0.0	0.0	0.0	-230.0	0.0	.3	0.0	.1
B032C5	.1	0.0	0.0	0.0	-217.5	0.0	.3	0.0	.1
B032C6	.1	0.0	.1	0.0	-205.0	0.0	.3	0.0	.2
B032C7	.1	0.0	0.0	0.0	-192.5	0.0	.7	0.0	.2
B032C8	.3	0.0	0.0	0.0	-180.0	0.0	.9	0.0	.1
B032C9	.7	.1	.2	0.0	-167.5	0.0	1.9		.4
B032C10	1.1	.3	.2	0.0	-155.0	0.0	3.0		.6
B032C11	1.2	.5	.2	0.0	-142.5	0.0	3.1	1.0	.5
C032C4	.2	0.0	0.0	50.0	-230.0	0.0	.4	0.0	.1
C032C5	0.0	0.0	0.0	50.0	-217.5	0.0	0.0	0.0	0.0
C032C6	.3	.2	0.0	50.0	-205.0	0.0	.8		.1
C032C7	.3	.2	0.0	50.0	-192.5	0.0	.9		.1
C032C8	.4	.1	.1	50.0	-180.0	0.0	1.0		.2
C032C9	.6	.2	.1	50.0	-167.5	0.0	1.5		.3
C032C10	.6	.1	.2	50.0	-155.0	0.0	1.5		.4
C032C11	.7	.3	.1	50.0	-142.5	0.0	1.8		.3
D032C4	0.0	0.0	0.0	100.0	-230.0	0.0	0.0	0.0	0.0
D032C5	.1	0.0	.1	100.0	-217.5	0.0	.2	0.0	.2
D032C6	.2	0.0	.1	100.0	-205.0	0.0	.5	0.0	.2
D032C7	.2	0.0	0.0	100.0	-192.5	0.0	.6	0.0	.1
D032C8	.3	0.0	.1	100.0	-180.0	0.0	.8	0.0	.2
D032C9	.7	.2	.1	100.0	-167.5	0.0	1.8		.5
D032C10	1.1	.4	.2	100.0	-155.0	0.0	2.7	1.0	.6
D032C11	1.4	.5	.2	100.0	-142.5	0.0	3.7	1.1	.4
E032C4	.5	.2	.1	150.0	-177.5	0.0	1.1		.4
E032C5	.5	.2	.1	150.0	-165.0	0.0	1.3		.5
E032C6	.7	.4	.1	150.0	-152.5	0.0	1.9	1.0	.6
E032C7	1.2	.4	.2	150.0	-140.0	0.0	2.9	1.1	.6
E032C8	1.3	.6	.2	150.0	-127.5	0.0	3.1	1.4	.6
E032C9	1.5	.8	.2	150.0	-115.0	0.0	3.3	1.9	.7
E032C10	1.6	.8	.2	150.0	-102.5	0.0	4.3	2.3	.8
E032C11	1.4	.8	.2	150.0	-90.0	0.0	3.5	2.2	.7
J032C4	.5	.1	.2	175.0	-177.5	0.0	1.1	.4	.4
J032C5	.4	.2	.1	175.0	-165.0	0.0	1.1	.4	.4
J032C6	.6	.1	.1	175.0	-152.5	0.0	1.6	.7	.5
J032C7	.8	.2	.1	175.0	-140.0	0.0	2.1	.8	.5
J032C8	.9	.4	.2	175.0	-127.5	0.0	2.5	.9	.6
J032C9	1.0	.4	.2	175.0	-115.0	0.0	2.7	.9	.6
J032C10	.8	.2	.2	175.0	-102.5	0.0	2.2	.7	.5
J032C11	1.0	.4	.2	175.0	-90.0	0.0	2.6	1.1	.5
F032C4	1.0	.4	.2	200.0	-87.5	0.0	2.6	1.1	.6
F032C5	1.0	.4	.2	200.0	-75.0	0.0	2.7	1.1	.7
F032C6	1.1	.3	.3	200.0	-62.5	0.0	2.9	.9	.7
F032C7	.7	.2	.2	200.0	-50.0	0.0	2.1	.5	.5
F032C8	.6	0.0	.1	200.0	-37.5	0.0	1.5	0.0	.2
F032C9	.4	.1	.1	200.0	-25.0	0.0	1.1	.2	.3
F032C10	.5	.1	.1	200.0	-12.5	0.0	1.3	.2	.3
F032C11	.2	0.0	0.0	200.0	0.0	0.0	.6	0.0	.1
K032C4	1.3	.6	.3	175.0	-77.5	0.0	3.2	1.5	.7
K032C5	1.1	.3	.3	175.0	-65.0	0.0	2.9	.8	.7
K032C6	1.1	.2	.2	175.0	-52.5	0.0	2.9	.4	.6
K032C7	1.0	.1	.2	175.0	-40.0	0.0	2.8	.3	.5
K032C8	.6	0.0	.1	175.0	-27.5	0.0	1.5	0.0	.3
K032C9	.4	0.0	.1	175.0	-15.0	0.0	1.1	0.0	.2
K032C10	.1	0.0	.1	175.0	-2.5	0.0	.4	0.0	.2
K032C11	.1	0.0	0.0	175.0	10.0	0.0	.4	0.0	.2

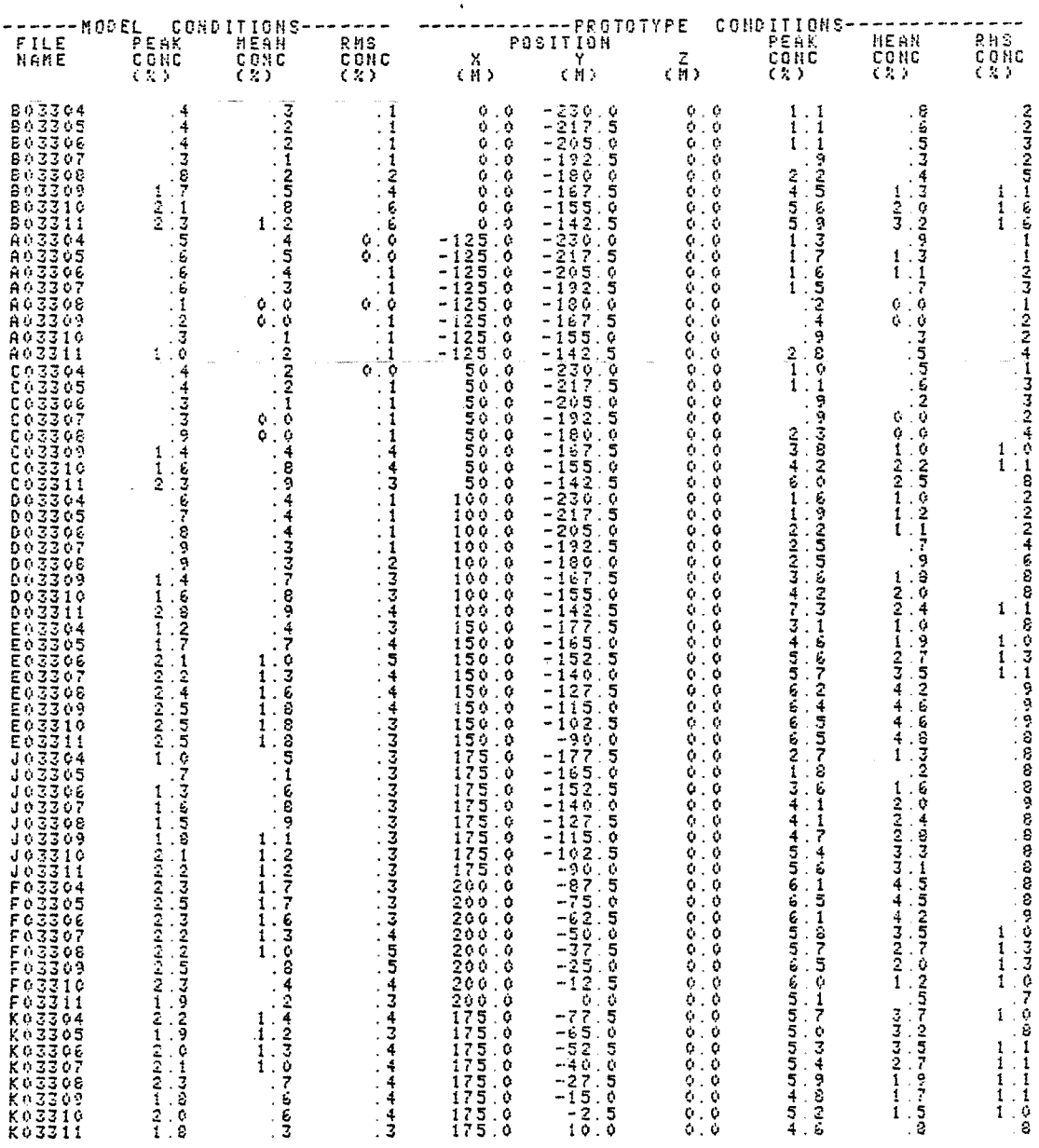

MODEL CONDITIONS				PROTOTYPE CONDITIONS					
FILE NAME	PEAK CONC (%)	MEAN CONC (%)	RMS CONC (%)	POSITION X (M)	Y (M)	Z (M)	PEAK CONC (%)	MEAN CONC (%)	RMS CONC (%)
C03404	.3	.2	.1	50.0	-230.0	0.0	.8	.5	.2
C03405	1.0	.8	.1	50.0	-217.5	0.0	2.8	2.2	.2
C03406	1.0	.8	.1	50.0	-205.0	0.0	2.6	2.1	.2
C03407	1.8	.6	.2	50.0	-192.5	0.0	4.8	1.6	.5
C03408	2.0	.5	.4	50.0	-180.0	0.0	5.3	1.5	1.1
C03409	2.4	1.3	.5	50.0	-167.5	0.0	6.3	3.3	1.4
C03410	4.1	2.1	.7	50.0	-155.0	0.0	10.4	5.3	1.7
C03411	5.2	2.8	.7	50.0	-142.5	0.0	13.6	7.2	1.7
D03404	.4	.2	0.0	100.0	-230.0	0.0	1.0	.6	.1
D03405	.5	.4	.1	100.0	-217.5	0.0	1.5	1.2	.2
D03406	.9	.3	.2	100.0	-205.0	0.0	2.3	.8	.4
D03407	1.3	.3	.3	100.0	-192.5	0.0	3.5	.8	.7
D03408	1.5	.4	.4	100.0	-180.0	0.0	3.8	1.0	1.0
D03409	2.0	.9	.5	100.0	-167.5	0.0	5.1	2.3	1.1
D03410	1.9	1.0	.4	100.0	-155.0	0.0	5.0	2.6	1.1
D03411	1.6	.7	.3	100.0	-142.5	0.0	4.2	1.9	.8
E03404	1.3	.6	.3	150.0	-177.5	0.0	3.5	1.6	.8
E03405	1.4	1.0	.2	150.0	-165.0	0.0	3.6	2.6	.6
E03406	1.1	.4	.3	150.0	-152.5	0.0	2.9	1.1	.7
E03407	1.3	.5	.3	150.0	-140.0	0.0	3.4	1.4	.8
E03408	1.7	.7	.3	150.0	-127.5	0.0	4.3	1.8	.7
E03409	1.7	1.0	.3	150.0	-115.0	0.0	4.4	2.6	.7
E03410	1.7	1.0	.3	150.0	-102.5	0.0	4.4	2.6	.7
E03411	1.7	1.1	.2	150.0	-90.0	0.0	4.4	2.9	.5
J03404	1.5	.7	.3	175.0	-177.5	0.0	3.9	1.8	.7
J03405	1.5	.9	.2	175.0	-165.0	0.0	3.9	2.4	.5
J03406	1.1	.4	.2	175.0	-152.5	0.0	2.9	1.1	.6
J03407	1.4	.6	.3	175.0	-140.0	0.0	3.7	1.6	.7
J03408	1.6	.9	.3	175.0	-127.5	0.0	4.1	2.3	.8
J03409	1.9	1.1	.3	175.0	-115.0	0.0	5.0	2.8	.8
J03410	1.8	1.0	.3	175.0	-102.5	0.0	4.8	2.6	.8
J03411	1.7	.9	.3	175.0	-90.0	0.0	4.4	2.3	.8
K03404	1.9	1.2	.3	175.0	-72.5	0.0	4.9	3.1	.8
K03405	.9	0.0	.3	175.0	-65.0	0.0	2.5	0.0	.7
K03406	2.1	1.0	.4	175.0	-52.5	0.0	5.5	2.7	1.1
K03407	2.3	.8	.4	175.0	-40.0	0.0	6.1	2.2	1.1
K03408	1.8	.6	.4	175.0	-27.5	0.0	4.7	1.6	.9
K03409	1.5	.5	.3	175.0	-15.0	0.0	4.1	1.3	.7
K03410	1.1	0.0	.3	175.0	-2.5	0.0	2.8	0.0	.5
K03411	1.0	.1	.2	175.0	10.0	0.0	2.7	.2	.5
F03404	1.6	1.0	.2	200.0	-87.5	0.0	4.3	2.7	.5
F03405	1.3	.8	.2	200.0	-75.0	0.0	3.5	2.2	.5
F03406	.9	.4	.2	200.0	-62.5	0.0	2.3	1.1	.5
F03407	1.2	.6	.2	200.0	-50.0	0.0	3.4	1.7	.6
F03408	1.7	.8	.3	200.0	-37.5	0.0	4.4	2.2	.8
F03409	1.8	.7	.4	200.0	-25.0	0.0	4.8	2.0	1.0
F03410	1.8	.6	.3	200.0	-12.5	0.0	4.7	1.6	.8
F03411	1.6	.5	.3	200.0	0.0	0.0	4.3	1.3	.7

FILE NAME	MODEL CONDITIONS PEAK CONC (%)	MEAN CONC (%)	RMS CONC (%)	PROTOTYPE CONDITIONS POSITION X (M)	Y (M)	Z (M)	PEAK CONC (%)	MEAN CONC (%)	RMS CONC (%)
B039004	.2	.1	.1	0.0	-230.0	0.0	.6	.1	.2
B039005	.2	0.0	.1	0.0	-217.5	0.0	.4	0.0	.1
B039006	.1	0.0	.2	0.0	-205.0	0.0	.2	0.0	.1
B039007	.1	0.0	.1	0.0	-192.5	0.0	.2	0.0	.1
B039008	.1	0.0	0.0	0.0	-180.0	0.0	.3	0.0	.1
B039009	.1	0.0	.1	0.0	-167.5	0.0	.4	0.0	.2
B039010	.3	0.0	.1	0.0	-155.0	0.0	.8	0.0	.3
B039011	.3	0.0	.1	0.0	-142.5	0.0	.9	0.0	.3
C039004	.2	0.0	.1	50.0	-230.0	0.0	.7	0.0	.2
C039005	0.0	0.0	0.0	50.0	-217.5	0.0	0.0	0.0	0.0
C039006	.1	0.0	.1	50.0	-205.0	0.0	.3	0.0	.1
C039007	.1	0.0	.1	50.0	-192.5	0.0	.2	0.0	.2
C039008	.2	0.0	.1	50.0	-180.0	0.0	.5	0.0	.2
C039009	.3	0.0	.1	50.0	-167.5	0.0	.8	0.0	.3
C039010	.5	0.0	.1	50.0	-155.0	0.0	1.5	0.0	.4
C039011	.9	.1	.2	50.0	-142.5	0.0	2.4	.3	.6
D039004	.2	0.0	.1	100.0	-230.0	0.0	.6	0.0	.3
D039005	.2	0.0	.1	100.0	-217.5	0.0	.6	0.0	.3
D039006	.2	0.0	.2	100.0	-205.0	0.0	.7	0.0	.4
D039007	.1	0.0	.1	100.0	-192.5	0.0	.2	0.0	.2
D039008	.2	0.0	.1	100.0	-180.0	0.0	.5	0.0	.3
D039009	.2	0.0	.2	100.0	-167.5	0.0	.8	0.0	.4
D039010	.3	0.0	.3	100.0	-155.0	0.0	.9	0.0	.5
D039011	.8	.1	.2	100.0	-142.5	0.0	2.2	.4	.9
E039004	.5	0.0	.3	150.0	-177.5	0.0	1.2	0.0	.8
E039005	.3	.3	.4	150.0	-165.0	0.0	1.5	.8	1.0
E039006	.3	.4	.9	150.0	-152.5	0.0	.9	.9	1.0
E039007	1.1	1.2	.7	150.0	-140.0	0.0	3.1	1.1	1.9
E039008	1.0	1.2	.5	150.0	-127.5	0.0	4.1	1.1	1.3
E039009	.9	1.8	.4	150.0	-115.0	0.0	4.7	1.1	1.0
E039010	.7	1.6	.4	150.0	-102.5	0.0	4.9	1.1	.9
E039011	.7	1.7	.3	150.0	-90.0	0.0	4.5	1.0	.7
J039004	.3	.3	.2	175.0	-177.5	0.0	.9	.3	.5
J039005	.3	.4	.4	175.0	-165.0	0.0	1.2	.4	.9
J039006	.3	.4	.6	175.0	-152.5	0.0	1.2	.5	1.3
J039007	.6	.6	.5	175.0	-140.0	0.0	1.5	.6	1.4
J039008	.4	1.0	.5	175.0	-127.5	0.0	2.5	.6	1.3
J039009	.3	1.0	.5	175.0	-115.0	0.0	2.6	.6	1.2
J039010	.9	.4	.4	175.0	-102.5	0.0	2.5	.6	1.2
J039011	.7	1.3	.4	175.0	-90.0	0.0	2.6	.6	1.1
F039004	1.9	.8	.4	200.0	-87.5	0.0	1.8	.4	1.0
F039005	1.6	.6	.4	200.0	-75.0	0.0	1.7	.4	1.1
F039006	1.7	.5	.5	200.0	-62.5	0.0	1.2	.4	1.2
F039007	1.8	.5	.5	200.0	-50.0	0.0	1.2	.4	1.3
F039008	1.8	.5	.4	200.0	-37.5	0.0	1.2	.4	1.1
F039009	1.5	.2	.3	200.0	-25.0	0.0	.9	.2	.7
F039010	1.6	.1	.3	200.0	-12.5	0.0	.4	.2	.4
F039011	.8	.1	.1	200.0	0.0	0.0	.2	.2	.4
K039004	2.4	1.4	.5	175.0	-77.5	0.0	3.8	1.3	1.3
K039005	2.4	1.0	.5	175.0	-65.0	0.0	3.6	1.3	1.3
K039006	1.9	.7	.6	175.0	-52.5	0.0	2.5	1.0	1.5
K039007	1.8	.5	.5	175.0	-40.0	0.0	2.4	1.0	1.2
K039008	2.0	.5	.5	175.0	-27.5	0.0	2.6	1.0	1.2
K039009	2.0	.4	.4	175.0	-15.0	0.0	2.5	1.0	1.1
K039010	2.2	.5	.3	175.0	-2.5	0.0	2.7	1.1	1.3
K039011	1.2	.3	.2	175.0	10.0	0.0	3.1	.7	.8

MODEL CONDITIONS				PROTOTYPE CONDITIONS					
FILE NAME	PEAK CONC (%)	MEAN CONC (%)	RMS CONC (%)	POSITION X (M)	Y (M)	Z (M)	PEAK CONC (%)	MEAN CONC (%)	RMS CONC (%)
B04104	0.0	0.0	0.0	0.0	-230.0	0.0	0.0	0.0	0.0
B04105	.3	.1	0.0	0.0	-217.5	0.0	.7	.3	.1
B04106	.8	.5	.1	0.0	-205.0	0.0	2.0	1.5	.2
B04107	.1	.1	0.0	0.0	-192.5	0.0	.4	.2	.1
B04108	.1	.1	0.0	0.0	-180.0	0.0	.4	.2	.1
B04109	.2	.1	0.0	0.0	-167.5	0.0	.5	.2	.1
B04110	.3	.1	.1	0.0	-155.0	0.0	.9	.3	.2
B04111	.6	.3	.1	0.0	-142.5	0.0	1.6	.8	.3
C04104	0.0	0.0	0.0	50.0	-230.0	0.0	0.0	0.0	0.0
C04105	.3	.2	.1	50.0	-217.5	0.0	.9	.5	.3
C04106	.4	.2	.1	50.0	-205.0	0.0	1.2	.7	.4
C04107	.3	.1	.1	50.0	-192.5	0.0	.7	.4	.2
C04108	.2	.1	0.0	50.0	-180.0	0.0	.5	.2	.1
C04109	.3	.1	.1	50.0	-167.5	0.0	.7	.3	.2
C04110	.6	.1	.2	50.0	-155.0	0.0	1.5	.6	.3
C04111	.6	.1	.1	50.0	-142.5	0.0	1.5	.7	.3
D04104	.3	.1	.1	100.0	-230.0	0.0	.7	.3	.2
D04105	.1	0.0	.1	100.0	-217.5	0.0	.2	.1	.1
D04106	.5	.2	.1	100.0	-205.0	0.0	1.2	.6	.2
D04107	.2	0.0	.1	100.0	-192.5	0.0	.6	.2	.1
D04108	.2	0.0	0.0	100.0	-180.0	0.0	.5	.2	.1
D04109	.4	.2	.1	100.0	-167.5	0.0	.9	.5	.2
D04110	.8	.2	.2	100.0	-155.0	0.0	1.8	.6	.3
D04111	1.4	.5	.3	100.0	-142.5	0.0	3.0	1.3	.6
E04104	0.0	0.0	0.0	150.0	-177.5	0.0	0.0	0.0	0.0
E04105	0.0	0.0	0.0	150.0	-165.0	0.0	0.0	0.0	0.0
E04106	1.5	.6	.2	150.0	-152.5	0.0	4.0	1.5	.5
E04107	2.0	.7	.4	150.0	-140.0	0.0	5.1	1.9	.7
E04108	2.6	1.4	.4	150.0	-127.5	0.0	6.5	3.7	1.1
E04109	2.9	2.0	.3	150.0	-115.0	0.0	7.5	5.2	1.0
E04110	3.3	2.4	.3	150.0	-102.5	0.0	8.4	6.3	.8
E04111	3.2	2.7	.3	150.0	-90.0	0.0	8.0	6.7	.8
J04104	0.0	0.0	0.0	175.0	-177.5	0.0	0.0	0.0	0.0
J04105	.6	.3	.2	175.0	-165.0	0.0	1.5	.8	.4
J04106	2.1	1.0	.2	175.0	-152.5	0.0	5.3	2.6	.6
J04107	2.0	1.0	.4	175.0	-140.0	0.0	5.1	2.5	1.1
J04108	2.0	1.3	.3	175.0	-127.5	0.0	5.0	3.3	.8
J04109	2.8	1.8	.3	175.0	-115.0	0.0	7.0	4.6	.8
J04110	3.0	2.2	.3	175.0	-102.5	0.0	7.4	5.5	.8
J04111	3.3	2.5	.3	175.0	-90.0	0.0	8.0	6.2	.8
F04104	0.0	0.0	0.0	200.0	-87.5	0.0	0.0	0.0	0.0
F04105	3.3	2.3	.4	200.0	-75.0	0.0	8.4	5.8	1.0
F04106	3.6	2.8	.3	200.0	-62.5	0.0	9.2	7.1	.8
F04107	2.8	1.9	.4	200.0	-50.0	0.0	7.1	4.8	.9
F04108	3.2	1.7	.5	200.0	-37.5	0.0	8.1	4.3	1.2
F04109	3.0	1.7	.5	200.0	-25.0	0.0	7.7	4.3	1.1
F04110	2.9	1.8	.6	200.0	-12.5	0.0	7.3	4.5	1.5
F04111	3.2	1.4	.5	200.0	0.0	0.0	8.2	3.6	1.3
K04104	2.9	2.0	.4	175.0	-77.5	0.0	7.4	5.1	1.1
K04105	3.1	2.3	.3	175.0	-65.0	0.0	8.0	5.9	.8
K04106	3.4	2.5	.3	175.0	-52.5	0.0	8.6	6.5	.8
K04107	3.1	2.2	.4	175.0	-40.0	0.0	8.0	5.6	1.1
K04108	2.8	1.0	.5	175.0	-27.5	0.0	7.3	2.6	1.1
K04109	2.2	.9	.4	175.0	-15.0	0.0	5.5	2.4	1.1
K04110	2.2	.7	.3	175.0	-2.5	0.0	5.4	1.9	.7
K04111	1.5	.6	.2	175.0	10.0	0.0	4.0	1.7	.5

FILE NAME	MODEL CONDITIONS PEAK CONC (%)	MEAN CONC (%)	RMS CONC (%)	PROTOTYPE CONDITIONS POSITION X (M)	Y (M)	Z (M)	PEAK CONC (%)	MEAN CONC (%)	RMS CONC (%)
D04304	0.0	0.0	0.0	150.0	-125.0	0.0	0.0	0.0	0.0
D04305	.5	.2	.1	150.0	-112.5	0.0	1.3	.7	.3
D04306	.8	.5	.1	150.0	-100.0	0.0	2.2	1.4	.4
D04307	.2	.1	0.0	150.0	-87.5	0.0	.7	.2	.1
D04308	.1	0.0	0.0	150.0	-75.0	0.0	.3	0.0	.1
D04309	.2	0.0	0.0	150.0	-62.5	0.0	.5	0.0	.1
D04310	0.0	0.0	0.0	150.0	-50.0	0.0	0.0	0.0	0.0
D04311	0.0	0.0	0.0	150.0	-37.5	0.0	0.0	0.0	0.0
C04304	0.0	0.0	0.0	100.0	-200.0	0.0	0.0	0.0	0.0
C04305	.5	.2	.1	100.0	-187.5	0.0	1.4	.6	.2
C04306	.6	.4	.1	100.0	-175.0	0.0	1.7	1.0	.3
C04307	.4	.2	.1	100.0	-162.5	0.0	1.0	.5	.1
C04308	.3	.1	0.0	100.0	-150.0	0.0	.7	.3	.1
C04309	.3	.2	0.0	100.0	-137.5	0.0	.9	.6	.1
C04310	.2	0.0	.1	100.0	-125.0	0.0	.6	0.0	.2
C04311	.1	0.0	0.0	100.0	-112.5	0.0	.1	0.0	.1
E04304	0.0	0.0	0.0	200.0	-87.5	0.0	0.0	0.0	0.0
E04305	.1	0.0	.1	200.0	-75.0	0.0	.2	0.0	.2
E04306	.2	0.0	.1	200.0	-62.5	0.0	.4	0.0	.3
E04307	.1	0.0	.1	200.0	-50.0	0.0	.3	0.0	.2
E04308	.2	0.0	.1	200.0	-37.5	0.0	.5	0.0	.2
E04309	.6	.2	.2	200.0	-25.0	0.0	1.2	.6	.5
E04310	.8	.2	.3	200.0	-12.5	0.0	2.2	.6	.7
E04311	.7	.3	.2	200.0	0.0	0.0	1.8	.8	.5
F04304	.9	.6	.1	200.0	12.5	0.0	2.5	1.5	.3
F04305	.8	.4	.1	200.0	25.0	0.0	2.2	1.1	.3
F04306	.8	.4	.1	200.0	37.5	0.0	2.2	1.2	.4
F04307	.4	.1	.1	200.0	50.0	0.0	1.1	.4	.2
F04308	.3	.1	.1	200.0	62.5	0.0	.8	.4	.2
F04309	.6	.3	.1	200.0	75.0	0.0	1.5	.7	.4
F04310	.5	.1	.2	200.0	87.5	0.0	1.3	.2	.4
F04311	.5	.2	.1	200.0	100.0	0.0	1.3	.5	.3
G04304	0.0	0.0	0.0	150.0	112.5	0.0	0.0	0.0	0.0
G04305	.4	.1	.1	150.0	125.0	0.0	1.0	.2	.2
G04306	.5	.2	.1	150.0	137.5	0.0	1.2	.6	.3
G04307	.3	.1	.1	150.0	150.0	0.0	.8	.3	.2
G04308	.2	.1	0.0	150.0	162.5	0.0	.7	.4	.1
G04309	.5	.3	.1	150.0	175.0	0.0	1.3	.9	.1
G04310	.6	.4	.1	150.0	187.5	0.0	1.6	1.1	.2
G04311	.4	.3	.1	150.0	200.0	0.0	1.0	.7	.1
H04304	.5	.3	.1	100.0	125.0	0.0	1.3	.7	.3
H04305	.4	.2	.1	100.0	137.5	0.0	1.1	.7	.2
H04306	.4	.3	.1	100.0	150.0	0.0	1.1	.7	.3
H04307	.3	.1	.1	100.0	162.5	0.0	.7	.3	.2
H04308	.1	0.0	0.0	100.0	175.0	0.0	.3	0.0	.1
H04309	.2	.1	0.0	100.0	187.5	0.0	.5	0.0	.1
H04310	.2	0.0	.1	100.0	200.0	0.0	.5	0.0	.2
H04311	.1	.1	0.0	100.0	212.5	0.0	.4	.1	.1
I04304	.6	.3	.1	50.0	150.0	0.0	1.5	.8	.2
I04305	.5	.2	.1	50.0	162.5	0.0	1.2	.6	.2
I04306	.3	.2	.1	50.0	175.0	0.0	.9	.5	.1
I04307	.2	0.0	0.0	50.0	187.5	0.0	.5	0.0	.1
I04308	.1	.1	0.0	50.0	200.0	0.0	.4	.2	.1
I04309	.3	.2	0.0	50.0	212.5	0.0	.8	.4	.1
I04310	.3	.1	.1	50.0	225.0	0.0	.7	.1	.2
I04311	.2	.1	0.0	50.0	237.5	0.0	.6	.3	.1

FILE NAME	MODEL CONDITIONS PEAK CONC (%)	MEAN CONC (%)	RMS CONC (%)	PROTOTYPE CONDITIONS POSITION X (M)	Y (M)	Z (M)	PEAK CONC (%)	MEAN CONC (%)	RMS CONC (%)
C04404	0.0	0.0	0.0	50.0	-230.0	0.0	0.0	0.0	0.0
C04405	.1	0.0	0.0	50.0	-215.5	0.0	.3	0.0	.1
C04406	.5	.4	.1	50.0	-201.5	0.0	1.4	1.0	.2
C04407	0.0	0.0	0.0	50.0	-192.5	0.0	0.0	0.0	0.0
C04408	.2	.1	0.0	50.0	-180.5	0.0	.5	.3	.1
C04409	.4	.2	.1	50.0	-167.5	0.0	1.1	.7	.2
C04410	.4	.2	.1	50.0	-155.5	0.0	1.1	.6	.2
C04411	.6	.5	.1	50.0	-142.5	0.0	1.7	1.3	.2
D04404	0.0	0.0	0.0	100.0	-230.0	0.0	0.0	0.0	0.0
D04405	.0	.0	.1	100.0	-215.5	0.0	1.4	.7	.1
D04406	.9	.5	.1	100.0	-201.5	0.0	2.3	1.5	.2
D04407	0.0	0.0	.1	100.0	-192.5	0.0	.6	0.0	.2
D04408	.2	.1	0.0	100.0	-180.5	0.0	.6	.2	.1
D04409	.4	.2	.1	100.0	-167.5	0.0	1.1	.6	.2
D04410	.4	.2	.1	100.0	-155.5	0.0	1.1	.6	.2
D04411	.7	.5	0.0	100.0	-142.5	0.0	.9	.5	.1
E04404	.3	.2	.1	150.0	-177.5	0.0	.9	.5	.2
E04405	.4	.2	.1	150.0	-165.5	0.0	1.1	.5	.2
E04406	.7	0.0	.2	150.0	-152.5	0.0	1.8	0.0	.6
E04407	0.0	0.0	0.0	150.0	-140.5	0.0	0.0	0.0	0.0
E04408	.3	.2	0.0	150.0	-127.5	0.0	.9	.5	.1
E04409	.4	.3	0.0	150.0	-115.5	0.0	1.2	.7	.1
E04410	.5	.2	.1	150.0	-102.5	0.0	1.3	.6	.3
E04411	.7	.4	.1	150.0	-90.5	0.0	1.8	1.1	.2
F04404	.3	.3	.1	200.0	-87.5	0.0	1.5	.8	.2
F04405	.8	.4	.1	200.0	-75.5	0.0	2.1	1.1	.3
F04406	1.1	.8	.1	200.0	-60.5	0.0	3.0	2.0	.3
F04407	.8	.4	.1	200.0	-55.5	0.0	2.0	1.1	.2
F04408	.6	.2	.1	200.0	-37.5	0.0	1.6	.6	.3
F04409	.7	.3	.1	200.0	-25.5	0.0	1.8	.8	.3
F04410	.4	0.0	.1	200.0	-1	0.0	1.0	0.0	.3
F04411	.4	0.0	.1	200.0	0	0.0	1.0	0.0	.3
G04404	.5	.3	.1	200.0	12.5	0.0	1.3	.8	.2
G04405	.3	0.0	.1	200.0	25.5	0.0	.7	0.0	.2
G04406	0.0	0.0	0.0	200.0	37.5	0.0	0.0	0.0	0.0
G04407	0.0	0.0	0.0	200.0	50.5	0.0	0.0	0.0	0.0
G04408	0.0	0.0	0.0	200.0	62.5	0.0	0.0	0.0	0.0
G04409	.6	.3	.1	200.0	75.5	0.0	1.5	.9	.2
G04410	.6	.2	.1	200.0	87.5	0.0	1.5	.7	.3
G04411	.5	.2	.1	200.0	100.0	0.0	1.4	.7	.3
H04404	1.2	.6	.2	150.0	25.5	0.0	3.1	1.6	.4
H04405	1.4	.5	.2	150.0	37.5	0.0	3.6	1.4	.5
H04406	1.3	.9	.1	150.0	50.5	0.0	3.3	2.3	.4
H04407	.9	.4	.1	150.0	62.5	0.0	2.4	1.1	.3
H04408	.8	.4	.1	150.0	75.5	0.0	2.2	1.2	.3
H04409	1.2	.8	.1	150.0	87.5	0.0	3.2	2.0	.3
H04410	1.5	.7	.2	150.0	100.0	0.0	3.9	2.0	.4
H04411	.8	.6	.1	150.0	112.5	0.0	2.2	1.7	.2
I04404	.7	.5	.1	105.0	175.5	0.0	1.8	1.4	.2
I04405	.5	.3	0.0	105.0	187.5	0.0	1.2	.8	.1
I04406	.8	.5	.1	105.0	200.5	0.0	2.0	1.5	.2
I04407	.3	.2	.1	105.0	212.5	0.0	.8	.4	.1
I04408	.3	0.0	0.0	105.0	225.5	0.0	.4	0.0	.1
I04409	.4	.1	.1	105.0	237.5	0.0	.8	.3	.1
I04410	.4	0.0	.2	105.0	250.0	0.0	1.2	0.0	.4
I04411	.3	.1	.1	105.0	262.5	0.0	.8	.4	.2

FILE NAME	MODEL CONDITIONS PEAK CONC (%)	MEAN CONC (%)	RMS CONC (%)	PROTOTYPE CONDITIONS POSITION X (M)	Y (M)	Z (M)	PEAK CONC (%)	MEAN CONC (%)	RMS CONC (%)
E04504	0.0	0.0	0.0	200.0	-87.5	0.0	0.0	0.0	0.0
E04505	.2	0.0	.1	200.0	-75.0	0.0	.7	0.0	.3
E04506	.3	0.0	.1	200.0	-62.5	0.0	.7	0.0	.3
E04507	0.0	0.0	0.0	200.0	-50.0	0.0	0.0	0.0	0.0
E04508	.6	.1	.1	200.0	-37.5	0.0	1.6	.2	.3
E04509	.8	.2	.2	200.0	-25.0	0.0	2.2	.5	.5
E04510	1.2	.4	.3	200.0	-12.5	0.0	3.2	1.0	.8
E04511	1.6	.8	.3	200.0	0.0	0.0	4.1	2.1	.8
F04504	1.6	.9	.3	200.0	12.5	0.0	4.2	2.5	.8
F04505	1.7	.8	.4	200.0	25.0	0.0	4.6	2.2	1.0
F04506	.7	0.0	.3	200.0	37.5	0.0	1.9	0.0	.7
F04507	1.1	.1	.2	200.0	50.0	0.0	3.0	.3	.7
F04508	1.1	.1	.2	200.0	62.5	0.0	3.0	.3	.5
F04509	1.1	.2	.2	200.0	75.0	0.0	2.8	.5	.5
F04510	.9	.1	.2	200.0	87.5	0.0	2.4	.2	.5
F04511	.8	.4	.1	200.0	100.0	0.0	2.1	1.0	.3
G04504	1.1	.5	.2	200.0	112.5	0.0	3.0	1.3	.5
G04505	1.1	.4	.2	200.0	125.0	0.0	3.0	1.0	.5
G04506	.9	.2	.2	200.0	137.5	0.0	2.5	.5	.5
G04507	.6	0.0	.1	200.0	150.0	0.0	1.7	0.0	.2
G04508	.1	0.0	0.0	200.0	162.5	0.0	.3	0.0	.2
G04509	.2	.1	.1	200.0	175.0	0.0	.6	.2	.2
G04510	.2	0.0	.1	200.0	187.5	0.0	.6	0.0	.2
G04511	.1	0.0	.1	200.0	200.0	0.0	.2	0.0	.2
H04504	3.6	2.1	.4	150.0	0.0	0.0	9.2	5.4	1.0
H04505	4.9	2.6	.6	150.0	12.5	0.0	12.1	6.8	1.4
H04506	6.0	2.2	.9	150.0	25.0	0.0	14.6	5.7	2.2
H04507	5.6	1.2	.9	150.0	37.5	0.0	13.8	3.1	2.2
H04508	2.5	.6	.4	150.0	50.0	0.0	6.4	1.5	.9
H04509	2.6	.6	.3	150.0	62.5	0.0	6.8	1.5	.8
H04510	3.2	.6	.3	150.0	75.0	0.0	8.3	1.6	.9
H04511	2.6	.9	.3	150.0	87.5	0.0	6.7	2.4	.9
I04504	2.1	.4	.3	150.0	100.0	0.0	5.4	1.0	.9
I04505	1.8	.4	.4	150.0	112.5	0.0	4.8	1.2	1.0
I04506	1.8	.3	.4	150.0	125.0	0.0	4.8	.9	1.1
I04507	.6	0.0	.2	150.0	137.5	0.0	1.7	0.0	.5
I04508	.2	0.0	0.0	150.0	150.0	0.0	.5	0.0	.2
I04509	.2	0.0	.1	150.0	162.5	0.0	.4	0.0	.2
I04510	.1	0.0	.1	150.0	175.0	0.0	.3	0.0	.2
I04511	0.0	0.0	0.0	150.0	187.5	0.0	0.0	0.0	0.0

FILE NAME	MODEL CONDITIONS PEAK CONC (%)	MEAN CONC (%)	RMS CONC (%)	PROTOTYPE CONDITIONS POSITION X (M)	Y (M)	Z (M)	PEAK CONC (%)	MEAN CONC (%)	RMS CONC (%)
E04604	.2	0.0	.1	150.0	-177.5	0.0	.6	0.0	.3
E04605	.1	.1	0.0	150.0	-165.0	0.0	.4	.1	.1
E04606	.2	.1	.1	150.0	-152.5	0.0	.5	.2	.1
E04607	.2	.1	0.0	150.0	-140.0	0.0	.5	.2	.1
E04608	.2	0.0	0.0	150.0	-127.5	0.0	.6	0.0	.1
E04609	.3	.1	0.0	150.0	-115.0	0.0	.8	.4	.1
E04610	.4	.2	.1	150.0	-102.5	0.0	1.1	.5	.2
E04611	.3	.1	.1	150.0	-90.0	0.0	.8	.3	.2
J04604	.2	.1	0.0	175.0	-177.5	0.0	.4	.2	.1
J04605	.3	.2	0.0	175.0	-165.0	0.0	.7	.4	.1
J04606	.2	.1	0.0	175.0	-152.5	0.0	.6	.3	.1
J04607	.1	0.0	0.0	175.0	-140.0	0.0	.3	0.0	.1
J04608	.3	.2	0.0	175.0	-127.5	0.0	.9	.4	.1
J04609	.2	0.0	.1	175.0	-115.0	0.0	.4	0.0	.2
J04610	.1	0.0	.1	175.0	-102.5	0.0	.3	0.0	.2
J04611	.1	0.0	.1	175.0	-90.0	0.0	.3	0.0	.2
K04604	.6	.4	.1	175.0	-77.5	0.0	1.6	1.0	.2
K04605	.3	.1	0.0	175.0	-65.0	0.0	1.1	.3	.1
K04606	.4	.3	.1	175.0	-52.5	0.0	1.1	.7	.2
K04607	.4	.2	.1	175.0	-40.0	0.0	1.1	.5	.2
K04608	.3	.1	.1	175.0	-27.5	0.0	.8	.4	.1
K04609	.2	0.0	.1	175.0	-15.0	0.0	.4	0.0	.2
K04610	.2	0.0	.1	175.0	-2.5	0.0	.5	0.0	.2
K04611	.1	0.0	.1	175.0	10.0	0.0	.4	0.0	.2
H04604	1.6	.8	.2	150.0	25.0	0.0	4.2	2.1	.4
H04605	1.1	.5	.1	150.0	37.5	0.0	3.9	1.4	.4
H04606	1.1	.7	.2	150.0	50.0	0.0	3.0	1.9	.4
H04607	1.0	.5	.1	150.0	62.5	0.0	2.6	1.4	.4
H04608	.6	.1	.1	150.0	75.0	0.0	1.5	.3	.4
H04609	1.0	.4	.1	150.0	87.5	0.0	2.7	1.1	.3
H04610	.8	.5	.1	150.0	100.0	0.0	2.3	1.2	.3
H04611	.7	.4	.1	150.0	112.5	0.0	1.8	1.0	.2

MODEL CONDITIONS				PROTOTYPE CONDITIONS					
FILE NAME	PEAK CONC (%)	MEAN CONC (%)	RMS CONC (%)	POSITION X (M)	Y (M)	Z (M)	PEAK CONC (%)	MEAN CONC (%)	RMS CONC (%)
C04704	.1	0.0	0.0	50.0	-230.0	0.0	.3	0.0	.1
C04705	.1	0.0	0.0	50.0	-217.5	0.0	.2	0.0	.1
C04706	.2	.1	0.0	50.0	-205.0	0.0	.6	.2	.1
C04707	.2	.1	0.0	50.0	-192.5	0.0	.5	.3	.1
C04708	.1	0.0	.1	50.0	-180.0	0.0	.2	0.0	.2
C04709	0.0	0.0	0.0	50.0	-167.5	0.0	0.0	0.0	0.0
C04710	0.0	0.0	0.0	50.0	-155.0	0.0	0.0	0.0	0.0
C04711	.1	0.0	0.0	50.0	-142.5	0.0	.2	0.0	.1
D04704	.1	0.0	.1	100.0	-230.0	0.0	.3	0.0	.2
D04705	.1	0.0	.1	100.0	-217.5	0.0	.2	0.0	.2
D04706	0.0	0.0	0.0	100.0	-205.0	0.0	0.0	0.0	0.0
D04707	0.0	0.0	0.0	100.0	-192.5	0.0	0.0	0.0	0.0
D04708	0.0	0.0	0.0	100.0	-180.0	0.0	0.0	0.0	0.0
D04709	0.0	0.0	0.0	100.0	-167.5	0.0	0.0	0.0	0.0
D04710	.1	0.0	0.0	100.0	-155.0	0.0	.3	0.0	.1
D04711	.5	0.0	.1	100.0	-142.5	0.0	1.2	0.0	.2
E04704	.2	.1	0.0	150.0	-177.5	0.0	.6	.3	.1
E04705	.3	.2	0.0	150.0	-165.0	0.0	.7	.4	.1
E04706	.6	.2	.1	150.0	-152.5	0.0	1.5	.6	.2
E04707	.9	.3	.2	150.0	-140.0	0.0	2.4	.7	.2
E04708	1.5	.4	.3	150.0	-127.5	0.0	4.0	1.0	.3
E04709	1.7	.8	.3	150.0	-115.0	0.0	4.3	2.0	.7
E04710	1.8	.8	.3	150.0	-102.5	0.0	4.8	2.1	.7
E04711	2.2	.6	.3	150.0	-90.0	0.0	5.7	1.5	.7
J04704	.1	0.0	0.0	175.0	-177.5	0.0	.2	0.0	.1
J04705	.2	0.0	0.0	175.0	-165.0	0.0	.5	0.0	.1
J04706	.4	.1	.1	175.0	-152.5	0.0	1.2	.2	.3
J04707	.8	.1	.2	175.0	-140.0	0.0	2.1	.3	.5
J04708	.8	.2	.2	175.0	-127.5	0.0	2.1	.6	.6
J04709	.9	.3	.2	175.0	-115.0	0.0	2.3	.8	.6
J04710	.9	.4	.2	175.0	-102.5	0.0	2.4	1.0	.6
J04711	.9	.3	.2	175.0	-90.0	0.0	3.3	.9	.8
K04704	1.2	.4	.3	175.0	-77.5	0.0	3.3	1.0	.8
K04705	1.1	.3	.3	175.0	-65.0	0.0	2.9	.8	.7
K04706	.5	0.0	.2	175.0	-52.5	0.0	1.4	0.0	.5
K04707	.9	.2	.2	175.0	-40.0	0.0	2.5	.6	.5
K04708	.9	.1	.1	175.0	-27.5	0.0	2.3	.4	.4
K04709	.8	.3	.1	175.0	-15.0	0.0	2.0	.9	.3
K04710	.6	.4	.1	175.0	-2.5	0.0	1.7	1.0	.2
K04711	.5	.3	.1	175.0	10.0	0.0	1.4	.8	.1

FILE NAME	MODEL PEAK CONC (%)	MODEL MEAN CONC (%)	MODEL RMS CONC (%)	PROTOTYPE POSITION X (M)	PROTOTYPE POSITION Y (M)	PROTOTYPE POSITION Z (M)	PROTOTYPE PEAK CONC (%)	PROTOTYPE MEAN CONC (%)	PROTOTYPE RMS CONC (%)
C04804	.3	.2	.1	100.0	-200.0	0.0	.9	.5	.2
C04805	.5	.4	0.0	100.0	-187.5	0.0	1.3	1.1	.1
C04806	.4	.3	0.0	100.0	-175.0	0.0	1.1	.8	.1
C04807	.4	.3	0.0	100.0	-162.5	0.0	1.1	.8	.1
C04808	.2	.1	0.0	100.0	-150.0	0.0	.6	.3	.1
C04809	1.1	.9	.1	100.0	-137.5	0.0	2.9	2.4	.2
C04810	.4	.2	.1	100.0	-125.0	0.0	1.2	.6	.2
C04811	.2	0.0	.1	100.0	-112.5	0.0	.4	0.0	.2
D04804	.5	.3	.1	150.0	-125.0	0.0	1.3	.7	.2
D04805	.5	.3	.1	150.0	-112.5	0.0	1.4	.9	.1
D04806	.5	.4	0.0	150.0	-100.0	0.0	1.2	1.0	.1
D04807	.5	.3	.1	150.0	-87.5	0.0	1.4	.8	.2
D04808	.3	.1	.1	150.0	-75.0	0.0	.7	.3	.1
D04809	.8	.6	.1	150.0	-62.5	0.0	2.1	1.5	.1
D04810	.3	.1	.1	150.0	-50.0	0.0	.8	.3	.2
D04811	.3	.1	.1	150.0	-37.5	0.0	.9	.4	.2
E04804	.1	0.0	.1	200.0	-87.5	0.0	.4	0.0	.2
E04805	.2	0.0	0.0	200.0	-75.0	0.0	.5	0.0	.1
E04806	0.0	0.0	0.0	200.0	-62.5	0.0	0.0	0.0	0.0
E04807	0.0	0.0	0.0	200.0	-50.0	0.0	0.0	0.0	0.0
E04808	.3	.1	.1	200.0	-37.5	0.0	.7	.2	.2
E04809	.6	.3	.1	200.0	-25.0	0.0	1.6	.7	.2
E04810	.5	.3	.1	200.0	-12.5	0.0	1.4	.7	.2
E04811	.6	.4	.1	200.0	0.0	0.0	1.6	1.1	.2
F04804	.1	0.0	.1	200.0	12.5	0.0	.3	0.0	.2
F04805	0.0	0.0	0.0	200.0	25.0	0.0	0.0	0.0	0.0
F04806	.3	.1	.1	200.0	37.5	0.0	.9	.3	.2
F04807	.3	0.0	.1	200.0	50.0	0.0	.8	0.0	.2
F04808	.4	.2	.1	200.0	62.5	0.0	1.1	.5	.2
F04809	1.1	.9	.1	200.0	75.0	0.0	2.8	2.3	.2
F04810	.7	.4	.1	200.0	87.5	0.0	1.8	1.1	.2
F04811	.7	.4	.1	200.0	100.0	0.0	1.9	1.1	.2
G04804	.4	0.0	.1	150.0	112.5	0.0	1.0	0.0	.2
G04805	.1	0.0	.1	150.0	125.0	0.0	.4	0.0	.2
G04806	.1	0.0	.1	150.0	137.5	0.0	.3	0.0	.2
G04807	.1	0.0	.1	150.0	150.0	0.0	.3	0.0	.1
G04808	0.0	0.0	0.0	150.0	162.5	0.0	0.0	0.0	0.0
G04809	0.0	0.0	0.0	150.0	175.0	0.0	0.0	0.0	0.0
G04810	.2	.1	0.0	150.0	187.5	0.0	.5	.2	.1
G04811	.1	0.0	0.0	150.0	200.0	0.0	.2	0.0	.1
H04804	2.2	1.9	.1	100.0	125.0	0.0	5.7	4.9	.3
H04805	.2	.1	0.0	100.0	137.5	0.0	.6	.2	.1
H04806	.3	0.0	.1	100.0	150.0	0.0	.8	0.0	.2
H04807	.2	.1	0.0	100.0	162.5	0.0	.5	.3	.1
H04808	.1	0.0	0.0	100.0	175.0	0.0	.3	0.0	.1
H04809	0.0	0.0	0.0	100.0	187.5	0.0	0.0	0.0	0.0
H04810	.5	.2	.1	100.0	200.0	0.0	1.2	.6	.2
H04811	.3	.1	.1	100.0	212.5	0.0	.8	.3	.2

FILE NAME	MODEL CONDITIONS PEAK CONC (%)	MEAN CONC (%)	RMS CONC (%)	PROTOTYPE CONDITIONS POSITION X (M)	Y (M)	Z (M)	PEAK CONC (%)	MEAN CONC (%)	RMS CONC (%)
C04904	.3	.2	.1	100.0	-200.0	0.0	.8	.4	.2
C04905	.3	.2	0.0	100.0	-187.5	0.0	.7	.4	.1
C04906	.3	.2	.1	100.0	-175.0	0.0	.9	.5	.2
C04907	.2	.1	0.0	100.0	-162.5	0.0	.5	.3	.1
C04908	.2	0.0	.2	100.0	-150.0	0.0	.7	0.0	.4
C04909	.4	.1	.1	100.0	-137.5	0.0	.9	.4	.1
C04910	.6	.2	.1	100.0	-125.0	0.0	1.6	.5	.2
C04911	1.1	.3	.2	100.0	-112.5	0.0	3.0	.7	.3
D04904	.5	.2	.1	150.0	-125.0	0.0	1.4	.4	.2
D04905	.8	.4	.1	150.0	-112.5	0.0	2.1	1.0	.3
D04906	.7	.3	.1	150.0	-100.0	0.0	1.7	.9	.3
D04907	.7	.3	.1	150.0	-87.5	0.0	1.7	.8	.3
D04908	1.2	.3	.1	150.0	-75.0	0.0	3.2	.8	.3
D04909	1.1	.3	.2	150.0	-62.5	0.0	2.9	.7	.5
D04910	1.7	.3	.3	150.0	-50.0	0.0	4.6	.9	.7
D04911	1.7	.5	.2	150.0	-37.5	0.0	4.4	1.3	.7
F04904	1.3	.2	.3	200.0	12.5	0.0	3.4	.5	.9
F04905	.5	0.0	.2	200.0	25.0	0.0	1.4	0.0	.5
F04906	.5	0.0	.1	200.0	37.5	0.0	1.4	0.0	.3
F04907	.1	0.0	.1	200.0	50.0	0.0	.3	0.0	.2
F04908	.3	0.0	.1	200.0	62.5	0.0	.7	0.0	.2
F04909	.3	0.0	.1	200.0	75.0	0.0	.8	0.0	.2
F04910	.2	0.0	.1	200.0	87.5	0.0	.6	0.0	.2
F04911	.2	0.0	.1	200.0	100.0	0.0	.5	0.0	.2
E04904	.5	.2	.1	200.0	-87.5	0.0	1.4	.4	.2
E04905	.5	.3	.1	200.0	-75.0	0.0	1.4	.7	.2
E04906	.9	.4	.1	200.0	-62.5	0.0	2.4	1.1	.3
E04907	1.0	.3	.2	200.0	-50.0	0.0	2.5	.8	.5
E04908	1.4	.4	.3	200.0	-37.5	0.0	3.8	1.2	.8
E04909	1.8	.5	.4	200.0	-25.0	0.0	4.7	1.4	1.1
E04910	1.6	.5	.4	200.0	-12.5	0.0	4.2	1.3	1.1
E04911	1.3	.6	.3	200.0	0.0	0.0	3.5	1.5	.8
L04904	0.0	0.0	0.0	212.5	-87.5	0.0	0.0	0.0	0.0
L04905	0.0	0.0	0.0	212.5	-75.0	0.0	0.0	0.0	0.0
L04906	0.0	0.0	0.0	212.5	-62.5	0.0	0.0	0.0	0.0
L04907	.3	0.0	.1	212.5	-50.0	0.0	.7	0.0	.2
L04908	.5	.1	.1	212.5	-37.5	0.0	1.4	.3	.4
L04909	.4	0.0	.2	212.5	-25.0	0.0	1.1	0.0	.4
L04910	.8	.2	.2	212.5	-12.5	0.0	2.3	.5	.5
L04911	.8	.2	.2	212.5	0.0	0.0	2.2	.4	.5

FILE NAME	MODEL CONDITIONS PEAK CONC (%)	MEAN CONC (%)	RMS CONC (%)	PROTOTYPE CONDITIONS POSITION X (M)	Y (M)	Z (M)	PEAK CONC (%)	MEAN CONC (%)	RMS CONC (%)
C05004	.3	.2	.1	150.0	-225.0	0.0	.9	.5	.2
C05005	.2	.1	0.0	150.0	-212.5	0.0	.5	.3	.1
C05006	.2	0.0	.1	150.0	-200.0	0.0	.5	0.0	.2
C05007	0.0	0.0	0.0	150.0	-187.5	0.0	0.0	0.0	0.0
C05008	.3	.2	0.0	150.0	-175.0	0.0	.8	.5	.1
C05009	.7	.5	.1	150.0	-162.5	0.0	1.8	1.3	.2
C05010	.4	.2	.1	150.0	-150.0	0.0	1.2	.6	.2
C05011	.4	.2	.1	150.0	-137.5	0.0	1.0	.5	.2
D05004	0.0	0.0	0.0	200.0	-187.5	0.0	0.0	0.0	0.0
D05005	0.0	0.0	0.0	200.0	-175.0	0.0	0.0	0.0	0.0
D05006	0.0	0.0	0.0	200.0	-162.5	0.0	0.0	0.0	0.0
D05007	0.0	0.0	0.0	200.0	-150.0	0.0	0.0	0.0	0.0
D05008	.1	0.0	0.0	200.0	-137.5	0.0	.4	0.0	.1
D05009	.4	.2	0.0	200.0	-125.0	0.0	1.0	.5	.1
D05010	.4	.2	.1	200.0	-112.5	0.0	1.0	.5	.2
D05011	.4	.2	0.0	200.0	-100.0	0.0	1.1	.7	.1
E05004	.4	.2	.1	200.0	-87.5	0.0	1.0	.4	.1
E05005	.3	.1	0.0	200.0	-75.0	0.0	.8	.3	.1
E05006	.2	.1	.1	200.0	-62.5	0.0	.7	.3	.2
E05007	.3	.2	.1	200.0	-50.0	0.0	.8	.4	.2
E05008	.2	0.0	.1	200.0	-37.5	0.0	.6	0.0	.2
E05009	.6	.3	.1	200.0	-25.0	0.0	1.5	.8	.2
E05010	.3	0.0	.1	200.0	-12.5	0.0	.8	0.0	.2
E05011	.4	.1	.1	200.0	0.0	0.0	1.1	.4	.2
H05004	.4	.1	.1	150.0	0.0	0.0	1.0	.4	.2
H05005	.3	0.0	.1	150.0	12.5	0.0	.7	0.0	.4
H05006	.3	0.0	.1	150.0	25.0	0.0	.7	0.0	.3
H05007	.2	0.0	.1	150.0	37.5	0.0	.6	0.0	.2
H05008	.3	.1	.1	150.0	50.0	0.0	.8	.3	.2
H05009	.5	.2	.1	150.0	62.5	0.0	1.3	.5	.2
H05010	.2	0.0	.1	150.0	75.0	0.0	.7	0.0	.2
H05011	.2	0.0	.1	150.0	87.5	0.0	.6	0.0	.2
I05004	.2	0.0	.1	150.0	100.0	0.0	.5	0.0	.2
I05005	.3	.2	.1	150.0	112.5	0.0	.8	.4	.1
I05006	.6	.4	.1	150.0	125.0	0.0	1.5	1.0	.2
I05007	.4	.2	.1	150.0	137.5	0.0	.9	.6	.1
I05008	.3	.2	0.0	150.0	150.0	0.0	.7	.4	.1
I05009	.5	.4	0.0	150.0	162.5	0.0	1.3	1.0	.1
I05010	.4	.2	.1	150.0	175.0	0.0	1.0	.6	.1
I05011	.3	.2	0.0	150.0	187.5	0.0	.9	.6	.1
J05004	.5	.3	.1	100.0	150.0	0.0	1.3	.7	.2
J05005	.4	.2	.1	100.0	162.5	0.0	1.1	.6	.2
J05006	.4	.3	.1	100.0	175.0	0.0	1.1	.7	.2
J05007	.3	.2	0.0	100.0	187.5	0.0	.9	.5	.1
J05008	.3	0.0	.2	100.0	200.0	0.0	.8	0.0	.6
J05009	.3	.2	0.0	100.0	212.5	0.0	.7	.5	.1
J05010	.3	.2	.1	100.0	225.0	0.0	.7	.4	.1
J05011	.3	.2	0.0	100.0	237.5	0.0	.7	.4	.1
K05004	.4	.2	.1	50.0	175.0	0.0	1.2	.6	.2
K05005	.3	.2	0.0	50.0	187.5	0.0	.7	.4	.1
K05006	.2	.1	0.0	50.0	200.0	0.0	.5	.3	.1
K05007	.2	.1	0.0	50.0	212.5	0.0	.5	.2	.1
K05008	0.0	0.0	0.0	50.0	225.0	0.0	0.0	0.0	0.0
K05009	.2	.1	0.0	50.0	237.5	0.0	.6	.4	.1
K05010	.3	.2	0.0	50.0	250.0	0.0	.8	.4	.1
K05011	.2	.1	0.0	50.0	262.5	0.0	.4	.3	.1

FILE NAME	MODEL CONDITIONS PEAK CONC (%)	MEAN CONC (%)	RMS CONC (%)	PROTOTYPE CONDITIONS POSITION X (M)	Y (M)	Z (M)	PEAK CONC (%)	MEAN CONC (%)	RMS CONC (%)
E05104	.3	.1	.1	200.0	-87.5	0.0	.8	.4	.1
E05105	.2	.1	.1	200.0	-75.0	0.0	.6	.2	.1
E05106	.1	0.0	.1	200.0	-62.5	0.0	.4	0.0	.1
E05107	.2	0.0	.1	200.0	-50.0	0.0	.5	0.0	.1
E05108	.4	.2	.1	200.0	-37.5	0.0	1.1	.7	.2
E05109	.3	.1	.1	200.0	-25.0	0.0	.9	.3	.2
E05110	.5	.2	.1	200.0	-12.5	0.0	1.4	.7	.3
E05111	.8	.4	.1	200.0	0.0	0.0	2.1	1.0	.3
F05104	1.7	.6	.2	200.0	12.5	0.0	4.3	1.7	.5
F05105	1.2	.4	.2	200.0	25.0	0.0	3.2	1.0	.5
F05106	.4	0.0	.2	200.0	37.5	0.0	1.0	0.0	.4
F05107	.3	0.0	.1	200.0	50.0	0.0	.7	0.0	.2
F05108	.4	0.0	.1	200.0	62.5	0.0	1.0	0.0	.2
F05109	.4	.1	.1	200.0	75.0	0.0	1.0	.1	.2
F05110	.4	.1	.1	200.0	87.5	0.0	1.2	.4	.2
F05111	.4	.2	.1	200.0	100.0	0.0	1.1	.6	.2
H05104	1.9	1.0	.3	150.0	0.0	0.0	5.0	2.7	.7
H05105	2.6	1.2	.4	150.0	12.5	0.0	6.7	3.1	1.1
H05106	2.7	1.1	.5	150.0	25.0	0.0	7.0	2.9	1.3
H05107	2.9	.8	.4	150.0	37.5	0.0	7.6	2.1	1.1
H05108	3.1	.6	.4	150.0	50.0	0.0	7.8	1.5	1.1
H05109	1.7	.3	.2	150.0	62.5	0.0	4.4	.9	.7
H05110	.9	.2	.2	150.0	75.0	0.0	2.4	.6	.5
H05111	.6	.1	.1	150.0	87.5	0.0	1.6	.2	.3
I05104	.7	.2	.1	150.0	100.0	0.0	1.9	.5	.3
I05105	.9	.3	.2	150.0	112.5	0.0	2.4	.8	.4
I05106	1.0	.2	.2	150.0	125.0	0.0	2.8	.4	.4
I05107	.2	0.0	.1	150.0	137.5	0.0	.5	0.0	.3
I05108	.1	0.0	0.0	150.0	150.0	0.0	.3	0.0	.1
I05109	.2	0.0	.1	150.0	162.5	0.0	.4	0.0	.1
I05110	.2	0.0	0.0	150.0	175.0	0.0	.4	0.0	.1
I05111	.1	0.0	0.0	150.0	187.5	0.0	.3	0.0	.1

APPENDIX C

CONCENTRATION DATA WITH LNG SPILL RATE OF 7000 gpm FOR 10 MINUTES DURATION

	MODEL CONDITIONS					PROTOTYPE CONDITIONS										
FILE NAME	PEAK CONC. (%)	1% ARR. TIME (SEC)	PEAK TIME (SEC)	1% END TIME (SEC)	SUM (X-S)	X (M)	POSITION Y (M)	Z (M)	PEAK CONC. (%)	5% ARR. TIME (SEC)	15% ARR. TIME (SEC)	PEAK TIME (SEC)	15% END TIME (SEC)	5% END TIME (SEC)	SUM (X-S)
B03604	.3	0.0	23.1	0.0	.13	0.0	-230.0	0.0	.8	0.	0.	304.	0.	0.	4.65
B03605	.2	0.0	20.7	0.0	.02	0.0	-217.5	0.0	.6	0.	0.	272.	0.	0.	.84
B03606	.3	0.0	23.1	0.0	.02	0.0	-205.0	0.0	.8	0.	0.	303.	0.	0.	.55
B03607	.2	0.0	24.3	0.0	.05	0.0	-192.5	0.0	.6	0.	0.	319.	0.	0.	1.84
B03608	.1	0.0	32.0	0.0	.02	0.0	-180.0	0.0	.3	0.	0.	420.	0.	0.	.54
B03609	.2	0.0	38.1	0.0	.05	0.0	-167.5	0.0	.5	0.	0.	501.	0.	0.	1.64
B03610	.5	0.0	57.5	0.0	.06	0.0	-155.0	0.0	1.4	0.	0.	755.	0.	0.	2.08
B03611	.8	0.0	69.2	0.0	.34	0.0	-142.5	0.0	2.1	0.	0.	909.	0.	0.	12.16
C03604	.1	0.0	127.9	0.0	.18	50.0	-230.0	0.0	.4	0.	0.	1680.	0.	0.	6.47
C03605	.2	0.0	183.6	0.0	.01	50.0	-217.5	0.0	.4	0.	0.	2439.	0.	0.	.34
C03606	.2	0.0	9.8	0.0	.17	50.0	-205.0	0.0	.4	0.	0.	129.	0.	0.	6.14
C03607	.1	0.0	14.9	0.0	.22	50.0	-192.5	0.0	.2	0.	0.	196.	0.	0.	7.78
C03608	.1	0.0	86.8	0.0	.14	50.0	-180.0	0.0	.3	0.	0.	1140.	0.	0.	5.05
C03609	.1	0.0	71.4	0.0	.21	50.0	-167.5	0.0	.4	0.	0.	938.	0.	0.	7.60
C03610	.1	0.0	84.3	0.0	.24	50.0	-155.0	0.0	.4	0.	0.	1107.	0.	0.	8.63
C03611	.2	0.0	64.8	0.0	.15	50.0	-142.5	0.0	.5	0.	0.	852.	0.	0.	5.50
D03604	.2	0.0	78.3	0.0	.02	100.0	-230.0	0.0	.5	0.	0.	1029.	0.	0.	.63
D03605	.1	0.0	69.3	0.0	.04	100.0	-217.5	0.0	.4	0.	0.	911.	0.	0.	1.31
D03606	.3	0.0	171.8	0.0	.08	100.0	-205.0	0.0	.7	0.	0.	2258.	0.	0.	2.67
D03607	.1	0.0	75.8	0.0	.02	100.0	-192.5	0.0	.4	0.	0.	996.	0.	0.	.80
D03608	.1	0.0	10.2	0.0	.01	100.0	-180.0	0.0	.2	0.	0.	134.	0.	0.	.29
D03609	.2	0.0	85.0	0.0	.04	100.0	-167.5	0.0	.4	0.	0.	1117.	0.	0.	1.39
D03610	.4	0.0	84.8	0.0	.11	100.0	-155.0	0.0	1.2	0.	0.	1115.	0.	0.	3.79
D03611	.8	0.0	60.6	0.0	.17	100.0	-142.5	0.0	2.2	0.	0.	796.	0.	0.	5.94
E03604	.5	0.0	84.7	0.0	.24	150.0	-177.5	0.0	1.3	0.	0.	1113.	0.	0.	8.62
E03605	.3	0.0	60.8	0.0	.02	150.0	-165.0	0.0	.8	0.	0.	799.	0.	0.	.59
E03606	.8	0.0	81.5	0.0	.43	150.0	-152.5	0.0	2.2	0.	0.	1071.	0.	0.	15.21
E03607	1.5	59.4	59.7	60.4	.34	150.0	-140.0	0.0	3.8	0.	0.	784.	0.	0.	12.17
E03608	1.4	46.3	59.0	60.4	.55	150.0	-127.5	0.0	3.6	0.	0.	775.	0.	0.	19.30
E03609	1.5	43.2	56.1	72.7	.78	150.0	-115.0	0.0	3.8	0.	0.	737.	0.	0.	27.48
E03610	1.3	42.9	59.3	76.9	.77	150.0	-102.5	0.0	3.4	0.	0.	779.	0.	0.	26.89
E03611	1.3	48.7	68.8	77.0	.80	150.0	-90.0	0.0	3.4	0.	0.	903.	0.	0.	28.02
J03604	.4	0.0	68.8	0.0	.29	175.0	-177.5	0.0	1.2	0.	0.	903.	0.	0.	10.25
J03605	.6	0.0	67.9	0.0	.31	175.0	-165.0	0.0	1.5	0.	0.	892.	0.	0.	10.91
J03606	1.2	61.0	79.7	80.5	.54	175.0	-152.5	0.0	3.2	0.	0.	1048.	0.	0.	19.02
J03607	1.3	62.1	79.0	79.5	.45	175.0	-140.0	0.0	3.5	0.	0.	1038.	0.	0.	15.88
J03608	1.0	78.4	78.4	78.5	.51	175.0	-127.5	0.0	2.8	0.	0.	1031.	0.	0.	18.10
J03609	.9	0.0	73.6	0.0	.43	175.0	-115.0	0.0	2.5	0.	0.	967.	0.	0.	15.17
J03610	1.1	52.7	52.8	53.3	.40	175.0	-102.5	0.0	2.9	0.	0.	693.	0.	0.	14.18
J03611	1.1	49.3	49.9	52.7	.55	175.0	-90.0	0.0	3.0	0.	0.	655.	0.	0.	19.42
K03604	1.0	0.0	62.3	0.0	.62	175.0	-77.5	0.0	2.6	0.	0.	818.	0.	0.	21.82
K03605	.8	0.0	57.5	0.0	.51	175.0	-65.0	0.0	2.0	0.	0.	756.	0.	0.	17.88
K03606	.6	0.0	69.0	0.0	.16	175.0	-52.5	0.0	1.7	0.	0.	907.	0.	0.	5.55
K03607	.6	0.0	70.1	0.0	.02	175.0	-40.0	0.0	1.5	0.	0.	922.	0.	0.	.81
K03608	.4	0.0	73.8	0.0	.07	175.0	-27.5	0.0	1.0	0.	0.	970.	0.	0.	2.35
K03609	.2	0.0	72.9	0.0	.19	175.0	-15.0	0.0	.5	0.	0.	958.	0.	0.	6.63
K03610	.2	0.0	66.3	0.0	.25	175.0	-2.5	0.0	.5	0.	0.	871.	0.	0.	8.78
K03611	.2	0.0	71.8	0.0	.03	175.0	10.0	0.0	.6	0.	0.	944.	0.	0.	1.24
F03604	.9	0.0	49.8	0.0	.39	200.0	-87.5	0.0	2.5	0.	0.	655.	0.	0.	13.70
F03605	1.0	0.0	48.5	0.0	.47	200.0	-75.0	0.0	2.6	0.	0.	638.	0.	0.	16.55
F03606	1.1	43.8	45.0	69.0	.54	200.0	-62.5	0.0	3.0	0.	0.	592.	0.	0.	19.12
F03607	.9	0.0	48.8	0.0	.33	200.0	-50.0	0.0	2.5	0.	0.	642.	0.	0.	11.72
F03608	.8	0.0	49.2	0.0	.19	200.0	-37.5	0.0	2.1	0.	0.	647.	0.	0.	6.79
F03609	.6	0.0	77.1	0.0	.12	200.0	-25.0	0.0	1.7	0.	0.	1014.	0.	0.	4.17
F03610	.6	0.0	75.9	0.0	.13	200.0	-12.5	0.0	1.6	0.	0.	997.	0.	0.	4.59
F03611	.3	0.0	75.7	0.0	.01	200.0	0.0	0.0	.8	0.	0.	995.	0.	0.	.52
X03604	.3	0.0	139.5	0.0	.03	150.0	-177.5	2.5	.8	0.	0.	1833.	0.	0.	1.21
X03605	.3	0.0	136.2	0.0	.01	150.0	-165.0	2.5	.8	0.	0.	1790.	0.	0.	.27
X03606	.4	0.0	119.0	0.0	.20	150.0	-152.5	2.5	1.2	0.	0.	1563.	0.	0.	7.18
X03607	.6	0.0	59.5	0.0	.26	150.0	-140.0	2.5	1.5	0.	0.	781.	0.	0.	9.22
X03608	.5	0.0	56.5	0.0	.18	150.0	-127.5	2.5	2.2	0.	0.	742.	0.	0.	6.33
X03609	.8	0.0	84.0	0.0	.26	150.0	-115.0	2.5	2.2	0.	0.	1103.	0.	0.	9.33
X03610	.7	0.0	87.0	0.0	.08	150.0	-102.5	2.5	1.8	0.	0.	1143.	0.	0.	2.83
X03611	.6	0.0	85.5	0.0	.10	150.0	-90.0	2.5	1.6	0.	0.	1124.	0.	0.	3.70
Y03604	.2	0.0	60.1	0.0	.03	150.0	-177.5	5.0	.7	0.	0.	790.	0.	0.	1.11
Y03605	.2	0.0	9.3	0.0	.23	150.0	-165.0	5.0	.4	0.	0.	123.	0.	0.	8.24
Y03606	.4	0.0	34.4	0.0	.05	150.0	-152.5	5.0	1.0	0.	0.	452.	0.	0.	1.77
Y03607	.6	0.0	62.4	0.0	.08	150.0	-140.0	5.0	1.7	0.	0.	819.	0.	0.	3.02
Y03608	.8	0.0	59.6	0.0	.03	150.0	-127.5	5.0	2.1	0.	0.	783.	0.	0.	.87
Y03609	.8	0.0	58.7	0.0	.04	150.0	-115.0	5.0	2.1	0.	0.	771.	0.	0.	1.41
Y03610	.6	0.0	45.9	0.0	.15	150.0	-102.5	5.0	1.5	0.	0.	604.	0.	0.	1.58
Y03611	.6	0.0	48.1	0.0	.15	150.0	-90.0	5.0	1.5	0.	0.	632.	0.	0.	1.54

MODEL CONDITIONS						PROTOTYPE CONDITIONS									
FILE NAME	PEAK CONC (%)	1% ARR. TIME (SEC)	PEAK TIME (SEC)	1% END TIME (SEC)	SUM (X-S)	X (M)	POSITION Y (M)	Z (M)	PEAK CONC. (%)	5% ARR. TIME (SEC)	15% ARR. TIME (SEC)	PEAK TIME (SEC)	15% END TIME (SEC)	5% END TIME (SEC)	SUM (X-S)
C04004	.3	0.0	95.9	0.0	0.00	50.0	-230.0	0.0	.8	0.	0.	1248.	0.	0.	.98
C04005	.3	0.0	46.5	0.0	.09	50.0	-217.5	0.0	.8	0.	0.	611.	0.	0.	3.29
C04006	.5	0.0	13.9	0.0	.23	50.0	-205.0	0.0	1.4	0.	0.	183.	0.	0.	7.98
C04007	.4	0.0	95.0	0.0	.03	50.0	-192.5	0.0	1.2	0.	0.	1248.	0.	0.	1.15
C04008	.2	0.0	14.5	0.0	.01	50.0	-180.0	0.0	.4	0.	0.	191.	0.	0.	.31
C04009	.2	0.0	103.1	0.0	.05	50.0	-167.5	0.0	.5	0.	0.	1355.	0.	0.	1.75
C04010	.5	0.0	95.0	0.0	.14	50.0	-155.0	0.0	1.5	0.	0.	1248.	0.	0.	4.90
C04011	1.0	0.0	63.8	0.0	.05	50.0	-142.5	0.0	2.6	0.	0.	839.	0.	0.	1.75
D04004	.0	0.0	.0	0.0	.37	100.0	-230.0	0.0	.1	0.	0.	1.	0.	0.	13.10
D04005	.0	0.0	.0	0.0	0.00	100.0	-217.5	0.0	.1	0.	0.	1.	0.	0.	0.00
D04006	.0	0.0	.0	0.0	0.00	100.0	-205.0	0.0	.0	0.	0.	1.	0.	0.	.01
D04007	.0	0.0	61.3	0.0	.03	100.0	-192.5	0.0	.1	0.	0.	805.	0.	0.	1.24
D04008	.1	0.0	.5	0.0	.08	100.0	-180.0	0.0	.3	0.	0.	7.	0.	0.	2.74
D04009	.2	0.0	133.5	0.0	0.00	100.0	-167.5	0.0	.5	0.	0.	1754.	0.	0.	.10
D04010	.7	0.0	136.0	0.0	.32	100.0	-155.0	0.0	1.8	0.	0.	1787.	0.	0.	11.14
D04011	.8	0.0	64.0	0.0	.37	100.0	-142.5	0.0	2.1	0.	0.	841.	0.	0.	13.02
E04004	.3	0.0	148.4	0.0	.06	150.0	-177.5	0.0	.6	0.	0.	1956.	0.	0.	2.28
E04005	.5	0.0	147.1	0.0	.03	150.0	-165.0	0.0	1.3	0.	0.	1933.	0.	0.	1.91
E04006	1.4	29.9	33.3	34.1	.34	150.0	-152.5	0.0	3.8	0.	0.	437.	0.	0.	12.92
E04007	1.8	32.3	46.2	100.4	.56	150.0	-140.0	0.0	4.8	0.	0.	607.	0.	0.	19.56
E04008	1.7	27.4	56.4	59.1	.81	150.0	-127.5	0.0	4.4	0.	0.	741.	0.	0.	28.49
E04009	1.7	25.7	53.2	105.2	.79	150.0	-115.0	0.0	4.5	0.	0.	699.	0.	0.	27.65
E04010	1.1	42.9	105.0	105.6	.62	150.0	-102.5	0.0	3.0	0.	0.	1380.	0.	0.	21.86
E04011	.9	0.0	35.8	0.0	.56	150.0	-90.0	0.0	2.4	0.	0.	470.	0.	0.	19.72
J04004	.5	0.0	154.9	0.0	.13	175.0	-177.5	0.0	1.2	0.	0.	2035.	0.	0.	4.56
J04005	.4	0.0	154.1	0.0	.01	175.0	-165.0	0.0	1.1	0.	0.	2025.	0.	0.	.40
J04006	.7	0.0	43.7	0.0	.05	175.0	-152.5	0.0	2.6	0.	0.	575.	0.	0.	1.94
J04007	.7	0.0	17.7	0.0	.13	175.0	-140.0	0.0	2.0	0.	0.	232.	0.	0.	4.53
J04008	.8	0.0	18.3	0.0	.03	175.0	-127.5	0.0	2.1	0.	0.	240.	0.	0.	1.14
J04009	.8	0.0	33.6	0.0	.19	175.0	-115.0	0.0	2.1	0.	0.	442.	0.	0.	6.53
J04010	1.1	33.2	33.4	49.2	.36	175.0	-102.5	0.0	3.0	0.	0.	439.	0.	0.	12.44
J04011	1.2	48.5	48.7	51.9	.52	175.0	-90.0	0.0	3.0	0.	0.	640.	0.	0.	18.29
K04004	1.2	45.9	47.5	52.1	.36	175.0	-77.5	0.0	3.2	0.	0.	625.	0.	0.	12.57
K04005	.8	0.0	48.5	0.0	.21	175.0	-65.0	0.0	2.1	0.	0.	638.	0.	0.	7.45
K04006	1.1	49.9	59.4	59.6	.34	175.0	-52.5	0.0	2.9	0.	0.	786.	0.	0.	12.02
K04007	.7	0.0	96.1	0.0	.11	175.0	-40.0	0.0	1.8	0.	0.	1282.	0.	0.	3.93
K04008	.5	0.0	74.3	0.0	.07	175.0	-27.5	0.0	1.3	0.	0.	977.	0.	0.	2.39
K04009	.6	0.0	75.1	0.0	.15	175.0	-15.0	0.0	1.6	0.	0.	987.	0.	0.	5.28
K04010	.6	0.0	95.6	0.0	.03	175.0	-2.5	0.0	1.7	0.	0.	1256.	0.	0.	1.20
K04011	.2	0.0	102.2	0.0	.01	175.0	10.0	0.0	.4	0.	0.	1343.	0.	0.	.37
F04004	.6	0.0	59.7	0.0	.05	200.0	-87.5	0.0	1.5	0.	0.	784.	0.	0.	1.73
F04005	.6	0.0	58.1	0.0	.07	200.0	-75.0	0.0	1.5	0.	0.	764.	0.	0.	2.52
F04006	1.2	54.2	58.6	79.7	.09	200.0	-62.5	0.0	3.2	0.	0.	762.	0.	0.	3.66
F04007	.5	0.0	54.2	0.0	.11	200.0	-50.0	0.0	1.3	0.	0.	712.	0.	0.	4.02
F04008	.4	0.0	66.4	0.0	.22	200.0	-37.5	0.0	1.0	0.	0.	873.	0.	0.	7.67
F04009	.4	0.0	63.2	0.0	.17	200.0	-25.0	0.0	1.2	0.	0.	830.	0.	0.	5.88
F04010	.4	0.0	169.6	0.0	.13	200.0	-12.5	0.0	1.0	0.	0.	2228.	0.	0.	4.56
F04011	.3	0.0	33.5	0.0	.11	200.0	0.0	0.0	.7	0.	0.	440.	0.	0.	3.84

FILE NAME	MODEL CONDITIONS PEAK CONC. (%)	1% ARR. TIME (SEC)	PEAK TIME (SEC)	1% END TIME (SEC)	SUM (X-S)	POSITION X (M)	POSITION Y (M)	POSITION Z (M)	PROTOTYPE CONDITIONS PEAK CONC. (%)	5% ARR. TIME (SEC)	15% ARR. TIME (SEC)	PEAK TIME (SEC)	15% END TIME (SEC)	5% END TIME (SEC)	SUM (X-S)
B04204	.2	0.0	155.2	0.0	.02	0.0	-230.0	0.0	.4	0.	0.	2040.	0.	0.	.85
B04205	0.0	0.0	0.0	0.0	0.00	0.0	-217.5	0.0	0.0	0.	0.	0.	0.	0.	0.00
B04206	.3	0.0	65.8	0.0	.05	0.0	-205.0	0.0	.7	0.	0.	862.	0.	0.	1.72
B04207	.1	0.0	143.9	0.0	.01	0.0	-192.5	0.0	.2	0.	0.	1891.	0.	0.	.42
B04208	.1	0.0	131.8	0.0	.02	0.0	-180.0	0.0	.2	0.	0.	1732.	0.	0.	.58
B04209	.1	0.0	112.6	0.0	.05	0.0	-167.5	0.0	.4	0.	0.	1480.	0.	0.	1.66
B04210	.3	0.0	129.4	0.0	.06	0.0	-155.0	0.0	.8	0.	0.	1700.	0.	0.	1.97
B04211	.4	0.0	32.8	0.0	.21	0.0	-142.5	0.0	1.1	0.	0.	432.	0.	0.	7.49
C04204	.1	0.0	148.0	0.0	.09	50.0	-230.0	0.0	.4	0.	0.	1944.	0.	0.	3.18
C04205	.2	0.0	126.5	0.0	.08	50.0	-217.5	0.0	.7	0.	0.	1662.	0.	0.	2.96
C04206	.2	0.0	126.5	0.0	.01	50.0	-205.0	0.0	.6	0.	0.	1662.	0.	0.	.51
C04207	.1	0.0	106.8	0.0	.02	50.0	-192.5	0.0	.3	0.	0.	1404.	0.	0.	.85
C04208	.1	0.0	52.9	0.0	.02	50.0	-180.0	0.0	.3	0.	0.	695.	0.	0.	.75
C04209	.1	0.0	126.4	0.0	0.00	50.0	-167.5	0.0	.4	0.	0.	1660.	0.	0.	.16
C04210	.2	0.0	126.5	0.0	.06	50.0	-155.0	0.0	.7	0.	0.	1662.	0.	0.	2.08
C04211	.1	0.0	154.9	0.0	.07	50.0	-142.5	0.0	.3	0.	0.	2035.	0.	0.	2.56
D04204	.1	0.0	46.1	0.0	.07	100.0	-230.0	0.0	.3	0.	0.	606.	0.	0.	2.53
D04205	.1	0.0	175.8	0.0	.10	100.0	-217.5	0.0	.3	0.	0.	2310.	0.	0.	3.61
D04206	.2	0.0	5.7	0.0	.07	100.0	-205.0	0.0	.4	0.	0.	75.	0.	0.	2.49
D04207	.1	0.0	31.8	0.0	.02	100.0	-192.5	0.0	.3	0.	0.	417.	0.	0.	.72
D04208	.1	0.0	159.1	0.0	0.00	100.0	-180.0	0.0	.3	0.	0.	2090.	0.	0.	.15
D04209	.3	0.0	156.4	0.0	.01	100.0	-167.5	0.0	.7	0.	0.	1977.	0.	0.	.53
D04210	.7	0.0	152.6	0.0	.05	100.0	-155.0	0.0	1.8	0.	0.	2005.	0.	0.	1.91
B04211	2.0	47.5	48.7	181.6	.52	100.0	-142.5	0.0	5.3	639.	0.	640.	0.	641.	18.39
E04204	.3	0.0	86.3	0.0	.03	150.0	-177.5	0.0	.8	0.	0.	1134.	0.	0.	.95
E04205	.3	0.0	42.9	0.0	.09	150.0	-165.0	0.0	.9	0.	0.	564.	0.	0.	3.17
E04206	.6	0.0	42.7	0.0	.14	150.0	-152.5	0.0	1.6	0.	0.	562.	0.	0.	5.02
E04207	1.5	93.1	94.1	94.9	.24	150.0	-140.0	0.0	4.0	0.	0.	1237.	0.	0.	8.34
E04208	2.2	51.4	104.0	105.6	.61	150.0	-127.5	0.0	5.8	1363.	0.	1366.	0.	1372.	21.27
E04209	1.4	43.2	102.6	114.5	.63	150.0	-115.0	0.0	3.8	0.	0.	1349.	0.	0.	21.98
E04210	2.0	45.5	91.7	115.8	.98	150.0	-102.5	0.0	5.2	965.	0.	1204.	0.	1206.	34.28
E04211	1.9	45.7	91.2	104.2	1.01	150.0	-90.0	0.0	5.0	1199.	0.	1199.	0.	1201.	35.38
J04204	.2	0.0	54.7	0.0	0.00	175.0	-177.5	0.0	.4	0.	0.	719.	0.	0.	.11
J04205	.1	0.0	21.8	0.0	.04	175.0	-165.0	0.0	.3	0.	0.	286.	0.	0.	1.36
J04206	.2	0.0	5.1	0.0	.10	175.0	-152.5	0.0	.4	0.	0.	68.	0.	0.	3.55
J04207	.1	0.0	32.0	0.0	.08	175.0	-140.0	0.0	.3	0.	0.	421.	0.	0.	2.78
J04208	.6	0.0	37.3	0.0	.08	175.0	-127.5	0.0	1.7	0.	0.	490.	0.	0.	2.74
J04209	.8	0.0	49.6	0.0	.22	175.0	-115.0	0.0	2.2	0.	0.	534.	0.	0.	7.84
J04210	.8	0.0	33.7	0.0	.14	175.0	-102.5	0.0	2.2	0.	0.	443.	0.	0.	4.82
J04211	1.0	0.0	44.9	0.0	.37	175.0	-90.0	0.0	2.6	0.	0.	590.	0.	0.	13.08
K04204	1.2	47.1	48.2	49.5	.37	175.0	-77.5	0.0	3.2	0.	0.	634.	0.	0.	13.16
K04205	1.0	45.3	45.3	45.6	.34	175.0	-65.0	0.0	2.8	0.	0.	596.	0.	0.	12.10
K04206	1.2	37.2	51.1	53.3	.27	175.0	-52.5	0.0	3.1	0.	0.	672.	0.	0.	9.53
K04207	1.5	38.7	42.5	54.8	.31	175.0	-40.0	0.0	4.0	0.	0.	558.	0.	0.	10.83
K04208	1.3	42.0	48.5	52.3	.15	175.0	-27.5	0.0	3.5	0.	0.	637.	0.	0.	5.20
K04209	1.5	48.2	49.2	51.2	.20	175.0	-15.0	0.0	3.9	0.	0.	647.	0.	0.	7.14
K04210	1.1	50.7	50.7	51.7	.30	175.0	-2.5	0.0	2.9	0.	0.	667.	0.	0.	10.48
K04211	.8	0.0	52.8	0.0	.35	175.0	10.0	0.0	2.0	0.	0.	694.	0.	0.	12.22

APPENDIX D

WIND TUNNEL MODELING OF LNG SPILLS
by R. N. Meroney, D. E. Neff, and J. E. Cermak,
Proceedings of AGA Transmission Conference,
Montreal, Canada, 8-10 May, 1978, 26 pp.

WIND TUNNEL MODELING OF LNG SPILLS

by

R. N. Meroney*, D. E. Neff†, and J. E. Cermak*

Paper Presented

Session 18
Tuesday, May 9 1:30 p.m.
Liquid Natural Gas II

AMERICAN GAS ASSOCIATION
TRANSMISSION CONFERENCE

Montreal, Canada
May 8-10, 1978

* Professor, Fluid Mechanics and Wind Engineering Program
Civil Engineering Department, Colorado State University, Fort Collins

† Graduate Research Assistant, Fluid Mechanics and Wind Engineering Program,
Civil Engineering Department, Colorado State University, Fort Collins

CEP77-78RNM-DEN-JEC49

Title: Wind Tunnel Modeling of LNG Spills

Authors: R. N. Meroney, D. E. Neff and J. E. Cermak

ABSTRACT

Motion in the atmospheric boundary layer can be simulated with sufficient accuracy to make laboratory studies of the dispersal of cold methane plumes resulting from LNG spills useful for planning measures. Performance envelopes have been prepared to identify LNG spill scenarios which may be simulated in meteorological wind tunnels. Satisfactory agreement between diffusion characteristics in the simulated and real atmosphere has been found whenever field data have been available for making comparisons.

Key Words: Vapor, Liquid natural gas, Spill, Hazards, Wind tunnel, Simulation, Models, Dispersion

WIND TUNNEL MODELING OF LIQUID NATURAL GAS SPILLS

R. N. Meroney, D. E. Neff, and J. E. Cermak
Colorado State University
Fort Collins, Colorado

I. INTRODUCTION

The primary purpose of this paper is to show through basic similarity analysis and comparisons of model and full-scale data that atmospheric transport of dense, cold natural gas clouds can be physically modeled in "meteorological" wind tunnels for a range of real boundary conditions which have great practical importance with respect to liquid natural gas (LNG) spill hazard analysis. The scales most accurately simulated will depend upon model scale, thermal stratification, and wind tunnel characteristics. Comparisons of natural gas concentrations for laboratory model tests of LNG spill configurations ranging in scale from 1:106 to 1:666 and an atmospheric prototype support the arguments for similarity of the physical model. Performance envelopes of a typical large meteorological wind tunnel indicate situations where physical modeling is credible.

A number of controlled laboratory experiments have been prepared previously to evaluate the significance of density on gaseous plume dispersion. Sakagami and Kato (1968) measured diffusion and vapor rise from a small 5 x 10 cm LNG well in the floor of a 50 x 50 cm cross-section x 200 cm length wind tunnel. They confirmed a tendency for the gas to remain concentrated at ground level. Boyle and Kneebone (1972) released LNG on water, precooled methane, and propane in a

specially built 1.5 x 1.2 m cross-section by 5 m long asbestos-wall wind tunnel. No attempt was made to scale the atmospheric surface layer velocity profile or turbulence. They concluded room-temperature propane simulated a LNG spill quite well, but the pre-cooled methane runs lofted suggesting to the authors incorrect release temperature or exaggerated heat transfer from the ground surface. Hoot and Meroney (1974) and Hall (1975) considered point source releases of heavy gases in wind tunnels at ground level. Hoot and Meroney found that releasing gases with specific gravities as great as 3.0 only slightly shifted the decay of maximum concentrations with distance despite significantly different plume cross-sections. Hall considered transient and continuous releases on a rough surface (plume height - roughness height) and on up and downhill slopes. Hall reported shallow, wide plumes whose shapes were considerably altered by 1 in 12 ground slopes.

Tests were conducted by Neff, et al., (1976) in wind tunnel facilities to evaluate the rate of dispersion and the extent of downwind hazards associated with the rupture of typical large LNG storage tanks. Concentration and temperature measurements, and photographic records were obtained for different wind speeds, wind direction and constant boiloff rates under both neutral and stable atmospheric stratifications. Subsequent measurements by Meroney, et al., (1977) examined transient releases in similar configurations as well as dense plumes on uphill slopes, and buoyant plume liftoff situations. Different model release gases were used to simulate the behavior of the cold methane plume - heavy isothermal gas mixtures (CO_2, Freon-12 and air, or Argon) or light-cold mixtures (He and N_2).

Since in many parts of the Nation there is the perception that current and planned LNG operations and facilities present an unacceptable risk to the public, the Division of Environmental Control Technology, Department of Energy, has proposed a comprehensive integrated RD & D program. The DOE (1978) program proposes to resolve the LNG safety and contral issues by developing a capability to predict the consequences of an accidental release of LNG.

Further tests to illuminate the missing physics of LNG spill behaviour would be appropriate. The purpose of this paper is to provide guidance for the planned use of wind tunnels to study the structure of vapor plumes resulting from LNG spills on land for a realistic range of meteorological variables, plus source and site features. Wind tunnel laboratory measurements permit a degree of control of safety, meteorological, source and site variables not often feasible or economic at full scale. Nonetheless simulation of dense plume behavior is not automatic, a discussion of some of the problems associated with this approach follows.

II. LABORATORY SIMULATION OF DENSE GAS PLUMES

The reliability of the use of wind tunnel shear layers for modeling atmospheric flows has been demonstrated by several investigators (Cermak, 1975). Specific problems associated with the dispersion of cold natural gas plumes have been previously discussed by Meroney, et al., (1976).

Wind tunnel flow characteristics and physical size are such that most of the requirements for similarity with the atmosphere can only be approximated with varying degrees of accuracy. This does not eliminate

the possibility of making useful studies of diffusion by means of small-scale models but limits the range of length scales and thermal conditions for which the studies are feasible. Each similarity requirement will be examined in an effort to determine the necessary approximations imposed by the physical model and the resulting limitations imposed upon the dispersion studies.

Grouping independent variables which govern LNG vapor dispersion into dimensionless parameters with air density, ρ_a, wind velocity at tank height, U_H, and tank height, H, as reference variables and where Q is volume boiloff rate of methane and ρ_g is methane gas density yields

$$\frac{U_H H}{\nu}$$ - Reynolds number

$$\frac{\rho_a U_H^2}{g(\rho_a - \rho_g)H}$$ - Modified Froude number

$$\frac{\rho_g Q^2}{\rho_a U_H^2 H^4}$$ - Momentum ratio

$$\frac{\rho_g - \rho_a}{\rho_a}$$ - Gas density ratio

$$\frac{Q}{U_H H^2}$$ - Non-dimensional spill rate

$\frac{g(T_H-T_o)H}{T\,U_H^2}$ - Bulk Richardson number of inverse atmospheric Froude number

$\frac{\delta}{H}, \frac{D}{H}, \frac{h}{H}, \frac{k}{H}$ - Various length scale ratios associated with shear layer thickness, δ, dike diameters, D; dike height, h; and roughness length, k.

For a model test to be completely representative of the full-scale event, values of at least these ten dimensionless numbers plus similarity in approach flow velocity and turbulence profiles should be the same in the model test as at full-scale. Since it is not possible to retain exactly the same values of all these numbers at full- and model scale some latitude must be tolerated. (Indeed in many cases the full-scale values are not even well defined.) One may accept variation in these parameters to the extent that such lassitude does not jeopardize the representativeness of the model.

The Reynolds number cannot be made equal for model and prototype for scales ranging from 1:100 to 1:600. Fortunately equality is not required if the magnitude and quality of the shear layer turbulence is similar to the full-scale--hence the use of specially designed meteorological wind tunnels (Cermak, 1975). It is possible to obtain full-scale values of the remaining non-dimensional parameters by reducing the reference velocity, U_H, to very low values (of the order of 0.2 m/s to simulate a 3 m/sec full-scale wind) and increasing the atmospheric temperature difference (T_H-T_o) as necessary. In some cases investigators modify the density ratio $\rho_a-\rho_g/\rho_a$ to permit the use of larger and more convenient values of U_H (Hall, et al., 1975). Unfortunately this also modifies inertial effects, time scale ratios, and volume dilution rates so this is not proposed herein.

Previous experiments by Hoot and Meroney (1974), Bodertha (1961), Van Ulden (1974), and Boyle and Kneebone (1973) have confirmed that the Froude number is the parameter which governs plume spread rate, trajectory, plume size and entrainment when gases remain negatively buoyant during their entire trajectory. In the case of spills of LNG buoyancy of the plume will be a function of both mole fraction of methane and temperature. Thus, depending upon the relative rate of entrainment of ambient gases versus rate of thermal transport from surrounding surfaces the state of buoyancy may vary from negative to positive.

To clarify this point Meroney, et al., (1976) proposed a simple one-dimensional mixing model including considerations of conservation of energy and mass plus thermodynamic definitions of mixture properties. Sample computations for methane spills suggest qualitative behavior as shown in Figures 1 and 2. If the relative humidity is zero, depending upon A (heat transfer rate) the behavior of buoyancy forces will vary markedly with dilution. Figure 3 depicts the potential variation in dense plume behavior in situations where the atmosphere is dry and stable with an insulative cool boundary versus a moist unstable day with a hot conductive boundary. Thus on initial consideration it is important to model not only the initial Froude number of a plume but its characteristic variation with dilution also. Room temperatures of air-Freon-12 mixtures (or alternatetively carbon dioxide or argon) will behave like the A = 0 case, and a release of nitrogen cooled to 217^{o}K will perform similar to a marginally buoyant methane spill (A = 1/3). For A = 0 but finite values of humidity it is seen in Figure 2 that humidities greater than 60 percent may produce

marginally buoyant plumes as a result of adiabatic mixing. A mixture of helium and nitrogen ($x_{He} = 0.5$, $x_{N_2} = 0.5$) adjusted to produce a molecular weight equal to that of methane, which is cooled to methane boiloff temperatures ($112^{o}K$) should simulate the variable Froude number characteristic but with a nonflammable gas.

Consideration of the heat transfer conditions suggests that surface heat transport from the ground will be a function of the Boundary Fourier Modulus function

$$BFM = \frac{\text{Plume time over surface}}{\text{Time constant to change surface temperature}}$$

Examination of the range of this term suggests that for field and wind tunnel configurations BFM << 1.0; thus, it is sufficient to maintain the surface temperature on the laboratory boundary constant. Since the turbulence characteristics of the flow are dominated by roughness, upstream profile shape, and stratification one expects that the Stanton number in the field will equal that in the model, i.e., $St_m = St_p$, and heat transfer rates in the two cases should be in proper relation to plume entrainment rates.

Earlier measurements (Neff, et al., (1976) and Meroney, et al., (1977) now suggest that heat transfer effects may be small over the significant time scales associated with non-calm situations (i.e., $U_p > 1$ m/sec); hence gas density should be adequately simulated by isothermal high molecular weight gas mixtures. This agrees with the result independently reported by Boyle and Kneebone (1972) that room temperature propane simulated an actual LNG spill quite well.

It is tempting to try to simulate the entire spill phenomenon in the laboratory including spill of LNG into the dike, heat transfer from the tank and dike materials to the cryogenic fluid, phase change of the LNG and subsequent dispersal of natural gas downwind. Unfortunately, the different scaling laws for the conduction and convection suggest that markedly different time scales occur for the various component processes as the scale changes. Since the volume of dike material storing sensible heat scales versus the cube of the length scale whereas the pertinent surface area scales as the square of the length scale one perceives that heat is transferred to a model cold plume much too rapidly within the model containment structures. This effect is apparently unavoidable since a material having a thermal diffusivity low enough to compensate for this effect does not appear to exist. Since calculations for the full scale situation suggest minimal heating of a cold natural gas plume by the tank-dike structure it suffices to cool the model tank-dike walls to reduce the heat transfer to a cold model vapor.

III. WIND TUNNEL PERFORMANCE ENVELOPE

It is instructive to consider the operational constraints on current large wind tunnels to determine those field situations which may be satisfactorily simulated. Operational limitations include:

1. The inability of most large wind tunnels to function satisfactorily at very low wind speeds (< 0.1 m/sec). At low wind speeds the wind tunnel becomes sensitive to small disturbances, both external and internal, which lead to unrealistic perturbations of the mean flow.

2. The associated inability to maintain large Reynolds number. When the characteristic Reynolds number falls below 3000 wake turbulence no larger remains similar to field conditions.
3. A minimum spatial resolution for concentration measurements of $\pm$ .25 cm. Minimum pertinant resolution in the field may be $\pm$ 1 m.
4. Lateral interference with a spreading dense plume by wind tunnel walls. Current wind tunnel facilities have widths up to about 4 m. One can estimate wind tunnel wall interference by utilizing the spread formulae proposed and tested against field spills by Van Ulden (1974). The expression relates spread to boiloff rate, wind speed, and gas density.

The four operational limitations listed above have been incorporated into the performance envelopes shown in Figures 4 and 5. Wind tunnel wall interference lines are conservative for the situation shown since they represent steady boiloff interaction at a distance of 20 diameters downwind of a 0.3 m diameter model source. Only the highest boiloff rates for the larger field situations must be eliminated from consideration and all relevant stable stratification conditions can be provided.

IV. WIND TUNNEL EXPERIMENT

Scale models (1:200 and 1:400) of two typical LNG storage tanks have been studied in meteorological wind tunnels for a neutral and stable atmosphere.

Tank facilities considered include a low dike configuration (39 m diameter tank, 36 m high surrounded by a 6.6 m high dike 93 m by 100 m

in area) and high dike configuration (73 m diameter, 39 m high tank surrounded by a concentric 81 m diameter dike 24 m high). Also examined was a 1:106 scale model of Test 044 from the Capistrano Series supported by the American Gas Association (1974) which involved a spill into a 25 meter diameter by 0.5 meter high dike. The 1:200 scale models shown in Figure 6 utilized for pre-cooled He-N_2 releases incorporated liquid nitrogen reservoirs within their structure to reduce temperature difference between the gas mixture and the tank/dike walls. This device prevented exaggerated heat transfer effects as discussed previously.

Concentration measurements were performed in the Colorado State University Meteorological Wind Tunnel. This tunnel, especially designed to study atmospheric flow phenomena, incorporates special features such as an adjustable ceiling to reduce model blockage, temperature controlled air stream and boundary walls, and a large test section (1.8 m x 1.8 m cross-section by 29 m long) to permit equilibrium development of typical atmospheric shear layer characteristics.

All results presented herein are modeled with pure carbon dioxide or pre-cooled helium-nitrogen mixtures adjusted to simulate boiloff densities of methane. Turbulent diffusion of simulated LNG plumes for the three different LNG tank and dike complexes, two model gas mixtures, two atmospheric stratifications, three scale ratios, and a number of wind speed and boiloff rate combinations were studied. Mean concentration measurements were obtained for as many as 23 different sample points distributed over a ground level zone up to 250 m wide, 50 to 2000 meters long, and in the vertical over a height

of 0 to 100 meters. A schematic of the model configuration and the associated concentration measuring equipment is shown in Figure 7.

To obtain an accurate prediction of the extent of hazard associated with the vaporization of LNG, the model should simulate the variable boiloff rate of the gaseous methane characteristic to that of the spill configuration. Typical boiloff curves for the prototype situation along with the actual model gas release for the Capistrano Test 044 are presented in Figure 8. These gas flow rate curves were obtained by use of a programmed cam to close a micrometer needle valve controlling the flow of simulation get at a predetermined rate.

The transient nature of the boiloff rates simulated necessitated the use of a fast response, temperature compensated concentration transducer. An aspirated dual film probe was designed for this project. As noted in Figure 9, dual films operated at different current levels permitted compensation for temperature drift, while a flared inlet reduced the noise of pressure fluctuations. Calibration suggests a noise level of 0.1% by volume CO_2 and an upper frequency response of 1000 Hz.

V. TEST PROGRAM RESULTS

The purpose of this paper is to demonstrate the feasibility of utilizing wind tunnels as a tool to study dense gas spills rather than present comprehensive results. Extended discussions of the LNG spill cases examined at CSU have been prepared by Neff, et al., (1976), Meroney, et al., (1977). Meroney and Neff (1977), R & D Associates, et al., (1977), and Harsha (1976).

Test results consisted of (1) a qualitative study of the flow field around the different tank and dike localities by visual observation of the plume released from the model area; and (2) a quantitative study of gas concentrations produced by the release of a tracer from the model area.

1. Continuous Boiloff Release Results

Continuous releases of CO_2 made from the high and low tank-dike configurations agree well with the earlier Freon-12-N_2 simulations performed by Neff, et al. (1976). The dimensionless concentration coefficient $X\bar{U}H_T^2/Q$ scales with non-dimensional downwind distance x/H_T (Figure 4). The dimensionless concentration coefficient curves asymptotically approach the slope of those given by the appropriate Pasquill diffusion category for both neutral and stable flow. No significant differentiation appeared between CO_2 and pre-cooled HeN_2 simulation gases.

2. Variable Boiloff Release Results

Figure 5 displays the dilution time history of the Capistrano Model Test and the field situation superimposed for the typical test position (320', 0', 0'). The time and magnitude of highest concentrations observed at most of the test locations is in good agreement. The arrival time of the transient plume at the measurement location is reasonably close. The model does not, however, predict the large and intermittent concentration peaks at late times as observed in the field. Such variations are likely due to gustiness and changes in wind direction recorded for the field case but not present in the wind tunnel, or possibly the long time response of the field sensors utilized (10 seconds).

Transient measurements made downwind of the typical high and low dike configurations reveal that mean concentration measurements made at constant boiloff rates appear to upper bound conditions to the maximum concentrations detected during a transient boiloff situation.

Motion in the atmospheric boundary layer can thus be simulated with sufficient accuracy to make laboratory studies of cold methane gas dispersal useful for planning measures. Satisfactory agreement between diffusion characteristics in the simulated and real atmosphere has been found whenever field data have been available for making comparisons.

VI. SUMMARY

The wind tunnel can simulate a range of conditions associated with vapor transport and dispersion downwind of LNG spills. Scaling criteria suggest that existing size facilities can simulate spills boiling from areas up to 150 meters diameter. Wind speeds at a 10 m reference heights may be simulated from lower magnitudes of 0.7 m/s for spills of 15 m diameter (scale ratio = 1/50) or 3.0 m/s for spills of 150 m diameter (scale ratio = 1/500) upwards. A desirable local resolution of 1 m limits model scale ratios to ~ 1/500 or less. Lateral spreading in a typical 4 m width wind tunnel may further limit maximum equivalent volume production of cold vapor at a given wind speed (i.e., for scale ratios = 1/200 a liquid boiloff rate of 25.4 mm/min produces wall interference effects beyong downwind distances of 300 m for velocities less than 3.0 m/sec). For rates less than liquid boiloff rates of 2.5 mm/min there should be no additional constraint. Vapor dispersion downwind of LNG spills has been reproduced for selected

cases of the 1974 AGA landspill program. Wind tunnel simulation provides a design tool to pre-scale trajectories and dispersion of cold LNG vapor clouds. This method will provide guidance for instrument placement and numerical model development during the 50 million dollar program planned by DOE to guide LNG hazard analysis.

REFERENCES

American Gas Association (1974) "LNG Safety Program Interim Report on Phase II Work", Report on American Gas Association Project IS-3-1, Battelle, Columbia Laboratories.

Bodurtha, F. T., Jr., (1961) "The Behavior of Dense Stack Gases," J. of APCA, Vol. II, No. 9, pp. 431-437.

Boyle, G. J. and Kneebone, A. (1973) "Laboratory Investigation Into the Characteristics of LNG Spills on Water, Evaporation, Spreading and Vapor Dispersion," Shell Research, Ltd., Report to API, March.

Cermak, J. E. (1975) "Applications of Fluid Mechanics to Wind Engineering--A Freeman Scholar Lecture," J. of Fluids Engineering, Vol. 97, Ser. 1, No. 1, pp. 9-38.

Department of Energy (DOE) (1978), An Approach to Liquified Natural Gas (LNG) Safety and Environmental Control Research, U.S. Department of Energy, Division of Environmental Control Technology, DOE/EW-0002, 446 pp.

Hall, D. J., Barrett, C. F. and Ralph, M. O. (1975) "Experiments on a Model of an Escape of Heavy Gas," Warren Spring Laboratory Report CR882(AP), Department of Trade and Industry, U. K.

Harsha, P. T. (1976) "LNG Safety Program Topical Report: Wind Tunnel Tests of Vapor Dispersion From Land Facilities," RDA-TR-1100-002, AGA Project IS-128-1, August (Draft).

Hoot, T. G. and Meroney, R. N. (1974) "The Behavior of Negatively Buoyant Stack Gases," 67th Annual Meeting APCA, 9-13 June, 1973, Denver, Colorado, Paper No. 74-210, 21 pp.

Meroney, R. N., Cermak, J. E., and Neff, D. E., (1976) "Dispersion of Vapor From LNG Spills - Simulation in a Meteorological Wind Tunnel," Proc. of 3rd AMS Symposium on Atmospheric Turbulence, Diffusion, and Air Quality, 19-22 Oct., Raleigh, N.C., pp. 243-246.

Meroney, R. N., Neff, D. E., Cermak, J. E., and Megahed, M., (1977) "Dispersion of Vapor From LNG Spills - Simulation in a Meteorological Wind Tunnel," Colorado State University, Fort Collins, 152 pp. Report No. CER76-77RNM-JEC-DEN-MM-57.

Meroney, R. N., and Neff, D. E. (1977) "Behavior of Negatively Buoyant Gas Plumes From an LNG Spill" 6th Australasian Hydraulics and Fluid Mechanics Conference, University of Adelaide, Australia, 4 p. December 5-9, 1977 (Colorado State University, Fort Collins, Report No. CEP77-78-RNM-DEN1).

REFERENCES (continued)

Neff, D. E., Meroney, R. N., and Cermak, J. E, (1976) "Wind Tunnel Study of the Negatively Buoyant Plume Due to an LNG Spill," Colorado State University, Fort Collins, 230 pp. Report No. CER76-77-22.

R & D Associates and Fluid Mechanics and Wind Engineering Program Staff, Colorado State University (1977) "LNG Wind Tunnel Simulation and Instrumentation Assessments," RDA-TR-105700-003, Prepared for ERDA, April (Draft)

Sakagami, J., and Kato, M., (1968) "Diffusion and Vapour Rise of Methane Vapour From a Real Source in Air Stream," Natural Science Report of Ochanomizu University, Japan, Vol. 19, #2, pp. 59-66.

Van Ulden, A. P., (1974) "On the Spreading of a Heavy Gas Released Near the Ground," Loss Prevention and Safety Promotion Seminar, Delft, Netherlands, 6 p.

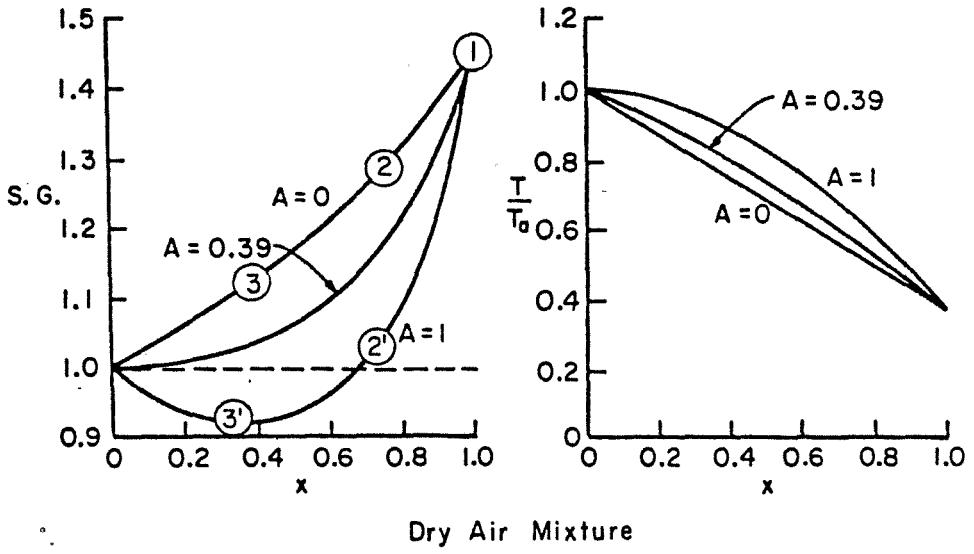

Figure 1. Theoretical Behavior of LNG Plumes

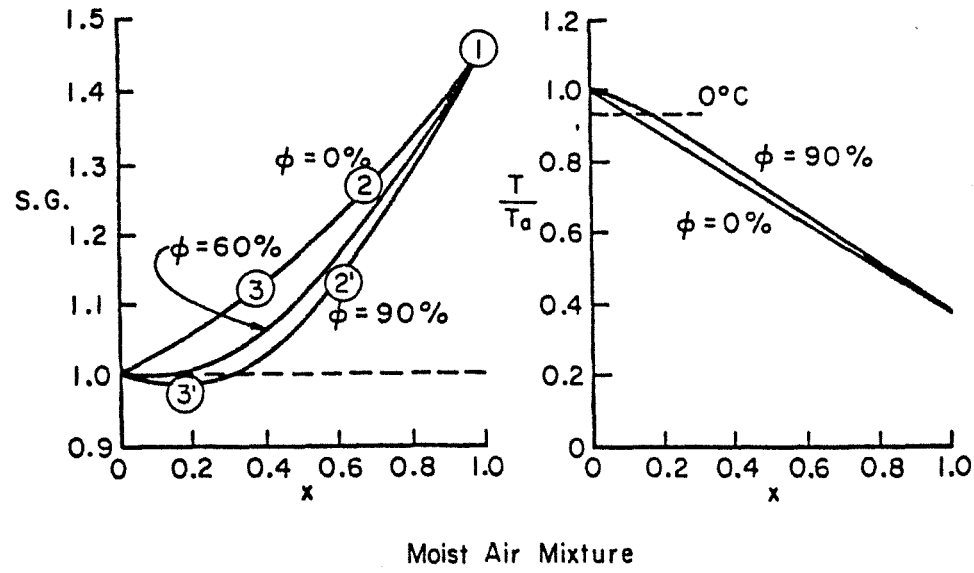

Figure 2. Theoretical Behavior of LNG Plumes

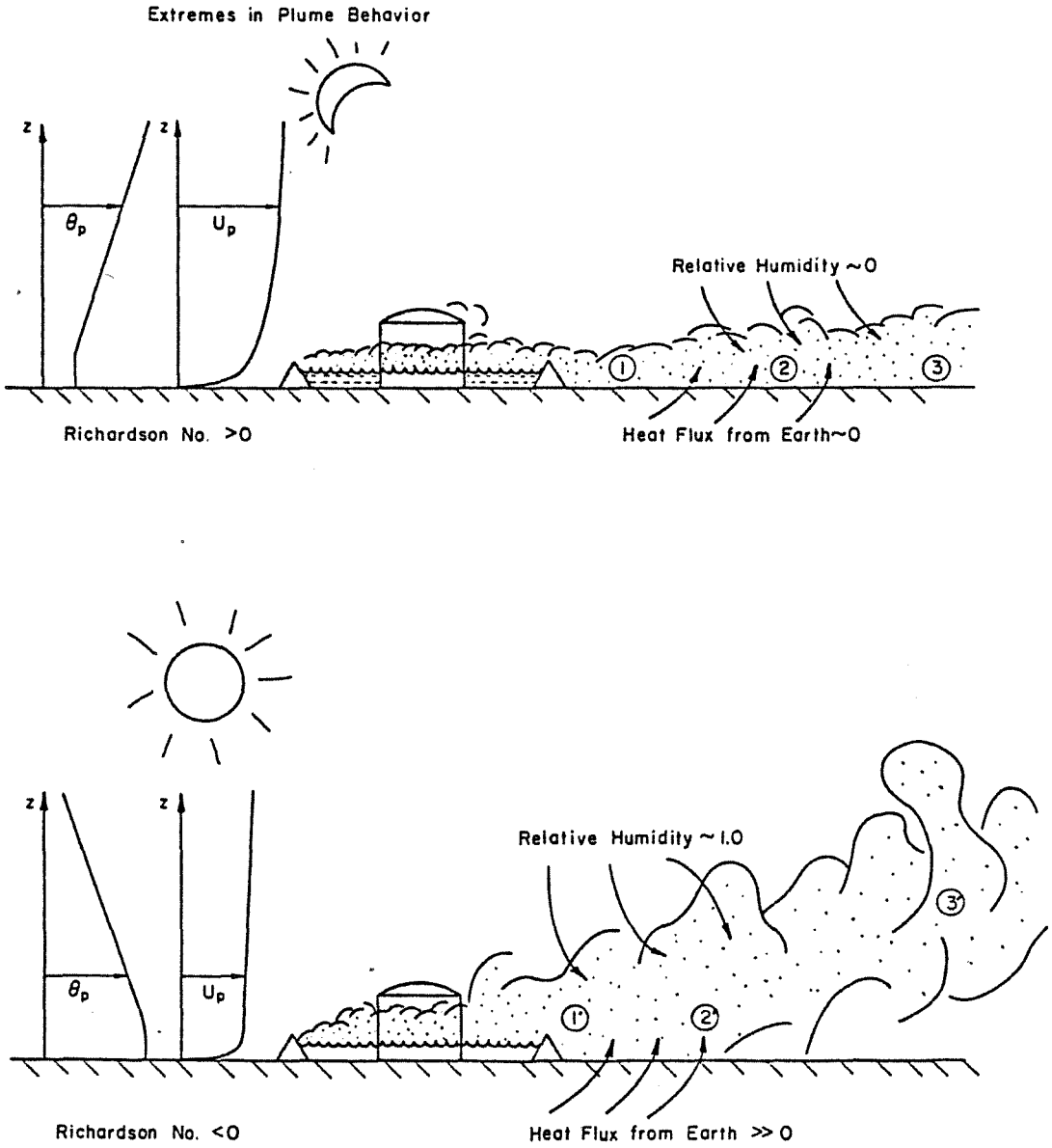

Figure 3. Extremes in Natural Gas Plume Behavior

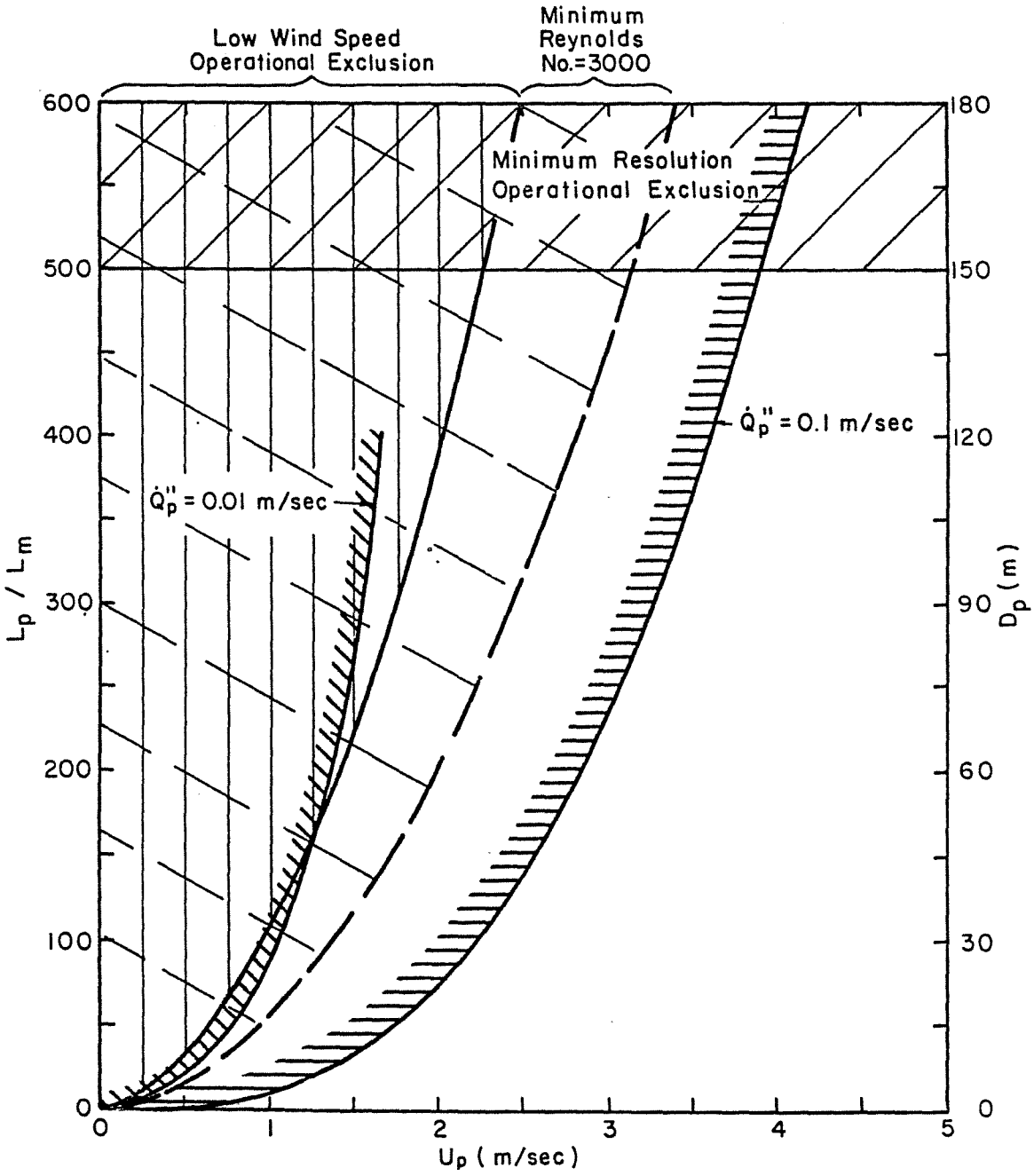

Figure 4. Performance Envelope to Simulate LNG Spills - Constant Boiloff Conditions

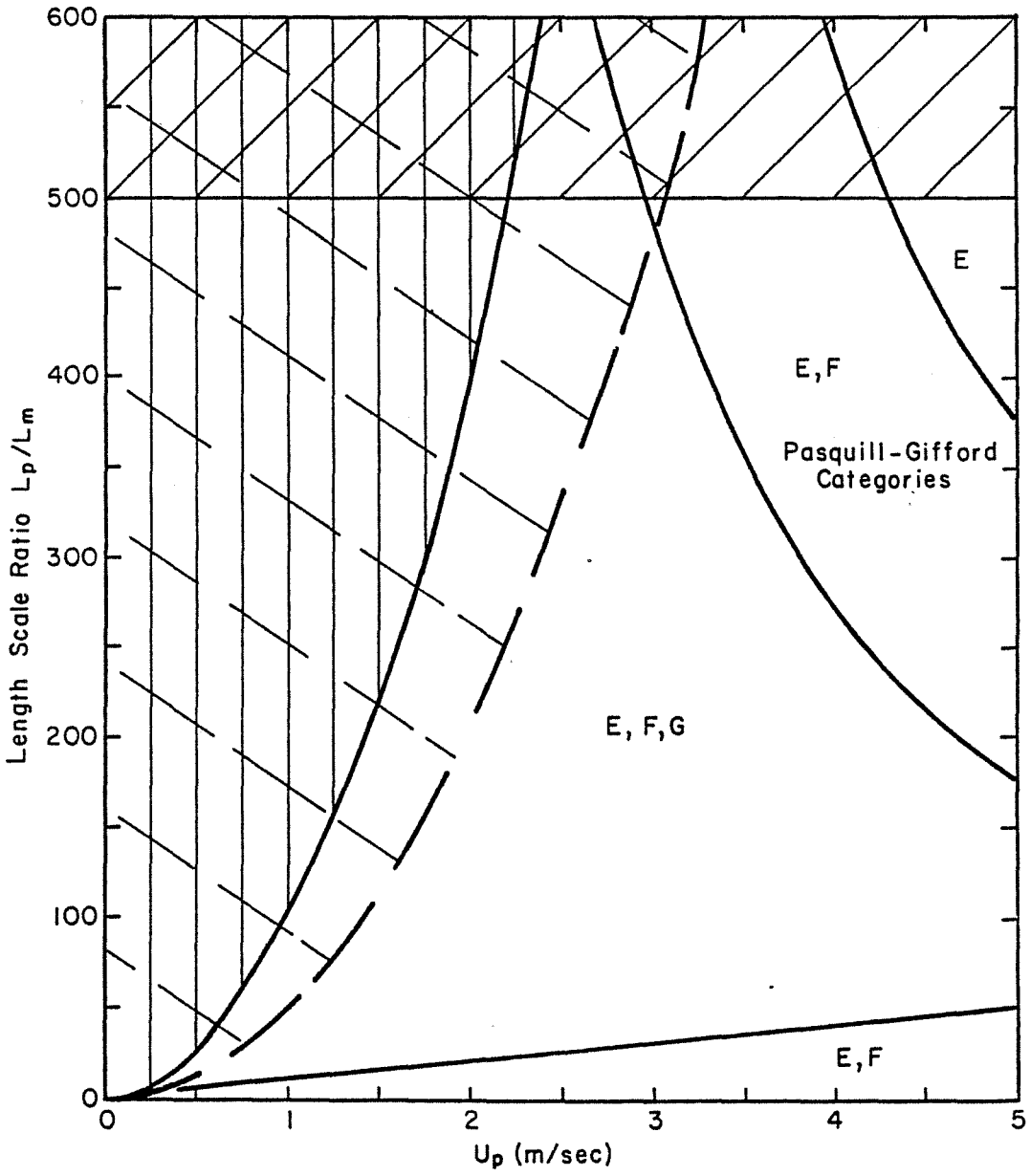

Figure 5. Performance Envelope - Atmospheric Stable Stratification on Envelope for Dm = 0.3 m

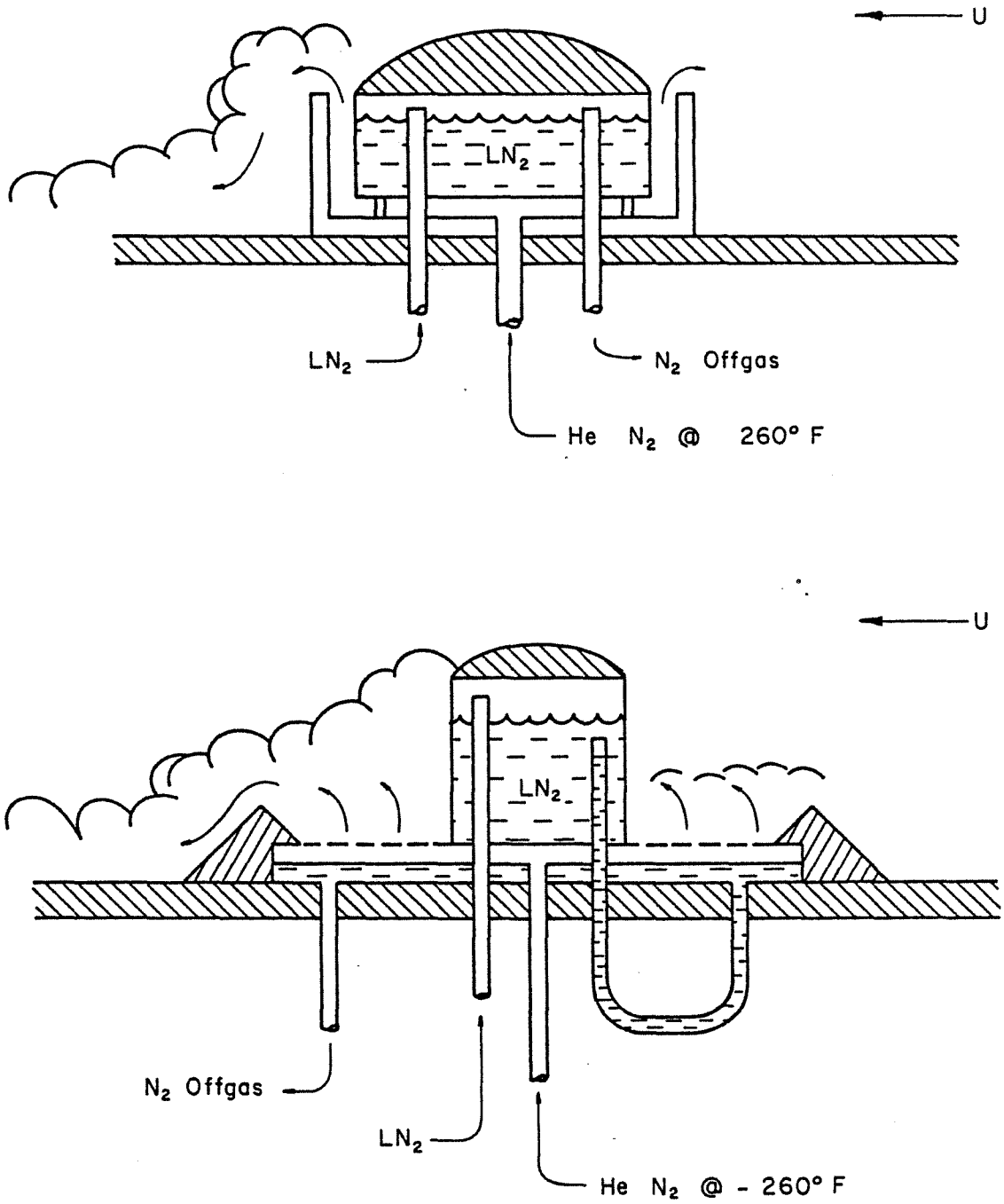

Figure 6. High and Low Dike Models for Simulation With Helium-Nitrogen Gas Mixture

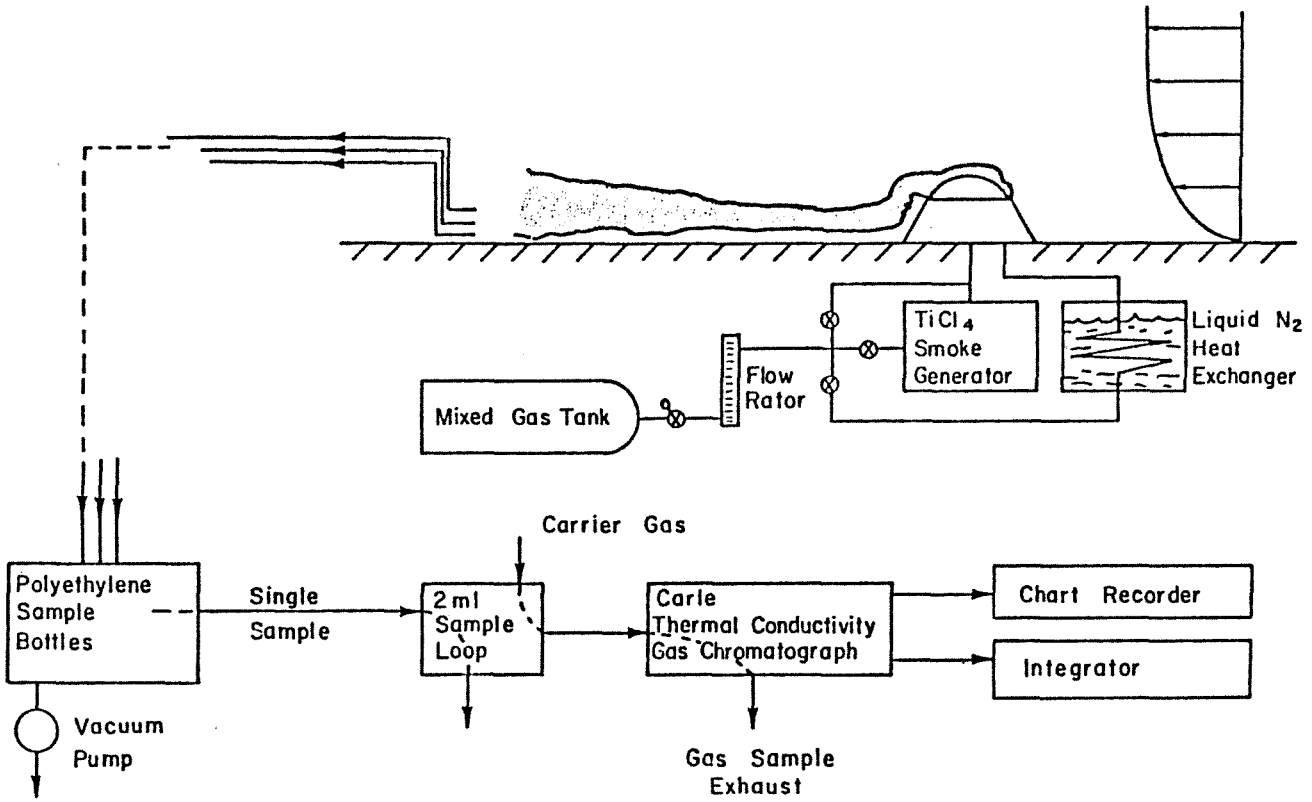

Figure 7. Flow Chart of Mean Concentration Sampling System

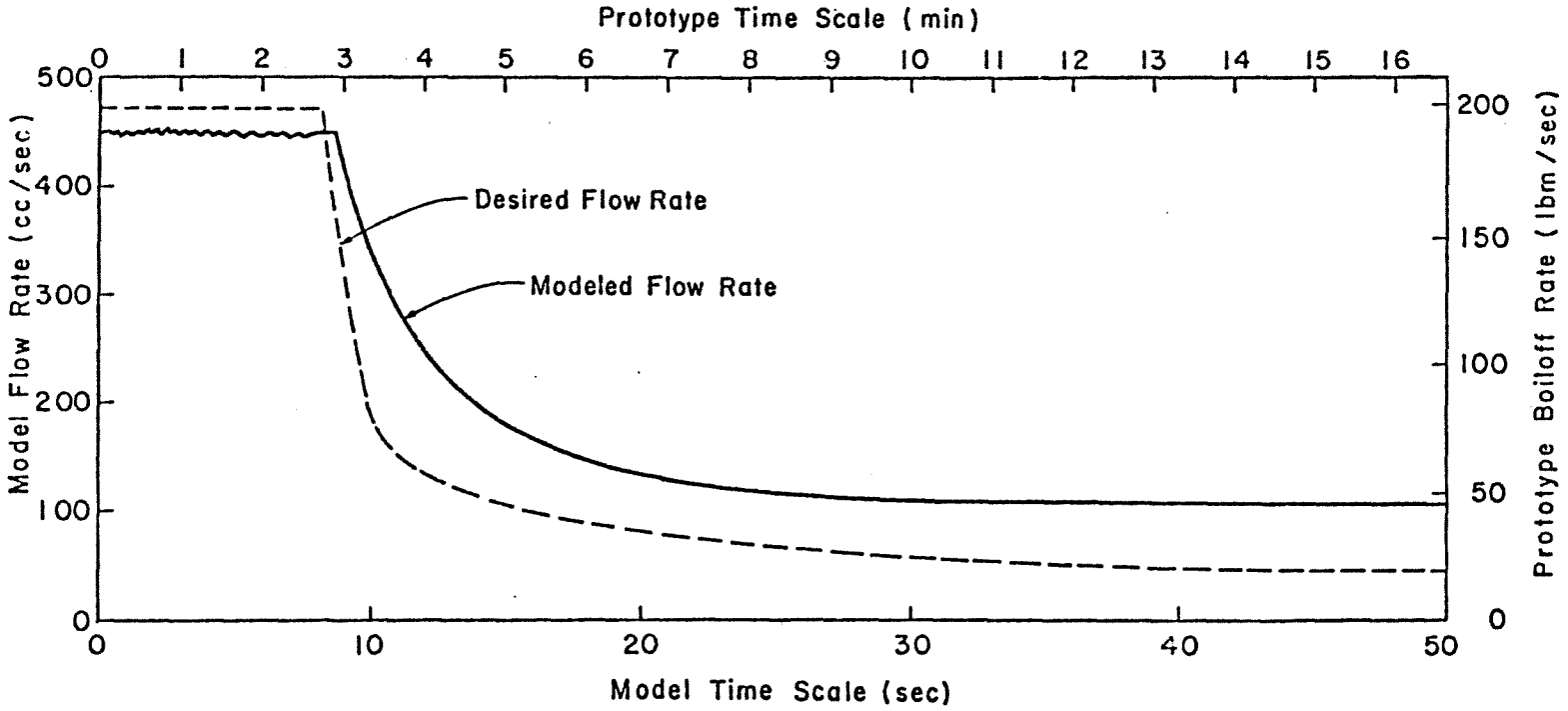

Figure 8. Capistrano 044 Gas Release Rates for Model and Prototype

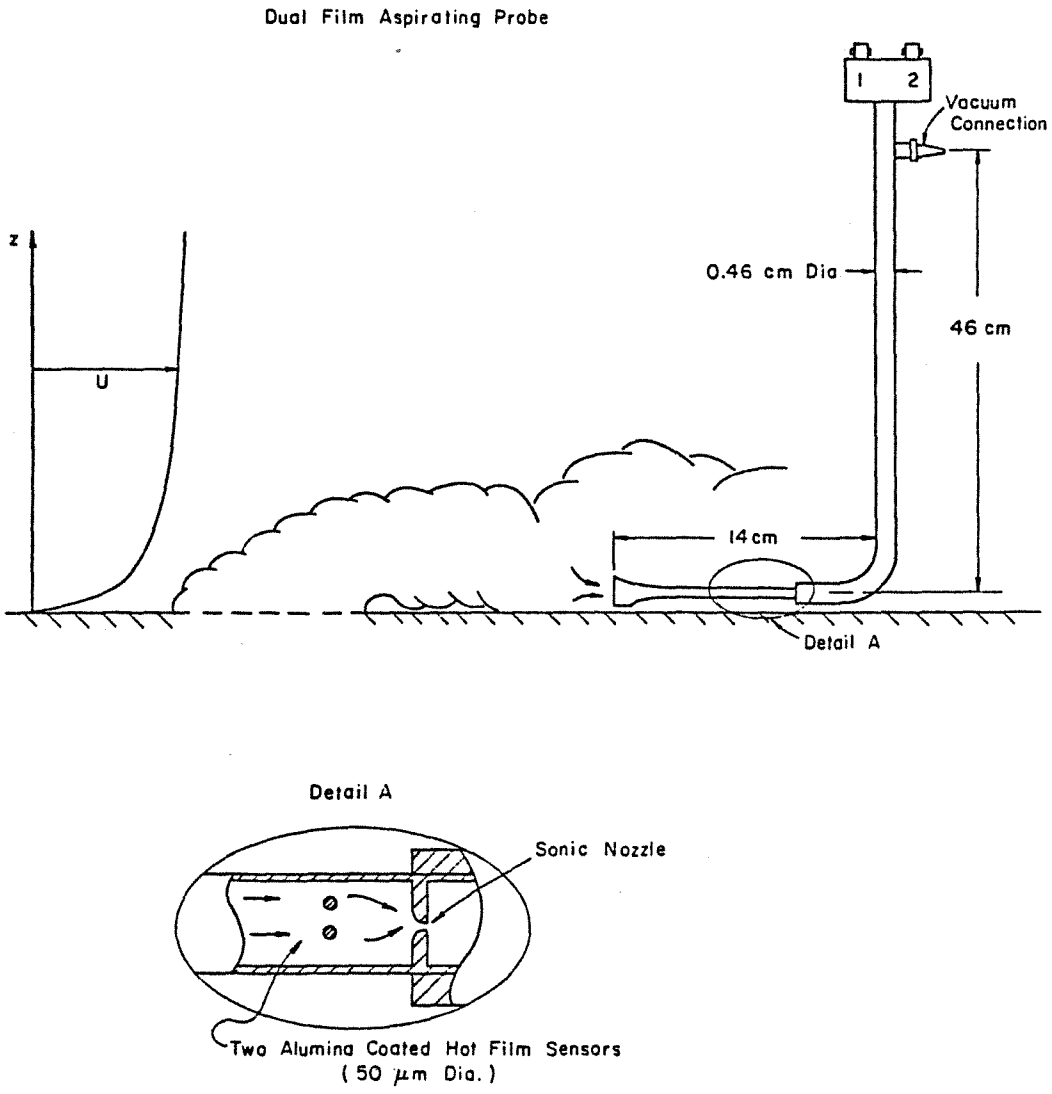

Figure 9. Dual Film Aspirating Concentration Probe

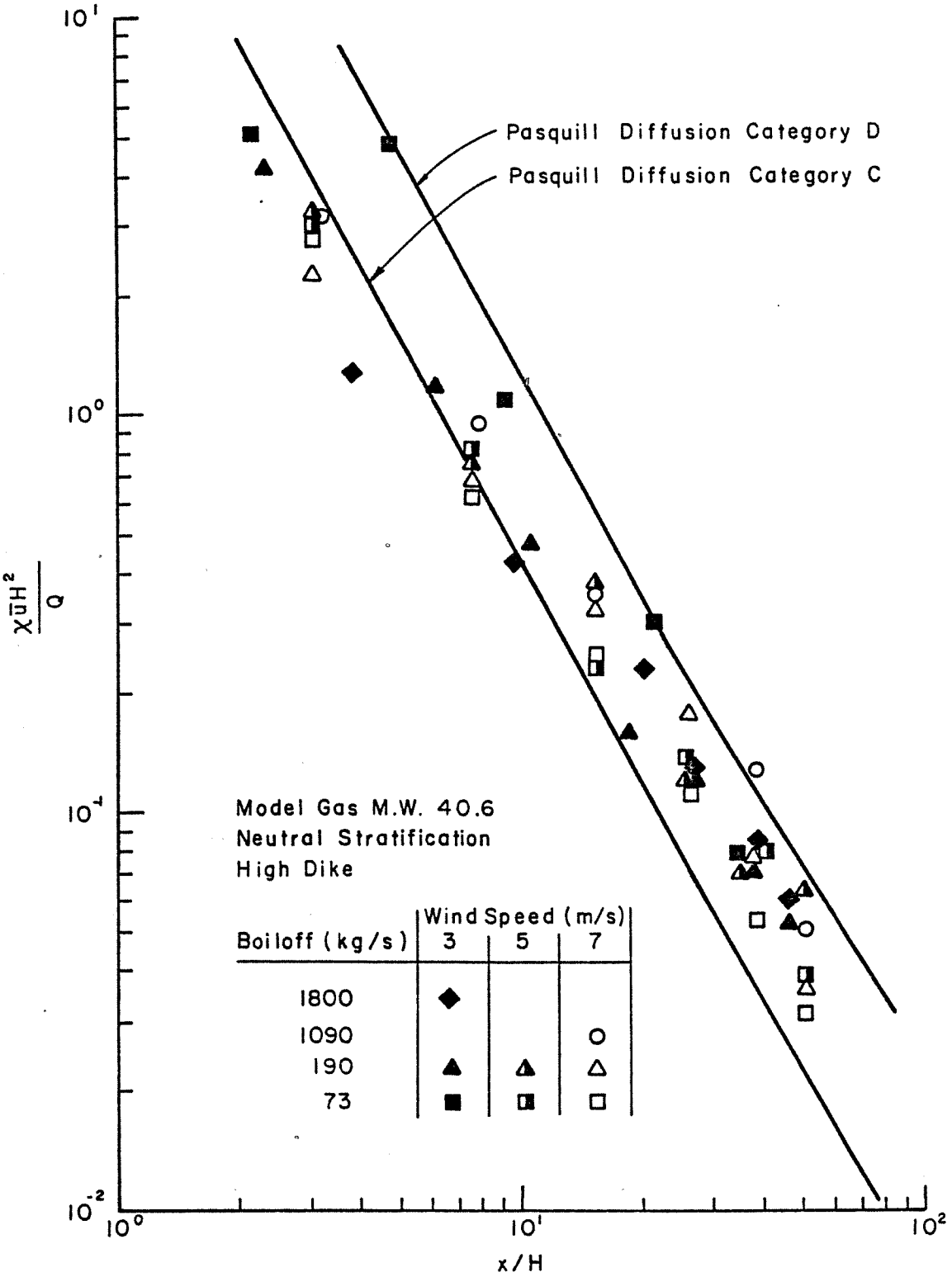

Figure 10. Dimensionless Concentration Coefficient Versus Non-Dimensional Downwind Distance

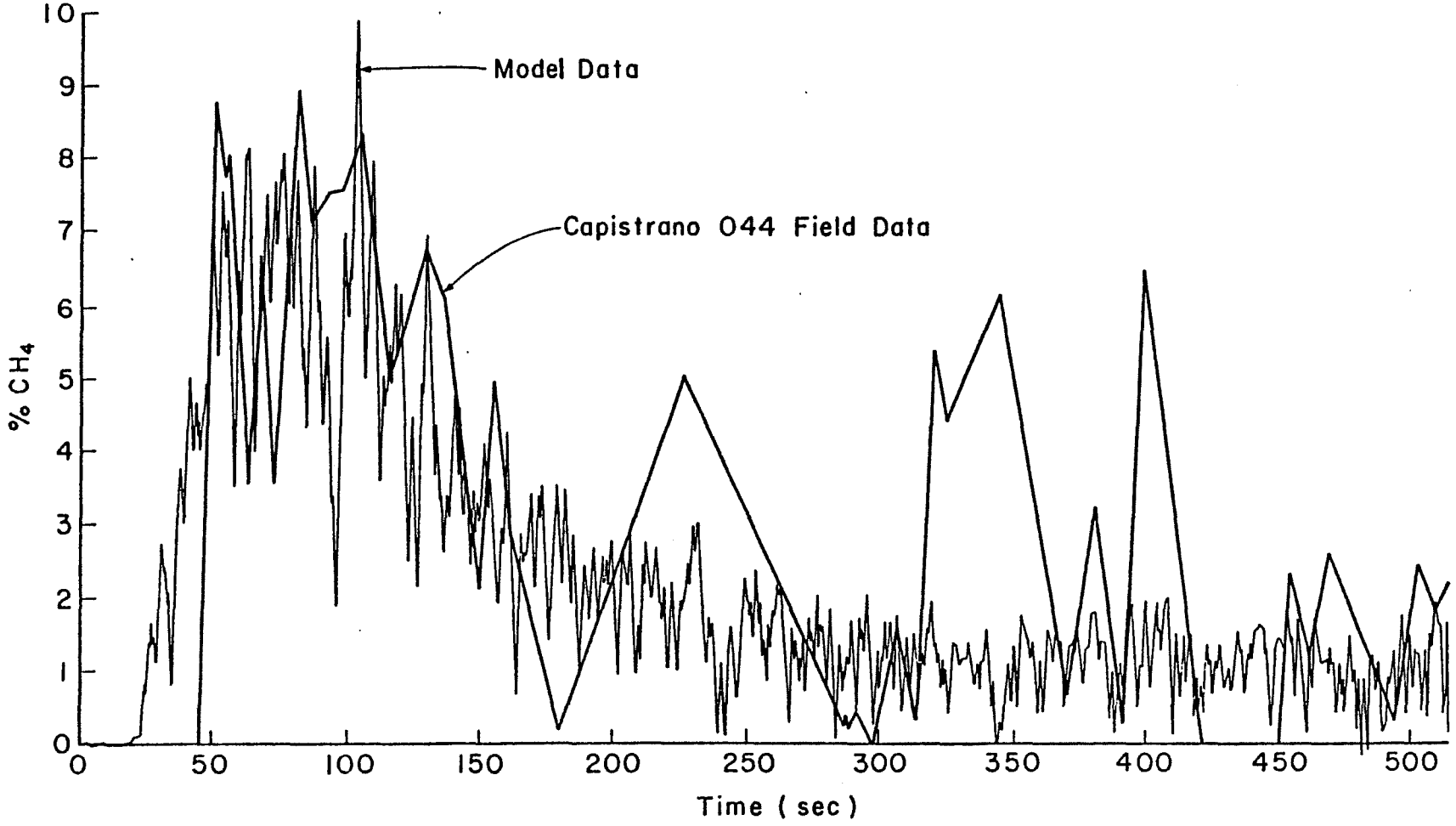

Figure 11. Comparison of Model Data With Capistrano 044 Field Data for a Sample Location at (320', 0', 0')

APPENDIX E

WIND-TUNNEL EXPERIMENTS ON DENSE GAS DISPERSION
by R. N. Meroney, (Review article for Journal of Hazardous Materials, to be published 1982), 36 pp.

WIND-TUNNEL EXPERIMENTS ON DENSE GAS DISPERSION

by

Robert N. Meroney, Ph.D.
Fluid Mechanics and Wind Engineering Program
Civil Engineering Department
Colorado State University
Fort Collins, Colorado 80523 USA

in

Journal of Hazardous Materials
Elsevier Scientific Publishing
Amsterdam

Special Issue on Dense Gas Dispersion

editor: Dr. Rex Britter
Cambridge University

Summary = A review of recent laboratory simulation and comparisons with models and field experiments.

July 1981 CEP81-82RNM1

WIND-TUNNEL EXPERIMENTS ON DENSE GAS DISPERSION

Summary

Laboratory simulation of negatively buoyant emissions into the earth's boundary layer is a valuable predictive tool to describe the motions of potentially hazardous chemicals such as propane, butane, chlorine, liquified natural gas, freon, etc. In this paper are discussed some of the simulation criteria, special instrumentation, and results of wind-tunnel investigations of dense plume behavior. Such wind-tunnel data can be correlated in a manner that yields an empirical prediction of vapor dispersion from full-scale releases; nonetheless, certain facility and gas specific limitations must be recognized when interpreting an experimental program.

WIND-TUNNEL EXPERIMENTS ON DENSE GAS DISPERSION

Robert N. Meroney
Fluid Mechanics and Wind Engineering Program
Colorado State University
Fort Collins, Colorado 80523

1.0 INTRODUCTION

Release of a dense gas from short stacks or near the ground is accompanied by initial descent and horizontal spreading caused by gravitational forces. Buoyancy forces tend to suppress advection by wind shear and dispersion by atmospheric turbulence. Such clouds will drift downwind from the source location at ground level, providing an opportunity for ignition if the gas is flammable or perhaps for acute toxic effects to life in its path. The mixing of such plumes is still only partially understood despite a significant research effort of many years.[1,2,3,] The relative influence of gravity forces, viscous forces, entrainment at the plume front, entrainment at the upper surface, and modification of the background turbulent field due to stratification effects have been active subjects of discussion.

Dispersion in the atmospheric boundary layer can be simulated today in meteorological wind tunnels with sufficient accuracy to permit realistic scaling of dense gas escape hazards, pretest planning for field experiments, and a post test opportunity to extend the value of limited field measurements. Laboratory experiments permit a degree of control of safety, meteorological, and site variables not often feasible or economic at full-scale.

This paper considers the results of experiments performed in wind tunnels to examine the behavior of dense plumes during periods of gravity spread/air entrainment dominance. The special features which

characterize dense gas dispersion and the associated similarity criteria are introduced. The behavior of elevated releases, surface releases, and dense gas plume interaction with surface obstructions are discussed in successive sections. Finally, sources of uncertainty and efforts to improve modeling procedures are presented.

2.0 DENSE GAS DISPERSION: GENERAL BEHAVIOR

Dense gas plumes may result whenever the fractional density ratio, Δ, is greater than zero, i.e.

$$\Delta \cong 1.0 - \frac{28.9}{m_o}\left(\frac{T_o}{T} - 8\,\frac{\dot{M}_w}{\dot{M}_o}\right) \tag{1}$$

where T_o is effluent temperature, m_o is the mean molecular weight of the effluent, and $\dot{M}_w$ and $\dot{M}_o$ are the mass flux of liquid water and total mass flux of the effluent respectively. If $\Delta > 0$ the plume is heavier than air. It may fall to the ground rather close to the source if

$$Fr = \frac{u}{\sqrt{g\Delta d_o}} < C \tag{2}$$

where C lies between 0.7 to 7.7 depending on surface roughness, wind speed and stratification condition. Prediction of the behavior of dense plumes is also often aggravated by the influence of surface interaction, heat transfer, latent heat release, and a transient character.

The effect of negative buoyancy on plume behavior and resulting downwind concentrations will be greatest when crosswinds are light, and turbulence intensities are low. The sinking velocity of the plume relative to the horizontal convective velocity will be much higher than under "normal" conditions. In such cases, the entrainment of outside

air into the plume and the resulting diffusion is a function of this interaction between the plume and the crosswind and approaches the behavior of a turbulent plume injected into a laminar crosswind. When the density is sufficient to bring a plume to ground level, large lateral spreading occurs after touchdown.

A ground-level release of a dense gas is characterized by rapid slumping toward the surface. Horizontal dimensions increase rapidly with an associated decrease in vertical dimension until such time as entrainment is significant. The ratio of vertical height to crosswind dimension remains quite small over most times of interest. The initial potential energy of the dense gas is converted rapidly to kinetic energy; however, this energy is also transmitted to the surrounding ambient fluid and is dissipated by turbulence.

The tendency for dense gases to remain near the ground enhances the importance of plume interaction with surface features. Slight changes of surface slope on the presence of buildings, fences, or dikes will effect plume behavior. These features produce three-dimensional secondary motions or local areas of enhanced turbulence; hence, laboratory models are often required to adequately predict dense gas dispersion.

3.0 PHYSICAL MODELING CRITERIA

Two systems at different geometric scales will exhibit similar behavior if geometric, kinematic, dynamic, and thermic similiarity are guaranteed by the equality of all pertinent ratios of forces, boundary conditions, and initial conditions.[4] When it is not possible to obtain a rigorous similarity in all variables it is necessary to neglect some contributors or phenomena; hence <u>partial</u> similarity. This is permissible when the contribution of such terms are small or their absence conservative.

3.1 Simulation of the Atmospheric Surface Layer

The atmospheric boundary layer is that portion of the atmosphere extending from ground level to approximately 600 meters within which the major exchanges of mass, momentum, and heat occur. Physical modeling in wind tunnels requires consideration of the physics of the atmospheric surface layer as well as the dynamics of plume motion. The reliability of wind-tunnel shear layers for modeling atmospheric shear layers has been demonstrated by many investigators;[5] hence only special aspects associated with dense gas dispersion need be discussed here.

The major practical limitations of accurate wind-tunnel simulation of dense gas dispersion are operational constraints, particularly the inability to obtain a steady wind profile or to accurately simulate atmospheric turbulence at the lowest wind speeds of interest, and Reynolds number constraints (as yet somewhat ill-defined) associated with the proper scaling of near-field turbulence. When combined with estimates of the restraint of plume expansion by the tunnel sidewalls, these considerations permit the development of a performance envelope for a particular wind-tunnel facility, examples of which are given by Meroney et al. (1978), (1979).[6,7]

3.2 Simulation of Dense Gas Dispersion

There exists in the literature descriptions of a variety of different wind-tunnel studies on the dispersion of neutral gas plumes in the atmosphere.[8-13] These referenced studies are significant in that simulation was confirmed by direct prototype measurements. Successful simulations exist for isolated plume behavior[8] as well as plume perturbation situations caused by buildings,[9,10,11] topography,[12,13] and stratification.[8,11,12,13]

When one considers the dynamics of gaseous plume behavior, exact similitude requires the simultaneous equivalence of mass, momentum and volume flux ratios, densimetric Froude number, Reynolds number, and specific gravity. Consideration of variable property, non-ideal gas, and thermal behavior of the plume mixture introduce additional constraints on specific heat capacity variations.[14]

Previous experiments by Hoot and Meroney, Bodurtha, Van Ulden, and Boyle and Kneebone have confirmed that the Froude number is the parameter which governs plume spread rate, trajectory, plume size and entrainment when gases remain negatively buoyant during their entire trajectory.[15,16,17,18] In the case of spills liquified inflammable gases like LNG and LPG buoyancy of the plume will be a function of both mole fraction of the gas and temperature. Thus, depending upon the relative rate of entrainment of ambient gases versus rate of thermal transport from surrounding surfaces the state of buoyancy may vary from negative to positive. Earlier measurements for cold gas releases now suggest that heat transfer effects may be small over the significant time scales associated with non-calm situations (i.e., $U_p > 1$ m/sec); hence gas density should be adequately simulated by isothermal high molecular weight gas mixtures. This agrees with the result independently reported by Boyle and Kneebone that room temperature propane simulated an actual LNG spill quite well.[18]

The Reynolds number cannot be made equal for model and prototype for scales ranging from 1:100 to 1:600. Fortunately, equality is not required if the magnitude and quality of the shear layer turbulence is similar to the full-scale--hence the use of specially designed meteorological wind tunnels.[5] It is possible to obtain full-scale values of

the remaining non-dimensional parameters by reducing the reference velocity to very low values (of the order of 0.2 m/s to simulate a 3 m/sec full-scale wind) and increasing the atmospheric temperature difference as necessary. In some cases investigators modify the density ratio $(\rho_a-\rho)/_g\rho_a$ to permit the use of larger and more convenient values of model velocity. Unforunately, this also modifies inertial effects, time scale ratios, and volume dilution rates.

A reasonably complete simulation may be obtained in some situations even when a modified initial specific gravity is stipulated. By increasing the specific gravity of the model gas compared to the prototype gas, one increases the reference velocity over the model. It is difficult to generate a flow which is similar to that of the atmospheric boundary layer in a wind tunnel run at very low wind speeds. Thus the effect of modifying the models specific gravity extends the range of flow situations which can be modeled accurately. Isyumov and Tanaka (1980) found that Froude number and volume flux equality provided conservative ground-level concentrations for buoyant plumes.[19] Skinner (1978) and Kothari and Meroney (1980) obtained similar plume trajectories when flux Froude number and momentum ratio equivalence are required.[20,21]

4.0 ELEVATED EMISSIONS OF DENSE GASES

Dense gases descending from elevated sources have been reported by several observers. Scorer reports cases of two power plants emitting wet-washed plumes with apparently insufficient elimination of free water, in which the subsequent evaporation of the free water cools the plume and causes it to sink.[22] Bodurtha observed descent of dense gases from chemical industry relief values.[16] The exit stack for the National

Transonic Wind Tunnel facility at Langley Research Center, NASA, will omit large quantities of cold nitrogen-air mixtures which produces ground fog under certain operational and meteorological conditions.[21]

Bodurtha conducted wind-tunnel tests of emission of freon-air mixtures into a crosswind. Various combinations of density, exit velocity, crosswind velocity and stack diameter were used in obtaining smoke pictures. The results were correlated by an expression for the maximum rise height:

$$H = 5.44\, D_o^{0.5}\, R^{0.75} \tag{3}$$

in which H is the maximum rise height of the plume centerline in feet, D_o is the stack diameter in feet, and R is the ratio of the exit velocity to the wind speed. This formula has the disadvantage of being dimensionally inhomogeneous, and the absence of relative density terms makes its application questionable as the specific gravity approaches unity.

Hoot and Meroney examined dense vertical plumes in a quiescent medium, and dense plume injected into both laminar and turbulent crosswinds.[15] The vertical plumes emitted into a quiescent atmosphere were observed to rise initially in a jet with almost linear growth of radius with vertical distance. This jet region appeared to encompass from 1/4 to 1/3 of the total rise height. The dense vertical plume appears to re-entrain some of the falling dense fluid, so that the flux of negative buoyancy increases with distance, rather than being constant. The point of maximum rise of the plume correlates as

$$\frac{\Delta h}{d_o} = 2.96\ F_R, \quad \text{where} \tag{4}$$

$$F_R = \frac{\sqrt{\rho}_o w_o}{\sqrt{(\rho_o - \rho_a) g d_o}}$$

where d_o is stack diameter, w_o is exit velocity, and ρ_o is exit density.

Plumes injected vertically into a crosswind initially lofted to some maximum height, subsequently descended to the ground, impacted with nearly a circular cross-sectional configuration, but then spread laterally as they dispersed downwind (Figure 1). Hoot and Meroney tuned an integral equation analytical plume theory with wind-tunnel experiments to estimate downwind surface concentrations. The components of the analysis required one to first estimate plume rise, Δh, as

$$\frac{\Delta h}{d_o} = 1.32\ (SG)^{2/3}\ (F_{RH})^{2/3}\ (R)\ , \tag{5}$$

where $SG = \rho_o/\rho_a$

$R = w_o/u$, and

$F_{RH} = u/\sqrt{g(SG-1.0)d_o}$; and

downwind distance to maximum plume rise, $\bar{x}$, as

$$\frac{\bar{x}}{d_o} = (SG)\ (F_{RH})^2\ (R)\ . \tag{6}$$

Touchdown distance, x_{TD}, may be evaluated from

$$\frac{x_{TD}-\bar{x}}{d_o} = 0.56 \left[\frac{\left(\frac{h_s}{d_o}\right) + 2\left(\frac{\Delta h}{d_o}\right)^3 - \left(\frac{\Delta h}{d_o}\right)^3}{R} \right]^{1/2} F_{RH}\ . \tag{7}$$

Symbols are defined in Figure 1.

Note that as $u \to 0$, $F_{RH} \to 0$, $\bar{x} \to 0$, $\Delta h \to 0$ and $x_{TD}/h_s \to 3\ F_{RH}$. The constant, 3, compares well to the value 4.5 proposed by Briggs based on Bodurtha's visualization experiments.

At touchdown the surface concentrations, C_{TD}, are of the order

$$K_c \equiv \frac{C_{TD} u d_o^2}{Q} \simeq 3.10 \left(\frac{2\Delta h + h_s}{2d_o}\right) - 2 \qquad (8)$$

Concentrations decrease from their touchdown values at a negative 0.65 power of distance, x, until the curve intercepts the -1.7 slope behavior of a ground source as shown in Figure 1.

Kothari and Meroney examined the behavior of a dense plume emitted from a 1:200 scale model of the National Transonic Facility exhaust stack at NASA, Langley. In this case the dense gases not only descended but interacted with local buildings as shown in Figure 2. Nonetheless, measurements made with and without buildings present suggested only second-order aerodynamic effects so results are compared to the predictive relations suggested by Hoot and Meroney in Table 1. The results are nearly equivalent except for the plume trajectory for the case of 1.8 m/sec wind and exhaust velocity of 23 m/sec. Streamline deflection by the NTF building is the likely explanation for this deviation.

5.0 SURFACE EMISSIONS OF DENSE GASES

A number of laboratory experiments have been performed to evaluate the influence of plume density on ground-level gaseous plume dispersion. Sakagami and Kato (1968) measured diffusion and vapor rise from a small 5 x 10 cm LNG well in the floor of a 50 x 50 cm cross section x 200 cm length wind tunnel. They confirmed a tendency for the gas to remain concentrated at ground level. Boyle and Kneebone (1972) released LNG on

water, precooled methane, and propane in a specially built 1.5 x 1.2 m cross section by 5 m long asbestos-wall wind tunnel. No attempt was made to scale the atmospheric surface layer velocity profile or turbulence. They concluded room-temperature propane simulated a LNG spill quite well, but the pre-cooled methane runs lofted suggesting to the authors incorrect release temperature or exaggerated heat transfer from the ground surface.

5.1 Point and Area Sources of Dense Gases

Hoot and Meroney, Hall et al., and Meroney et al., have considered the behavior of continuous ground-level point sources of heavy gases in wind tunnels.[15,23,24,25] The principle characteristic of such plumes is their very wide, shallow nature. In general, the plume size reduces rapidly with increasing wind speed, but it still retains a low, flat form with significant upwind and lateral travel. At higher wind speeds the plume upper boundary becomes more turbulent and unsteady, resulting in rapid vertical growth as local Richardson numbers decrease. Visualization tests performed over a simple ground-level area source revealed that the plumes upwind spread, L_U, and lateral spread at source center, L_{H_o}, correlate with the buoyancy length scale, $\ell_b = Qg(SG-1)/u^3$, for a wide range of source and shear flow conditions.[25] Britter reported similar results for dense salt plumes emitted in a water flume and liquified natural gas (LNG) plumes developing downwind of sea spills.[22] Specific gravity ratios considered ranged from 1.0 to 4.2 and lateral scales from 1.0 to 500 meters.

Along the plume centerline gas concentrations fall off rapidly with increasing windspeed. Although density differences were observed to have a significant effect on downstream diffusion pattern the effect on

centerline concentrations appear primarily multiplicative. Hoot and Meroney studied point source ground releases in both neutral and stably stratified turbulent boundary layers.[15] They found that varying specific gravity of the source gas from 1.0 to 3.0 increased maximum ground concentrations by no more than 40% while decay rates of concentration with distance remained the same.

5.2 Volume Sources and Short-Term Releases of Dense Gases

Short-term or instantaneous releases of dense gas may occur during explosions or boiloff of gases from limited spills of liquified gases such as ammonia or LNG. Meroney et al., released carbon dioxide in a 1:106 scale model simulation of test 044 from the Capistrano land spill field test series supported by the American Gas Association.[27] This test involved a spill of LNG into a 24.4 m diameter area surrounded by a 46 cm high dike. Figure 4 compares concentration sensor response at equivalent locations from the model and field measurements. The wind-tunnel simulation did not reproduce the large and intermittent concentration peaks at late times as observed in the field; however, it is believed that these perturbations may be due to gustiness, changes in wind direction, and cracking of the field test dike floor which produced spikes in the late boiloff rate.

Hall has compared data from short time releases of BCF gas in a wind-tunnel shear layer with Trial 33 from the Porton Field releases of freon mixtures.[34,28] Situations from the two sets of data existed which had equal modified Froude numbers. The scale of the model test was 1:34.2 based on the volume of gas released. Wind speeds were determined at a scaled reference height. As noted in Figure 5, the level of agreement between wind-tunnel model and field trial seems good. The peak

concentrations, the form of concentration distribution with time, and the plume arrival and departure times all match quite well when one considers that these field tests are separate realizations from some probability distribution about an ensemble behavior. Hall has also prepared figures based on laboratory experience which predict downwind hazard limits for propane or butane escape.[24]

During a 5 cubic meter LNG spill series onto a water basin at the Naval Weapons Center at China Lake, California, concentrations were measured at up to eight locations downwind.[29] Meroney and Neff replicated the meteorological, topography, and spill conditions to a scale of 1:85 for the four field tests.[30] Correlation of results ranged from poor to very good, probably because fluctuation present during the field tests were as large as ± 50° in wind direction and ± 1.8 m/s in wind speed. During field test LNG-21 wind conditions were more stationary, and Figure 6 displays good agreement between laboratory and field measured peak concentrations.

A sudden release of a volume of dense gas near the ground is characterized by a slumping of the volume toward the ground followed by a radial expansion preceeded by a gravity current head. Wind-tunnel model experiments with releases of dense gas volumes of 50 cm^3 reproduced dense plume behavior previously seen in field experiments at scales up to 350 times greater.[31] Lohmeyer et al., used a special source volume generator to quickly release measured volumes of Freon-12 gas (specific gravity = 4.17) at a wind-tunnel floor (Figure 7). A fast response katherometer system measured time dependent concentration variation. Measurements were compared with a modified version of the generalized box model for dense gases proposed by Fay.[32] In a calm

environment the radial variation of plume dilution, $V_{initial}/V$, versus dimensionless radius, $R^* = R/V_{initial}^{1/3}$, is shown in Figure 8. These measurements support the notion that the radial spreading speed is independent of dilution and directly proportional to the local excess hydroelastic head within the cloud, i.e.,

$$dR/dt = \alpha(g'H)^{1/2} \tag{9}$$

where α is equal to unity and that the entrainment velocities at the surface of the cloud are also proportional to excess hydrostatic head, i.e.,

$$u_z = c_z\,(g'H)^{1/2} \quad \text{and} \quad u_r = c_r\,(g'H)^{1/2} \tag{10}$$

and $$c_r \simeq c_z \simeq 0.10.$$

These measurements agree with those discussed by Simpson and Britter and Germeles and Drake.[33,34]

Wind shear superimposed over volume releases of dense gas initially displace higher concentrations further downwind with increasing wind speed. As shear flow mixing increases it begins to dominate over inertial/buoyancy entrainment mechanisms, hence at very high velocities the maximum peak concentrations retreat back toward the source. As velocities increase further the gravity dominated portion of the plume lifetime decreases until dispersion is essentially passive. Most of the data taken by Hall was for high wind speed or low modified Froude number conditions.[24] Figure 9 indicates that plume concentrations decay with time to a power of -3. Also shown are predictive lines for instantaneous point and finite width sources from Lagrangian similarity theory proposed by Yang and Meroney.[35] A ground-level neutrally buoyant point source will decay as

$$\left(\frac{\Psi_i}{\Psi}\right)_{max} = 0.298\ \tilde{\tilde{t}}^{-3} \quad \text{where} \tag{11}$$

$$\tilde{\tilde{t}} = \frac{t^*}{R_i^{1/2}} = \frac{t\ u}{\Psi_i^{1/3}} \quad ,$$

and a line source of width dimension equal to $2\ \Psi_i^{1/3}$ will decay as

$$\left(\frac{\Psi_i}{\Psi}\right)_{max} = (0.55/\tilde{\tilde{t}})^2\ [\text{erf}\ (0.483/\tilde{\tilde{t}})] \ . \tag{12}$$

Although some of Hall's releases were extended over considerable time all data assymptotically approaches the passive gas dispersion theory.

5.3 Dense Cold Gases Versus Dense Isothermal Gases

Exact variation of the density ratio for the entire life of a model plume is difficult to simulate for plumes which simultaneously vary in molecular weight and temperature. To emphasize this point more clearly, consider the mixing of two volumes of gas, one being the source gas, Ψ_s, the other being ambient air, Ψ_a. Consideration of the conservation of mass and energy for this system yields*

$$\frac{\rho_g}{\rho_a} = \frac{\left(\frac{\rho_s}{\rho_a}\Psi_s + \Psi_a\right)}{\left(\frac{T_a}{T_s}\Psi_s + \Psi_a\right)\left(\frac{C_{p_s} M_s}{C_{p_a} M_a}\Psi_s + \Psi_a\right)\left(\frac{C_{p_s} M_s}{C_{p_a} M_a}\frac{T_a}{T_s}\Psi_s + \Psi_a\right)}$$

If the temperature of the air, T_a, equals the temperature of the source gases, T_s, or if the product of the specific heat capacity and molecular weight, C_pM, is equal for both source gas and air then the equation reduces to:

*The pertinent assumption in this derivation is that the gases are ideal and properties are constant.

$$\frac{\rho_g}{\rho_a} = \frac{\frac{\rho_s}{\rho_a} \Psi_s + \Psi_a}{\Psi_s + \Psi_a} \quad .$$

Thus for two prototype cases: 1) an isothermal plume and 2) a thermal plume which is composed mostly of air, it does not matter how one produces the model density ratio as long as the initial density ratio value is equal for both model and prototype.

For a plume whose temperature, molecular weight, and specific heat are all different from that of the ambient air, i.e., a cold natural gas plume, equality in the variation of the density ratio upon mixing must be relaxed slightly if one is to model utilizing a gas different from that of the prototype. In most situations this deviation from exact similarity is very small.

Scaling of the effects of heat transfer by conduction, convection, radiation, or latent heat release from entrained water vapor cannot be reproduced when the model source gas and environment are isothermal. Fortunately in a large majority of industrial plumes the effects of heat transfer by conduction, convection, and radiation from the environment are small enough that the plume buoyancy essentially remains unchanged. The influence of latent heat release by moisture upon the plume's buoyancy is a function of the quantity of water vapor present in the plume and the humidity of the ambient atmosphere. Such phase change effects on plume buoyancy can be very pronounced in some prototype situations. Humidity effects are expected to reduce the extent in space and time of plume buoyancy dominance on plume motion. Hence a dry adiabatic model condition should be conservative.

The influence of heat transfer on cold dense gas dispersion due to cryogenic liquid spills can be divided into two phases. First, the temperature (and hence specific gravity) of the plume at exit from a containment tank on dike is dependent on the thermal diffusivity of the tank-dike-spill surface materials, the volume of the tank-dike structure, the actual boiloff rate, and details of the spill surface geometry. A second plume phase involves the heat transfer from the ground surface beyond the spill area which lowers plume density.

It is tempting to try to simulate the entire transient spill phenomenon in the laboratory including spill of cryogenic fluid into the dike, heat transfer from the tank and dike materials to the cryogenic fluid, phase change of the liquid and subsequent dispersal of cold gas downwind. Unfortunately, the different scaling laws for the conduction and convection suggest that markedly different time scales occur for the various component processes as the scale changes. Since the volume of dike material storing sensible heat scales versus the cube of the length scale whereas the pertinent surface area scales as the square of the length scale one perceives that heat is transferred to a model cold plume much too rapidly within the model containment structures. This effect is apparently unavoidable since a material having a thermal diffusivity low enough to compensate for this effect does not appear to exist. When calculations for the full-scale situation suggest minimal heating of a cold gas plume by the tank-dike structure it may suffice to cool the model tank-dike walls to reduce the heat transfer to a cold model vapor and study the resultant cold plume.

Boyle and Kneebone released under equivalent conditions room temperature propane and LNG onto a water surface. The density of

propane at ambient temperatures and methane at -161°C relative to air are the same.[18] Using the modified Froude number as a model law they concluded dispersion characteristics were equivalent within experimental error.

A mixture of 50% helium and 50% nitrogen pre-cooled to 115°K was released from model tank-dike systems by Meroney et al., to simulate equivalent LNG spill behavior.[27] There was no guarantee that these experiments reproduced quantitatively similar situations in the field. Rather it was expected the gross influences of different heat transfer conditions could be determined. Since the turbulence characteristics of the flow are dominated by roughness, upstream wind profile shape, and stratification one expects the Stanton number in the field will equal that in the model, and heat transfer rates in the two cases should be in proper relation to plume entrainment rates. On the other hand, if temperature differences are such that free convection heat transfer conditions dominate, scaling inequalities may exist; nonetheless, model dispersion rates would be conservative.

Visualization experiments performed with equivalent dense isothermal and dense cold plumes revealed no apparent change in plume geometry. Concentration data followed similar trends in both situations. No significant differentiation appeared between insulated versus heat conducting ground surfaces or neutral versus stratified approach flows.

5.4 Dense Gas Plume Interaction with Surface Features and Buildings

Measurements of dense gas dispersion downwind of isolated releases have resulted in the development of many predictive models. The variation of such predictions is significant in assessing credibility of

potential hazards, yet this uncertainty may well increase when the perturbations of building or structural aerodynamics is considered.[37]

Dense plumes emitted from short stacks rising above cubical model buildings were found to avoid significant entrainment or wake effects when ejection velocities were greater than wind speed at stack height and stack height exceeded twice the building height.[15] A criteria appropriate to assure that the dense plume does not fall back into the recirculating cavity region would be $\bar{x}/d_o \geq 3\ ^{h}b/d_o$.

Model tests have been conducted to evaluate the rate of dispersion and extent of downwind hazards associated with the rupture of large LNG storage tanks.[27] Tank facilities considered include a Low Dike configuration (73 m diameter, 39 m tank surrounded by a 6.6 m dike 93 m by 100 m in area) and a High Dike configuration (73 m diameter, 39 m tank surrounded by a concentric 81 m diameter dike 24 m tall). Dense plumes fell rapidly down over the dike walls to the ground and proceeded downwind in an undulating wave-like motion until the atmospheric turbulence started to penetrate and produce increased vertical dispersion. Figures 10 and 11 give an artist representation of these flows for the High Dike and Low Dike at 45°.

For the same dike geometry the rate of initial plume spread in the lateral directions varied directly with boiloff rate and inversely with wind speed. That is, to maintain approximately the same rate of spread with an increased boiloff, the wind speed would have to be increased and vice versa. At low wind speeds and high boiloff rates the gravity spread rate increases to a point where the plume would spread out to the walls of the tunnel and then crawl upwind of the dike complex in a front perpendicular to the wind direction. With stable stratification the

plume would spread out on the ground and migrate quite far upwind (300 meters) for the higher boiloff rates and low wind speeds. This upwind movement was present to some extent for the lower boiloffs and higher wind speeds.

The observed effects of the wake and cavity regions generated by the aerodynamics of the tank and dike structure varied with tank and dike geometry, wind speed, and stratification. For the Low Dike and Tank complex the effect of increased plume dispersion due to turbulence in its wake was insignificant. The only aerodynamic effect noticeable for this structure was that of a standing plume in the cavity regions of the tank and dike. For the High Dike and Tank the effect of increased plume dispersion due to turbulence in its wake was most significant. Strong vortices which formed near the ground on each side of dike structure would entrain a large amount of the plume and transport it downwind. This effect would give the plume a bifurcated form on the ground with what appears to be maximum concentrations traveling downwind at a separation distance slightly greater than that of the dike diameter. Another vortex was generated on the tank top and traveled slightly upward in the downwind direction. This vortex appeared to act as a vent to the standing plume in the cavity region.

Concentration measurements were obtained for as many as 50 different sample points distributed over an equivalent ground zone of 100 to 2000 meters long by 250 meters wind and in the vertical over a height of 0 to 120 meters. A series of vertical profiles revealed the shallow layer character of a dense gas plume. Ground-level contour plots of percent methane confirmed the presence of a bifurcated plume as suggested by the visualization photographs.

Even in the presence of the tank/dike wakes the decay of maximum downwind concentrations fell only slightly below values predicted by the Battelle Columbus Laboratories (BCL) correlation, which represents an upper bound of all concentration resulting from confined LNG land spills during the AGA phase II program, i.e.,

$$\frac{X_{max}\,\bar{u}\,L^2}{Q} \simeq 130\,\left(\frac{x}{L}\right)^{-2} \quad . \tag{13}$$

where L is same characteristic length scale, Q is a maximum volumetric release rate, and u is the wind speed at an elevation of 10 m.

Dirkmaat studied the effect of a 50 m long, 21 m wide, 17.5 m obstacle placed at various locations near a modeled sudden guillotine fractive of an LPG pipeline.[38] A release of 1000 kg/sec of LPG during 6 minutes was simulated. On the average the plume spread in streamwise direction and the maximum contour areas tended to decrease compared to the undisturbed situation. Although the cloud contours were capriciously affected by the obstacle, the overall effect on cloud dimensions was not dramatic. Little could be said however, about more complicated obstacle arrangements.

Terrain undulations can act to accelerate or depress dense gas dispersion. Hall and Meroney et al., both report extensive upwind motion for dense gases released on modest ground slope.[23,27] The presence of upwind obstacles tends to lessen the effects of ground slope when surface layer turbulence is enhanced.[27] Studies of simulated spills of 6 cubic meter LNG volumes on a pond suggest that slight hill slopes (1:10) can detour dense plumes and reduce longitudinal distances to the lower flammability limit. Shallow valleys or gorges channel the plume and sustain high concentrations.[25]

6.0 CONCLUSIONS

Wind tunnels have simulated a wide range of conditions associated with dense gas transport and dispersion. Scaling criteria suggest that existing facilities can simulate a wide range of release situations. Measurements of dense fluid behavior in both air and water facilities appear reproducible and consistent. Idealized release configurations appear optimal for testing and tuning numerical or analytical models. Wind tunnels are primarily limited by operational constraints associated with the necessary low wind speeds and low Reynolds numbers. Further effort is needed to quantify fully the effects of nonadiabatic heat transfer and humidity on cold plume model behavior.

ACKNOWLEDGMENTS

The author gratefully acknowledges the support of the Gas Research Institute provided through Contract No. 5014-352-0203.

REFERENCES

1. Liquified Gaseous Fuels Safety and Environmental Control Assessment Program: A Status Report, U.S. Department of Energy, DOE/EV-0036, May 1979.

2. Recommended Research on LNG Safety, U.S. Department of Energy, DOE/EV-10024-1, March 1981.

3. J. D. Reid, Dispersion of Denser-Than-Air Gases, Report AQRB-80-005-L, Atmospheric Environment Service, Ontario, Canada, 24 p.

4. S. J. Kline, Similitude and Approximation Theory, McGraw-Hill Book Co., New York (1965).

5. W. H. Snyder, Guidelines for Fluid Modeling of Atmospheric Diffusion, U.S. Environmental Protection Agency, Report EPA-600/8-81-009 (1981) 185 p.

6. R. N. Meroney, D. E. Neff, and J. E. Cermak, Wind-Tunnel Modeling of LNG Spills, Proceedings AGA Transmission Conference, Montreal, Canada, May 8-10, 1978, T217-T223.

7. R. N. Meroney and D. E. Neff, Laboratory Simulation of Liquid Natural Gas Vapor Dispersion over Land or Water, Wind Engineering, Pergamon Press, New York, Vol. 2 (1980), pp. 1139-1150.

8. F. H. Chaudhry and R. N. Meroney, A Laboratory Study of Diffusion in a Stably Stratified Flow, Atmospheric Environment, Vol. 7, No. 4, (1973), 443.

9. J. E. Martin, The Correlation of Wind Tunnel and Field Measurements of Gas Diffusion Using Kr-85 as a Tracer, Ph.D. Thesis, MMPP 272, University of Michigan, 1965.

10. N. Isyumov, T. Jondali, and A. G. Davenport, Model Studies and the Prediction of Full-Scale Levels of Stack Gas Concentration, Journal of APCA, Vol. 26, No. 10, (1976) 956.

11. K. M. Kothari, R. N. Meroney, and R. J. Bouwmeester, An Algorithm to Estimate Field Concentrations in the Wake of Power Plant Complexes under Nonsteady Meteorological Conditions from Wind-Tunnel Experiments, Journal of Applied Meteorology, to be published, (1981).

12. J. C. Yinst, et al., Review of Five Wind-Tunnel Modeling Results in Complex Terrain, 5th Symposium on Turbulence, Diffusion, and Air Pollution, Atlanta, Georgia, (1981) 148.

13. J. C. Weil, J. E. Cermak, and R. L. Petersen, Plume Dispersion about the Windward Side of a Hill at Short Range: Wind Tunnel Versus Field Measurements, 5th Symposium on Turbulence, Diffusion, and Air Pollution, Atlanta, Georgia, (1981) 159.

14. D. E. Neff and R. N. Meroney, Dispersion of Vapor from LNG Spills--Simulation in a Meteorological Wind Tunnel of Spills at China Lake Naval Weapons Center, California, Fluid Mechanics and Wind Engineering Report CER78-79DEN-RNM41, Colorado State University, Fort Collins, (1979) 77 p.

15. T. G. Hoot and R. N. Meroney, The Behavior of Negatively Buoyant Stack Gases, 67th Annual Meeting of APCA, Denver, Colorado, Paper 74-210 (1974) 20 p.

16. F. T. Bodurtha, Jr., The Behavior of Dense Stack Gases, J. of APCA, Vol. 11, No. 9 (1961) 431-437.

17. A. P. Van Ulden, On the Spreading of a Heavy Gas Released near the Ground, Loss Prevention and Safety Prevention Seminar, Delft, Netherlands (1974).

18. G. J. Boyle and A. Kneebone, Laboratory Investigations Into the Characteristics of LNG Spills on Water, Evaporation, Spreading and Vapor Dispersion, Shell Research, Ltd. Report to API (1972).

19. N. Isyumov and H. Tanaka, Wind-Tunnel Modeling of Stack Gas Dispersion--Difficulties and Approximations, Wind Engineering, Pergamon Press, New York, Vol. II (1980) 987-1002.

20. G. T. Skinner and G. R. Ludwig, Physical Modeling of Dispersion in the Atmospheric Boundary Layer, Calspan Advanced Technology Center, Carmel, New York, Calspan Report No. 201 (1978).

21. K. M. Kothari and R. N. Meroney, Building Effects on National Transonic Facility Exhaust Plume, NASA Contract NAS1-15925, Fluid Mechanics and Wind Engineering Report CER79-80KMK-RNM35, Colorado State University, Fort Collins, Colorado (1980) 43 p.

22. R. S. Scorer, The Behavior of Chimney Plumes, Int. J. Air Pollution, Vol. 1 (1959) 198-220.

23. D. J. Hall, C. F. Barrett, and M. O. Ralph, Experiments on a Model of an Escape of Heavy Gas, Warren Springs Laboratory Report LR 217 (AP) Dept. of Trade and Industry, United Kingdom (1974) 25 p.

24. D. J. Hall, Further Experiments on a Model of an Escape of Heavy Gas, Warren Springs Laboratory Report LR (312) AP, Dept. of Trade and Industry, United Kingdom, (1977) 47 p.

25. R. N. Meroney, D. E. Neff, and K. M. Kothari, Behavior of LNG Vapor Clouds: Tests to Define the Size, Shape and Structure of LNG Vapor Clouds: Annual Report for 1979-1980, Gas Research Institute Report GRI 79/0073, Chicago, Illinois (1980) 80 p.

26. R. Britter, The Ground-Level Extent of a Negatively Buoyant Plume in a Turbulent Boundary Layer, Atmospheric Environment, Vol. 14(7) (1980) 779-785.

27. R & D Associates and Colorado State University, Liquified Natural Gas Wind-Tunnel Simulation and Instrumentation Assessments, U.S. Dept. of Energy Report SAN/W1364-01 (1978) 390 p.

28. R. G. Picknett, Field Experiments on the Behavior of Dense Clouds: Part 1, Main Report, Report Ptn IL 1154/78/1, Chemical Defense Establishment, Porton Down, United Kingdom (1978) 93 p.

29. R. P. Koopman, B. R. Bowman, and D. L. Ermak, Data and Calculations of Dispersion on 5 m^3 LNG Spill Tests, Report UCRL-52876, Lawrence Livermore Laboratory, California (1979) 31 p.

30. R. N. Meroney and D. E. Neff, Dispersion of Vapor From LNG Spills--Simulation in a Meteorological Wind Tunnel: Six Cubic Meter China Lake Spill Series, Proceedings of 4th Colloquium on Industrial Aerodynamics, Achen, West Germany, June 18-20, 1980, 303-320.

31. A. Lohmeyer, R. N. Meroney, and E. J. Plate, Model Investigations on the Spreading of Heavy Gases Released From an Instantaneous Volume Source at the Ground, Proceedings of 11th NATO/CCMS Int. Tech. Mtg. on Air Pollution Modeling and Its Applications, Amsterdam, the Netherlands, November 25-28, 1980, 15 p.

32. J. A. Fay, Gravitational Spread and Dilution of Heavy Vapor Clouds, Proceedings of 2nd Intl. Symposium on Stratified Flows, Trondheim, Norway, June 24-27, 1980, 471-494.

33. J. E. Simpson and R. E. Britter, The Dynamics of the Head of a Gravity Current Advancing over a Horizontal Surface, J. Fluid Mech. Vol. 94 (1979) 477-495.

34. A. E. Germeles and E. M. Drake, Gravity Spreading and Atmospheric Dispersion of LNG Vapor Clouds, Proceedings of 4th Intl. Symp. on Transport of Hazardous Cargoes by Sea and Inland Waterway, Jacksonville, Florida (1975) 519-539.

35. B. T. Yang and R. N. Meroney, Construction of a Lagrangian Similarity Distribution Function for a Non-Stationary Atmospheric Diffusion Process, Proceedings of 3rd AMS Conf. on Probability and Statistics in Atmospheric Science, Boulder, Colorado, June 19-22, (1973) 6 p.

36. J. Havens, Predictability of LNG Vapor Dispersion From Catastrophic Spills Onto Water: An Assessment, U.S. Coast Guard, Dept. of Transportation, Report CG-M-09-87 (1977) 211 p.

37. R. N. Meroney, Turbulent Diffusion near Buildings, Ch. 11, Engineering Meteorology (ed. E. Plate), Elsevier, to be published in (1981).

38. J. J. Dirkmaat, Experimental Studies on the Dispersion of Heavy Gases in the Vicinity of Structures and Buildings, Proceedings of Symposium - Designing with the Wind, Nantes, France, Centre Scientifique et Technique du Baitment, June 15-19, (1981) pp III-3-1 to III-3-13.

FIGURE TITLES

Figure	Title
1	Dispersion of Dense Plumes from Short Stacks, Hoot and Meroney (1974).
2	Behavior of a Cold Dense Gas Plume Emitted from the Model National Transonic Facility Exhaust Stack, Model Scale 200:1, Kothari and Meroney (1979).
3	Spreading Characteristics of Dense Gas Area Sources: Upstream Travel Distances and Lateral Tunnel Distances, Meroney et al. (1980).
4	Comparison of Wind Tunnel and Field Data for the Capistrano 044 LNG Land Spill Experiments, Meroney et al. (1977): Wind Speed 5.4 m/s, Stability Category D-C, Wind Tunnel Scale Ratio 106:1.
5	Comparison of Wind Tunnel and Field Data for the Porton Field Test Trial No. 33: Wind Speed 1.0 m/s, Source Gas Specific Gravity = 2.2, Stability Category B-C; Wind-Tunnel Scale 34.2:1.
6	Comparison of Wind Tunnel and Field Data for the Six Cubic Meter LNG Spill Test No. LNG-21 at China Lake Naval Weapons Test Center, Neff and Meroney (1979): Wind Speed 4.9 m/s, Stability Category C; Wind-Tunnel Scale Ratio 85:1.
7	Experimental Configuration for Release of Instantaneous Volume Sources of Dense Gas, Lohmeyer et al. (1980).
8	Plume Dilution, $\forall_i/\forall$, versus Dimensionless Radius, $R^*=r/\forall^{1/3}$, $U_L^* = 0$, Lohmeyer et al. (1980).
9	Assymptotic Dilution of Short-Term Releases of Dense Gases: Comparison of Lagrangian Similarity Solution for Passive Sources, Yang and Meroney (1973) with Dense Gas Tests, Hall (1979).
10	Dense Plume Behavior Downwind of a High Dike/Tank Model.
11	Dense Plume Behavior Downwind of a Low Dike/Tank Model.

Table 1. Comparison of NTF Model Plume Characteristics with that Predicted by Hoot and Meroney (1974).

(w_o) m/s	(u) m/s @ 10 m Height	Downwind Distance to Maximum Plume Rise, $\bar{x}$ Meters		Touchdown Distance of Plume Center, x_{TD}, Meters		Plume Rise Δh Meters		K_c(maximum)	
		Calculated	Experimental	Calculated	Experimental	Calculated	Experimental	Calculated	Experimental
23	1.8	32	65	156	240	45	46	0.26	--
23	2.7	49	45	255	250	39	41	0.32	--
23	22	--	--	--	--	--	--	0.80	0.46*
46	1.8	63	70	255	325	89	75	0.09	--
46	2.7	98	90	410	330	77	70	0.11	--

*Wind direction = 180° and maximum measured value with NTF complex
All other experimental data are for wind direction = 0°

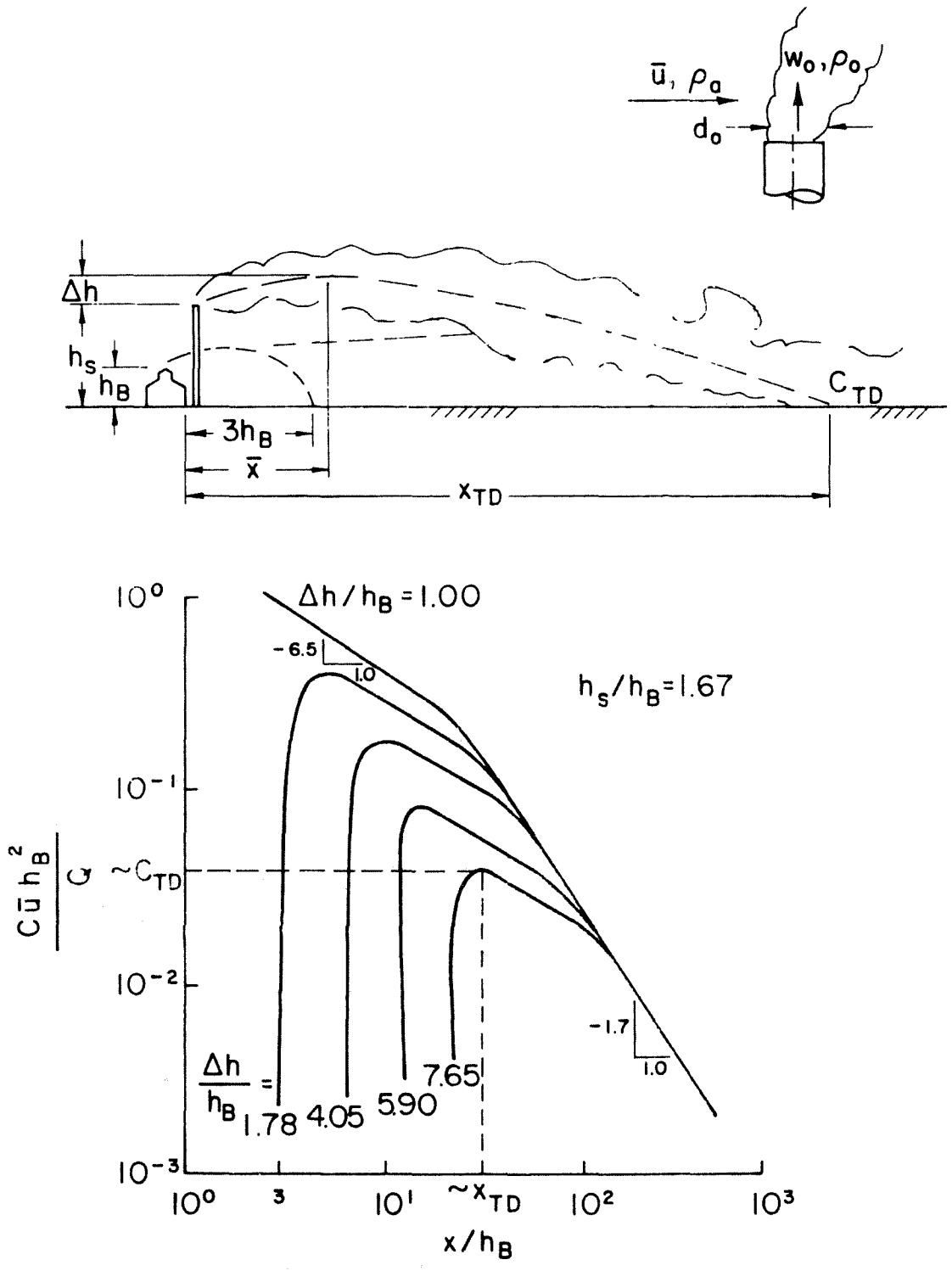

Figure 1. Dispersion of Dense Plumes from Short Stacks, Hoot and Meroney (1974).

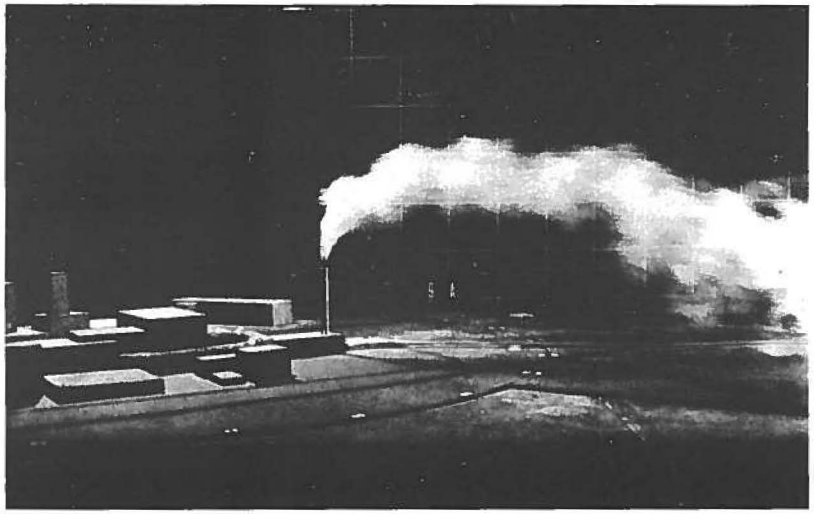

U = 1.8 m/s

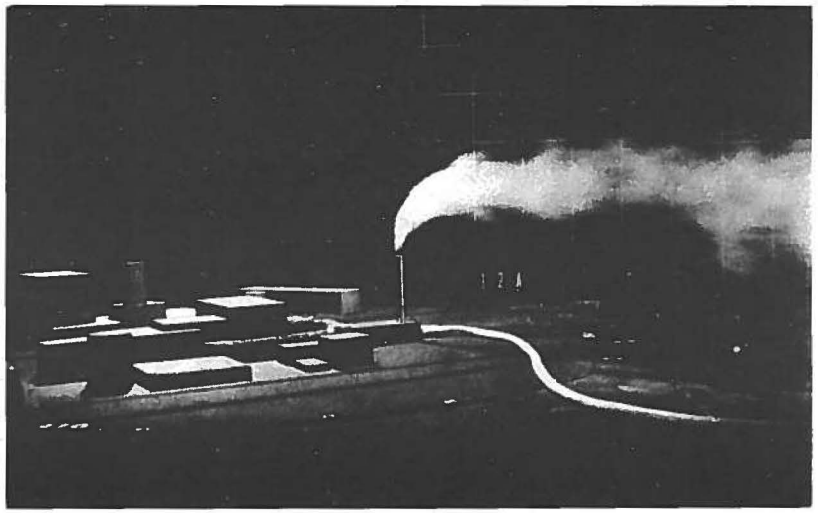

U = 2.7 m/s

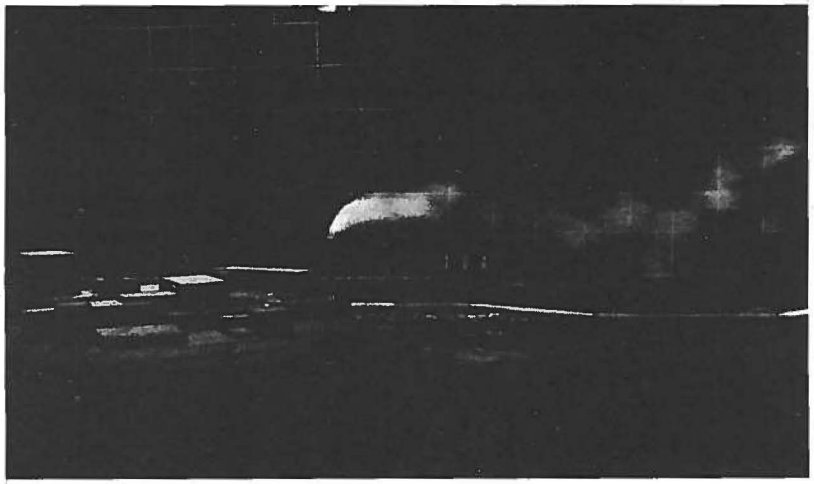

U = 4.5 m/s

Figure 2. Behavior of a Cold Dense Gas Plume Emitted from the Model National Transonic Facility Exhause Stack, Model Scale 200:1, Kothari and Meroney (1979). S.G. = 2.0, W_s = 23 m/s.

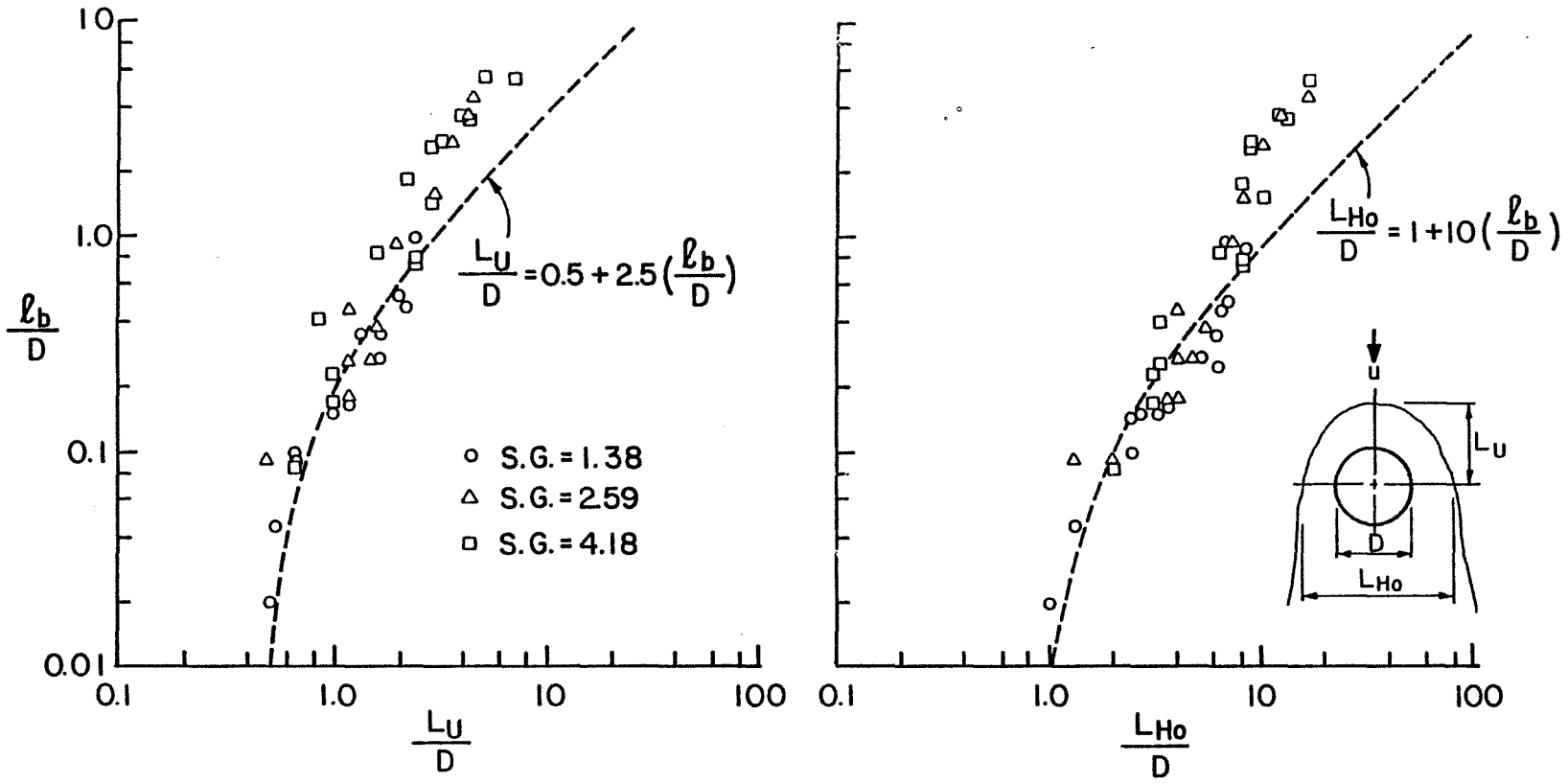

Figure 3. Spreading Characteristics of Dense Gas Area Sources: Upstream Travel Distances and Lateral Tunnel Distances, Meroney et al. (1980).

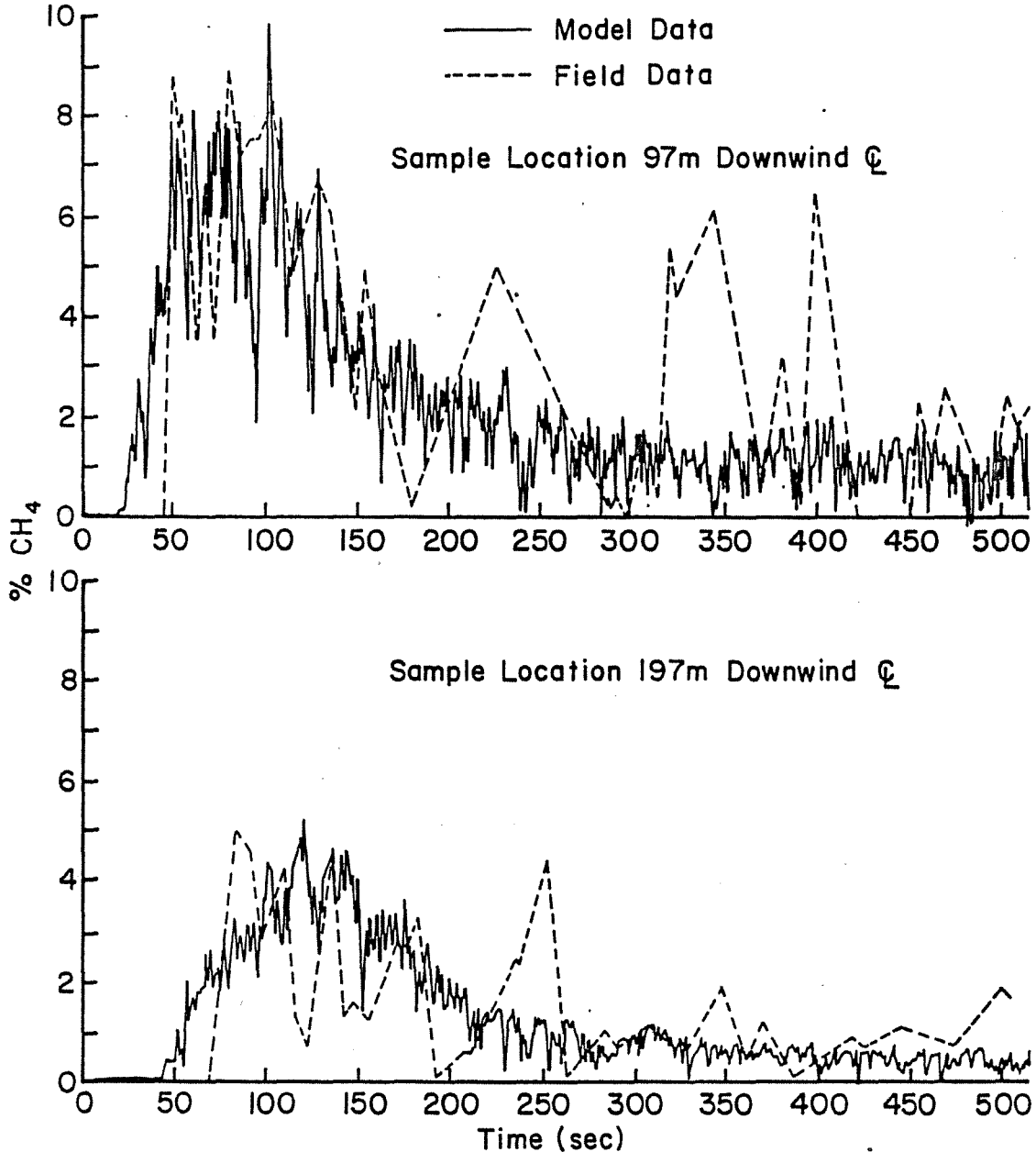

Figure 4. Comparison of Wind Tunnel and Field Data for the Capistrano 044 LNG Land Spill Experiments, Meroney et al. (1977): Wind Speed 5.4 m/s, Stability Category D-C, Wind Tunnel Scale Ratio 106:1.

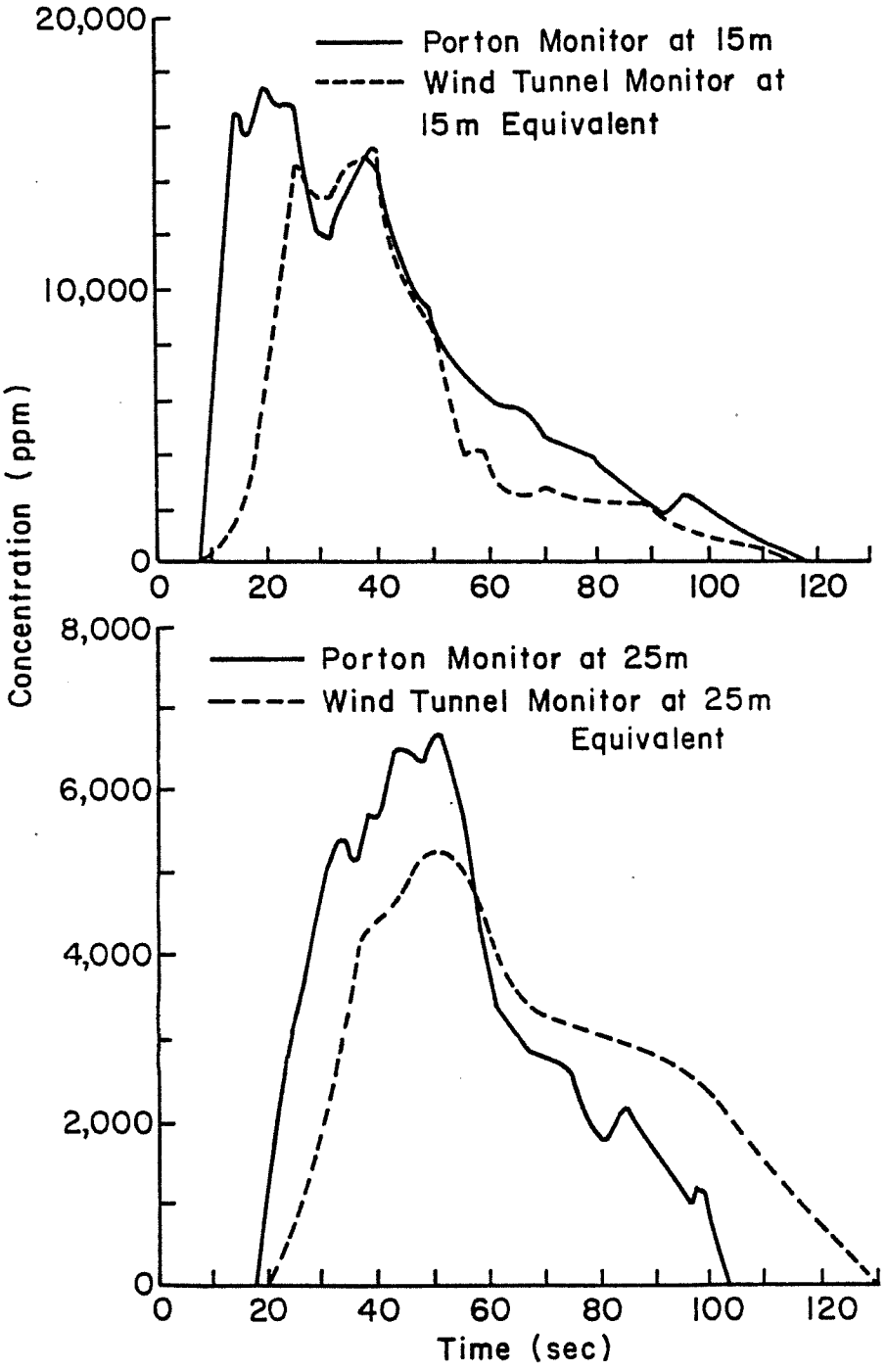

Figure 5. Comparison of Wind Tunnel and Field Data for the Porton Field Test Trial No. 33: Wind Speed 1.0 m/s, Source Gas Specific Gravity = 2.2, Stability Category B-C; Wind-Tunnel Scale 34.2:1.

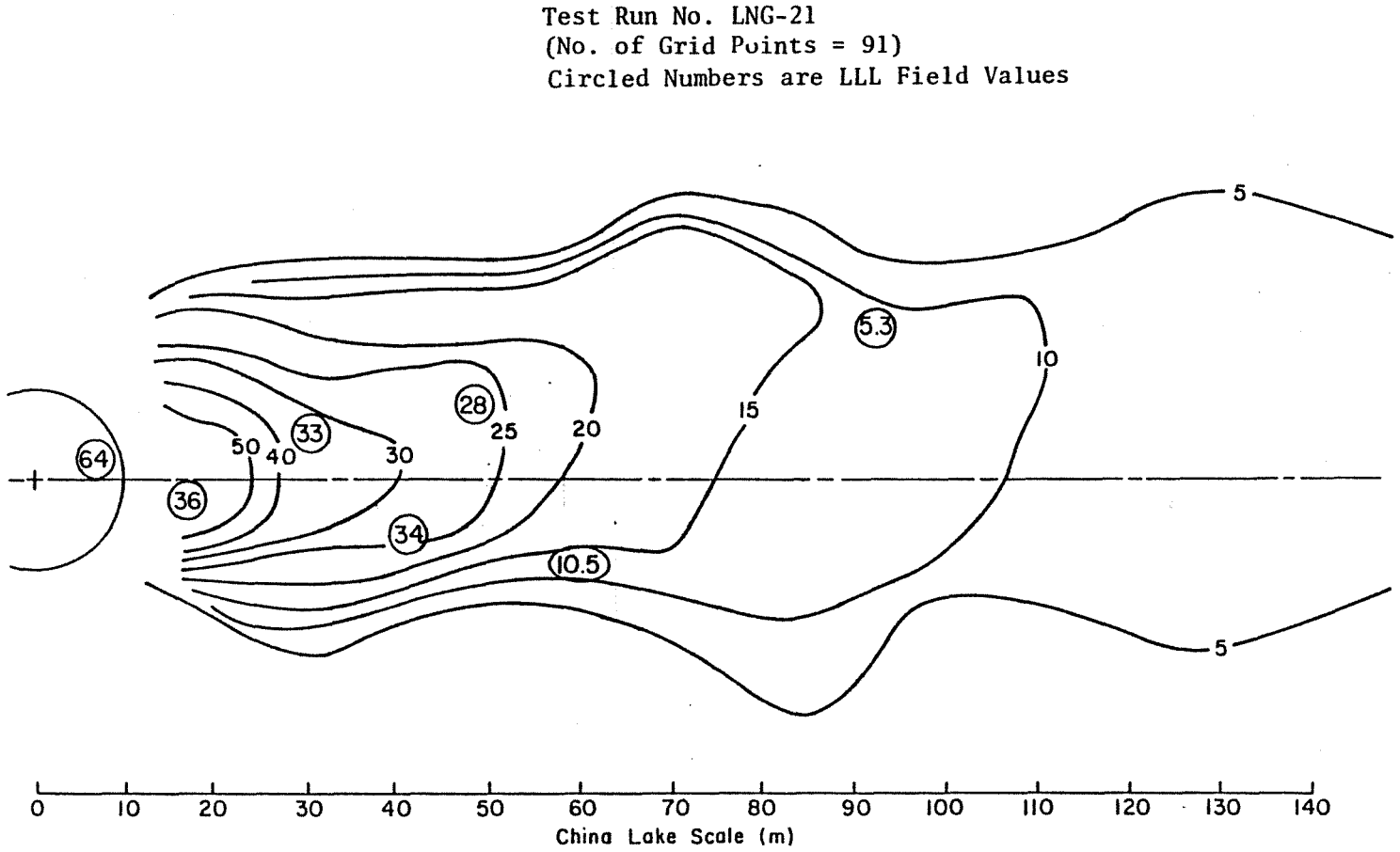

Figure 6. Comparison of Wind Tunnel and Field Data for the Six Cubic Meter LNG Spill Test No. LNG-21 at China Lake Naval Weapons Test Center, Neff and Meroney (1979): Wind Speed 4.9 m/s, Stability Category C; Wind-Tunnel Scale Ratio 85:1.

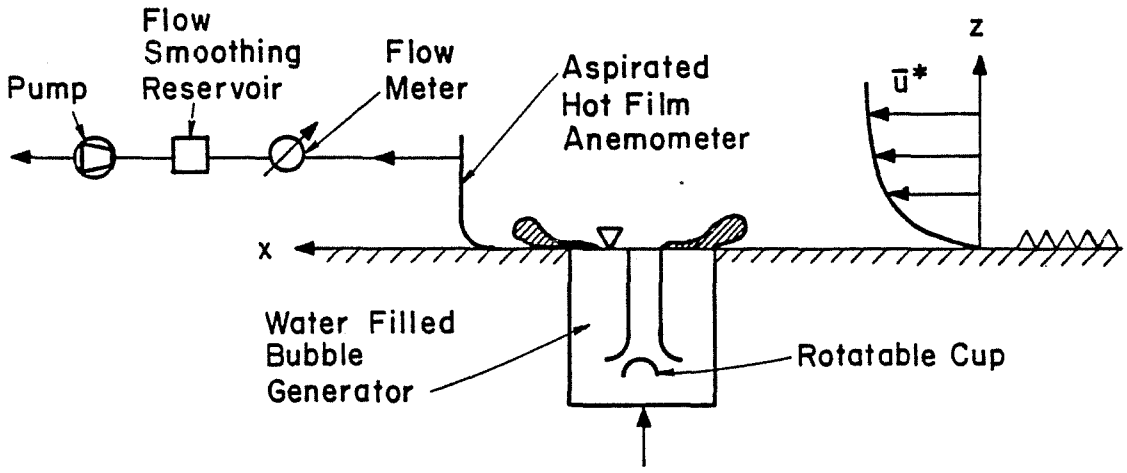

Figure 7. Experimental Configuration for Release of Instantaneous Volume Sources of Dense Gas, Lohmeyer et al. (1980).

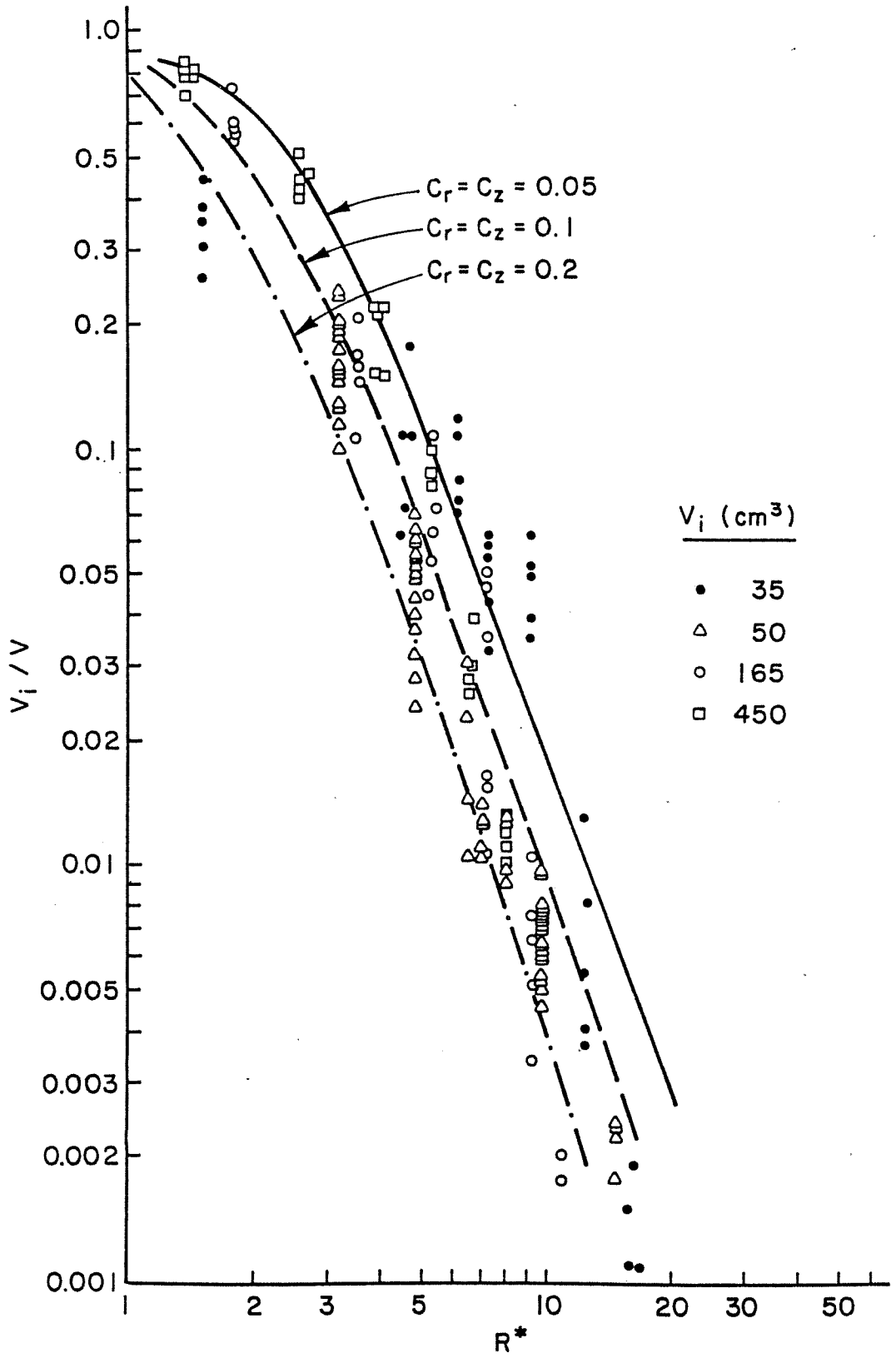

Figure 8. Plume Diultion, $\forall_i/\forall$, versus Dimensionless Radius, $R^* = r/\forall^{1/3}$, $U_L^* = 0$, Lohmeyer et al. (1980).

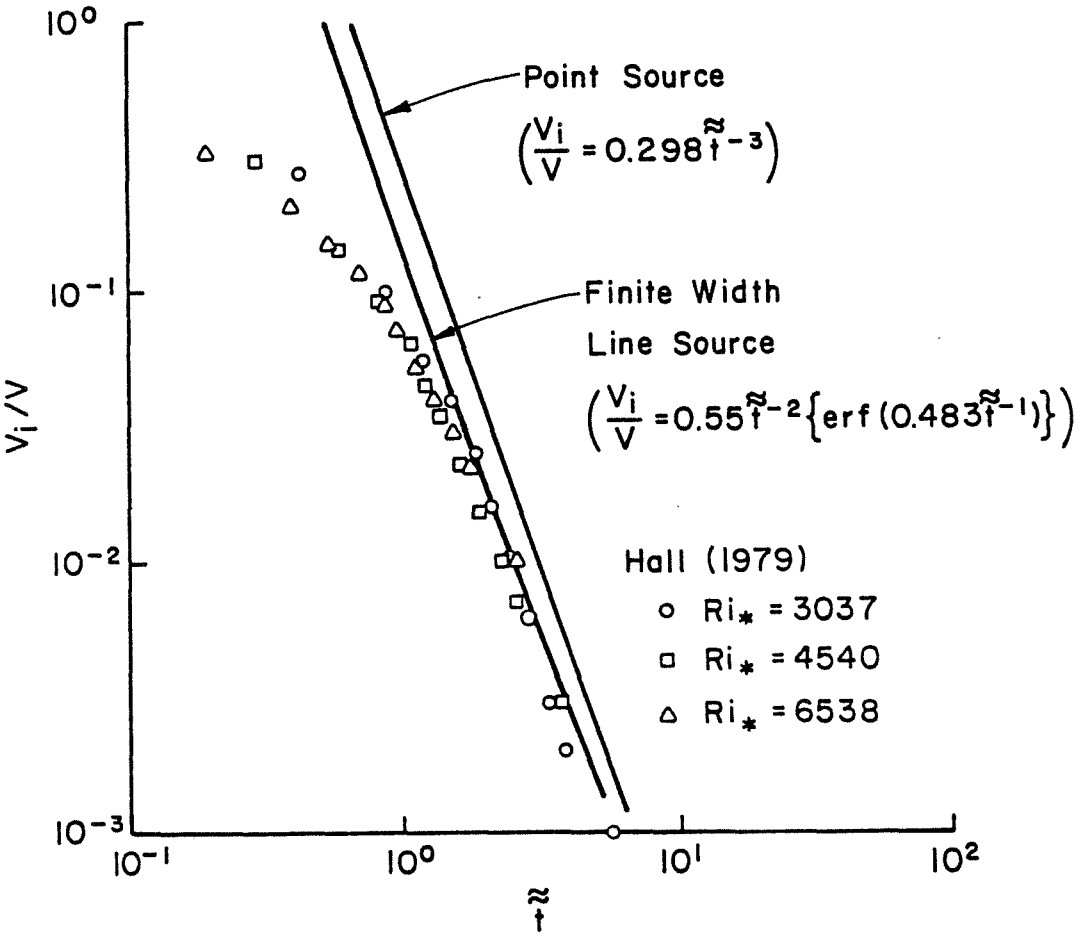

Figure 9. Assymptotic Dilution of Short-Term Releases of Dense Gases: Comparison of Lagrangian Similarity Solution for Passive Sources, Yang and Meroney (1973) with Dense Gas Tests, Hall (1979).

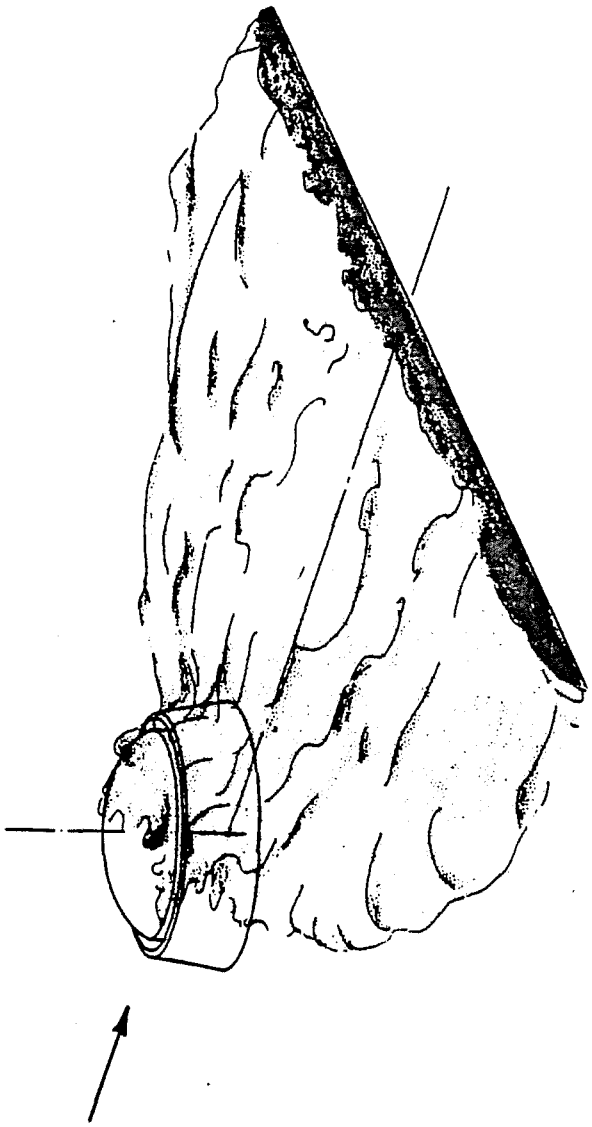

Figure 10. Dense Plume Behavior Downwind of a High Dike/Tank Model.

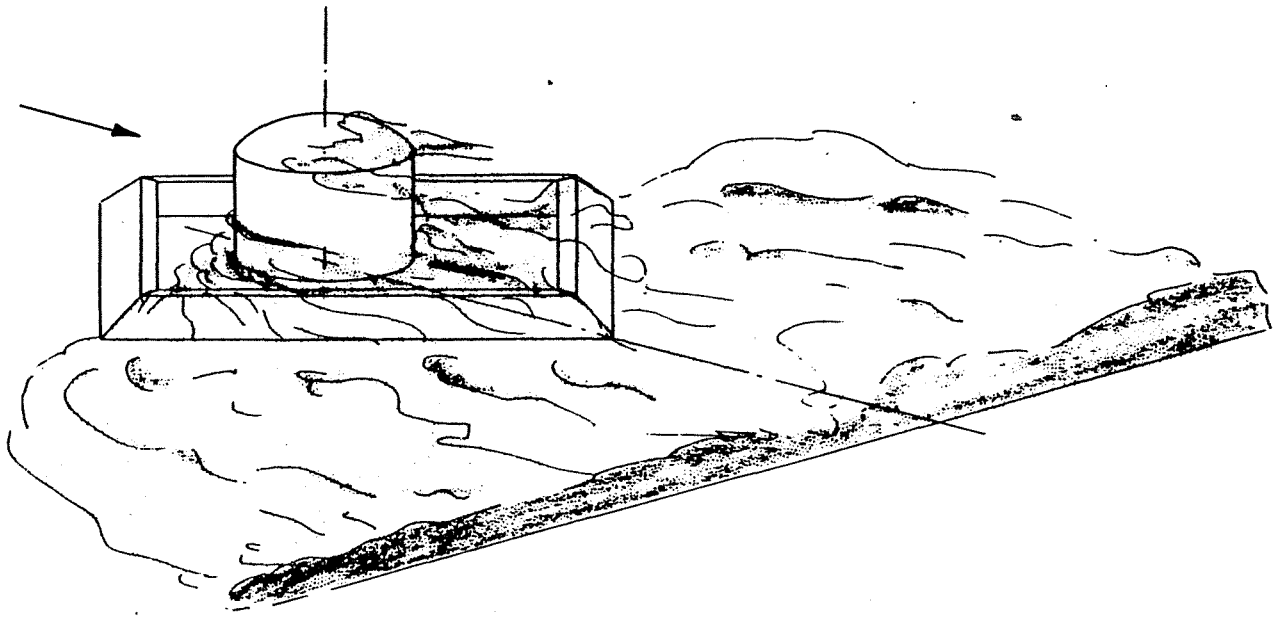

Figure 11. Dense Plume Behavior Downwind of a Low Dike/Tank Model.